Investigation into the antimicrobial activity of cationic antibacterials

Noëlle H. O'Driscoll

PhD **2011**

Investigation into the antimicrobial activity of cationic antibacterials

Noëlle H. O'Driscoll

A thesis submitted in partial fulfilment of the requirements of the Robert Gordon University for the degree of Doctor of Philosophy

August 2011

Declaration

This thesis has been composed by myself and has not been submitted in any previous application for a higher degree. The work that is documented was carried out by me. All verbatim extracts have been distinguished by quotation marks and the source of information specifically acknowledged.

Noëlle H. O'Driscoll

Abstract

The topic addressed by the 2011 WHO's World Health Day was antibacterial resistance. This action served to highlight the serious problem bacterial resistance now presents to healthcare professionals globally. This investigation focussed on the action of four cationic antimicrobial agents against *E. coli*, *S. aureus* and *P. aeruginosa*. Triclosan is widely used clinically and as an ingredient of personal care products that has come under renewed scrutiny by the FDA last year. Colistin is used clinically as salvage therapy against multi-drug resistant bacteria, particularly *P. aeruginosa* and *A. baumanii*. NP101 and NP108 are novel antimicrobial peptides, considered as a class with huge future potential in the treatment of not only bacterial but also viral and fungal infections in humans. The action of triclosan on all three test bacteria, including *P. aeruginosa*, historically considered resistant to triclosan, revealed concentration dependent bacteriostatic/bactericidal effects; reduction in bacterial growth; inhibition of second-phase logarithmic growth in *S. aureus*; induction of minimal K^+ loss in all bacterial species; non-septation and aggregation in all test species. Colistin use was abandoned clinically between 1970-2000 and is not used clinically against Gram-positive species. Colistin exposure induced a common response from test bacteria including the Gram-positive *S. aureus*; concentration dependent retardation in onset of bacterial growth, without reduction in final bacterial density; significant K^+ loss from *S. aureus* and *E. coli* but not *P. aeruginosa;* the development of resistance to the inhibitory colistin concentration by *P. aeruginosa* and *S. aureus* but not *E. coli*; production of small colony variants by *P. aeruginosa*; formation of spherical aggregates; membrane blebbing and inhibition of normal bacterial septation. Similar responses to NP101 and NP108 were observed to the test bacteria; an all or nothing effect on bacterial growth; prevention of second phase logarithmic growth in *S. aureus*; induction of

significant K^+ loss in all bacteria; size and shape alterations; extrusion of intracellular material, membrane blebbing; inhibition of bacterial septation and interruption of binary fission. Each of these peptides was incorporated into lyophilised wafers and tested for *in vitro* topical antibacterial efficacy and shown to have antibacterial activity against all test species.

Acknowledgements

I would like to express my sincere gratitude to everyone who has helped me undertake and complete this work.

I am deeply indebted to my principal supervisor Dr Andrew Lamb not only for accepting me as a PhD student but for his excellent supervision, planning and direction of the work undertaken in this thesis and for his guidance and friendship over the past years.

Special thanks also to the other members of my supervisory team, Dr Kerr Matthews and Dr Derry Mercer, for all the assistance, discussions and data analysis they provided over the course of this study.

I wish to express my deep gratitude to Novabiotics for providing me with the novel antimicrobial peptides which were used in this study.

I would like to express my grateful thanks to my friend and colleague Miss Vivienne Hamilton, who sadly passed away before this work was completed; for all the advice freely given when solicited, her encouragement, support and company in the laboratory from day one.

I wish to thank Dr Tim Cushnie for all his microbiological advice, insights and the help he provided me with over the duration of my studies; not least the great philosophical discussions we had in the laboratory.

Special thanks are due to Mr Steve Darwood (Beckman Coulter) for all the flow cytometry training, assistance in data analysis and for never failing to sort out the technical problems I encountered whilst using the Epics®XL™.

Grateful thanks are also due to Mrs Emily Hunter and Mr Iain Tough for all the training and their un-failing assistance in undertaking the Scanning Electron Microscopy work.

Many thanks also to Mrs Maureen Byers for all her help with the flame photometer operation and calibration which enabled me to carry out the potassium detection experiments.

I would like to express my sincere thanks to Mrs Mary Grant for all the help she provided during literature searches and referencing and for proof-reading my bibliography.

I am deeply grateful to Dr Hector Williams for all the statistical insight he provided and the invaluable discussion and data analysis sessions he provided.

Thanks also to Dr Stephen MacManus for his assistance with Chemsketch.

I would like to thank the many research students in RGU for their camaraderie and friendship while I was undertaking my studies.

My sincere appreciation and gratitude to Ms Olga Labovitiadi, Dr Ania Gryka and Dr Pramod Gadad, for their friendship, all the shared laughter and great times together during our PhD studies and in the Research Students Association.

Grateful thanks and deep appreciation are due to my Parents, family and friends for all the support and encouragement un-stingingly given not only during this project but in all my endeavours thus far; especially my sisters-in-law Brigid and Lisa for their un-failing hospitality and friendship and each of the following for their unique, individual contributions – Adam, Edel, Holly, Oliver, Coleman, John, Jonah, Chris, Debbie, Muireann, Moira, Evelyn, Gerry, Nancy, Celine, Kasia, Karolina and Elena.

Sincere thanks to my brother Hubert for all the complex mathematical computations he cheerfully undertook; his un-wavering support and refusal to admit defeat.

Last and best - special thanks are due to my brother Martin for his constant support, the countless technical problems he solved over the years; his encouragement and belief in my abilities and for his unique counselling style.

"There is a tide in the affairs of men,
Which, taken at the flood, leads on to fortune;
Omitted, all the voyage of their life
Is bound in shallows and in miseries.
On such a full sea are we now afloat,
And we must take the current when it serves,
Or lose our ventures".

Julius Caesar Act 4, Scene 3
William Shakespeare

Table of Contents

Abstract iv
Acknowledgements vi
Table of Contents ix
Index of Figures xv
Index of Tables xx
Abbreviations xxi
Chapter One 1
Introduction 1
1. Background on innate human defences 1
1.1 Development of antibiotics for clinical Use 1
1.1.2 Bacterial resistance 3
1.1.3 Host defence system 4
1.1.4 Inappropriate prescribing patterns 5
1.1.5 Reduction in bacterial fitness 6
1.1.6 Minimisation of resistance 7
1.2. Background on development of antimicrobial agents 7
1.2.1 Research and development strategies 7
1.2.2 New antimicrobial agents 9
1.3. Re-evaluating the anti-bacterial arsenal 10
1.3.1 Re-assessment and re-investigation 10
1.3.2 Triclosan 11
1.3.2.1 Triclosan; an atypical biocide 12
1.3.2.2 Triclosan Mechanisms of Action 13
1.3.2.3 Mechanisms of bacterial resistance to triclosan 15
1.3.2.4 Triclosan use and cross resistance to antibiotics 16
1.3.2.5 Triclosan toxicity 17
1.3.3 Colistin 18
1.3.3.1 Mechanism of action of colistin 19
1.3.3.2 Resistance to colistin 19
1.3.3.3 Therapeutic doses and risk factors 20
1.3.3.4 Colistin toxicity 20
1.3.3.5 Colistin anti-endotoxic activity 21
1.3.4 Cationic Antimicrobial Peptides (CAPs) 22
1.3.4.1 CAPs 22
1.3.4.2 CAP Composition 23
1.3.4.3 CAP mechanisms of action 24
1.3.4.4 CAP regulation in the human body 25
1.3.4.5 Resistance to CAPs 26
1.3.4.6 Presence and absence of CAPs in the human body 28
1.3.4.7 Synthetic CAPs 29
1.3.4.8 CAP detractions 30
1.3.4.9 CAP applications 30
1.3.4.10 Vehicles for the delivery of CAP therapeutics for clinical use 30
1.4 Project Aims: Investigation of cationic antibacterial agents 31
1.5 Objectives of the present study 32
Chapter Two 34
Materials and Methods 34
2.1 Chemicals and reagents 34

2.1.1 Antibacterial chemicals 34
2.1.2 Growth media and bacterial diluents 34
2.1.3 Miscellaneous chemical compounds 34
2.1.4 Fluorescent dyes 35
2.1.5 Laboratory equipment 35
2.2 Bacterial storage and sub-culture 35
2.2.1 Bacterial strains 35
2.2.2 Bacterial storage 35
2.2.3 Bacterial sub-culture 36
2.3 Preparation of bacterial enumeration graphs 36
2.3.1 Bacterial suspension preparation 36
2.3.2 Agar plate preparation 37
2.3.3 Dilution of bacterial suspensions and plating out 37
2.3.4 Determination of viable counts 37
2.3.5 Determination of bacterial growth under oxygentated and non-oxygenated conditions 38
2.3.6 Preparation of agarose plates 38
2.3.6.1 Agarose pour plates 38
2.3.6.2 Agarose spread plates 39
2.3.6.3 Determination of zones of inhibition 39
2.4 Dissolution of antibacterials 40
2.4.1 Triclosan 40
2.4.2 Colistin and CAPs 40
2.5 Determination of antimicrobial sensitivity 41
2.5.1 Preparation of micro-titre plates 41
2.5.2 Determination of minimum bactericidal concentration of test antibacterial 42
2.6 Sensitisation/de-sensitisation of antibacterial 42
2.6.1 Sensitisation of *E. coli* to triclosan 42
2.6.2 De-sensitisation of *E. coli* to triclosan 43
2.7 Assessment of loss of intracellular potassium 43
2.7.1 Calibration of the atomic emission spectrophotemeter 43
2.7.2 Quantification of total intracellular bacterial potassium 44
2.7.3 Assessment of potassium content of bacterial samples 45
2.8 Analysis of bacterial growth dynamics via flow cytometry 46
2.8.1 Calibration of flow cytometer 46
2.8.2 Preparation of bacterial samples for analysis 46
2.8.3 Assessment of rejuvenation of bacterial cultures on de-sensitisation to antimicrobial peptides 47
2.9 Examination of bacterial morphology via Scanning Electron Microscopy (S.E.M.) 48
2.10 Preparation of freeze dried antimicrobial wafers 49
2.10.1 Preparation of gels 49
2.10.2 Freeze drying process 49
2.10.3 Rheological analysis of gels 49
2.11 Statistical analysis 50
Chapter Three 51
Determination of antibacterial activity of cationic antimicrobial compounds 51
3.1 Introduction 51
3.2 Methodologies 52
3.2.1 Evaluation of bacterial growth under oxygenated and non-oxygenated conditions 52

3.2.2 Quantification of the antibacterial activity of test agents by broth macrodilution method 52
3.2.3 Quantification of the antibacterial activity of test agents by the broth microdilution method 52
3.2.4 Determination of minimum bactericidal concentration of test agents.. 53
3.2.5 Determination of MICs of *E. coli* sensitised/de-sensitised to triclosan . 53
3.3 Results 53
3.3.1 Bacterial growth under non-oxygenated, oxygenated and micro-titre plate reader conditions 53
3.3.2 Quantification of antimicrobial sensitivity 55
3.3.2.1 Triclosan 55
3.3.2.2 Colistin 57
3.2.2.3 CAPs 58
3.3.3 Bacterial growth in presence of cationic antibacterials 60
3.3.3.1 Triclosan 60
3.3.3.2 Colistin 66
3.3.3.3 NP101 72
3.3.3.4 NP108 77
3.4 Discussion 83
3.4.1 Optimum bacterial growth 83
3.4.2 Triclosan activity 83
3.4.3 Colistin activity 86
3.4.4 CAP activity 88
3.5 Conclusion 90
Chapter Four 92
Detection of cytoplasmic membrane damage by measuring loss of internal potassium induced by cationic antibacterials 92
4.1 Introduction 92
4.2 Methodologies 95
4.2.1 Detection and quantification of K^+ levels in extra pure de-ionised water and 1% SDS 95
4.2.2 Development of experimental protocol suitable for examination of K^+ loss from cationic antibacterial – treated bacteria 95
4.2.3 Quantification of total cytoplasmic K^+ present in *E. coli*, *S. aureus* and *P. aeruginosa* 96
4.2.4 Examination of the effect of 1% SDS and 5% chlorhexidine on K^+ loss from *E. coli*, *S. aureus* and *P. aeruginosa* 96
4.2.5 Examination of the effects of triclosan, colistin and NP108 on K^+ loss from cells of *E. coli*, *S. aureus* and *P. aeruginosa* 96
4.3 Results 96
4.3.1 Detection and quantification of K^+ levels in extra pure de-ionised water and 1% SDS 96
4.3.2 Detection and quantification of K^+ levels in 5% chlorhexidine 97
4.3.3 Development of an experimental protocol suitable for examination of K^+ loss from cationic antibacterial – treated bacteria 98
4.3.3.1 Comparison of the results obtained with ~1 x 10^6 cfu/ml and ~1 x 10^7 cfu/ml bacterial populations 98
4.3.4. Quantification of total K^+ present in *E. coli*, *S. aureus* and *P. aeruginosa* 99
4.3.5 Quantification of loss of K^+ in *E. coli*, *S. aureus* and *P. aeruginosa* due to incubation with 1% SDS 100

4.3.6 Quantification of loss of K^+ in *E. coli*, *S. aureus* and *P. aeruginosa* due to incubation with 5% chlorhexidine 101
4.3.7 Quantification of K^+ loss in *E. coli*, *S. aureus* and *P. aeruginosa* upon incubation with cationic antibacterials 103
4.3.7.1 Quantification of K^+ loss from *E. coli* and *S. aureus* exposed to triclosan 103
4.3.7.2 Quantification of K^+ loss from *E. coli*, *S. aureus* and *P. aeruginosa* exposed to colistin 105
4.3.7.3 Quantification of K^+ loss in *E. coli*, *S. aureus* and *P. aeruginosa* due to NP108 109
4.4 Discussion 113
4.4.1 K^+ content of bacterial cells 113
4.4.2 Loss of intracellular K^+ induced by triclosan 114
4.4.3 Loss of intracellular K^+ induced by colistin 116
4.4.4 Colistin mechanisms of action 117
4.4.5 K^+ loss induced by NP108 120
4.5 Conclusion 123
Chapter Five 124
Examination by flow cytometry growth dynamics and loss of bacterial viability upon incubation with cationic antimicrobial compounds 124
5.1 Introduction 124
5.1.1 Background 124
5.1.2 Components of a flow cytometer 124
5.1.3 Hydrodynamic focussing 126
5.1.4 Analysing the fluid stream 127
5.1.5 Fluorescent dyes 130
5.1.6 Acquisition 131
5.1.7 Aim of flow cytometry investigation 133
5.2 Methodologies 134
5.2.1 Preparation of samples for analysis by flow cytometry 134
5.2.2 Calibration of flow cytometer 134
5.2.3 Data analysis 134
5.3 Results 134
5.3.1 Examination of the effects of triclosan on *E. coli* and *S. aureus* 134
5.3.2 Examination of the effects of colistin on *E. coli*, *S. aureus* and *P. aeruginosa* 140
5.3.3 Effects of NP101 on *E. coli*, *S. aureus* and *P. aeruginosa* 145
5.3.4 Examination of the effects of NP108 on *E. coli*, *S. aureus* and *P. aeruginosa* 149
5.4 Discussion 153
5.4.1 Flow cytometry for analysing antimicrobial activity 153
5.4.2 Effect of triclosan upon *E. coli* and *S. aureus* 155
5.4.3 Effects of colistin on *E. coli*, *S. aureus* and *P. aeruginosa* 157
5.4.4 Effects of NP101 on *E. coli*, *S. aureus* and *P. aeruginosa* 159
5.4.5 Effects of NP108 on *E. coli*, *S. aureus* and *P. aeruginosa* 161
5.5 Conclusion 161
Chapter Six 163
Examination of the influence of cationic antibacterials upon test bacteria using scanning electron microscopy 163
6.1 Introduction 163
6.1.1 Electron Microscope 163
6.1.2 Scanning Electron Microscope 164

6.1.3 Bacterial responses to incubation with antibacterial agents.....164
6.1.4 Morphology of test species 165
6.2 Methodologies 167
6.2.1 Preparation of bacterial cultures for Scanning Electron Microscopy analysis.....167
6.2.2 Scanning Electron Microscope data collection.....167
6.2.3 Selection of suitable bacterial density 167
6.3 Results.....168
6.3.1 SEM images of *E. coli*, *S. aureus* and *P. aeruginosa* incubated with triclosan 168
6.3.2 SEM images of *E. coli*, *S. aureus* and *P. aeruginosa* incubated with colistin 183
6.3.3 SEM images of *E. coli*, *S. aureus* and *P. aeruginosa* incubated with NP101.....199
6.3.4 SEM images of *E. coli*, *S. aureus* and *P. aeruginosa* incubated with NP108.....214
6.4 Discussion 231
6.4.1 Introduction 231
6.4.2 Changes in morphology of *E. coli*, *S. aureus* and *P. aeuginosa* induced by triclosan.....232
6.4.2.1 Sub-inhibitory concentration 232
6.4.2.2 Inhibitory concentration 233
6.4.2.3 Supra-inhibitory concentration 234
6.4.2.4 Summary of bacterial responses to triclosan 234
6.4.3 Changes in morphology of *E. coli*, *S. aureus* and *P. aeuginosa* induced by colistin.....235
6.4.3.1 Sub-inhibitory concentration 235
6.4.3.2 Inhibitory concentration 236
6.4.3.3 Supra-inhibitory concentration 236
6.4.3.4 Summary of bacterial responses to colistin 237
6.4.4 Changes in morphology of *E. coli*, *S. aureus* and *P. aeuginosa* induced by CAPs 238
6.4.4.1 Sub-inhibitory concentration 238
6.4.4.2 Inhibitory and supra-inhibitory concentrations.....239
6.4.4.3 Summary of bacterial responses to CAPs 239
Chapter Seven 241
The production of lyophilised wafers as a formulation vehicle for the topical delivery of CAPs.....241
7.1 Introduction 241
7.1.2 Wounded and burned skin 241
7.1.3 Application of CAPs as topical therapeutic agents 242
7.1.4 Lyophilised wafers as topical drug delivery systems.....244
7.1.5 Freeze-drying process.....244
7.1.6 Chemical nature of NP101 and NP108 245
7.1.7 Selection of polymeric carrier 245
7.1.7 Objective of current investigation.....246
7.2 Methodologies 247
7.2.1 Preparation of guar gum gel 247
7.2.2 Freeze drying process.....247
7.2.3 Rheological analysis of gels 247
7.2.4 Preparation of agarose plates 247
7.2.5 Determination of zones of inhibition 247

7.3 Results 248
7.3.1 Rheological analysis of pre-lyophilised gels 248
7.3.2 Freeze dried lyophilised wafers 250
7.3.3 Determination of expansion and inhibition ratios of lyophilised 2% guar gum wafers via spread plates 251
7.3.3 Determination of expansion and inhibition ratios of guar gum 2% lyophilised wafers via pour plates 253
7.4 Discussion 255
7.4.1 Determination of inhibition ratios 255
7.4.2 Lyophilised wafers as topical formulations 255
7.4.3 CAP cell selectivity 256
7.4.4 Factors controlling drug residence in tissues 257
7.5 Conclusion 257
Chapter Eight 258
Discussion 258
8.1 Introduction 258
8.2 Measures to reduce antibacterial resistance 258
8.2 Membrane active agents 260
8.2.1 Membrane potential 260
8.2.2 Membrane enzymes 260
8.2.3 Membrane permeability 261
8.3 Quorum sensing 261
8.4 Small colony variants and persister cells 262
8.5 Antibacterial mechanism of action of triclosan 263
8.5 Antibacterial mechanism of action of colistin 265
8.6 Antibacterial mechanism of action of NP101 and NP108 267
8.7 Future work 270
8.8 Conclusions 270
Bibliography 273
Conference Publications 299

Index of Figures

Figure 1.1 Chemical structure of triclosan..... 11
Figure 1.2 (a) barrel stave, (b) carpet and (c) toroidal models. 24
Figure 3.1 Growth of 1x10^6 cfu/ml *E. coli* culture..... 54
Figure 3.2 Growth of 1x10^6 cfu/ml *S. aureus* culture. 55
Figure 3.3 *E. coli* 1x10^6 cfu/ml incubated with 0.008-1.12 µg/ml triclosan. 61
Figure 3.4 *E. coli* 1x10^8 cfu/ml incubated with 1.1-72 µg/ml triclosan 62
Figure 3.5 *E. coli* 1 x 10^6 cfu/ml serially passaged in 0.07 µg/ml triclosan..... 62
Figure 3.6 *E. coli* 1x10^6 cfu/ml serially passaged in triclosan for 96 hours..... 63
Figure 3.7 *S. aureus* 1x10^6 cfu/ml incubated with 0.014-1.76 µg/ml triclosan.... 64
Figure 3.8 *S. aureus* 1x10^8 cfu/ml incubated with 0.4-56 µg/ml triclosan..... 65
Figure 3.9 *P. aeruginosa* 1x10^6 cfu/ml incubated with 11-1445 µg/ml triclosan.. 66
Figure 3.10 *E. coli* 1x10^6 cfu/ml incubated with 0.02-0.28 µg/ml colistin. 67
Figure 3.11 *E. coli* 1x10^7 cfu/ml incubated with 0.3–39 µg/ml colistin. 68
Figure 3.12 *S. aureus* 1x10^6 cfu/ml incubated with 3–400 µg/ml colistin. 69
Figure 3.13 *S. aureus* 1x10^7 cfu/ml incubated with 2.5-312 µg/ml colistin. 70
Figure 3.14 *Ps. aeruginosa* 1x10^6 cfu/ml incubated with 0.09–12 µg/ml colistin. 71
Figure 3.15 *Ps. aeruginosa* 1x10^7 cfu/ml incubated with 0.3–39 µg/ml colistin. .. 71
Figure 3.16 *E. coli* 1x10^6 cfu/ml incubated with 0.008–1.0 mg/ml NP101. 72
Figure 3.17 *E. coli* 1x10^7 cfu/ml incubated with 0.08–10.0 mg/ml NP101. 73
Figure 3.18 *S. aureus* 1x10^6 cfu/ml incubated with 0.008–1.0 mg/ml NP101. 74
Figure 3.19 *S. aureus* 1x10^7 cfu/ml incubated with 0.08 – 10.0 mg/ml NP101 ... 75
Figure 3.20 *P. aeruginosa* 1x10^6 cfu/ml incubated with NP101. 76
Figure 3.21 *P. aeruginosa* 1x10^7 cfu/ml incubated with NP101 77
Figure 3.22 *E. coli* 1x10^6 cfu/ml incubated with 0.008–1.0 mg/ml NP108 78
Figure 3.23 *E. coli* 1x10^7 cfu/ml incubated with 0.016–2.0 mg/ml NP108 79
Figure 3.24 *S. aureus* 1x10^6 cfu/ml incubated with 0.008–1.0 mg/ml NP108. 80
Figure 3.25 *S. aureus* 1x10^7 cfu/ml incubated with 0.016–2.0 mg/ml NP108. 80
Figure 3.26 *P. aeruginosa* 1x10^6 cfu/ml incubated with NP108. 81
Figure 3.27 *P. aeruginosa* 1x10^7 cfu/ml incubated with NP108 82
Figure 4.1 K^+ loss in bacteria induced by incubation with 1% SDS.....101
Figure 4.2 K^+ loss in bacteria induced by incubation with 5 % chlorhexidine. 102
Figure 4.3 K^+ loss in bacteria induced by exposure to triclosan for 24 hours 104
Figure 4.4 K^+ loss induced by incubation with colistin over 24-hours 106
Figure 4.5 K^+ loss in 1 x 10^6 cfu/ml *S. aureus* induced by incubation with colistin for 60-minutes 108
Figure 4.6 K^+ loss in 1 x 10^6 cfu/ml *E. coli* induced by incubation with NP108 for 60 minutes.....109
Figure 4.7 K^+ loss in bacteria incubated with NP108.....111
Figure 5.1 Internal structure and components of a functional flow cytometer....125
Figure 5.2 Hydrodynamic focussing in a flow cytometer 127
Figure 5.3 Several graphical representations of the same flow cytometry data..132
Figure 5.4 *E. coli* 1x10^6 cfu/ml cultures incubated with different concentrations of triclosan 135
Figure 5.5 *E. coli* 1x10^6 cfu/ml cultures incubated with different concentrations of triclosan 138
Figure 5.6 *S. aureus* 1x10^6 cfu/ml incubated with different concentrations of triclosan 139

Figure 5.7 *E. coli* cultures inoculated with $1x10^6$ cfu/ml, incubated with different concentrations of colistin. 141
Figure 5.8 *S. aureus* cultures inoculated with $1x10^6$ cfu/ml, incubated with different concentrations of colistin. 142
Figure 5.9 *P. aeruginosa* cultures inoculated with $1x10^6$ cfu/ml, incubated with different concentrations of colistin 144
Figure 5.10 *E. coli* cultures inoculated with $1x10^6$ cfu/ml, incubated with different concentrations of NP101. 145
Figure 5.11 *S. aureus* cultures inoculated with $1x10^6$ cfu/ml, incubated with different concentrations of NP101. 147
Figure 5.12 *P. aeruginosa* cultures inoculated with $1x10^6$ cfu/ml, incubated with different concentrations of NP101 148
Figure 5.13 *E. coli* cultures inoculated with $1x10^6$ cfu/ml, incubated with different concentrations of NP108. 149
Figure 5.14 *S. aureus* cultures inoculated with $1x10^6$ cfu/ml, incubated with different concentrations of NP108. 151
Figure 5.15 *P. aeruginosa* cultures inoculated with $1x10^6$ cfu/ml, incubated with different concentrations of NP108 152
Figure 6.1 Components of a scanning electron microscope 163
Figure 6.2 Scanning electron micrograph of $1x10^8$ cfu/ml *E. coli* exposed to triclosan for 1 hour 169
Figure 6.3 Scanning electron micrograph of $1x10^8$ cfu/ml *E. coli* exposed to triclosan for 3 hours 169
Figure 6.4 Scanning electron micrograph of $1x10^8$ cfu/ml *E. coli* exposed to triclosan for 6 hours 170
Figure 6.5 Scanning electron micrograph of $1x10^6$ cfu/ml *E. coli* exposed to triclosan for 24 hours 171
Figure 6.6 Scanning electron micrograph of $1x10^6$ cfu/ml *E. coli* exposed to triclosan for 72 hours 172
Figure 6.7 Scanning electron micrograph of $1x10^6$ cfu/ml *E. coli* exposed to triclosan for 168 hours 173
Figure 6.8 Scanning electron micrograph of $1x10^8$ cfu/ml *S. aureus* exposed to triclosan for 1 hour 174
Figure 6.9 Scanning electron micrograph of $1x10^8$ cfu/ml *S. aureus* exposed to triclosan for 3 hours. 175
Figure 6.10 Scanning electron micrograph of $1x10^8$ cfu/ml *S. aureus* exposed to triclosan for 6 hoursl 176
Figure 6.11 Scanning electron micrograph of $1x10^6$ cfu/ml *S. aureus* exposed to triclosan for 24 hours 177
Figure 6.12 Scanning electron micrograph of $1x10^6$ cfu/ml *S. aureus* exposed to triclosan for 72 hours 178
Figure 6.13 Scanning electron micrograph of $1x10^6$ cfu/ml *S. aureus* exposed to triclosan for 168 hours 179
Figure 6.14 Scanning electron micrograph of $1x10^6$ cfu/ml *P. aeruginosa* exposed to triclosan for 4 hours 180
Figure 6.15 Scanning electron micrograph of $1x10^6$ cfu/ml *P. aeruginosa* exposed to triclosan for 8 hours 181
Figure 6.16 Scanning electron micrograph of $1x10^6$ cfu/ml *P. aeruginosa* exposed to triclosan for 24 hours 181
Figure 6.17 Scanning electron micrograph of $1x10^6$ cfu/ml *P. aeruginosa* exposed to triclosan for 32 hours 182

Figure 6.18 Scanning electron micrograph of $1x10^7$ cfu/ml *E. coli* exposed to colistin for 1 hour 184
Figure 6.19 Scanning electron micrograph of $1x10^7$ cfu/ml *E. coli* exposed to colistin for 3 hours 184
Figure 6.20 Scanning electron micrograph of $1x10^7$ cfu/ml *E. coli* exposed to colistin for 6 hours 185
Figure 6.21 Scanning electron micrograph of $1x10^7$ cfu/ml *E. coli* exposed to colistin for 24 hours 186
Figure 6.22 Scanning electron micrograph of $1x10^7$ cfu/ml *E. coli* exposed to colistin for 72 hours 187
Figure 6.23 Scanning electron micrograph of $1x10^7$ cfu/ml *E. coli* exposed to colistin for 168 hours 188
Figure 6.24 Scanning electron micrograph of $1x10^7$ cfu/ml *S. aureus* exposed to colistin for 30 minutes 189
Figure 6.25 Scanning electron micrograph of $1x10^7$ cfu/ml *S. aureus* exposed to colistin for 1 hour 189
Figure 6.26 Scanning electron micrograph of $1x10^7$ cfu/ml *S. aureus* exposed to colistin for 3 hours 190
Figure 6.27 Scanning electron micrograph of $1x10^7$ cfu/ml *S. aureus* exposed to colistin for 24 hours 191
Figure 6.28 Scanning electron micrograph of $1x10^7$ cfu/ml *S. aureus* exposed to colistin for 72 hours 192
Figure 6.29 Scanning electron micrograph of $1x10^7$ cfu/ml *S. aureus* exposed to colistin for 168 hours 193
Figure 6.30 Scanning electron micrograph of $1x10^7$ cfu/ml *P. aeruginosa* exposed to colistin for 2 hours 194
Figure 6.31 Scanning electron micrograph of $1x10^7$ cfu/ml *P. aeruginosa* exposed to colistin for 4 hours 195
Figure 6.32 Scanning electron micrograph of $1x10^7$ cfu/ml *P. aeruginosa* exposed to colistin for 8 hours 195
Figure 6.33 Scanning electron micrograph of $1x10^7$ cfu/ml *P. aeruginosa* exposed to colistin for 24 hours 196
Figure 6.34 Scanning electron micrograph of $1x10^7$ cfu/ml *P. aeruginosa* exposed to colistin for 72 hours 197
Figure 6.35 (a) Scanning electron micrograph of $1x10^7$ cfu/ml *P. aeruginosa* exposed to colistin for 168 hours 198
Figure 6.35 (b) High magnification scanning electron micrograph of $1x10^6$ cfu/ml *P. aeruginosa* exposed to MIC colistin for 168 hours 199
Figure 6.36 Scanning electron micrograph of $1x10^7$ cfu/ml *E. coli* exposed to NP101 for 1 hour 200
Figure 6.37 Scanning electron micrograph of $1x10^7$ cfu/ml *E. coli* exposed to NP101 for 3 hours 200
Figure 6.38 a) Scanning electron micrograph of $1x10^7$ cfu/ml *E. coli* exposed to NP101 for 6 hours 201
Figure 6.38 b) High magnification scanning electron micrograph of $1x10^7$ cfu/ml *E. coli* exposed to MIC NP101 for 6 hours 202
Figure 6.39 Scanning electron micrograph of $1x10^6$ cfu/ml *E. coli* exposed to NP101 for 24 hours 202
Figure 6.40 Scanning electron micrograph of $1x10^6$ cfu/ml *E. coli* exposed to NP101 for 72 hours 203
Figure 6.41 a) Scanning electron micrograph of $1x10^6$ cfu/ml *E. coli* exposed to NP101 for 168 hours 204

Figure 6.41 b) High magnification scanning electron micrograph of $1x10^6$ cfu/ml *E. coli* exposed to MIC NP101 for 168 hours.....205
Figure 6.42 Scanning electron micrograph of $1x10^7$ cfu/ml *S. aureus* exposed to NP101 for 1 hour.....205
Figure 6.43 Scanning electron micrograph of $1x10^7$ cfu/ml *S. aureus* exposed to NP101 for 3 hours.....206
Figure 6.44 Scanning electron micrograph of $1x10^7$ cfu/ml *S. aureus* exposed to NP101 for 6 hours.....207
Figure 6.45 Scanning electron micrograph of $1x10^6$ cfu/ml *S. aureus* exposed to NP101 for 24 hours.....207
Figure 6.46 Scanning electron micrograph of $1x10^6$ cfu/ml *S. aureus* exposed to NP101 for 72 hours.....208
Figure 6.47 Scanning electron micrograph of $1x10^6$ cfu/ml *S. aureus* exposed to NP101 for 168 hours.....209
Figure 6.48 Scanning electron micrograph of $1x10^7$ cfu/ml *P. aeruginosa* exposed to NP101 for 1 hour.....210
Figure 6.49 Scanning electron micrograph of $1x10^7$ cfu/ml *P. aeruginosa* exposed to NP101 for 3 hours.....210
Figure 6.50 Scanning electron micrograph of $1x10^7$ cfu/ml *P. aeruginosa* exposed to NP101 for 6 hours.....211
Figure 6.51 a) Scanning electron micrograph of $1x10^6$ cfu/ml *P. aeruginosa* exposed to NP101 for 24 hours.....212
Figure 6.51 b) High magnification scanning electron micrograph of $1x10^6$ cfu/ml *P. aeruginosa* exposed to $1/20^{th}$ MIC NP101 for 24 hours.....213
Figure 6.52 Scanning electron micrograph of $1x10^6$ cfu/ml *P. aeruginosa* exposed to NP101 for 72 hours.....213
Figure 6.53 Scanning electron micrograph of $1x10^6$ cfu/ml *P. aeruginosa* exposed to NP101 for 168 hours.....214
Figure 6.54 Scanning electron micrograph of $1x10^7$ cfu/ml *E. coli* exposed to NP108 for 1 hour.....215
Figure 6.55 Scanning electron micrograph of $1x10^7$ cfu/ml *E. coli* exposed to NP108 for 3 hours.....216
Figure 6.56 Scanning electron micrograph of $1x10^7$ cfu/ml *E. coli* exposed to NP108 for 6 hours.....216
Figure 6.57 Scanning electron micrograph of $1x10^6$ cfu/ml *E. coli* exposed to NP108 for 24 hours.....217
Figure 6.58 Scanning electron micrograph of $1x10^6$ cfu/ml *E. coli* exposed to NP108 for 72 hours.....218
Figure 6.59 a) Scanning electron micrograph of $1x10^6$ cfu/ml *E. coli* exposed to NP108 for 168 hours.....219
Figure 6.59 b) High magnification scanning electron micrograph of $1x10^6$ cfu/ml *E. coli* exposed to $1/20^{th}$ MIC NP108 for 168 hours.....220
Figure 6.60 Scanning electron micrograph of $1x10^7$ cfu/ml *S. aureus* exposed to NP108 for 1 hour.....220
Figure 6.61 Scanning electron micrograph of $1x10^7$ cfu/ml *S. aureus* exposed to NP108 for 3 hours.....221
Figure 6.62 a) Scanning electron micrograph of $1x10^7$ cfu/ml *S. aureus* exposed to NP108 for 6 hours.....222
Figure 6.62 b) High magnification scanning electron micrograph of $1x10^7$ cfu/ml *S. aureus* exposed to MIC NP108 for 6 hours.....222
Figure 6.63 Scanning electron micrograph of 1x107 cfu/ml S. aureus exposed to NP108 for 24 hours.....223

Figure 6.64 Scanning electron micrograph of $1x10^7$ cfu/ml *S. aureus* exposed to NP108 for 72 hours 224
Figure 6.65 Scanning electron micrograph of $1x10^7$ cfu/ml *S. aureus* exposed to NP108 for 168 hours 225
Figure 6.66 Scanning electron micrograph of $1x10^7$ cfu/ml *P. aerugionsa* exposed to NP108 for 1 hour. 226
Figure 6.67 Scanning electron micrograph of $1x10^7$ cfu/ml *P. aerugionsa* exposed to NP108 for 3 hours. 226
Figure 6.68 Scanning electron micrograph of $1x10^7$ cfu/ml *P. aerugionsa* exposed to NP108 for 6 hours 227
Figure 6.69 Scanning electron micrograph of $1x10^7$ cfu/ml *P. aerugionsa* exposed to NP108 for 24 hours 228
Figure 6.70 Scanning electron micrograph of $1x10^7$ cfu/ml *P. aerugionsa* exposed to NP108 for 72 hours 229
Figure 6.71 a) Scanning electron micrograph of $1x10^7$ cfu/ml *P. aerugionsa* exposed to NP108 for 168 hours 230
Figure 6.71 b) High magnification scanning electron micrograph of $1x10^6$ cfu/ml *P. aeruginosa* exposed to MIC NP108 for 168 hours 230
Figure 7.1 Chemical structure of guar gum 246
Figure 7.2 Rheological analysis of pre-lyophilised gels 248
Figure 7.3 Determination of log shear stress against log shear rate 249
Figure 7.4 Temperature profile of freeze-drying process 250
Figure 7.5 Expansion (a) and inhibition (b) ratios of lyophilised wafers 251
Figure 7.6 Expansion (a) and Inhibition (b) ratios of lyophilised wafers 253

Index of Tables

Table 1.1 Antibiotic class, mechanism of action and resistance mechanisms 2
Table 3.1 MICs of bacteria incubated with triclosan. 56
Table 3.2 Macro broth MICs of $1x10^6$ cfu/ml *E. coli* incubated in nutrient broth with triclosan for varying time periods. 56
Table 3.3 Macro broth MICs of $1x10^6$ cfu/ml *E. coli* de-sensitised to triclosan for varying time periods. 57
Table 3.4 MIC/MBCs of bacteria incubated with colistin. 58
Table 3.5 MIC and MBCs of $1x10^6$ cfu/ml test bacteria incubated with CAPs in polyethylene microtitre plates. 59
Table 3.6 MIC/MBCs of $1x10^6$ cfu/ml test bacteria incubated with CAPs in polycarbonate microtitre plates. 59
Table 3.7 MICs and MBCs of $1x10^7$ cfu/ml test bacteria incubated in polyethylene microtitre plates with CAPs. 60
Table 4.1 Assessment of K^+ content (mg/L) in 1% SDS via flame photometer. .. 97
Table 4.2 Assessment of K^+ content (mg/L) in 5% chlorhexidine via flame photometer. 98
Table 4.3 Total K^+ content of bacterial cells. 99
Table 5.1 EPICS® XL™ filters and detectors. 129
Table 7.1 Chemical nature and source of polymers 245
Table 7.2 Viscosity coefficient (consistency) η' (Pa.s), yield stress σ_o (Pa), rate index for control, NP101 and NP108 polymers in aqueous solution as analysed by the Herschel-Bulkley model.....248

Abbreviations

BZK	Banzalkonium chloride
CAPs	Cationic antimicrobial peptides
cfu	Colony forming unit
DMSO	Dimethyl sulphoxide
FDA	Food and Drug Administration (USA)
HPCV	Half peak co-efficient variation
iv	intravenous
K^+	Potassium ions
LPS	Lipopolysaccharide
MBC	Minimum bactericidal concentration
MHRA	Medicines and Healthcare Regulatory Agency
MIC	Minimum inhibitory concentration
MOA	Mechanism of action
NCTC	National Collection of Type Cultures
ND	Not determined
PMF	Proton-motive force
RGU	Robert Gordon University
rpm	Revolutions per minute
SDS	Sodium dodecyl sulphate
SEM	Scanning Electron Microscope
S.E.M.	Standard error of mean
UK	United Kingdom
USA	United States of America

Chapter One

Introduction

1. Background on innate human defences

1.1 Development of antibiotics for clinical Use

Before the introduction of sulphonamides in the 1930s, death due to infection was common and whether a patient lived or died from an illness was due in part to the strength of their immune system, the level of medical care received and availability of food (Jayarman 2009). Early antibiotics were seen as truly miraculous drugs and were initially reserved for military use during World War II (Alanis 2005). Many classes of antibiotic have been developed since (Table 1.1); unfortunately bacteria have developed at least one resistance factor to each of these antibacterials (Woods 2006).

The increase in microorganisms that have developed resistance to currently available antimicrobial agents has become a major cause for concern worldwide and while these organisms are widespread in hospitals they are becoming increasingly prevalent in the community (Alanis 2005). Resistance can be defined as, bacteria surviving exposure to a concentration of antimicrobial (biocide), which is lethal to the rest of the bacterial population (Maillard 2007). Penicillin was developed in 1943 and penicillin resistant bacteria were first detected in 1946 (Alanis 2005) while tetracycline was developed in 1948 and resistance emerged only five years later (Quadri Luis 2007). In 1945, while being interviewed by *The New York Times,* Sir Alexander Fleming predicted the development of resistant, mutant forms of *S. aureus* if penicillin was used inappropriately.

Class of antibacterial	Mode of action	Resistance mechanism
Penicillins, Cephalosporins, Carbapenems, Monobactams, Glycopeptides, cyclic Lipopeptides	Inhibition of cell wall synthesis	β-lactamases, alterations in penicillin-binding proteins
Tetracycline, Aminoglycosides, Oxazolidononones, Ketolides, Lincosamides, Macrolides, Streptogramins	Inhibition of protein synthesis	Active- efflux, Ribosomal alterations
Fluoroquinolones	Inhibition of DNA synthesis	Active- efflux, DNA-gyrase modifications
Rifampicin	Inhibition of RNA synthesis	Rifampicin resistant rna polymerase β-subunit
Sulphonamides, Trimethoprim	Inhibition of bacterial folic acid synthesis	Sulphonamide transposable element (Tnβ) dfrA1
Polymyxins	Membrane disrupting agents	Reduction of negative charges on bacterial surface
Metronidazole	Other mechanisms	Nonsense or deletion mutations in rdxA

Table 1.1 Antibiotic class, mechanism of action and resistance mechanisms

As more antibiotics were discovered their use became widespread and they were employed to treat trivial and non-susceptible infections (Alanis 2005). The consequences of antibiotic overuse are the alarming levels of bacterial resistance to existing antimicrobials and the dearth of effective antimicrobials for clinical use against multi drug resistant bacteria.

Serious infections caused by bacteria resistant to commonly used antibiotics are now a major problem in the 21st Century (Alanis 2005). The estimated cost of treating drug-resistant nosocomial bacterial infections in North America annually is 5 billion dollars and these infections result in over 63,000 deaths per annum (Kindrachuk et al. 2007). Some of these strains are multi-resistant and the agents available to treat infections caused by them are few and dwindling (Finch and Hunter 2006).

1.1.2 Bacterial resistance

Bacteria have developed resistance to antibiotics of natural (penicillins), semi-synthetic (cephalosporins) and completely synthetic origin (fluoroquinolones) as well as agents that do not even enter the bacterial cell (vancomycin) (Jayarman 2009). The most implicated factor in the development of antibiotic resistance is the un-necessary and un-controlled use of antibiotics in both community and hospitalised patients and in the care of animals for food production (Alanis 2005). Bacterial resistance to antibiotics can be intrinsic or acquired and can be transmitted horizontally as well as vertically. The most frequent resistance type seen is acquired; transmitted horizontally via conjugation by plasmids (Alanis 2005).

There are only two requirements necessary for bacterial antimicrobial resistance to occur, an antibiotic capable of inhibiting the majority of bacteria in a colony and one bacterium in the colony with the genetic make-up capable of developing resistance to that antibacterial (Levy and Marshall 2004). Once genetic mutation has occurred, resulting in a change in bacterial DNA, transfer of this genetic material to other bacteria can occur rapidly by conjugation, transformation or transduction (Alanis 2005).

A report " Overcoming Antimicrobial Resistance" in 2000, issued by the World Health Organisation (WHO) on bacterial resistance to antimicrobials, identified the problem as critical for public health due to the faster emergence and spread of resistant bacteria than previously observed, the global nature of resistance that is rapidly spread through international travel and the treatment of infections beset by either a total lack of effective antimicrobials or the exorbitant and prohibitive cost of new anti-infective agents (Finch and Hunter 2006). This increased level of bacterial resistance has produced pandrug-resistant isolates, i.e. bacteria resistant

to all available antibiotics. (Falagas and Bliziotis 2007) Untreatable pan-resistant bacterial infections have become far more frequent in the last five years (Projan and Bradford 2007). Deaths in patients following bacterial infections are increasing, even in patients infected with bacteria susceptible to current antimicrobials, as patients most at risk of contracting an infection caused by multidrug-resistant pathogens, are the most seriously ill patients. Multidrug-resistant infections in otherwise healthy adults are now frequently identified in the community setting, compared to this being a predominantly hospital phenomenon in the past (Projan and Bradford 2007).

Multiple solutions are required to combat this problem, amongst them, education of the public that antibiotics are not always necessary or needed, better global regulation of antimicrobial use, research to permit the development of new agents and increased worldwide monitoring of bacterial resistance (Finch and Hunter 2006).

1.1.3 Host defence system

Humans are constantly exposed to potentially harmful pathogens in normal everyday life. Our survival depends on an effective host defence system, comprised of the innate immune system and acquired immune responses (Reddy, Yedery and Aranha 2004). The function of the immune system is to identify invading pathogens, contain and neutralise the threat and restore health (Martin and Dodds 2006). Many factors comprise the innate immune defence system; physical barriers such as the stratum corneum of the skin; leukocytes such as macrophages and neutrophils monitor blood for potential pathogenic infection: while epithelia synthesise and secrete small cationic peptides to counteract infection (Schauber et al. 2006). The difference between the innate and acquired immune system is that

each human is born with an already functioning innate immune system whereas humans require exposure to infections in order to acquire immunity to them: thereby developing their acquired immune system. Generally once exposure to infection has occurred, humans produce antibodies to that antigen within four days (Wood 2006). The ability of the acquired immune system to carry out its function lies in its recognition of certain molecules as foreign to the human body. These are distinct, evolutionary conserved, molecular patterns such as lipopolysaccharide, peptidoglycan and flagellin in bacteria (Martin and Dodds 2006). As these molecules are specific for bacteria and essential for their survival, ceasing their production to avoid detection by the immune system is not possible. The host cell receptors that recognise these bacterial molecules are termed pattern recognition receptors, which include Toll-like receptors (TLRs) and Nod like receptors (NLRs) (Wood 2006). TLRs are located throughout the human body from epithelial cells to the endothelial cells of coronary arteries; once molecules are bound to these receptors a cascade of responses is released including the transcription of antimicrobial peptides (Martin and Dodds 2006).

1.1.4 Inappropriate prescribing patterns

Prescribing guidelines were developed in the 1980s and 1990s to promote appropriate prescribing and reduce the risk of resistance. Towards the end of the 1990s, the Consensus Group on Resistance and Prescribing in Respiratory Tract Infections was set up to optimise treatment for lower respiratory tract infections (RTI). They targeted primary care antibiotic prescribing which accounted for 80% of antibiotic prescriptions, 75% of which are prescribed for RTIs (Ball 2007). Antibacterial prescribing for the common cold in the US alone is reported as 36%, (Gilberg et al. 2003) yet the medical profession is well aware that the causative

factor in the majority of colds is an adenovirus which is unaffected by the prescribed antibacterial.

The importance of RTIs as a cause of death is rising and it is estimated by 2020 the number of deaths due to chronic obstructive pulmonary disease and pneumonia will be surpassed only by chronic heart disease and stroke (Murray and Lopez 1997). Three bacterial species, *Streptococcus pneumoniae, Haemophilus influenzae* and *Moxarella catarrhalis* are mainly involved in respiratory disease and drug resistance in clinical isolates of all three species is rising (Ball 2007). SENTRY and PROTEKT, two global surveillance studies, have shown the worldwide increase in penicillin-resistant isolates of *S. pneumoniae*.

1.1.5 Reduction in bacterial fitness

Studies have shown that by whatever means antibiotic resistance is acquired by bacteria, there is a cost involved, which may be manifested as a reduction in bacterial growth, virulence or transmission between patients (Andersson 2006). Experimental studies have demonstrated the cost of resistance is a main determinant of both the rate and extent of resistance development whilst under a given antibiotic pressure (Andersson 2006). The cost of resistance can also be measured by examining the rate by which resistance declines if antibiotic use is reduced (Andersson 2006). If the resistance-conferring gene is linked genetically with other selected genetic markers, that resistance-conferring gene could remain in the bacterial population (even though it exerts a fitness cost) solely due to the genetic link - as shown by the prevalence of sulphonamide resistance to date (40/45%) in *E. coli* despite a 97% reduction in sulphonamide use since the 1990's (Enne et al. 2004). Sulphonamide resistance is carried on *sul2*-encoding plasmids which normally reduce the competitive fitness of the host but these plasmids also

encode resistance to at least one other currently used antimicrobial suggesting maintenance in the bacterial population is due to the clinical use of these agents (Enne et al. 2004). Unfortunately studies of fitness costs of resistance on bacteria have shown that resistant bacteria do not disappear even if antibiotic use is reduced but persist long term even in the absence of antibiotic selective pressure (Andersson 2006).

1.1.6 Minimisation of resistance

Because bacteria have developed resistance to so many existing antibacterial agents, any factors that can help slow the development of resistance to both current and future antibacterials should be utilised. Properly conducted epidemiological studies of risk factors for the development of antibiotic resistance are essential for interventions, based on these studies, to be effective in curbing the rising tide of resistance (Gasink et al. 2007).

For example, early *in vitro* studies revealed exposure of *E. coli* to fluoroquinolones resulted in selection of resistance mutations conferring fluoroquinolone resistance. (Watanabe et al. 1990)(MacAdam et al. 2006). Ecological studies also observed a strong correlation between fluoroquinolone-resistant *E. coli* and the increase in the use of fluoroquinolones (Lautenbach et al. 2004)(MacAdam et al. 2006). Logically, clinical studies investigating risk factors for fluoroquinolone-resistant *E. coli* should utilise this information in formulating treatment guidelines (MacAdam et al. 2006).

1.2. Background on development of antimicrobial agents

1.2.1 Research and development strategies

In spite of nearly seven decades using antimicrobial agents, infectious diseases continue to have a massive impact both on human morbidity and mortality

throughout the world and place a major burden on healthcare services. The antibacterial drugs poised for licensing in the US are mostly active against Gram-positive bacteria, particularly MRSA, but the growing unmet medical need of antibacterials to treat multi-drug resistant Gram-negative infections remains currently un-addressed (Projan and Bradford 2007).

The Infectious Diseases Society of America has called for a "10 x 20 initiative", requesting a global commitment to deliver a minimum of 10 new antibacterials by 2020 (Moellering Jr. 2011). The search for new antimicrobial agents possessing wide antibacterial activity, little potential for selection of resistant mutants in combination with minimal human toxicity, is now urgent (Kindrachuk et al. 2007).

Amongst the factors that have contributed to the lack of new antimicrobials entering clinical use, is the global consolidation of pharmaceutical companies since 1990 and the lack of interest by the remaining big pharma companies in the development of new antibacterial agents (Moellering Jr. 2011). Increasing development costs of new drugs coupled with a 10-14 year span from discovery of a promising drug candidate to the development of a new medicine, combined with regulatory agencies requiring ever increasing volumes of data on safety and efficacy of these drugs from clinical trials, has caused pharmaceutical companies to reassess their research portfolio in favour of medicines which show the greatest return for the money invested over a lengthy product lifetime (Moellering Jr. 2011).

It makes sound financial sense for pharmaceutical companies to develop therapeutic agents such as anti-hypertensives, which once prescribed for the patient are life long medicines, maximising the long term financial return for the pharmaceutical company holding the patent. Compare this to a similar time and monetary investment by the same company for the production of an antimicrobial

agent with a prescribing pattern for short tem, infrequent clinical use and it is immediately apparent that the development of antimicrobial agents is not in the best long term financial interest of pharmaceutical companies.

Another factor affecting drug development is that the patent life of a medicine only lasts 20 years from the date of discovery (Shlaes and Moellering 2002). The nature of the product being developed also discourages financial investment; if the antimicrobial agent is novel and clinically effective an embargo will initially be imposed on its use in an effort to curtail the development of resistance and thereafter the product will only show a financial return while clinically effective, before bacterial resistance to this agent develops, ending the financial reward for the company involved (Projan and Bradford 2007).

1.2.2 New antimicrobial agents

Mapping of the first bacterial genome that of *Haemophilus influenzae,* occurred in 1995, whereupon the focus of development of new antibacterials fell on targets elucidated from the genomic sequencing of bacteria (Brötz-Oesterhelt and Brunner 2008). This strategy of one gene one target has not been successful in the development of novel antimicrobials and is contrary to the complex mechanisms of action of developed antibacterials, where bacterial inactivation is not merely due to the binding of a unique enzyme target (Brötz-Oesterhelt and Brunner 2008). Strategies used in the development of new antibacterial agents range from classic screening methods, chemical modification of existing antimicrobial agents, potentiation of activity of known compounds, to synergistic combinations of agents (Moellering Jr. 2011). Through development of a novel screening method for un-culturable microorganisms, Novobiotics has discovered the glycosylated macrolactams; novolactamycin and novobiomycin (Moellering Jr. 2011).

Novelty in future drugs requires in essence a molecular target, previously un-used in drug formulation and original drug core architecture (Quadri Luis 2007). For this to happen, innovation is required in the target and lead discovery phases to produce a new arsenal of anti-infective weapons (Quadri Luis 2007). This work is hoped to result in an array of drugs that prevent pathogens producing infections due to antimicrobial activity and drugs that do so by other activities, as for example the inhibition of a bacterial iron scavenging mechanism, as iron is essential for correct multiplication in most bacteria (Quadri Luis 2007).

1.3. Re-evaluating the anti-bacterial arsenal

1.3.1 Re-assessment and re-investigation

The dearth of new antimicrobials in the antibacterial development pipeline for clinical use has focussed the spotlight on the existing agents in the antimicrobial arsenal. The FDA identified Triclosan for re-evaluation in 2010, in response to reports of altered thyroid function and changes to bacterial resistance by the bisphenol (Focus on Surfactants 2010a) (Focus on Surfactants 2010b). Triclosan was developed in the early 1960's and is marketed as Irgasan DP300 for use in skin products and Irgacare MP for oral care formulations (Jones et al. 2000). Triclosan was launched onto the healthcare market in 1972 as a surgical scrub (Jones et al. 2000).

Re-examination of discarded antibiotics such as polymyxins is currently being undertaken (Woods 2006.) The clinical use of Colistin (polymyxin E) was abandoned worldwide around 1980 except in the treatment of cystic fibrosis patients, due to reports of serious nephrotoxicity and neurotoxicity problems (Falagas and Michalopoulos 2006). Colistin use has been revived recently and it is

currently used as a salvage treatment against multi-drug resistant Gram-negative bacteria (Zavascki et al. 2007).

Under-investigated areas such as antimicrobial peptides are being re-examined; antimicrobial proteins - lactoferrin and histones – were first reported in 1930, but the discovery of antibiotics, which were much easier to synthesise, drew the attention of researchers away from these antimicrobial proteins (Lupetti et al. 2003).

1.3.2 Triclosan

Triclosan (Irgasan DP 300; 2,4,4'-trichloro-2'-hydroxydiphenyl ether) is a chlorinated diphenyl ether or bisphenol that is employed in a variety of ways, including incorporation into mouthwashes, cosmetic preparations and plastics due to its high anti-bacterial activity and safety profile (Gomez- Escalada et al. 2005).

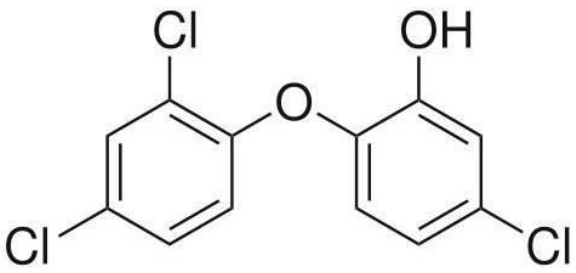

Figure 1.1: Chemical structure of triclosan

Triclosan is a tasteless, white, non-ionic, odourless crystalline powder (Qian, Guan and Xiao 2008), which is highly lipophilic, requiring sufficiently alkaline pH for significant aqueous solubility in anionic form (Amiri et al. 2007). The typical concentration of the diphenyl ether in healthcare products ranges from 0.1 - 0.3% and the widespread use of such products has led to the identification of triclosan

in 2002 as one of seven most commonly detected compounds in a United States freshwater survey (Liu et al. 2009.)

Triclosan exhibits high activity against *Escherichia coli* and *Staphylococcus aureus* while *Pseudomonas aeruginosa* is highly resistant (Russell 2004)(Russell 2004). Triclosan enters all three organisms by diffusion, the rate of which has been reported as proportional to the lipid content of the cell membrane (Schweizer 2001). Triclosan displays activity against many Gram-positive and Gram-negative non-sporulating bacteria, *Plasmodium falciparium*, some fungi and *Toxoplasma gondii* (Russell 2004). Triclosan is bacteriostatic at low concentrations (sub-inhibitory) but bactericidal at higher concentrations (supra-inhibitory) (Russell 2004).

1.3.2.1 Triclosan; an atypical biocide

Triclosan has been termed an atypical biocide, through targeting only one specific site within the bacterial cell, namely the gene fabI (Russell 2002). Characteristically biocides possess many target sites upon which they exert their action within a bacterium. (Suller and Russell 2000) Biocide composition can include several active compounds resulting in multiple bacterial intracellular targets (Randall et al. 2007).

Concentration is the most important factor governing the antimicrobial activity of a biocide, even at low concentrations biocides exert a selective pressure upon a bacterial population and a stress response is induced from the bacteria (Maillard and Denyer 2009). High biocide concentrations for disinfection and antiseptic use greatly exceed bacterial MICs, resulting in rapid microbial kill through interaction with multiple target sites, with little possibility of the development of bacterial resistance (Maillard 2005). Unfortunately high biocide concentration does not guarantee the absence of microorganisms, as contaminated formulations

incorporating a high biocide concentration have been reported (Maillard and Denyer 2009).

Increased public awareness of microbial contamination and infection has greatly increased biocide use in the domestic and healthcare market, resulting in the commercial availability of products containing low concentrations of biocides (Maillard and Denyer 2009). The dilution factor in the environment of these low biocide concentrations and their subsequent effects on bacteria remains unevaluated (Maillard 2007). Some researchers have proposed that it is the residual concentrations of Triclosan in the environment that may play a role in selecting for organisms with reduced susceptibility (Aiello et al. 2004).

1.3.2.2 Triclosan Mechanisms of Action

Triclosan exerts antibacterial activity by targeting a specific site within bacterial cells, namely an NADH-dependent enoyl-acyl carrier protein reductase, FabI (Yu, Kim and Pan 2010). The *fabI* gene encodes this enoyl reductase enzyme, which uses NADH to reduce double bonds during fatty acid elongation, making this an important element of lipid synthesis (Suller and Russell 2000). *E. coli*, *S. aureus* and *P. aeruginosa* all possess *fabI* however *P. aeruginosa* also possesses *fabK*, a triclosan resistant gene which catalyses fatty acid synthesis in this bacterium (Escalada et al. 2005).

Levy *et al* reported the formation of a ternary complex in *E. coli* between FabI, NAD^+ and triclosan (Levy et al. 1999)(Levy and Marshall 2004). Heath *et al* have demonstrated that FabI is the target of Triclosan in *S. aureus* (Heath et al. 2000). *E. coli* FabI specifically requires NADH whereas *S. aureus* FabI exhibits specific and positive co-operative binding of NADPH (Heath et al. 2000). *P. aeruginosa* is reported to be inherently resistant to triclosan as it possesses a non-susceptible enoyl reductase (Yu, Kim and Pan 2010). Bacterial growth is inhibited by blocking

lipid synthesis through inhibition of this reductase in susceptible bacteria (Yu, Kim and Pan 2010).

Escalada *et al* demonstrated though complete inhibition of fatty acid biosynthesis was achieved via triclosan's targeting of enoyl reductase, significant reductions in viable bacterial counts were not recorded (Escalada et al. 2005). The action of triclosan at the concentrations employed was therefore bacteriostatic, though long-term prevention of lipid synthesis would result in bacterial death (Escalada et al. 2005). If inhibition of fatty acid synthesis is the primary target of triclosan, when complete inhibition of fatty acid synthesis by triclosan was demonstrated by Escalada *et al*, this did not correlate to a bactericidal effect but rather to a bacteriostatic effect prompting Escalada *et al* to suggest that triclosan possesses another as yet un-determined bactericidal mechanism of action, un-connected to fatty acid biosynthesis (Escalada et al. 2005).

A.D. Russell attributed triclosan to have more than one mechanism of action due to its biocide nature (Russell 2004)(Russell 2004). Other research groups have proposed that the antibacterial action of triclosan is due to more than inhibition of *fabI* (Yu, Kim and Pan 2010). Suller *et al* showed logarithmic and stationary phases in *S. aureus* were equally sensitive to triclosan (Suller and Russell 2000). Were *fabI* the only triclosan target in the bacterium the logarithmic growth phase should have been more severely affected than every other phase of bacterial growth and this was clearly shown not to be the case (Suller and Russell 2000). Other studies have proposed the action of triclosan is due in part to its effect on bacterial membranes, where triclosan was incorporated into phospholipid membranes interacting with them without inducing lysis but resulting in the formation of perturbed membrane structures, this usually occuring at higher triclosan concentrations (Russell 2002)(Russell 2003)(Russell 2003)(Villalaín et al.

2001). Triclosan has also been shown to inhibit F-ATPase, glycolytic enzymes, transmembrane protein carriers and biofilm formation in oral bacteria (Yu, Kim and Pan 2010).

1.3.2.3 Mechanisms of bacterial resistance to triclosan

Bacterial resistance mechanisms to biocides include changes in permeability of bacterial membranes; resulting in decreased concentration of biocide entering the cells and increased bacterial efflux that reduces biocide concentration in the cytoplasm (Russell 2003)(Russell 2003). Efflux pumps are transport proteins that remove toxic substrates from within cells to the external environment. These proteins are found in Gram-negative and Gram-positive bacteria and may be specific for one substrate or may transport structurally dissimilar compounds. As antibiotic sensitive as well as resistant bacteria carry and express genes encoding efflux transporters it is possible that the pumps arose so that noxious substances could be transported out of the organism permitting survival.

Biocide resistance through mutation of target sites is unusual but triclosan's activity at low concentrations is through inhibition of *fabI*; therefore mutation or over expression of this gene could lead to the development of resistance (Russell 2003). Bacteria develop triclosan resistance through target mutations, enzymatic modification and active efflux (Chuanchuen, Karkhoff-Schweizer and Schweizer 2003). The presence of a *fabI* homologue is responsible for resistance to triclosan in *S. aureus* (Tkachenko et al. 2007). The high triclosan resistance level of *P. aeruginosa* has been attributed to its constitutive MexAB-OprM efflux system (Champlin et al. 2005). Development of triclosan resistance in *E. coli* is through up-regulation of RND efflux pumps or mutation of *fabI* (McBain and Gilbert 2001).

1.3.2.4 Triclosan use and cross resistance to antibiotics

The potential for cross resistance to develop occurs when the same target is attacked by different anti-microbial agents, when two agents initiate a common pathway to cell death, or when antimicrobials share a common route of access to different targets (Chapman 2003). Chuanchuen *et al* described exposure of *P. aeruginosa* to triclosan that resulted in the development of a high level of resistance not only to triclosan but also to ciprofloxacin through induction of expression of a multi drug efflux pump (Chuanchuen, Karkhoff-Schweizer and Schweizer 2003). By whatever means cross-resistance is achieved the end result is identical; the development of resistance to a particular antibacterial agent is co-joined to resistance being displayed to another agent (Chapman 2003).

Triclosan is a biocide that has been implicated as a possible cause for the selection and persistence of bacterial strains with low-level antibiotic resistance (Russell 2002). The development of cross-resistance between triclosan and antibiotics through utilisation of target mutations, enzymatic modification and active efflux has been demonstrated in bacteria under laboratory conditions (Schweizer 2001). A recent community based clinical trial examined biocide usage and development of antimicrobial resistance in bacteria (Carson et al. 2008). At baseline Carson *et al* demonstrated no significant association between high triclosan MICs and high benzalkonium chloride (BZK) MICs for any bacteria tested. After completion of the one-year study their data showed a significant association in community isolates of high BZK MICs, high triclosan MICs and resistance to one or more antibiotics. The selective pressure of biocides on bacteria has the potential to result in the co-selection of genes, which could bestow reduced susceptibility to both biocides and antibiotics (Carson et al. 2008).

Cottell *et al* in their 2009 study demonstrated increased susceptibility to aminoglycosides by triclosan tolerant *E. coli*. The authors speculated the link between triclosan tolerance and aminoglycoside susceptibility in *E. coli,* as attributable to plasmid loss or changes in outer bacterial membranes (Cottell et al. 2009). Increased tolerance to antibiotics such as gentamicin and quinolones has been shown in triclosan tolerant *S. aureus* (Cottell et al. 2009). Tkachenko *et al* credit alteration in structural and functional proteins of bacterial cell membranes with triclosan/ciprofloxacin resistance in *S. aureus* (Tkachenko et al. 2007).

1.3.2.5 Triclosan toxicity

Triclosan has been shown to possess a favourable mammalian safety profile (Liu et al. 2009)(Jones et al. 2000)(Escalada et al. 2005). Though triclosan's efficacy in preventing gingivitis through incorporation in toothpaste has been demonstrated (Focus on Surfactants 2010a) (Focus on Surfactants 2010b), infrequent incidents of immuno- and neurotoxic reactions have been reported (Latosińska, Tomczak and Kasprzak 2008).

Reported concentrations of triclosan in human breast milk have varied from 0 up to 2100 µg/kg lipid (Paul et al. 2010). Other noted triclosan side effects include interactions with thyroid hormones and skin irritations (Latosińska, Tomczak and Kasprzak 2008). In 2010 an animal study conducted by Paul *et al* reported reduced levels of thyroxine and triiodothyronine after exposure to triclosan (Paul et al. 2010). Reports of interactions with human pregnane X receptor, P450-dependent enzymes and UDP-glucuronosyltransferases by triclosan also exist (Krishnan et al. 2010). Inhibition of a type I fatty acid synthase in breast cancer cells by triclosan has been described (Escalada et al. 2005).

Laboratory studies conducted by Ciba Speciality Chemicals have identified the mineralization half-life of triclosan varies between 15 – 35 days (Thompson et al.

2005). Combined with the efficiency of UK water treatment plants in triclosan removal from waste water ranging from 58-98%, there is a potential for significant triclosan exposure for all living organisms (Thompson et al. 2005). Given the very polar nature of triclosan, bioaccumulation of the diphenyl ether is likely (Thompson et al. 2005). The long term significance, if any of these various interactions by triclosan on humans remain to be unequivocally determined (Krishnan et al. 2010).

1.3.3 Colistin

Colistin is marketed as colistin sulphate for oral and topical use and as colistimethate sodium (an inactive pro-drug) for parenteral and inhalation administration (Maviglia, Nestorini and Pennisi 2009). The polypeptide was discovered in 1949 and used clinically from the 1950s (Montero et al. 2009). Colistin, also known as polymyxin E, is a decapeptide antibiotic with an antimicrobial spectrum which includes Gram-negative bacteria (Falagas and Michalopoulos 2006). Narrow spectrum of activity coupled with a rapid concentration dependent bactericidal onset of action against most Gram-negative aerobic bacilli are colistin's best attributes (Maviglia, Nestorini and Pennisi 2009). Colistin is not active against Gram-positive bacteria or anaerobes (Falagas, Rafailidis and Matthaiou 2010)(Falagas et al. 2010). Knowledge of the effect of colistin on bacteria is lacking as licensing bodies such as the Medicines and Healthcare Regulatory Agency (MHRA) were not in existence and the body of microbiological and pharmacological evidence that would have to be submitted nowadays in order to license an antibiotic simply was not required (Nation and Li 2009).

1.3.3.1 Mechanism of action of colistin

Colistin exerts a bactericidal effect on bacteria by permeabilizing the outer Gram-negative bacterial membrane (Vaara 2010). Colistin binds to and de-stabilizes the lipopolysaccharide (LPS) layer by displacing the calcium and magnesium bridges, entering the bacterium through the self-promoted uptake pathway (Zavascki et al. 2007). Thus neither diffusion nor any transport mechanism is required by colistin to reach the bacterial cytoplasmic membrane, upon which colistin exerts its bactericidal effect through a surface detergent mechanism of action (Nasnas, Saliba and Hallak 2009). This results in leakage of cell components and subsequent cell death (Maviglia, Nestorini and Pennisi 2009). Colistin has also demonstrated bactericidal activity through inhibition of cell growth, at concentrations far lower than those required for breaching membrane permeability, through as yet unknown mechanism of action (Maviglia, Nestorini and Pennisi 2009).

1.3.3.2 Resistance to colistin

The reason multi-drug resistant Gram-negative bacteria have not acquired any significant degree of colistin resistance to date is very probably due to the infrequent clinical use of polymyxins over the last few decades (Zavascki et al. 2007). Not only is resistance to colistin seldom seen, it appears as a result of chromosomal mutation which is manifested as decreased permeability of the bacterial wall to colistin (Nasnas, Saliba and Hallak 2009). Modification of the outer bacterial membrane structure is the most significant resistance mechanism to colistin (Falagas, Rafailidis and Matthaiou 2010)(Falagas et al. 2010)(Falagas and Michalopoulos 2006). These LPS modifications prevent or reduce the initial interaction between the Gram-negative bacterium and colistin. *P. aeruginosa* and *E. coli* modify lipid A reducing the overall net negative LPS charge, hence reducing colistin binding and increasing resistance to the antimicrobial (Zavascki et al.

2007). As this resistance mechanism compromises the normal functioning of the outer bacterial membrane, permeability of other antimicrobial agents may be enhanced (Vaara 2010). Plasmid mediated resistance has not been reported to date for colistin (Nasnas, Saliba and Hallak 2009).

Global resistance to colistin is generally less than 10%, however certain areas such as Korea and Singapore exhibit higher resistance levels (Falagas, Rafailidis and Matthaiou 2010). A report in 2010 from Milne *et al* noted a 16% resistance rate to colistin amongst cystic fibrosis patients in Scotland (Milne and Gould 2010). Concerns have been raised that sub-optimal colistin dosing is responsible for the development of resistance to the polymyxin agent (Rattanaumpawan, Ungprasert and Thamlikitkul 2011).

1.3.3.3 Therapeutic doses and risk factors

A 2010 study examining colistin use over a 12-month period gave the median duration of therapy and cumulative dose of IV colistin to onset of nephrotoxicity as 7 days and 1200mg respectively (Rattanaumpawan, Ungprasert and Thamlikitkul 2011). The authors also list a number of independent risk factors in the development of nephrotoxicity to be considered with colistin use, notably; concomitant use of vancomycin, old age and long duration coupled with high IV colistin doses (Rattanaumpawan, Ungprasert and Thamlikitkul 2011).

1.3.3.4 Colistin toxicity

As previously mentioned the clinical use of colistin was largely abandoned due to perceived toxicity problems. The most serious reported toxicity was renal damage, which may be explained by the extensive tubular re-absorption of colistin, leading to the accumulation of and subsequent damage by the polymyxin to the renal proximal tubular cells (Vaara 2010).

A recent retrospective review of patients treated with intravenous colistin in a Beirut hospital identified no renal failure or major neurological toxicity under treatment (Nasnas, Saliba and Hallak 2009). The average cumulative dose of colistin administered to patients during this study was 86 x 10^6 international units, with durations of treatment ranging from 16 to 65 days (Nasnas, Saliba and Hallak 2009). A systematic review of colistin use has shown higher reported rates of nephrotoxicity in studies undertaken prior to 1995 compared to those carried out after 1995 (Hartzell et al. 2009). This could be partly attributed to impairment in renal function being defined by different standards, chemical impurities in the earlier synthesis of colistin, better modern critical care unit monitoring of patients in conjunction with non-administration of concurrent known nephrotoxic medication (Falagas and Rafailidis 2009)(Falagas et al. 2010).

Hartzell *et al* identified that it is the total cumulative dose of colistin that is associated with nephrotoxicity, therefore shortening the duration of colistin administration should reduce the rate at which nephrotoxicity develops (Hartzell et al. 2009).

1.3.3.5 Colistin anti-endotoxic activity

Death or division of bacteria can result in release of lipopolysaccharide (LPS) from the surface of bacteria into the bloodstream of the host. This can be a potent stimulus for the activation of an immune response leading to sepsis and septic shock with potentially fatal consequences for the patient (Gutsmann, T. 2005). Sepsis is the response of the body to infection, which can deteriorate to an uncontrolled immunological reaction with the potential to result in multiple organ failure and death from septic shock (Giuliani, Pirri and Rinaldi 2010).

Some antibiotics kill bacteria while simultaneously facilitating unwanted release of endotoxin, but cannot bind or neutralise endotoxin (Gutsmann et al. 2005).

Endotoxin is responsible for >2% of total hospital admissions annually in the US and >400,000 deaths there per year (Zhang and Falla 2006). Polymyxins B and E are the only antibiotics in current clinical use that can bind and neutralise endotoxin (Nasnas, Saliba and Hallak 2009).

A two-step approach is thought to be the mechanism by which colistin binds to LPS; the correct orientation and position of polymyxin and LPS is achieved through electrostatic interaction of the positively charged polymyxin ring followed by binding of the polymyxin hydrophobic acyl chain to the non-polar centre of the LPS lamellar phase (Davies and Cohen 2011, Davies and Maillard 2001).

Japan has been using a specially designed polymyxin column for use in patients suffering from severe sepsis since 1994 (Davies and Cohen 2011). The polymyxin is attached to polystyrene fibres in the column via covalent bonding; blood is passed through the cartridge and LPS is removed through binding to the polymyxin via the remaining charged amino acid groups (Davies and Cohen 2011). Despite widespread clinical use of endotoxin removal devices in Japan, lack of efficacy from clinical trials for these devices has meant worldwide adoption of this procedure has not yet occurred, however further clinical trials are on going (Davies and Cohen 2011).

1.3.4 Cationic Antimicrobial Peptides (CAPs)

1.3.4.1 CAPs

CAPs, once recognised as nature's antibiotics are now regarded as promising candidates for development as novel antimicrobials (Hale and Hancock 2007). The presence of CAPs has been identified in practically every living entity, ranging from bacteria to humankind (Hale and Hancock 2007). More than 1000 natural cationic peptides have been identified while many others possessing equivalent spectrums

of activity as their natural counterparts, have been synthesised (Hale and Hancock 2007). CAPs are broad-spectrum antimicrobials, active against Gram-positive and Gram-negative bacteria, viruses, fungi and parasites (Zhang and Falla 2006)(Zaiou 2007).

CAPs enter Gram-negative bacterial cells in a similar manner to colistin, through the self-promoted uptake pathway (Hancock and Sahl 2006, Hancock and Chapple 1999). Evidence indicates that antimicrobial peptides such as α and β defensins and cathelicidins, link the innate with the acquired immune response (Lupetti et al. 2003). Compared to the acquired immune response, the constitutively expressed or induced endogenous CAPs provide a fast response to bacterial invasion (Reddy, Yedery and Aranha 2004)(Hale and Hancock 2007).

John K. Spitznagel and colleagues were pioneers in 1963 for the quest for antimicrobial proteins and studied the polymorphonuclear leukocyte (PMN). They showed that there were a number of cationic antimicrobial proteins associated with the granules of PMN that coated bacteria during phagocytosis. Little research in the area of CAPs was conducted until the 1980s, when technology was sufficiently developed to permit investigators to isolate, purify and sequence these proteins. The identification of proteins with antimicrobial activity from PMN such as the α defensins was instrumental in moving this field forward (Pereira 2006).

1.3.4.2 CAP Composition

CAPs are gene-encoded, ribosomally synthesised polypeptides that diffuse rapidly into cells due to their small size and quickly neutralise a broad range of microorganisms (Perron, Zasloff and Bell 2005)(Hale and Hancock 2007)(Papagianni 2003)(Reddy, Yedery and Aranha 2004). CAPs are generally composed of between 12 – 50 amino acids; possess an overall positive charge between +2 to +9 and are hydrophobic (Hale and Hancock 2007)(Hancock and Sahl

2006). CAPs can be classified into five major types namely; α-helical, β-sheet, looped, extended and cyclic (Hancock and Sahl 2006)(Zhang and Falla 2006). Primary and secondary structures display variability but CAPs display common structural arrangement at tertiary level, through the formation of amphiphilic molecules with the segregation into groups of charged (polar) and hydrophobic residues on membrane interaction (Hale and Hancock 2007)(Papagianni 2003).

1.3.4.3 CAP mechanisms of action

CAPs can be divided into membrane lytic and non-membrane lytic agents (Zhang and Falla 2006). Membrane lysis is induced via several recognised modes of action; barrel stave, carpet, toroidal and aggregate models (Hale and Hancock 2007)(Reddy, Yedery and Aranha 2004)(Brogden 2005).

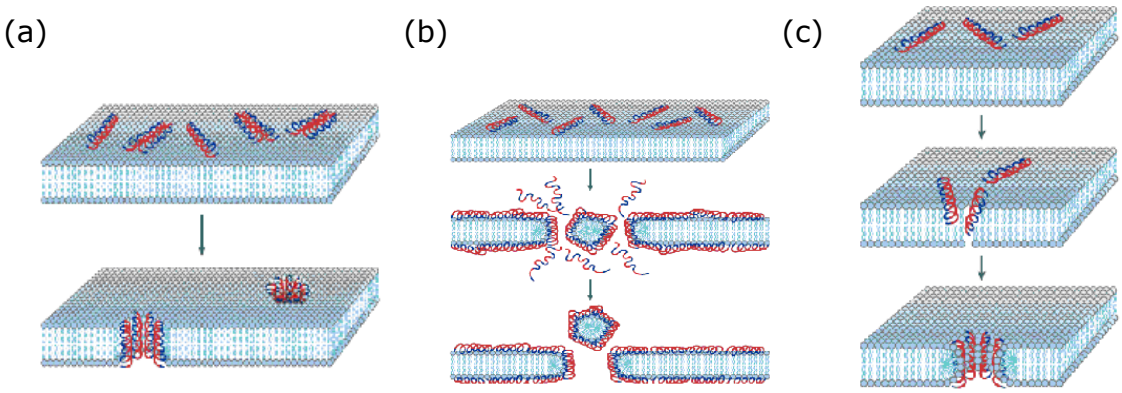

Figure 1.2 (a) barrel stave, (b) carpet and (c) toroidal models. Adapted from (Brogden 2005)

It has been suggested that all CAPs can induce membrane perturbation if the concentration employed is higher than a physiologically relevant one (Hale and Hancock 2007). Similar mechanisms of action have been observed for non-membrane lytic agents and sub-MIC concentrations of membrane lytic agents, through interference of cell division, inhibiting synthesis of intracellular macromolecules and disruption of gene regulation (Hale and Hancock 2007)(Zhang

and Falla 2006). Activation of autolytic enzymes, inhibition of DNA and protein synthesis has also been recorded (Zaiou 2007)(Reddy, Yedery and Aranha 2004). CAPs have been shown to form ion channels through which loss of K^+ and other cellular components are induced (Reddy, Yedery and Aranha 2004). CAPs also possess non-antimicrobial activities, including reduction in inflammation and promoting wound healing (Zhang and Falla 2006). Chemokine like activities through binding of CAPs with some chemokine receptors have also been recorded (Zaiou 2007).

1.3.4.4 CAP regulation in the human body

Six α defensins have been identified in humans; human neutrophil proteins 1-4 (HNP1-4) are predominantly produced by granulocytes and certain leukocytes and function as danger signals at concentrations well below those required for their antimicrobial action (Kim and Kaufmann 2006). Micromolar concentrations of α defensins are necessary to disrupt bacterial membranes, inhibit activation of NADPH or interact with complement compared to nanomolar concentrations of α defensins necessary for chemotactic, mitogenic and corticostatic activities (Yang et al. 2000)(Yang et al. 2010).

The concentration of HNP1-3 in plasma under normal physiological conditions is approximately 40 ng ml^{-1} but can rise to 0.9-170 µg ml^{-1} during severe infections on stimulation of their production (Kim and Kaufmann 2006). Evidence suggests the antimicrobial activity of HNP1-3 is effected through binding to specific bacterial receptors rather than permeabilising bacterial membranes (Kim and Kaufmann 2006). HNP1-3 promote wound healing by stimulating cell proliferation and have been shown to neutralize toxins secreted by bacterial pathogens including lethal factor from *Bacillus anthracis* (Kim and Kaufmann 2006). HNP1-3 also block the fibrinolytic activities of staphylokinase produced by *S. aureus* by binding to the

Lys74 position of staphylokinase used in interaction with human plasminogen (Kim and Kaufmann 2006).

1.3.4.5 Resistance to CAPs

There are very few naturally peptide-resistant organisms such as *Burkholderia*, *Proteus* and *Serratia* species (Hale and Hancock 2007)(Marr, Gooderham and Hancock 2006). The development of resistance to CAPs that are, and have been, effective in tackling bacterial infections in humans for 10^8 years, seems remote (Perron, Zasloff and Bell 2005). The huge variety of CAPs in the human body together with the obligatory interaction of these peptides with the bacterial cytoplasmic membrane plus the multiple CAP targets within cells, challenges bacterial machinery on many levels before resistance to CAPs can occur (Perron, Zasloff and Bell 2005).

Some resistance mechanisms have been described (Marr, Gooderham and Hancock 2006). However the resulting recorded increase in resistance was only two to four-fold, with no general peptide cross-resistance mechanism in existence whereby bacteria are resistant to every single peptide, probably as a result of CAP diversity (Marr, Gooderham and Hancock 2006). Certain bacteria such as *S. aureus* and *P. aeruginosa* have reduced their sensitivy to CAPs through increased incorporation of positively charged protein in their membranes, thereby reducing the overall net negative charge (Brogden 2005). Bacteria have developed resistance to CAPs by production of proteolytic enzymes; for example, cathelecidin LL-37 is cleaved and inactivated by a *S. aureus* metalloproteinase, termed aureolysin (Brogden 2005).

Active efflux, trapping proteins and modification of host cellular processes are other resistance mechanisms elucidated through experimental investigations (Zaiou 2007). Bader *et al* in 2005 have raised the possibility that intracellular pathogens can tap into the innate immune program of their host and trigger a defence system

that gives resistance to CAPs as well as other virulence traits (Bader et al. 2005). One of the most significant ways in which pathogens assess host environments is through their two-component regulatory systems; Bishop *et al* in 2005 showed the PhoP-PhoQ system of *Salmonella* is activated by binding to CAPs and in doing so gene transcription necessary for *Salmonella* survival within the human or mouse host is promoted (Bishop and Finlay 2006). Perron *et al* in 2005 documented the experimental evolution of resistance to a CAP known as pexiganan, by growing bacterial colonies in continuously increasing CAP concentrations for 600/700 generations under laboratory conditions (Perron, Zasloff and Bell 2005).

Other experimental work has shown that 30 passages in sub-MIC peptide concentrations was necessary to increase resistance in *Ps. aeruginosa* by two- to four-fold i.e. from 8 to 16 µg/ml or 16 to 64 µg/ml (Zhang et al. 2005)(Marr, Gooderham and Hancock 2006). Under the same conditions resistance to the aminoglycoside antibiotic gentamicin increased by 190-fold or from 0.5 to 90 µg/ml (Steinberg et al. 1997)(Marr, Gooderham and Hancock 2006).

Resistance evolution however is linked to the extent of exposure as has been seen with naturally occurring antibiotics such as penicillins and streptomycin, bacterial resistance to these antibiotics was low when their widespread clinical use began in the 1940's, whereas nowadays resistant strains are commonplace (Buckling and Brockhurst 2005). The bactericidal nature of CAPs plus their diverse mechanisms of action are the reasons quoted by many for a low frequency of resistance to CAPs emerging (Zhang and Falla 2006) (Zhang and Falla 2010). Nonetheless, there is concern that the therapeutic use of CAPs could lead to the evolution of resistance and the subsequent possibility of cross-resistance to human defence peptides (Perron, Zasloff and Bell 2005).

1.3.4.6 Presence and absence of CAPs in the human body

Low levels of CAPs are associated with severe pathogenic conditions; people lacking α-defensins due to a specific granule deficiency syndrome suffer regular and severe bacterial infections (Zaiou 2007). Patients suffering from Morbus Kostmann condition are afflicted with frequent oral bacterial infections and severe periodontal disease due to a deficiency in human cathelicidin peptide LL-37 and human neutrophil peptides (HNP 1-3) (Zaiou 2007). Cathelicidins are also involved in protecting the gastric mucosa against *Helicobacter pylori*; down regulation of cathelicidin expression in colon epithelium by *Shigella* allows these cells to penetrate the mucosa (Schauber et al. 2006)(Schauber and Gallo 2008).

The skin scales of people suffering from psoriasis (a common immune mediated, chronic skin condition) contain several CAPs, which are credited with protecting the inflamed skin from infections as psoriasis sufferers rarely suffer from skin infections (Harder 2008)(Zaiou 2007). Some peptides are salt sensitive and under physiological conditions lose their antibacterial activity; this has important implications for certain patients, in particular cystic fibrosis patients, where increased salinity of the broncho-pulmonary fluid is due to the defective chloride channel causing the disease. The subsequent impairment of the β-defensin bactericidal activity against *P. aeruginosa,* results in persistent chronic lung infections caused by the bacterium in these patients (Marr, Gooderham and Hancock 2006).

Crohn's disease and ulcerative colitis are chronic inflammatory bowel diseases; the pathology of Crohn's disease is due in part to diminished levels of human α-defensins, while ulcerative colitis is considered to be partly due to the inability of CAPs to cope with pathogenic bacteria in the intestine (Zaiou 2007).

1.3.4.7 Synthetic CAPs

As previously mentioned synthetic CAPs have been shown to possess equivalent spectrums of activity as naturally occurring CAPs. Appelt *et al* formulated a set of non-peptide compounds possessing antimicrobial activity based on 3D structures of natural CAPs (Appelt et al. 2007). All of the compounds they formulated exhibited antibacterial activity using the carpet model mode of membrane permeabilization and the activity of the synthetic non-peptide compounds matched that of the original CAPs, prompting them to propose that CAP activity is due to the precise arrangement of relevant functional groups and not to the inherent CAP peptidic nature (Appelt et al. 2007).

They further demonstrated experimentally that the peptide backbone acted as scaffolding, allowing appropriate orientation of the side chains of the amino acids, while a sufficient number of indole rings and guanidinium groups was critical for antimicrobial activity (Appelt et al. 2007).

Activity was also linked to distance between the charged groups and the aromatic rings as compounds with pentane chains demonstrated far superior antimicrobial activity compared to compounds with ethane linkers (Appelt et al. 2007). Fluorinated versions of a potent amphibian CAP – pexiganan - were formulated by Marsh *et al* in 2007 (Ritter 2007). The purpose of this was to enhance the stability of CAPs and enhance CAP efficacy as antibiotics for systemic delivery (Ritter 2007). The resulting fluorinated CAPs were significantly more stable than the non-fluorinated versions, when subjected to thermal and chemical denaturation (Ritter 2007). This experimental work has delivered a huge boost to CAPs and their potential uses as systemically deliverable, site-specific human medicines (Ritter 2007).

1.3.4.8 CAP detractions

Susceptibility to proteases, short half-lives, stability issues, loss of activity under physiological conditions, unwanted systemic side effects and high production costs are some of the problems associated with development of CAP therapeutics (Zhang and Falla 2006)(Zhang and Falla 2010)(Zaiou 2007). CAP limitations include cytotoxicity, the higher the antimicrobial activity the more acute the toxicity, as exemplified by the gramicidins; while the less toxic CAPs, though potential compounds for treating systemic infections, do not possess very high *in vitro* antimicrobial activity compared to conventional antibiotics (Deming 2007).

1.3.4.9 CAP applications

The range of biological roles of CAPs also includes endotoxin neutralization, chemokine–like activity and immuno-modulatory activities (Zaiou 2007)(Marr, Gooderham and Hancock 2006). Several CAPs including cathelicidin LL-37 have been shown to bind to and disrupt LPS aggregates and *in vitro* models have shown the ability of CAPs to suppress pro-inflammatory responses triggered by LPS. Therefore the development of these compounds could provide an excellent clinical tool for the treatment of Gram-negative sepsis (Giuliani, Pirri and Rinaldi 2010)(Pereira 2006). Initiation of therapy within one hour of diagnosis of septic shock in patients is believed to be a critical requirement to promote their survival (Ewig 2011). Death from septic shock in US Critical Care Units has been shown to exceed 60% with an estimated cost per year of $16.7 billion (Giuliani, Pirri and Rinaldi 2010).

1.3.4.10 Vehicles for the delivery of CAP therapeutics for clinical use

Several CAP based therapies are currently under development or undergoing clinical trials, for example talactoferrin which is in Phase II development as first line treatment of advanced non-small cell lung cancer for combined clinical use with

chemotherapy (Zhang and Falla 2006). As previously mentioned the main problems associated with the development of CAPs as therapeutic agents are, degradation by proteases, un-wanted systemic side effects and loss of efficacy under physiological conditions (Zhang and Falla 2006)(Zaiou 2007). If used as topically active agents however these drawbacks are no longer significant. Not only do CAPs possess antimicrobial activity, some CAPs also exhibit anti-inflammatory and wound healing activities, making them ideal agents for treating chronic wounds (Zhang et al. 2005)(Zhang and Falla 2006).

A novel topical delivery system for the treatment of infected wounds is through targeted delivery of antimicrobials into the wound bed via lyophilised wafers. Freeze-drying polymer solutions, suspensions or gels produce lyophilised wafers (Matthews et al. 2008). Studies have shown that lyophilised wafers act as stable and effective vehicles for the delivery of insoluble therapeutic agents to wound beds (Matthews et al. 2005). The release rate of the incorporated therapeutic agent is dependent on the polymer selected for use and once in use, the rheological properties of the gel state (Matthews et al. 2008)(Matthews et al. 2006). Should lyophilised wafers prove to be a compatible and effective vehicle for the topical delivery of CAPs for the treatment of infected wounds, this could offer a huge therapeutic treatment application for CAPs.

1.4 Project Aims: Investigation of cationic antibacterial agents

Two antimicrobial agents in current clinical use, namely triclosan and colistin, as well as two novel CAPs, NP101 and NP108 were selected for investigation in this study. As agreed with Novabiotics, information as regards structure and composition of NP101 and NP108 will not be discussed. Triclosan has been shown to be active against Gram positive and Gram negative bacteria whilst colistin is

reputedly active against Gram negative but not Gran positive bacteria and the spectrum of activity of NP101 and NP108 is unknown. Three bacterial species, *Escherichia coli*, *Staphylococcus aureus* and *Pseudomonas aeruginosa* were selected to assess the antimicrobial activity of each of these agents and to observe effects exerted by each antimicrobial agent on actively growing cultures of each bacterial species, to elucidate mechanisms of action of each agent.

Triclosan and colistin have both been attributed as being membrane active agents and NP101 and NP108 being CAPs; which as a group are all reported to be membrane active; these novel CAPs will be investigated for the exhibition of this mechanism of action. Quantification of potassium loss from each bacterial species induced by incubation with concentrations ranging from sub to supra MIC of each antimicrobial will be undertaken.

If the novel CAPs display antimicrobial efficacy against Gram positive and negative species, the use of lyophilised wafers as a vehicle permitting their use as topical antimicrobial agents for the treatment of infected wounds will then be undertaken.

1.5 Objectives of the present study

The objectives of the present study were as follows:

i. To quantitatively assess the antibacterial activity of triclosan, colistin and two developmental synthetic cationic antimicrobial peptides NP101 and NP108 against *Escherichia coli*, *Pseudomonas aeruginosa* and *Staphylococcus aureus* (Chapter 3).

ii. To seek to examine the activity of these test antimicrobial agents upon the cytoplasmic membrane of the selected bacteria, through quantification of potassium loss when exposed to the antimicrobials (Chapter 4).

iii. To assess via flow cytometry putative changes in the dynamics of bacterial cell viability as well as analysis of population responses when exposed to triclosan, colistin, NP101 and NP108 (Chapter 5).

iv. To examine via scanning electron microscopy effects upon test bacterial populations post incubation with triclosan, colistin, NP101 and NP108, specifically examining for any induced changes of bacterial morphology (Chapter 6).

v. To evaluate potential of the synthetic CAPs as topical antimicrobials through formulation within antimicrobial wafers. (Chapter 7).

Chapter Two

Materials and Methods

2.1 Chemicals and reagents

2.1.1 Antibacterial chemicals

Triclosan was obtained from Ciba Speciality Chemicals (Grenzach-Wyhlen, Germany) as Irgasan DP 300. Colistin sulphate was purchased from Sigma (Sigma-Aldrich Company Ltd., Poole, UK.) Antimicrobial peptides NP101 and NP108 were kindly supplied by NovaBiotics (Novabiotics Ltd., Craibstone, Aberdeen, AB21 9TR, Scotland.).

2.1.2 Growth media and bacterial diluents

Nutrient broth and agar were supplied by Oxoid Ltd. (Basingstoke, UK.) and all media was autoclaved at 121^{o}C for 15 minutes by moist heat sterilisation. Agarose was purchased from Fisher Scientific UK Ltd. (Loughborough, UK.) and was autoclaved at 121^{o}C for 15 minutes by moist heat sterilisation. General-purpose grade NaCl 0.9% was obtained in crystalline form from Fisher Scientific UK Ltd. (Loughborough, UK.). Phosphate buffered saline (PBS) tablets were purchased from Sigma.

2.1.3 Miscellaneous chemical compounds

Potassium dihydrogen orthophosphate SLR and glutaraldehyde were purchased from Fisons Scientific Apparatus (Loughborough, Leics, England). Sodium carbonate in crystalline form was obtained from British Drug House (BDH), (Poole, UK.). Acetone (technical grade reagent), formaldehyde, sodium dodecyl sulphate, chlorhexidine digluconate 20% and propidium iodide dye were obtained from Fisher

Scientific UK Ltd. Isopropanol (99+%), dimethyl sulphoxide (DMSO), guar gum and sodium phosphate were obtained from Sigma-Aldrich Company Ltd. Ethanol was purchased from Hayman Ltd. (Witham, UK.). Polyanetholesulfonic acid sodium salt (PASA) was kindly supplied by Novabiotics.

2.1.4 Fluorescent dyes

The LIVE/DEAD Bac*Light*™ Kit and sytox green 5 mM dye were purchased from Molecular Probes ((Invitrogen Ltd., Paisley, UK.).

2.1.5 Laboratory equipment

All plastic sterile disposable equipment was bought from Fisher Scientific. Plastic tips and 1.5 ml micro centrifuge tubes were sterilised by autoclaving at 134 ^{o}C for 3¼ minutes as a porous load. All glassware was sterilised at 160 ^{o}C for 2 hours by dry heat sterilisation.

2.2 Bacterial storage and sub-culture

2.2.1 Bacterial strains

Pseudomonas aeruginosa NCTC 6750, *Escherichia coli* NCTC 4174 and *Staphylococcus aureus* NCTC 6571 were obtained from the National Collection of Type Cultures (NCTC, Porton Down, Salisbury, UK.).

2.2.2 Bacterial storage

Bacteria were stored in Protect Bacterial Preservers (Technical Service Consultants Ltd., Lancashire, UK.) at –80 ^{o}C (Upright freezer TS80-140; Life Sciences International, Colchester, UK.).

2.2.3 Bacterial sub-culture

Organisms were sub-cultured by inoculating single beads from the appropriate Protect Bacterial Preserver into 10 ml aliquots of nutrient broth and incubating statically for 18 to 24 hours at 37 ^{o}C (Mark II proportional temperature controller; LEEC Ltd., Nottingham, UK.). Master plates were prepared by streaking a loopful of this overnight culture onto plates containing 20 ml of nutrient agar and incubating these statically for 18 to 24 hours at 37 ^{o}C. These master plates were stored at 4 ^{o}C (Hotpoint 'Iced Diamond' refrigerator; Indesit Company, Ancona, Italy.) and used to inoculate fresh plates each week for a maximum of four weeks. After this time the master plates were discarded and fresh Protect Bacterial Preserver Beads were taken from the freezer.

Bacterial stock cultures were sub-cultured weekly by streaking out onto nutrient agar and incubated at 37 ^{o}C for 24 hours in a static incubator, these stock plates stored at 4 ^{o}C until discarded. A single colony from this plate was used to prepare broth cultures daily. These were prepared by aseptically transferring the bacterial colony into a 250 ml Erlenmeyer conical flask containing 100 ml of sterile nutrient broth. Flasks were incubated at 37 ^{o}C for 24 hours in an orbital incubator set at 100 rpm (1OX400.XX2.C; Sanyo Gallenkamp PLC, Loughborough, UK.).

2.3 Preparation of bacterial enumeration graphs

Graphs of optical density versus concentration of bacterial cells (colony forming unit per ml (cfu/ml)) were prepared by the following viable count dilution method.

2.3.1 Bacterial suspension preparation

One hundred ml of a 24-hour culture grown in nutrient broth was centrifuged at 4000 rpm for 10 minutes using an MSE Chilspin (Fisons, Loughborough, UK.). The

supernatant was carefully decanted and the pellet re-suspended in 5 ml of 0.9% (w/v) sodium chloride and re-centrifuged as previously described. The pellet was re-suspended in 5 ml of 0.9% (w/v) sodium chloride, from which cell concentrations were prepared by dilution, to yield seven suspensions ranging in absorbency from 0.1 to 0.2 at 500 nm, as determined by a Helios *E* spectrophotometer (Thermo Spectronic Corporation, Madison, US.).

2.3.2 Agar plate preparation

Fourteen nutrient agar plates (90 mm diameter with triple vents) were over dried by placing them upright with open lids in a sterile cabinet at room temperature (Horizontal Laminar Flow Cabinet 5HLF B/U; Hepaire Manufacturing Ltd., Avon, UK.) for one hour. The base of each plate was divided into four quadrants labelled for dilutions $1x10^{-5}$ down to $1x10^{-8}$.

2.3.3 Dilution of bacterial suspensions and plating out

Each of the seven suspensions prepared in Section 2.3.1 was diluted ten-fold in a step-wise manner in 0.9% (w/v) sodium chloride down to $1x10^{-8}$. Five aliquots of 20 μl were carefully pipetted onto each quadrant of a pre-dried agar plate, using dilutions 10^{-5}, 10^{-6}, 10^{-7} and 10^{-8} from each suspension. Duplicate agar plates were prepared for each suspension; the inoculated plates were inverted and statically incubated for 24 hours at 37 ^{o}C.

2.3.4 Determination of viable counts

All agar plates were examined post incubation and the level of bacterial growth was quantified by identifying the dilution yielding between 40-120 colonies. The colonies in all ten spots (from duplicate plates) were counted and a mean value calculated. The concentration of cells in the original culture (measured in cfu/ml) was then

calculated. A graph was plotted once the original cell density values were determined for all seven suspensions. Graphs were plotted for each bacterial strain and were used for all subsequent enumeration.

2.3.5 Determination of bacterial growth under oxygentated and non-oxygenated conditions

Four 250 ml Erlenmeyer conical flasks each containing 100 ml of $1x10^6$ cfu/ml test bacterial culture were prepared. Two of these flasks were incubated in a shaking water bath (DMS360, Fisher Scientific) at 37 ^oC and 150 revolutions per minute. The remaining two flasks were placed in an identical non-agitating water bath at 37 ^oC. One ml samples were obtained from each flask at 15-minute intervals over a nine-hour period and again at 24 hours. Each sample was pipetted into a sterile semi-micro cuvette and the absorbance at 650 nm read and recorded. Graphs of optical density versus time were then plotted for bacterial growth under each condition.

2.3.6 Preparation of agarose plates

2.3.6.1 Agarose pour plates

Antimicrobial peptides are known to interact and bind with polysaccharide in agar (personal communication Dr Derry Mercer 2010), which necessitated the identification of a suitable inert, but translucent solidifying agent to act as both a growth medium and a base for the determination of zones of growth inhibition produced by the peptide containing wafers. Literature sources identified agarose gel as a suitable base, so a 1.5% solution was prepared using sterile water and autoclaved. The sterile Petri dish was initially seeded with the bacterial culture to yield a final cell density of $1x10^6$ cfu/ml (approximately 30 μl of overnight culture)

to which was added 20 ml of a molten sterile suspension of agarose. The plates were allowed to set by placing them upright with partially open lids in a laminar airflow cabinet. The 2 cm diameter antimicrobial impregnated wafer to be tested was placed in the centre of the solidified agarose plate and this incubated at 37 ^{o}C for 24 hours. After incubation the plates were removed and the diameter of resulting zones of growth inhibition measured.

2.3.6.2 Agarose spread plates

A 1.5% solution was prepared using sterile water and autoclaved. Approximately 20 ml of agar was poured into each petri dish and allowed to set with partially open lids in a laminar airflow cabinet. A final cell density of $1x10^{6}$ cfu/ml (approximately 30 μl of overnight culture) of test bacterial culture was spread using a sterile glass spreader over the surface of the agarose plate. The 2 cm diameter antimicrobial impregnated wafer to be tested was placed in the centre of the spread agarose plate and this incubated at 37 ^{o}C for 24 hours. After incubation the plates were removed and the diameter of resulting zones of growth inhibition measured.

2.3.6.3 Determination of zones of inhibition

The initial diameter (D_0) of a circular control or antimicrobial wafer was measured by digital vernier callipers (Mitutoyo, Scottish Enterprise Technology Park, East Kilbride, Glasgow, Scotland), prior to placement of the wafer on the centre of a seeded or spread agarose plate. The plates were then incubated at 37 ^{o}C for 24 hours. The diameter of inhibition of the antimicrobial wafer was measured using a rigid steel engineering ruler (Mitutoyo) from one edge of the circular zone of inhibition to the other. The zone of inhibition was calculated by taking the average of two measurements of the diameter of the inhibition zone, measured at a 90^{o} angle to each other. The mean diameter of the inhibition zone is termed D_i. The

final swollen diameter of each wafer (D_t) was also measured after incubation using the steel ruler. Wafer expansion was calculated as the ratio of D_t/D_o. The antimicrobial activity of NP101 or NP108 was determined as an inhibition ratio (IR) of D_i/D_o.

2.4 Dissolution of antibacterials

2.4.1 Triclosan

A 5 mM triclosan stock solution was prepared in 0.1 M sodium carbonate. Triclosan was weighed in a glass weighing boat on a 4 place digital balance (Metter AE 50; Vitrium Ltd., Aberdeen, Scotland) and transferred to a 100 ml volumetric flask. 0.1 M Sodium carbonate was added, and the flask placed in an ultrasonic water bath (FS Minor, Decon Laboratories Ltd., Hove, UK.) for 10 minutes to aid dissolution. The triclosan stock solution was stored at 4 ^{o}C for up to 5 days. All subsequent dilutions of the 5 mM triclosan stock solution were prepared using 0.1 M sodium carbonate.

DMSO

An iso-osmotic concentration of DMSO was prepared by diluting 100% DMSO to a concentration of 1.96% (v/v) in sterile de-ionised water. Triclosan powder was weighed as described above, added to a volumetric flask and made up to volume using the iso-osmotic DMSO solution. The flask was placed in an ultrasonic water bath for 10 minutes to aid dissolution. The triclosan stock solution in DMSO was stored at 4 ^{o}C for up to 5 days.

2.4.2 Colistin and CAPs

Colistin and CAPs were weighed in a similar manner to triclosan, transferred to volumetric flasks and made up to required volume with sterile distilled water. Each

flask was placed in an ultrasonic water bath for 5 to 10 minutes to ensure total antibacterial dissolution. The colistin and CAPs stock solutions were stored at 4 ^{o}C for up to 5 days.

2.5 Determination of antimicrobial sensitivity

Minimum inhibitory concentrations (MICs) were determined using both macro and micro broth dilution techniques.

2.5.1 Preparation of micro-titre plates

The Versamax Microplate Reader (Molecular Devices Ltd., Wokingham, Berkshire, UK.) was optimised to read in a non-agitating mode every 30 minutes for 24-hours duration, at a wavelength of 650 nm. To avoid inaccurate results (due to formation of condensation on the plate seal) only the first eight columns of the micro-titre plate (96 well, gamma-irradiated; Bibby Sterilin Ltd., Stone, UK.) were utilised. A final volume of 200 µl was transferred into each well by multi-channel pipette (Transferpette-8; Brandtech Scientific Inc., Wertheim, Germany). Two hundred µl volumes of test agent were pipetted into each well of the first row of test rows C, D, E and F and negative control H. 100 µl aliquots of sterile distilled water were pipetted into each well of columns 2 to 8 of these rows. Transferring 100 µl volumes of solution from each well in column 1 to column 2 using a multi-channel pipette then performed a two-fold serial dilution. This process was repeated until column 8 where 100 µl volumes of solution were aspirated from the five wells and discarded. 100 µl of sterile double strength nutrient broth was then added to each well in row H. The test bacterial strain was sub-cultured, harvested and washed as described in Section 2.3.1. The bacterial concentration was adjusted to ~$2x10^8$ cfu/ml using the previously prepared enumeration graph. Immediately prior to inoculation the bacterial cell density was adjusted to ~$2x10^6$ cfu/ml by pipetting 0.2

ml of the ~2x10^8 cfu/ml bacterial suspension into 19.8 ml of 200/99 strength nutrient broth. All wells in columns 1 to 8 of test rows C, D, E, and F and row A (positive control) were then inoculated with 100 μl of this ~ 2 x 10^6 cfu/ml bacterial suspension using a multichannel pipette. A Gilson pipette (Anachem Ltd. Luton, UK.), was used to pipette 100 μl of sterile distilled water into each well of row A. The micro-titre plate was then sealed with an optically clear and gas-impermeable seal obtained from Fisher Scientific and incubated as described above.

2.5.2 Determination of minimum bactericidal concentration of test antibacterial

Once incubation of the micro-titre plate was completed, the gas tight seal was carefully removed and a 96-pin multi point replicator (140500 Boekel Scientific, Feasterville PA, US.) was used to check the bactericidal/bacteriostatic effect of varying concentrations of test antibacterial. One μl was transferred on the replicator pin tip from each micro-titre well and placed on the surface of a large 13.5 mm diameter nutrient agar plate, which was then inverted and incubated at 37 ^oC for 24 hours. After incubation the plate was checked for bacterial growth, confirming the effect of each concentration of test antibacterial employed.

2.6 Sensitisation/de-sensitisation of antibacterial

2.6.1 Sensitisation of *E. coli* to triclosan

The minimum inhibitory concentration (MIC) of *E. coli* NCTC 4174 1x10^6 cfu/ml against Triclosan was determined by macro and micro-broth assay. An Erlenmeyer flask containing a 1x10^6 cfu/ml *E. coli* culture in nutrient broth was incubated in the presence of the MIC of Triclosan for 24 hours in an orbital incubator. Macro and micro broth MIC assays of this culture against Triclosan were performed and the

culture was re-incubated for a further 72 hours (96 hours in total), with MICs repeated every 24 hours.

2.6.2 De-sensitisation of *E. coli* to triclosan

A $1x10^6$ cfu/ml *E. coli* culture in nutrient broth incubated (at 37 ^oC and 100 rpm) with the MIC of Triclosan for 24 hours was examined for de-sensitisation to the agent in the following way. 5 ml of the overnight suspension was aseptically transferred into 95 ml of fresh nutrient broth lacking triclosan in a 250 ml Erlenmeyer flask and incubated for 24 hours in an orbital incubator set at 100 rpm. A macro broth MIC assay was then performed on this culture. This *E. coli* strain was further de-sensitised to Triclosan by aseptically transferring 5 ml of this 24 hour de-sensitised suspension, into 95 ml of fresh nutrient broth and re-incubated for a further 24 hours. The previous step was repeated for a total of 5 x 24 hours de-sensitisation growth cycles and the MIC checked after every desensitisation cycle.

2.7 Assessment of loss of intracellular potassium

2.7.1 Calibration of the atomic emission spectrophotemeter

Assessment of internal potassium content of bacterial cells was undertaken on a flame atomic absorption spectrophotometer (Model AA3110, Perkin Elmer Las UK, Beaconsfield, UK.). The instrument mode was set for standard flame emission for detection of potassium at 766.5 nm, slit at 0.2/0.4 nm, powered by air/acetylene gas mixture (B.O.C., Worsley, Manchester, UK.). A stock solution containing 1000 $\mu g/cm^3$ potassium was prepared by diluting 1.907 g of potassium in 1000 ml of ultra pure deionised water. Five standards were prepared from this stock solution containing 1.0, 2.0, 3.0, 4.0, and 5.0 $\mu g/cm^3$ potassium, in polypropylene bottles (Azlon; Fisher Scientific). The five standards were used to calibrate the flame

photometer and the supernatant samples were processed once a correlation co-efficient of 0.998 was obtained. A one in ten dilution was performed on all samples reading 5.0 $\mu g/cm^3$ or higher in ultra pure de-ionised water. Graphs of percentage potassium loss versus time were then plotted.

2.7.2 Quantification of total intracellular bacterial potassium

One ml of overnight bacterial suspension was pipetted into each of four sterile 1.5 ml micro centrifuge tubes, inserted into a micro- centrifuge (Technico Maxi, Fisher Scientific) and spun at 14,000 rpm for 10 minutes. The supernatant was aspirated and the bacterial pellets re-suspended in sterile ultra pure de-ionised water and used to prepare 2 x 5 ml each of $1x10^6$ and $1x10^7$ cfu/ml cultures from previously prepared bacterial enumeration graphs, using sterile plastic centrifuge tubes. A one ml sample acting as control was removed from the centrifuge tube before sonication and plated out after serial dilution in normal saline to confirm bacterial density. The sonicator, a Misonix XL 2010 Ultrasonic Liquid Processor (Heat Systems, Farmingdale, NY, US.) was used at setting 10 to deliver 4 x 30 second sonication pulses to each test sample, paused after each 30 second sonication pulse to place the centrifuge tube on ice, both to cool the culture heated during sonication and to assist in rupturing the cells. One ml of the sonicated sample was pipetted into each of six sterile 1.5 ml micro centrifuge tubes and these were analysed for potassium content using a flame photometer. A duplicate check on bacterial viability was performed by serial dilution of one ml of each sonicated culture in 0.9 % sodium chloride, of which the $1x10^1$, $1x10^2$, $1x10^3$, and $1x10^4$ dilutions were plated out on agar, incubated at 37 ^oC for 24 hours and then examined for bacterial colonies.

2.7.3 Assessment of potassium content of bacterial samples

The test bacterial strain was sub-cultured, harvested and washed as described in Section 2.3.1. with final re-suspension of the bacterial pellet in sterile ultra pure de-ionised water. The bacterial concentration was adjusted to ~$1x10^6$ cfu/ml in de-ionised water using the previously prepared enumeration graph. A control flask was prepared for each test antibacterial concentration analysed. All potassium detection triclosan experiments employed DMSO as solvent and an equivalent concentration of DMSO was added to each control flask for every triclosan concentration analysed. Concentrations of test antibacterials analysed were $1/20^{th}$ MIC, MIC and either 2xMIC or 10xMIC, at a bacterial concentration of $1x10^6$ cfu/ml. All control and test cultures were prepared using high purity de-ionised water, in sterile polymethylpentene thermoplastic conical flasks (Nalgene; Fisher Scientific UK.), as potassium is known to adsorb to glass. The flasks were incubated in a shaking water bath (DMS360, Fisher Scientific) at 37 ^oC and 150 revolutions per minute. One ml samples were withdrawn at timed intervals, pipetted into sterile 1.5 ml sterile micro centrifuge tubes and centrifuged at 14,000 rpm for 60 seconds. The 1.5 ml sterile micro centrifuge tubes were carefully removed without disturbing the contents and 800 µl of supernatant aspirated and pipetted into sterile 1.5 ml sterile micro centrifuge tubes. Potassium content of the samples was then analysed via flame emission photometry.

2.8 Analysis of bacterial growth dynamics via flow cytometry

2.8.1 Calibration of flow cytometer

Prior to each experiment, the laser alignment was checked using Flow Check™ Fluorospheres and the test samples were processed once the half peak co-efficient variation (HPCV) was ≤ 2% on FL1, FL2, FL3 and FL4.

2.8.2 Preparation of bacterial samples for analysis

Flow cytometric analysis was undertaken using an Epics©XL MCL flow cytometer (Beckman Coulter United Kingdom Ltd., High Wycombe, Buckinghamshire, UK.). Sheath fluid, Flow Check™ Fluorospheres and all plastic disposable equipment was purchased from Beckman Coulter. Concentrations of test antibacterials analysed were $1/20^{th}$ MIC, MIC and either 2xMIC or 10xMIC, at a bacterial concentration of $1x10^6$ cfu/ml and all flasks were incubated at 37 ^oC in an orbital incubator. A control flask was prepared for each test antibacterial concentration analysed. The absorbance of the overnight culture was determined in a spectrophotometer blanked with nutrient broth at 500 nm and the cell density was calculated using the appropriate calibration curve. All cultures to be analysed were prepared in nutrient broth and incubated in an orbital incubator at 37 ^oC for 7 days. Samples were withdrawn at 24, 72 and 168 hours and prepared for analysis by flow cytometer using the LIVE/DEAD Bac*Light*™ Bacterial Viability and Counting Kit as per manufacturer's instructions. A live and dead control were prepared by centrifuging two 1ml samples of test overnight bacterial culture at 10,000 rpm for 3 minutes to pellet the cells; the supernatant was aspirated and one pellet was re-suspended in 1ml of 0.85% NaCl (live control), while the second pellet was re-suspended in 1 ml of 70% isopropyl alcohol (dead control). Both controls were incubated at room

temperature for 45 minutes and vigorously mixed every 15 minutes. The controls were centrifuged at 10,000 rpm for 3 minutes, then both controls were washed in 1 ml of 0.85% NaCl at 10,000rpm for 3 minutes and both controls were re-suspended in 1 ml of 0.85% NaCl. Each test bacterial culture whether control or bacteria incubated with either 1/20th MIC, MIC or 2/10xMIC of test antimicrobial were prepared for flow cytometry analysis as follows; 987 µl of 0.85% NaCl was pipetted into a sterile labelled micro-centrifuge tube, 1.5 µl of SYTO 9 and 1.5 µl of propidium iodide was pipetted into the micro-centrifuge tube and 10 µl of the required bacterial suspension was then added to the micro-centrifuge tube and incubated for 15 minutes at room temperature whilst protected from light, before being run on the flow cytometer. The bacterial sample to be analysed wass pipetted into a flow cytometer polystyrene tube and sufficient 0.9% NaCl is added to bring the sample volume to a minimum of 100 µl. A detection time of 300 seconds per sample was set in which to enumerate bacteria whilst a detection limit of 10,000 bacteria per sample was also invoked. Each flow cytometer tube was gently inverted prior to immediate analysis by the flow cytometer. Once the sample results had been obtained, overlay histograms of control, 1/20th MIC, MIC and 2 or 10xMIC were prepared using Beckman Coulter software.

2.8.3 Assessment of rejuvenation of bacterial cultures on de-sensitisation to antimicrobial peptides

After incubation of test bacteria with MIC or 2xMIC NP101 or NP108 for seven days, 5 ml suspension was aspirated from each control, MIC or 2xMIC flask and pipetted into 95 ml of fresh nutrient broth, which was then incubated for 24 hours. Samples were prepared for flow cytometric analysis as described in 2.8.1, to check for changes in bacterial growth dynamics once the antimicrobial peptide challenge had

been removed. These flasks were re-incubated at 37 ^{o}C for a total of 168 hours, with flow cytometry analysis every 24 hours.

2.9 Examination of bacterial morphology via Scanning Electron Microscopy (S.E.M.)

Bacterial cultures incubated for less than 24 hours employed 1x10^7 cfu/ml concentration for SEM analysis. Bacterial cultures incubated between 24 and 168 hours employed a 1x10^6 cfu/ml concentration. Cells were concentrated from an initial 10 ml sample volume to 2.5 ml final volume by a three-step centrifugation (each centrifugation step run at 10,000 rpm x 10 minutes) and re-suspension process using 0.1 M phosphate buffer. Cells were trapped on a sterile 0.2 µm Whatman nylon membrane filter (Camlab, Cambridge, UK.) contained within an autoclaved Swinnex re-usable filter holder (Merck Millipore, Darmstadt, Germany). Bacteria trapped on the membrane filter were fixed using 5% v/v glutaraldehyde in 0.1 M phosphate buffer (pH 7.4), which was left in contact with the monolayer for a minimum of 3 hours. The filter was then sequentially dehydrated for 20-minute intervals in 70, 80% (v/v in absolute alcohol) and 100% acetone. Filters were subsequently critically point dried in a Polaron critical point drier B7010 (Agar Scientific Ltd., Stansted, Essex, UK.), using acetone and CO_2, (B.O.C., Worsley, Manchester, UK.). The filters were mounted on aluminium stubs and sputter coated with a fine metal coating of gold (Gold Sputter Coater, aluminium stubs and gold metal coating – Polaron SC7640, Quorum Technologies Ltd., Ashford, Kent, UK.). Samples were analysed using a variable pressure scanning electron microscope (Leo S430 Scanning Electron Microscope, Carl Zeiss SMT Ltd., Cambridge, UK.).

2.10 Preparation of freeze dried antimicrobial wafers

2.10.1 Preparation of gels

Three gel batches were prepared using 2% guar gum (Sigma Aldrich) in distilled water; control, NP101 1.0 mg/ml (2xMIC) and NP108 0.5 mg/ml (2xMIC). The gels were mixed by propeller mixer (Heidolph RZR 2102, Cole-Parmer Instrument Co. Ltd, Hanwell, London, UK.), with the mixer speed initially set at 630 rpm and gradually increased to maximum speed of 2,000 rpm over 15 minutes, until a homogenous gel was formed.

2.10.2 Freeze drying process

Each gel was cast in a 12 well polystyrene plate (Costar, Sigma Aldrich) used as a mould for the freeze-drying process. Each well of diameter 2 cm contained 1.5 g ± 0.02 g of gel. Twenty-four wafers were prepared from each gel, control - containing only distilled water; NP101 wafers containing 14.71 mg of peptide per wafer and NP108 wafers containing 7.36 mg of peptide per wafer. The plates were then placed in a VirTis adVantage freeze drier (Biopharma Process Systems, Winchester, Hampshire, UK.) until the freeze drying cycle was completed after 24 hours. When the plates were removed these were sealed with parafilm (Fisher Scientific) and stored under cool, dry conditions.

2.10.3 Rheological analysis of gels

Analysis of guar gum flow and deformation was investigated by rheological measurements. Three samples of guar gum control, guar gum with NP101 and guar gum with NP108 were characterised by continuous flow rheometry at 25 ^{o}C. A cone and plate geometry was used (40 mm/ 2^{o} steel) and flow measurements were performed at continuous shear rates from 0 to 600 s^{-1} using a dynamic rheometer

(TA Instrument AR 1000, Nickel Electro Ltd. Weston-S-Mare, Somerset, UK.) The descending flow curves were analysed with the system software using the Herschel-Bulkley model given below;

$$\sigma = \eta'\gamma^n + \sigma_o$$

where σ = shear stress (Pa), η' = viscosity coefficient (Pa.s), γ = shear rate (s^{-1}), n = rate index of pseudoplasticity, σ_o = yield stress (Pa).

2.11 Statistical analysis

All statistical analysis was carried out using Minitab® 14 software (Minitab Inc., Philadelphia, PA, USA) and GraphPad Software (GraphPad Software, Inc., Inc., California, USA). Assumptions of normality and equal variances were confirmed using the Minitab and GraphPad software. Analyses of variance – ANOVA – were performed at 95% confidence interval. Levels of statistical significance were annotated on graphs and legends as follows: *p*-value < 0.05 *; *p*-value <0.01 **; *p*-value <0.001 *** or alternatively *p*-value < 0.05 $^{\#}$; *p*-value <0.01$^{\#\#}$; *p*-value <0.001$^{\#\#\#}$.

Chapter Three

Determination of antibacterial activity of cationic antimicrobial compounds

3.1 Introduction

The potency of each test agent was assessed by determination of both the minimum inhibitory concentration (MIC) and minimum bactericidal concentrations (MBCs) against *E. coli*, *S. aureus* and *P. aeruginosa*. The MIC of an antibacterial compound is the minimum concentration at which the compound inhibits growth of the test bacterium. MIC values can be determined using the broth macrodilution assay, the broth microdilution assay or the agar dilution assay (Clinical and Laboratory Standards Institute (CLSI) 2006). Broth macrodilution and microdilution assays were performed for triclosan and colistin. Broth microdilution assays only, were performed for CAPs, to conserve stock supplies, as minimal quantities of test agents were required to generate data using this assay. The growth of test bacteria under oxygenated (via agitating water bath), non-oxygenated (via non-agitating water bath) and micro-titre plate reader (static) conditions was first examined, to determine whether equivalent bacterial growth was obtainable under each of these test conditions.

The MBC of an antibacterial compound is the minimum concentration at which the compound prevented growth of the test bacterium. MBCs were determined using broth microdilution assays. MBCs and MICs are rarely identical; the MBC of an antimicrobial compound is always higher than the MIC, sometimes by several multiples. These experiments were undertaken to quantitatively assess the antibacterial activity of triclosan, colistin, NP101 and NP108 against *Escherichia coli*, *Pseudomonas aeruginosa* and *Staphylococcus aureus.*

3.2 Methodologies

3.2.1 Evaluation of bacterial growth under oxygenated and non-oxygenated conditions

Examination of bacterial growth under oxygenated/non-oxygenated conditions was performed as described in Section 2.3.4. Assays were performed in triplicate to verify reproducibility of results.

3.2.2 Quantification of the antibacterial activity of test agents by broth macrodilution method

Macro broth assays were performed according to the guidelines detailed by The Clinical and Laboratory Standards Institute (CLSI) 2006. Assays were performed in triplicate to verify reproducibility of results.

3.2.3 Quantification of the antibacterial activity of test agents by the broth microdilution method

Solutions of cationic antibacterials were prepared daily as described in Section 2.4.1 and 2.4.2. These solutions were used in the broth microdilution assay (Section 2.5.1) to establish antibacterial activity against *E. coli*, *S. aureus* and *P. aeruginosa.* MICs were determined by examination of microtitre plates over an 18 to 24 hour period of incubation at 37 ^{o}C and identifying the minimum concentration of test agent that inhibited bacterial growth. Assays were performed in triplicate (four replicates per assay) for each agent and each bacterial strain to verify the reproducibility of the results.

3.2.4 Determination of minimum bactericidal concentration of test agents

MBCs were determined as outlined in Section 2.5.2 as the minimum concentration that prevented bacterial growth. Assays were performed in triplicate (four replicates per assay) for each agent and each bacterial strain to verify reproducibility of results.

3.2.5 Determination of MICs of *E. coli* sensitised/de-sensitised to triclosan

MICs of *E. coli* sensitised/de-sensitised to triclosan were prepared as indicated in Section 2.6.1 and 2.6.2. Assays were performed in triplicate to verify reproducibility of results.

3.3 Results

3.3.1 Bacterial growth under non-oxygenated, oxygenated and micro-titre plate reader conditions

Growth of *E. coli* under oxygenated or static non-oxygenated cultures in 100 ml Erlenmeyer flasks and static micro-titre plate settings was examined (Figure 3.1)). Results were analysed and indicated after 24 hours of growth *E. coli* yielded an optical density of 1.20 at 650 nm under oxygenated conditions: short lag phase, onset of steep log phase at 2 hours with stationary phase commencing at 6 hours. A shorter lag phase was observed under micro-titre plate reader conditions with onset of steep log phase at 3 hours, which increased gradually until stationary phase commenced at 21 hours incubation, resulting in *E. coli* growth of optical density 1.2 after 24 hours incubation.

S. aureus cultures (Figure 3.2)) also achieved optimum growth under micro-titre plate reader conditions where after 24 hours of growth *S. aureus* yielded an optical density of 1.1 at 650 nm under oxygenated conditions; onset of log phase commenced at 2 hours with stationary phase observed at 13 hours. A longer lag phase was visualised under oxygenated macro broth conditions and a slowly increasing log phase yielded *S. aureus* growth after 24 hours of optical density 1.05 at 650 nm.

Growth under static non-oxygenated macro broth conditions for both bacteria showed similar lag and onset of log phase but very poor bacterial growth was achieved over the 24-hour incubation. Automated analysis of bacterial growth was better than manual process due to increased surface area to volume ratio within the wells of a microtitre plate compared to ratios of conical flasks.

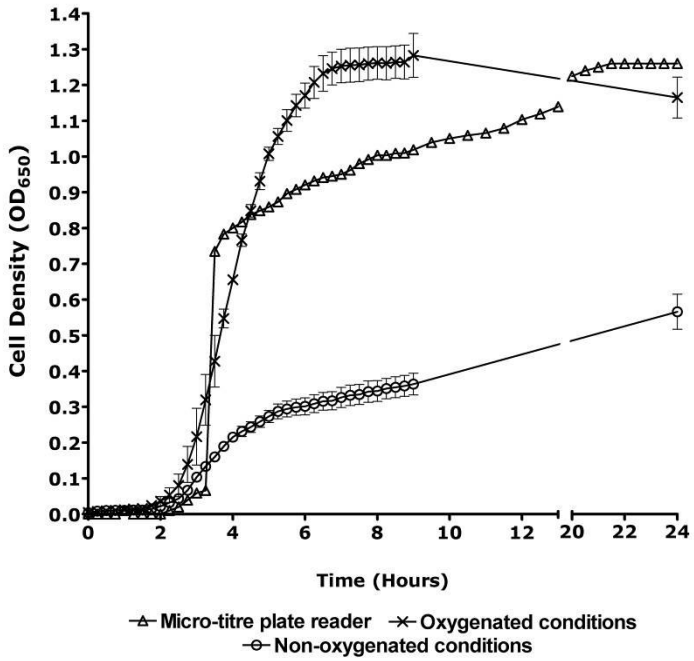

Figure 3.1 Growth of 1x10^6 cfu/ml *E. coli* culture. N=3. Standard error of mean (S.E.M.)

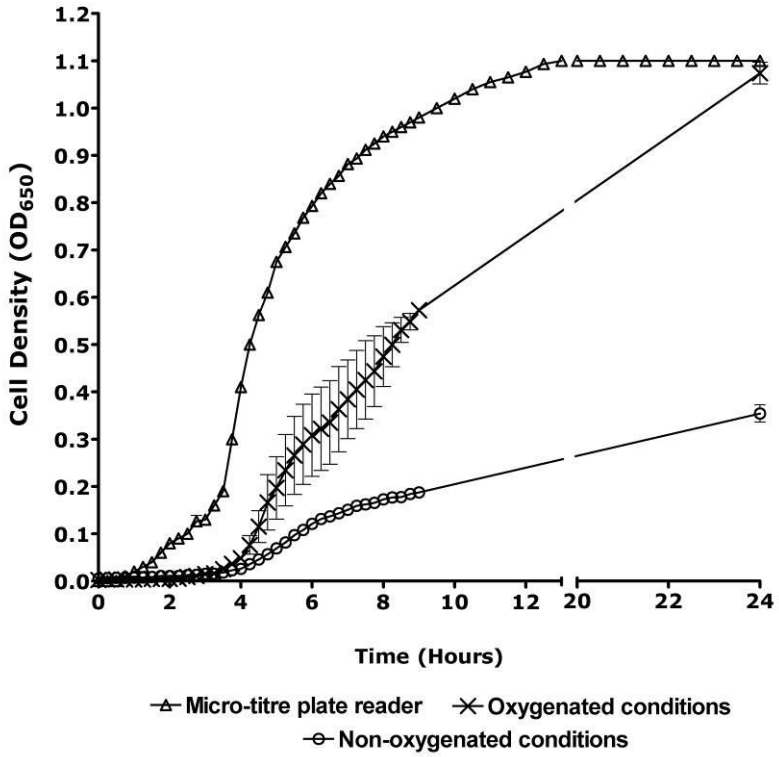

Figure 3.2 Growth of $1x10^6$ cfu/ml *S. aureus* culture. N=3. S.E.M.

3.3.2 Quantification of antimicrobial sensitivity

3.3.2.1 Triclosan

A two-fold difference in MIC values of triclosan against test bacteria (Table 3.1) was recorded for macro and micro broth assays. A two-fold difference in values was recorded between MIC/MBC results for the $1x10^6$ cfu/ml *S. aureus* cultures, whereas MBC values for $1x10^8$ cfu/ml cultures were 24 times higher than recorded MIC values for $1x10^8$ cfu/ml *E. coli* and 26 times higher than $1x10^8$ cfu/ml MIC values for *S. aureus.*

E. coli that was sensitised to triclosan (Table 3.2) for 24 hours showed a 32 fold increase in macro broth MIC values and 64 fold increase in micro broth MIC value. This increase in MIC values by *E. coli* appeared to be stably retained (Table 3.3), as

MIC values recorded during a total of five separate 24-hour de-sensitisation periods of cultivation and sub-culture, retained an increased MIC value.

Assay conditions		**MIC**			**MBC**	
Assay	**Cell Density (cfu/ml)**	***E. coli* (μg/ml)**	***S. aureus* (μg/ml)**	***P. aeruginosa* (μg/ml)**	***E. coli* (μg/ml)**	***S. aureus* (μg/ml)**
Macro broth	$1x10^6$	0.07	0.06	ND	ND	ND
Micro broth	$1x10^6$	0.14	0.11	360	0.14	0.22
Micro broth	$1x10^8$	18.0	14.0	ND	425	360

Table 3.1 MICs of bacteria incubated with triclosan. N=3. S.E.M. ND = not determined

Length of exposure of *E. coli* to MIC of triclosan 0.07 μg/ml (Hours)		**Macro broth assay**		**Micro broth assay**	
Number of culture passages (Hours)	**Total exposure time (Hours)**	**Culture Viability (cfu/ml)**	**MIC (μg/ml)**	**Culture Viability (cfu/ml)**	**MIC (μg/ml)**
1x24	24	$5.83x10^8$	2.26	$6.84x10^8$	4.5
2x24	48	$6.31x10^8$	2.26	$5.93x10^8$	4.5
3x24	72	$5.76x10^8$	2.26	$5.67x10^8$	4.5
4x24	96	$5.70x10^8$	2.26	$5.7x10^8$	9.0

Table 3.2 Macro broth MICs of $1x10^6$ cfu/ml *E. coli* incubated in nutrient broth with triclosan for varying time periods. Viabilities of cultures were checked after every 24 hour incubation period. N=3. S.E.M.

Number of 24 hour de-sensitisation cycles	Total de-sensitisation time of *E. coli* to triclosan (Hours)	Culture Viability (cfu/ml)	Macro broth MIC (μg/ml)
1x24	24	$6.8x10^8$	2.26
2x24	48	$8.29x10^8$	1.13
3x24	72	$7.44x10^8$	1.13
4x24	96	$6.58x10^8$	1.13
5x24	120	$7.72x10^8$	1.13

Table 3.3 Macro broth MICs of $1x10^6$ cfu/ml *E. coli* de-sensitised to triclosan for varying time periods. Viabilities of cultures were checked after every 24 hour incubation period. N=3. S.E.M.

3.3.2.2 Colistin

Identical MIC and MBC results were recorded for colistin against all three test bacteria (Table 3.4). A considerable difference in macro and micro-broth MICs was obtained for *E. coli*, whereas identical MIC values for both assays were determined for *P. aeruginosa*. Of note, the macro broth MIC value for *S. aureus* against colistin was 35 times higher than that obtained for *E. coli* and 70 times higher than *P. aeruginosa,* a clear indication of why the agent is only used to treat Gram-negative species in clinical practice. It should also be pointed out that the lower MIC/MBC value recorded for colistin against $1x10^7$ cfu/ml *S. aureus* culture compared to the $1x10^6$ cfu/ml culture, was due to refinement of the concentration scale employed.

Assay	Cell Density cfu/ml	*E. coli* MIC/MBC μg/ml	*S. aureus* MIC/MBC (μg/ml)	*P. aeruginosa* MIC/MBC (μg/ml)
Macro broth	$1x10^6$ cfu/ml	3	100	1.5
Micro broth	$1x10^6$ cfu/ml	0.28	200	1.5
Micro broth	$1x10^7$ cfu/ml	9.8	156	4.9

Table 3.4 MIC/MBCs of bacteria incubated with colistin. N=6. S.E.M.

3.2.2.3 CAPs

Identical MIC and MBC values were recorded for all CAPs against *E. coli*, *S. aureus* and *P. aeruginosa* (Table 3.5, Table 3.6 and Table 3.7). As peptides are reputed to bind to plastics, MIC/MBC assays were undertaken in polyethylene and polycarbonate micro titre plates but no difference in values were recorded. A higher MIC/MBC value for NP101 was recorded for *E. coli* compared to *P. aeruginosa* and *S. aureus*.

The reason a lower MIC/MBC value for NP101 against $1x10^7$ cfu/ml *E. coli* culture was recorded compared to the $1x10^6$ cfu/ml culture was due to refinement of the concentration scale employed. Identical MIC/MBC values were recorded for NP108 against $1x10^6$ and $1x10^7$ cfu/ml *S. aureus* cultures (Table 3.5 and Table 3.7).

Bacterial species	CAP	MIC of CAP using polyethylene microtitre plates (μg/μl)	MBC of CAP using polyethylene microtitre plates (μg/μl)
E. coli	NP101	0.5	0.5
E. coli	NP108	0.25	0.25
S. aureus	NP101	0.25	0.25
S. aureus	NP108	0.25	0.25
P. aeruginosa	NP101	0.25	0.25
P. aeruginosa	NP108	0.25	0.25

Table 3.5 MIC and MBCs of $1x10^6$ cfu/ml test bacteria incubated with CAPs in polyethylene microtitre plates. N=6. S.E.M.

Bacterial species	CAP	MIC of CAP using polycarbonate microtitre plates (μg/μl)	MBC of CAP using polycarbonate microtitre plates (μg/μl)
E. coli	NP108	0.25	0.25
S. aureus	NP101	0.25	0.25

Table 3.6 MIC/MBCs of $1x10^6$ cfu/ml test bacteria incubated with CAPs in polycarbonate microtitre plates. N=6. S.E.M.

Bacterial species	CAP	MIC (μg/μl)	MBC (μg/μl)
E. coli	NP101	0.31	0.31
E. coli	NP108	0.5	0.5
S. aureus	NP101	0.31	0.31
S. aureus	NP108	0.25	0.25
P. aeruginosa	NP101	0.31	0.31
P. aeruginosa	NP108	0.5	0.5

Table 3.7 MICs and MBCs of $1x10^7$ cfu/ml test bacteria incubated in polyethylene microtitre plates with CAPs. N=6. S.E.M.

3.3.3 Bacterial growth in presence of cationic antibacterials

3.3.3.1 Triclosan

a) *Escherichia coli*

Triclosan exerted a concentration dependent retardation in onset of log phase bacterial growth coupled with reduction in logarithmic growth on $1x10^6$ *E. coli* culture (Figure 3.3) over a 24-hour experimental period. Onset of log phase in *E. coli* control commenced at 2 hours and bacterial growth of optical density 1.2 was attained at 24 hours. The retardation and reduction effects on logarithmic bacterial growth of *E. coli* increased as the concentration of triclosan increased and were highest at 0.07 μg/ml triclosan where onset of logarithmic growth in *E. coli* commenced at 14 hours and growth of optical density 0.85 was achieved over the experimental period. Concentrations greater than the MIC resulted in complete inhibition of growth and are not plotted in order to maintain clarity.

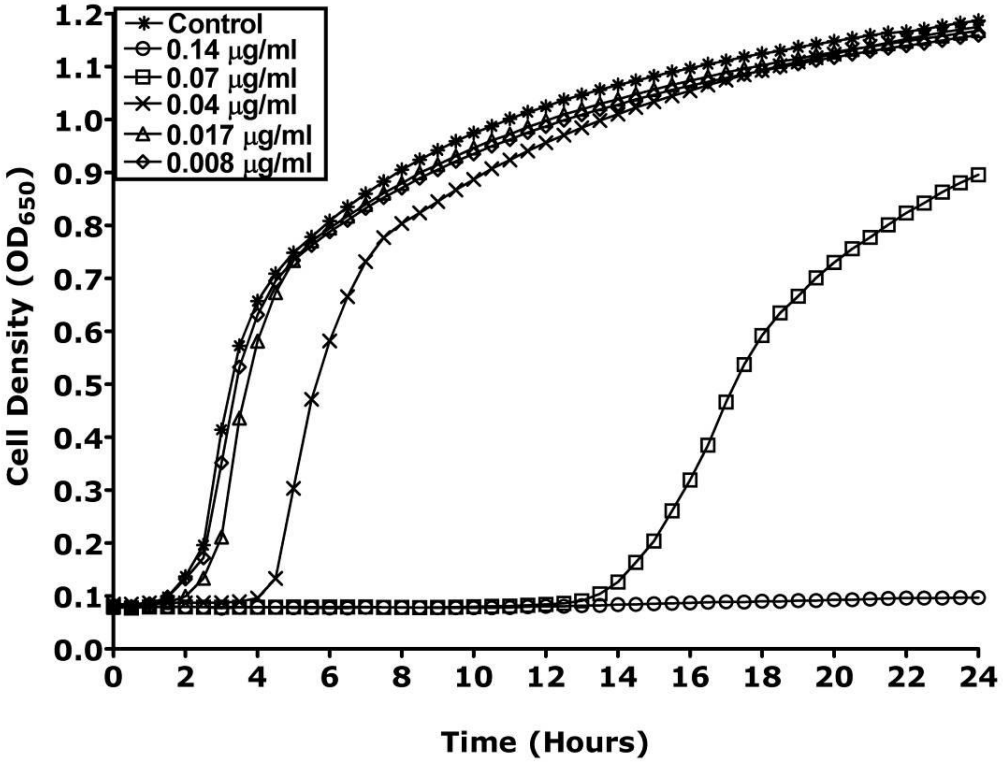

Figure 3.3 *E. coli* 1x10^6 cfu/ml incubated with 0.008-1.12 μg/ml triclosan. MIC = 0.14 μg/ml triclosan. N=3. S.E.M.

A greater *E. coli* density of 1x10^8 cfu/ml exposed to a higher triclosan concentration range (Figure 3.4) revealed little retardation of onset of log phase however significant reduction of final density of bacterial growth was apparent.

These dual effects of triclosan were also visualised in a 1x10^6 cfu/ml *E. coli* culture that had been serially passaged for 2x24-hour cycles in 0.07 μg/ml triclosan (MIC) for a total of 48 hours (Figure 3.5) and then incubated with a higher triclosan concentration scale. Control bacteria displayed onset of log phase growth at 2 hours with a final bacterial density of 1.2, compared to onset of log phase growth at 11 hours for the serially passaged *E. coli* incubated with 2.25 μg/ml triclosan and a final cell density of 0.5.

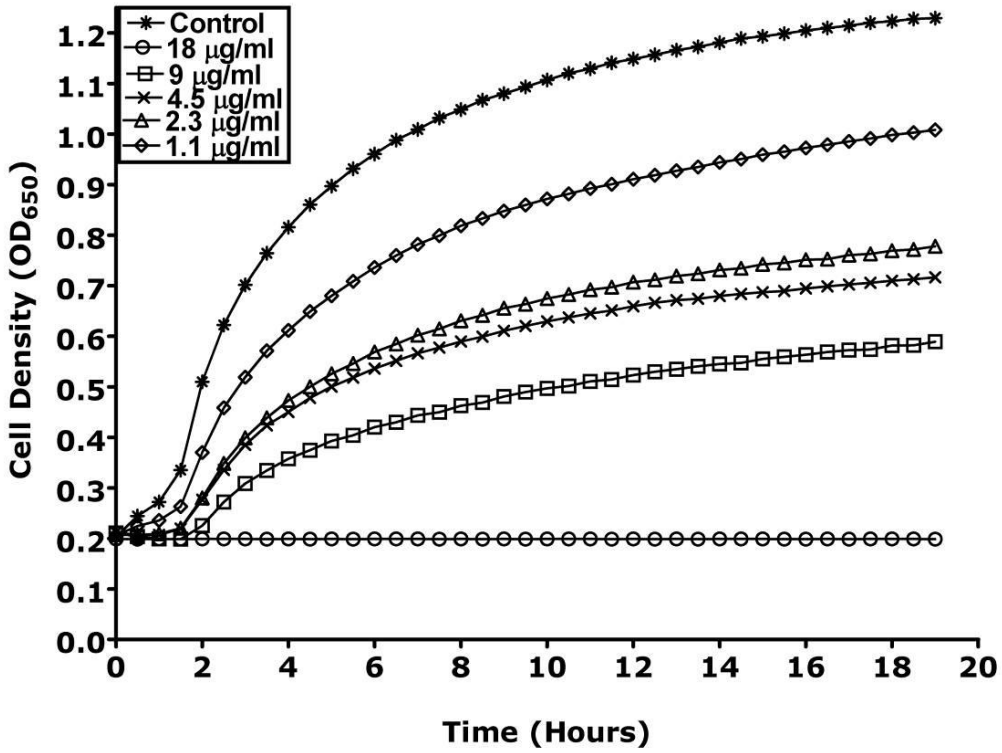

Figure 3.4 *E. coli* 1x10^8 cfu/ml incubated with 1.1-72 μg/ml triclosan. MIC = 18 μg/ml triclosan. N=3. S.E.M.

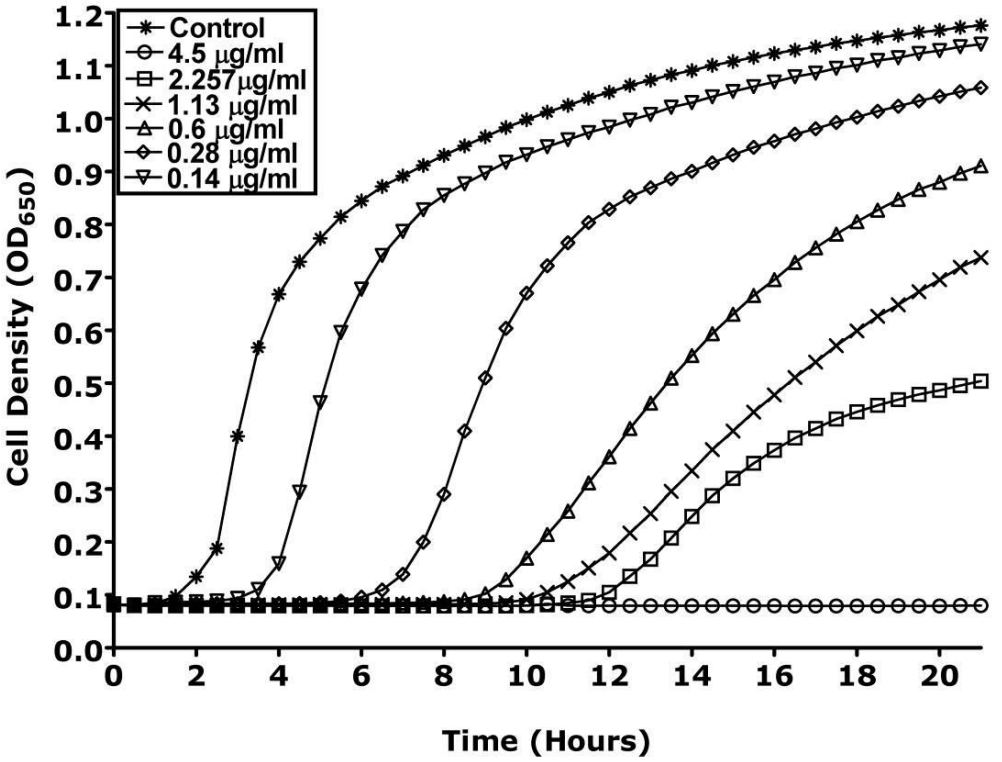

Figure 3.5 *E. coli* 1 x 10^6 cfu/ml serially passaged in 0.07 μg/ml triclosan for 48 hours. MIC = 4.5 μg/ml triclosan. N=3. S.E.M.

After 96 hours (four separate 24-hour periods of growth and sub-culture) this serially passaged *E. coli* culture (Figure 3.6) was again re-incubated with a high triclosan concentration scale and the delayed onset of log phase growth coupled with severe retardation of logarithmic bacterial growth was still visible compared to control bacteria, though the MIC value had doubled and *E. coli* growth was now apparent at 4.5 µg/ml triclosan concentration.

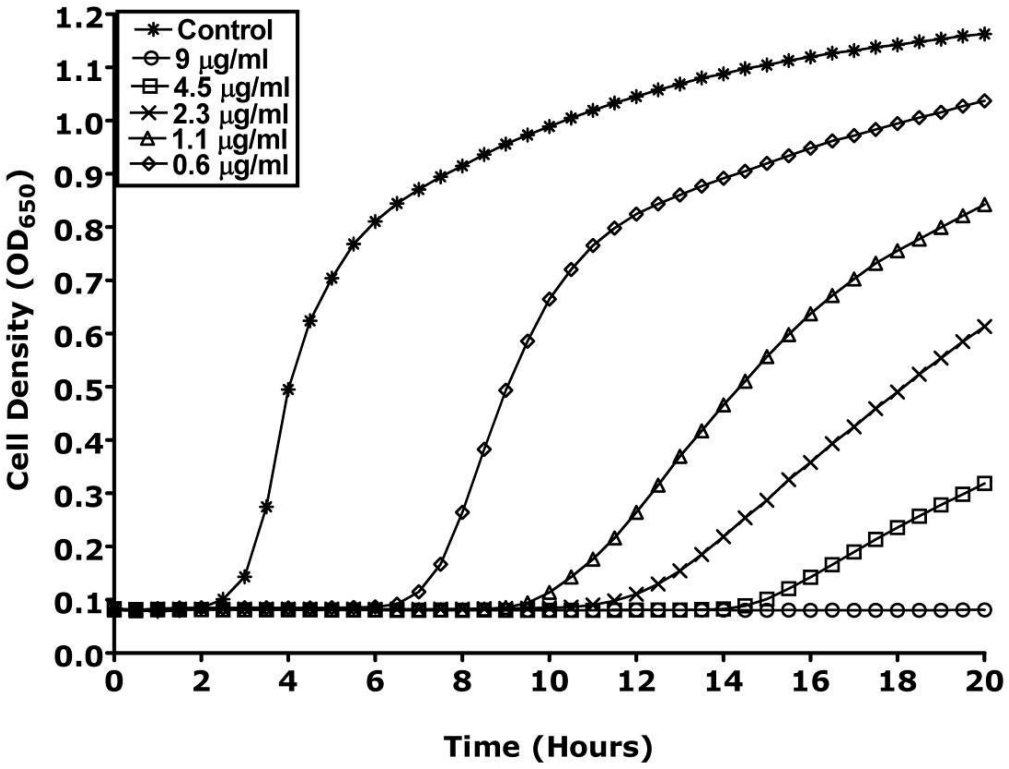

Figure 3.6 *E. coli* 1x10^6 cfu/ml serially passaged in 0.07 µg/ml triclosan for 96 hours. MIC = 9 µg/ml triclosan. N=3. S.E.M.

b) *Staphylococcus aureus*

S. aureus 1x10^6 cfu/ml bacteria (Figure 3.7)) incubated with triclosan demonstrated a concentration dependent inhibition in onset of log phase growth in conjunction with slight retardation of this logarithmic bacterial growth, compared to control. The dual phase growth demonstrated by the control bacteria was also absent in the growth of the triclosan incubated bacteria.

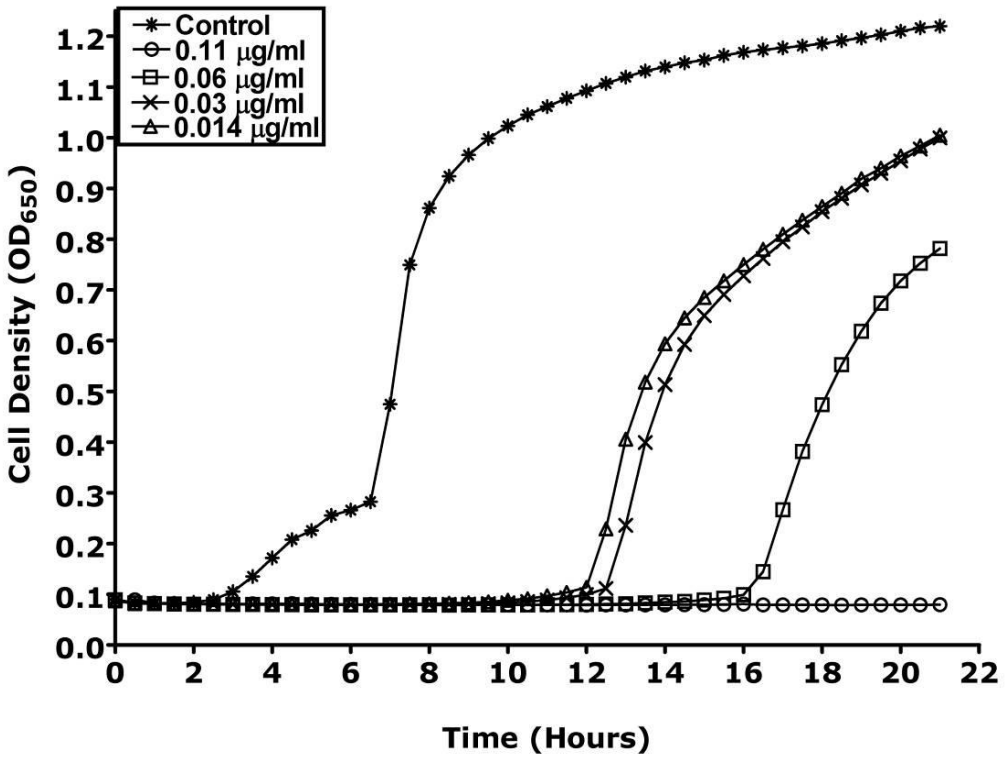

Figure 3.7 *S. aureus* 1x10^6 cfu/ml incubated with 0.014-1.76 μg/ml triclosan. MIC = 0.11 μg/ml triclosan. N=3. S.E.M.

Onset of log phase growth in *S. aureus* control occurred at 2.25 hours and reached an optical density of 1.2 over the experimental period whereas onset of logarithmic growth in *S. aureus* incubated with 0.06 μg/ml triclosan was at 16 hours with a final bacterial density of 0.75 over the same time period. As observed with *E. coli* 1x10^8 cfu/ml cultures incubated with triclosan, little retardation in onset of log phase growth was visualised in the growth of 1x10^8 cfu/ml *S. aureus* bacteria incubated with triclosan (Figure 3.8) but similarly a marked reduction in logarithmic bacterial growth over the experimental was observed, compared to control, with the dual phase growth pattern of control bacteria absent in the triclosan incubated bacteria.

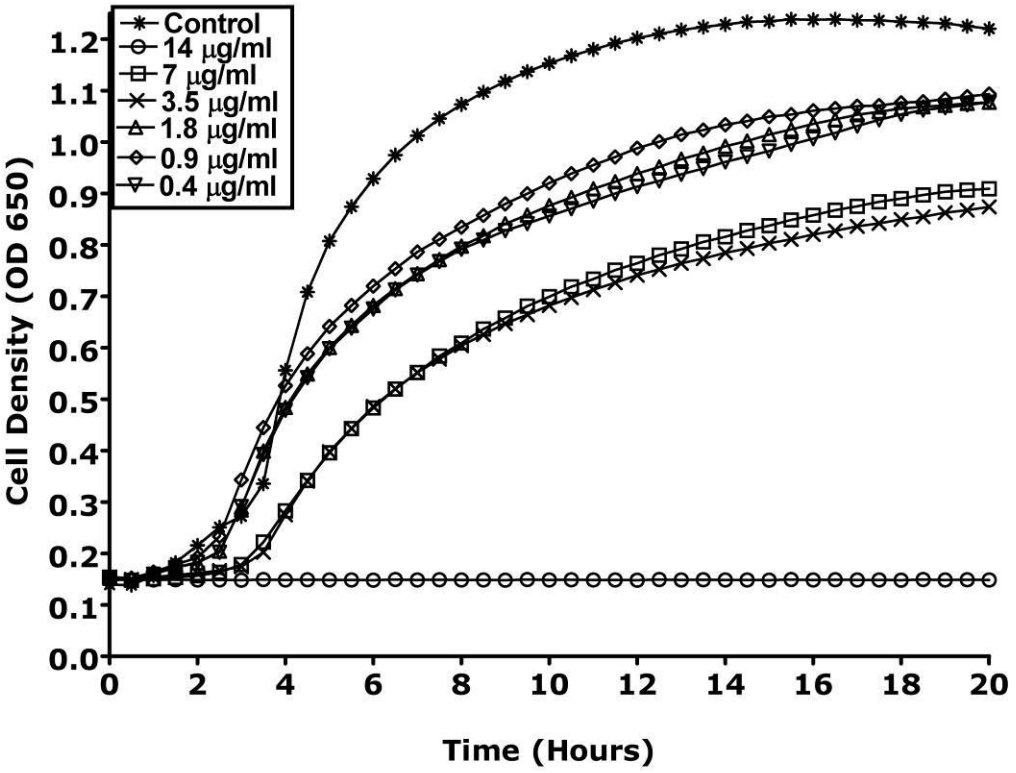

Figure 3.8 *S. aureus* 1x10^8 cfu/ml incubated with 0.4-56 μg/ml triclosan. MIC = 14 μg/ml triclosan. N=3. S.E.M.

c) *Pseudomonas aeruginosa*

P. aeruginosa 1x10^6 cfu/ml incubated with a substantially higher triclosan range (Figure 3.9) also exhibited the dual effects of concentration dependent retardation of onset on logarithmic bacterial growth with significant reduction in this bacterial growth compared to control. Onset of logarithmic growth in *P. aeruginosa* control bacteria commenced at 4 hours and reached a final density of 1.2 at 24 hours, compared to onset of logarithmic growth at 7 hours for *P. aeruginosa* incubated with 180 μg/ml triclosan, with a final recorded bacterial density of 0.85 over the experimental period. Due to the extremely high tolerance of *P. aeruginosa* towards triclosan, attempts to determine an MIC for 1x10^8 cfu/ml *P. aeruginosa* culture against triclosan were restricted by the solubility of triclosan.

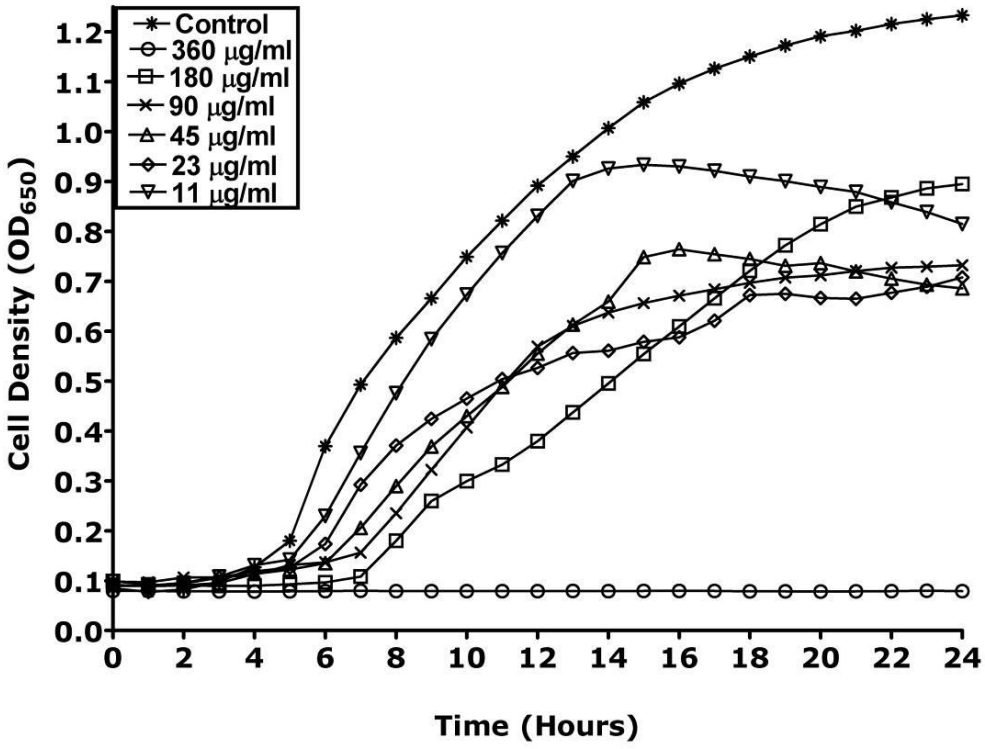

Figure 3.9 *P. aeruginosa* 1x10^6 cfu/ml incubated with 11-1445 μg/ml triclosan. MIC = 360 μg/ml triclosan. N=3. S.E.M.

3.3.3.2 Colistin

a) *Escherichia coli*

Growth of *E. coli* 1x10^6 cfu/ml (Figure 3.10) incubated with colistin revealed a moderate concentration dependent retardation of onset of log phase bacterial growth coupled with slight reduction in final bacterial density, compared to control. Logarithmic growth of control bacteria commenced at 1.5 hours with a final density of 1.2, compared to onset of log phase growth at 3 hours with a final optical density of 1.05 for 0.14 μg/ml colistin incubated *E.coli*. These data show that colistin appears to have the equivalent of an all or nothing effect on growth of *E. coli* at a density of 1x10^6 cfu/ml.

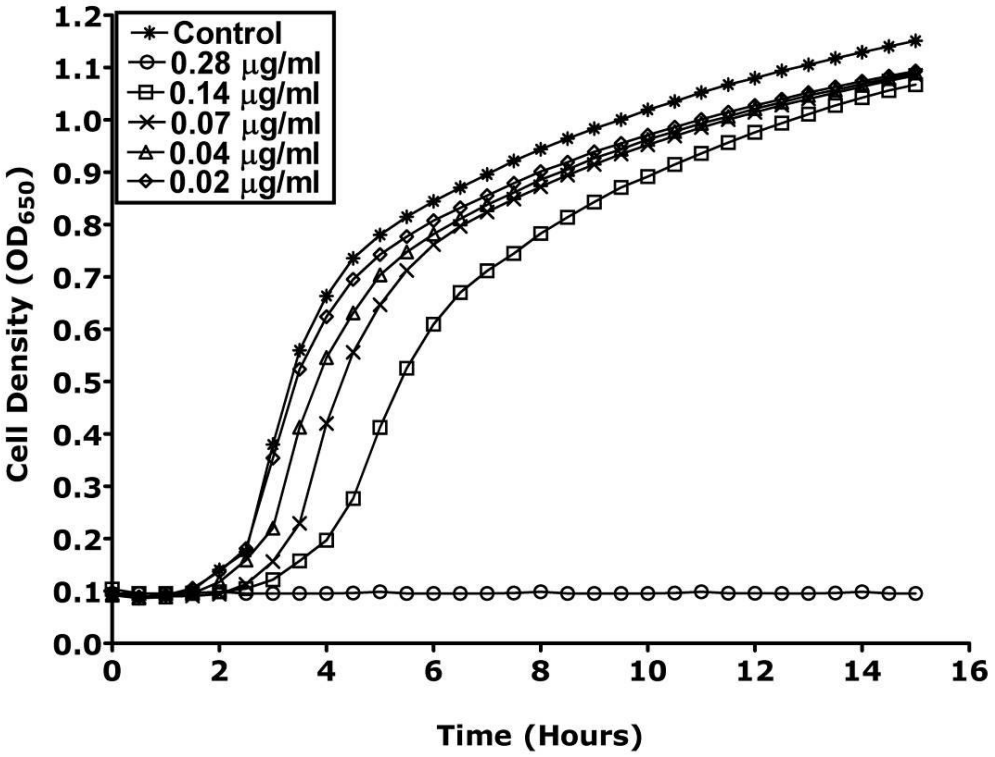

Figure 3.10 *E. coli* 1x10^6 cfu/ml incubated with 0.02-0.28 μg/ml colistin. MIC/MBC = 0.28 μg/ml colistin. N=6. S.E.M.

Both retardation of onset of logarithmic growth and minimal reduction in bacterial density, were visualised in the growth of the 1x10^7 cfu/ml *E. coli* culture (Figure 3.11). Onset of log phase growth for control bacteria at one hour and final optical density of 1.2, compared to onset of log phase growth at 8 hours for bacteria incubated with 4.9 μg/ml colistin and an optical density of 1.1 at the end of the experimental period. The higher *E. coli* inoculum employed in this experiment demonstrated bacterial density is an important factor in the ability of this bacterium to withstand the effects of colistin, as growth was visualised at far higher colistin concentrations compared to the 1x10^6 cfu/ml culture, though the retardation effects of colistin on onset of logarithmic bacterial growth were far more severe.

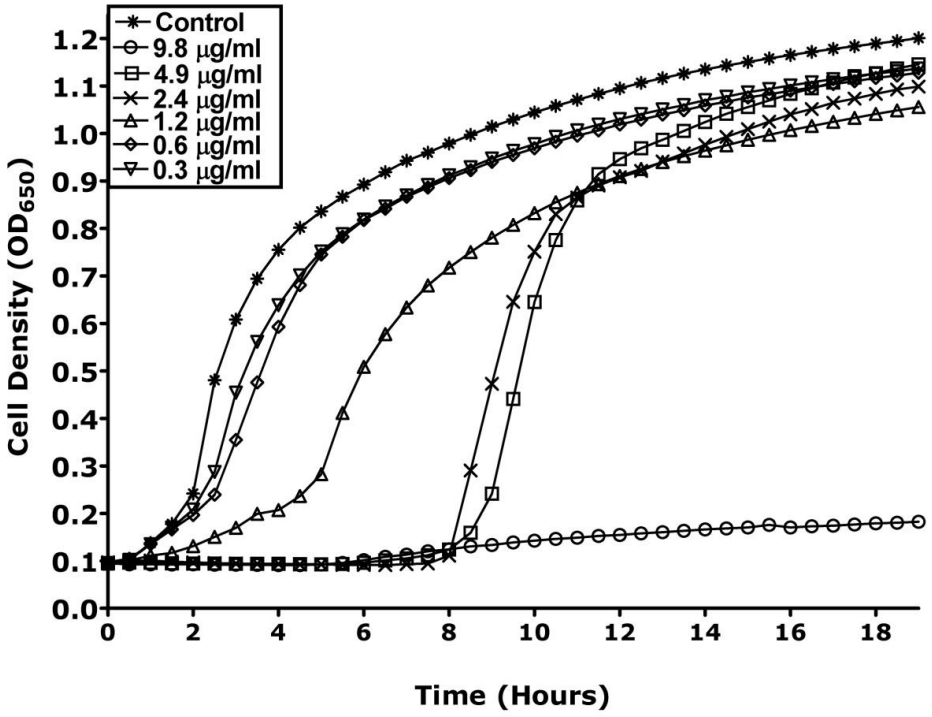

Figure 3.11 *E. coli* 1x10^7 cfu/ml incubated with 0.3–39 μg/ml colistin. MIC/MBC was 9.8 μg/ml colistin. N=6. S.E.M.

b) *Staphylococcus aureus*

A biphasic growth pattern was displayed by both *S. aureus* 1x10^6 cfu/ml control and colistin incubated bacteria (Figure 3.12). Reduction in final density achieved, coupled with retardation in onset of logarithmic growth was also manifested by *S. aureus* incubated with colistin when compared to control. However the rate of growth, once log phase had commenced, was equivalent in all concentrations of colistin up to that immediately below the MIC. *S. aureus* control bacteria demonstrated onset of logarithmic phase bacterial growth after incubation for 1 hour, followed by a further spurt of exponential growth which commenced at 4 hours, achieving a final density of 1.2 after 24 hours. A simultaneous onset of logarithmic bacterial growth for all concentrations of colistin incubated *S. aureus* occurred at 3 - 4 hours. Subsequently, a concentration dependent retardation in onset of a second phase of exponential growth occurred at 8 hours for *S. aureus*

incubated with 3 and 6.25 µg/ml colistin and at 13 hours for 100 µg/ml colistin incubated *S. aureus*. Markedly reduced final bacterial densities for all colistin incubated bacteria were recorded at 24 hours.

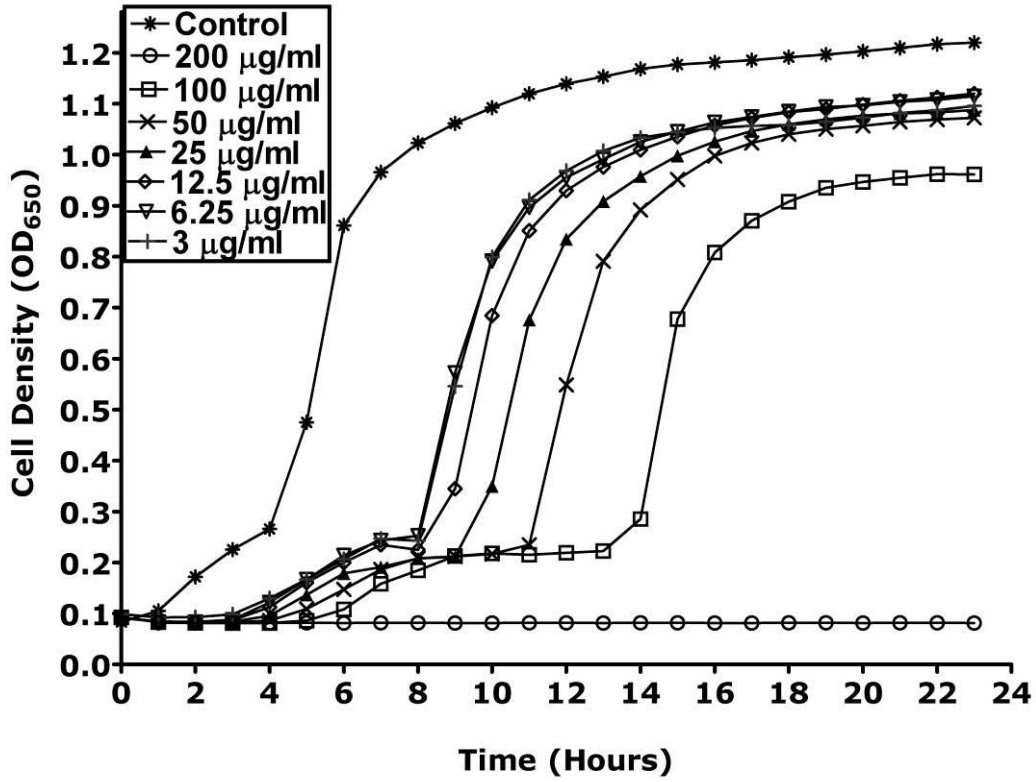

Figure 3.12 *S. aureus* $1x10^6$ cfu/ml incubated with 3–400 µg/ml colistin. MIC/MBC = 200 µg/ml colistin. N=6. S.E.M.

Similar biphasic growth patterns for control and colistin incubated bacteria were recorded for $1x10^7$ cfu/ml *S. aureus* (Figure 3.13). The higher *S. aureus* density used in this experiment demonstrated as with *E. coli,* the greater ability of the bacterium to withstand the effects of colistin. Onset of logarithmic growth for all bacteria, other than 78 µg/ml treated cells, commenced at 2 hours with a concentration dependent staggered onset of a further phase of exponential bacterial growth for control and all colistin incubated bacteria ranging from 5 hours for control bacteria. With *S. aureus* incubated with 78 µg/ml colistin growth occurred at 7-8 hours with the second phase occurring at 11 hours achieving a final bacterial

density of 1.1, compared to a final density of 0.9 for *S. aureus* $1x10^6$ cfu/ml culture incubated with 100 µg/ml colistin. Bacterial inoculum density therefore is significant in the ability of bacteria to withstand the effects of colistin.

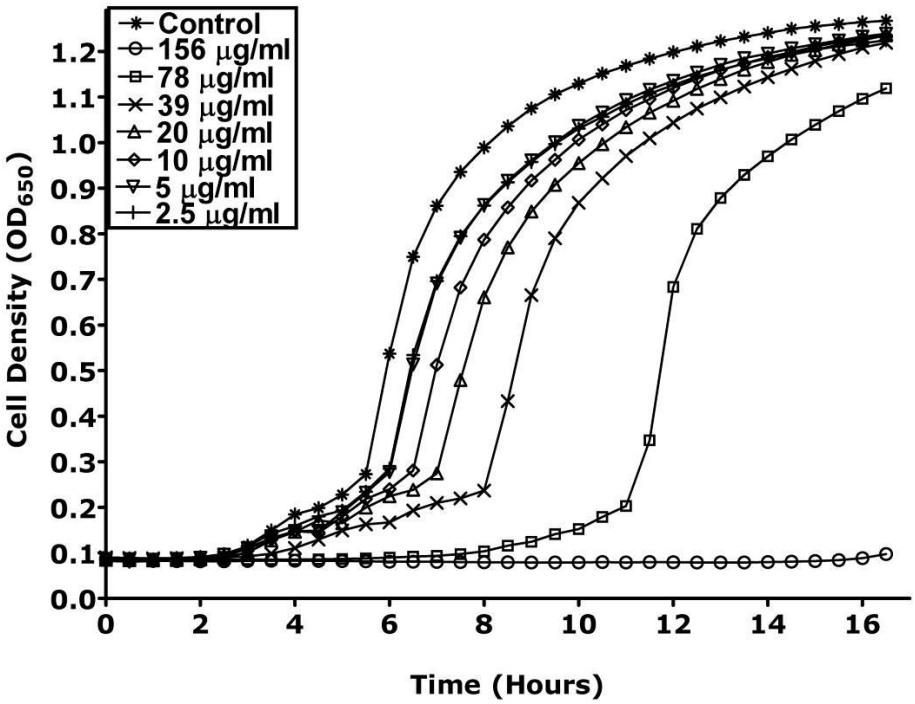

Figure 3.13 *S. aureus* $1x10^7$ cfu/ml incubated with 2.5-312 µg/ml colistin. MIC/MBC = 156 µg/ml colistin. N=6. S.E.M.

c) *Pseudomonas aeruginosa*

As with *E. coli* and *S. aureus*, the effects of colistin on *P. aeruginosa* varied with the bacterial density employed. Colistin incubated $1x10^6$ cfu/ml *P. aeruginosa* culture (Figure 3.14) demonstrated a concentration dependent inhibition in onset of log phase bacterial growth with final bacterial densities similar to control.

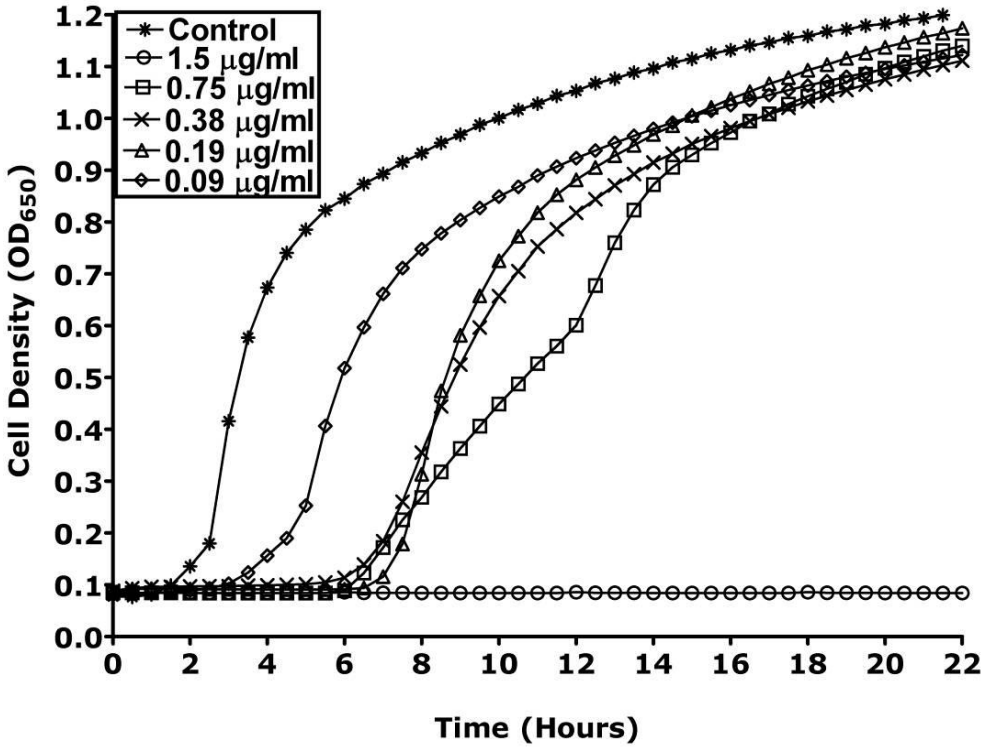

Figure 3.14 *Ps. aeruginosa* $1x10^6$ cfu/ml incubated with 0.09–12 μg/ml colistin. MIC/MBC = 1.5 μg/ml colistin. N=6. S.E.M.

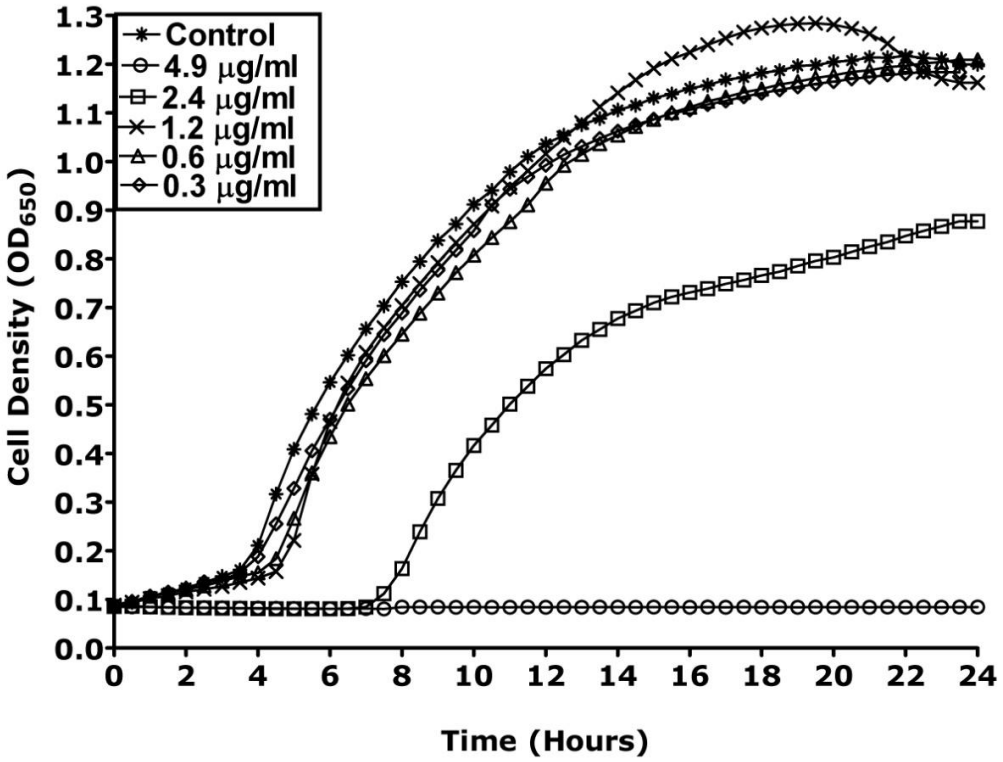

Figure 3.15 *Ps. aeruginosa* $1x10^7$ cfu/ml incubated with 0.3–39 μg/ml colistin. MIC/MBC = 4.9 μg/ml colistin. N=6. S.E.M.

No reduction or retardation of bacterial growth compared to control was visualised in $1x10^7$ cfu/ml *P. aeruginosa* colistin incubated culture (Figure 3.15) except for bacteria incubated with 2.4 µg/ml colistin, which displayed delayed onset of logarithmic growth and marked reduction in final bacterial density.

3.3.3.3 NP101

a) *Escherichia coli*

Recorded bacterial growth of *E. coli* $1x10^6$ cfu/ml cultures incubated with NP101, were similar at all time points compared to control (Figure 3.16). The spike in measurements observed and visible during the first hour of incubation can be attributed to an interaction between the CAP and the nutrient broth which resulted in a short term reduction in solubility of the CAP. After approximately 2 hours the CAP had solubilised fully along with a reduction in recorded optical density.

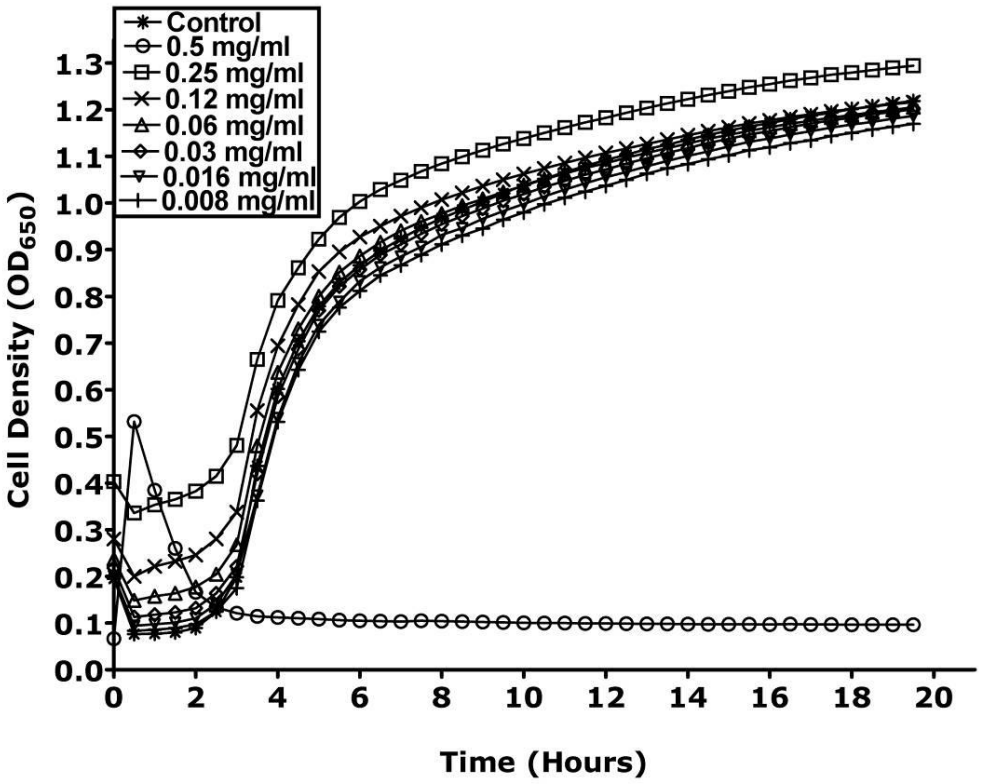

Figure 3.16 *E. coli* $1x10^6$ cfu/ml incubated with 0.008–1.0 mg/ml NP101. MIC/MBC = 0.5 mg/ml NP101. N=6. S.E.M.

The *E. coli* 1x10^7 cfu/ml cultures incubated with NP101 (Figure 3.17) also displayed very similar bacterial growth compared to control for the 0.08 and 0.16 mg/ml cultures. Again, interaction between the CAP and broth gave an initial high reading and then dropped to an optical density of 0.15 due to a solubility issue with the CAP, and is not indicative of bacterial growth. After 5 hours incubation a steady slight increase in optical density of the 0.31 mg/ml CAP culture was noted this is most probably due to replication of survivor bacterial cells. While MBC analysis confirmed no viable bacteria, slowly growing persister cells are most likely responsible for the increasing bacterial density.

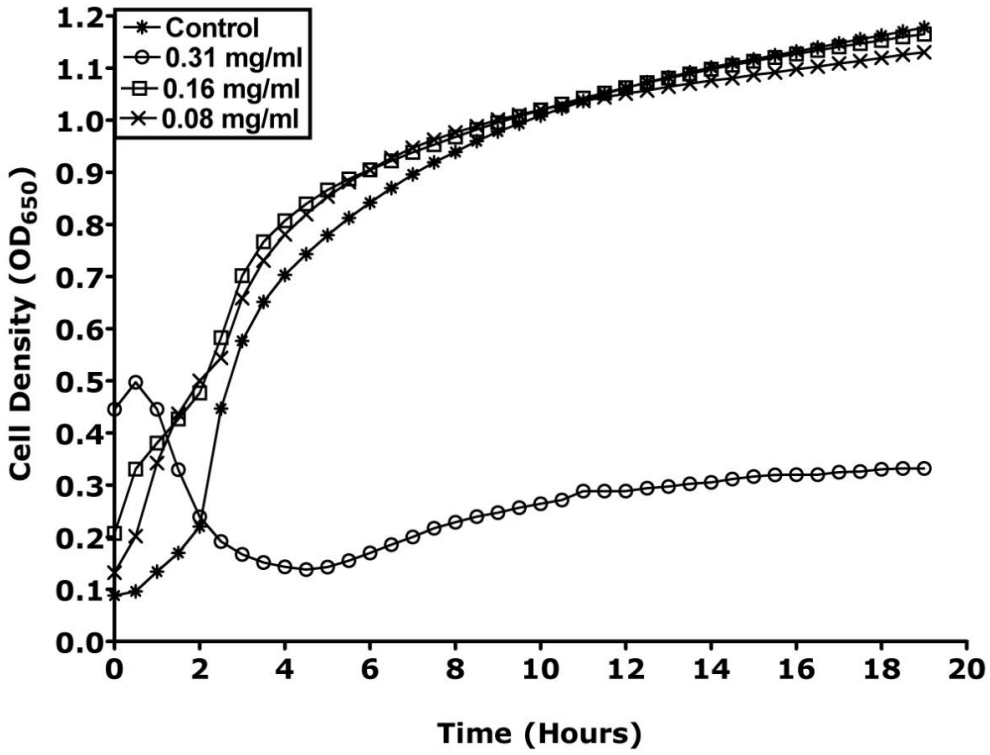

Figure 3.17 *E. coli* 1x10^7 cfu/ml incubated with 0.08–10.0 mg/ml NP101. MIC/MBC = 0.31 mg/ml NP101. N=6. S.E.M.

b) *Staphylococcus aureus*

S. aureus 1x10^6 cfu/ml (Figure 3.18) displayed an all or nothing effect when incubated with NP101; when bacterial growth occurred in tolerated CAP

concentrations, onset of growth and final density was equivalent to that of control. No fitness cost to withstand the effects of increasing concentrations of NP101 was exhibited by *S. aureus*. Bacterial growth equivalent to control occurred or no bacterial growth was manifested. The inference that can be drawn from this is that when the MIC/MBC concentration of NP101 against *S. aureus* was reached, the mechanism of action by which NP101 killed these bacteria was very rapid, allowing no registration of bacterial growth. A noticeable absence from the growth of all NP101 incubated *S. aureus* was the biphasic growth pattern displayed by the control bacteria. Thus NP101 exerted an effect on *S. aureus* that altered the normal growth pattern of the bacterium.

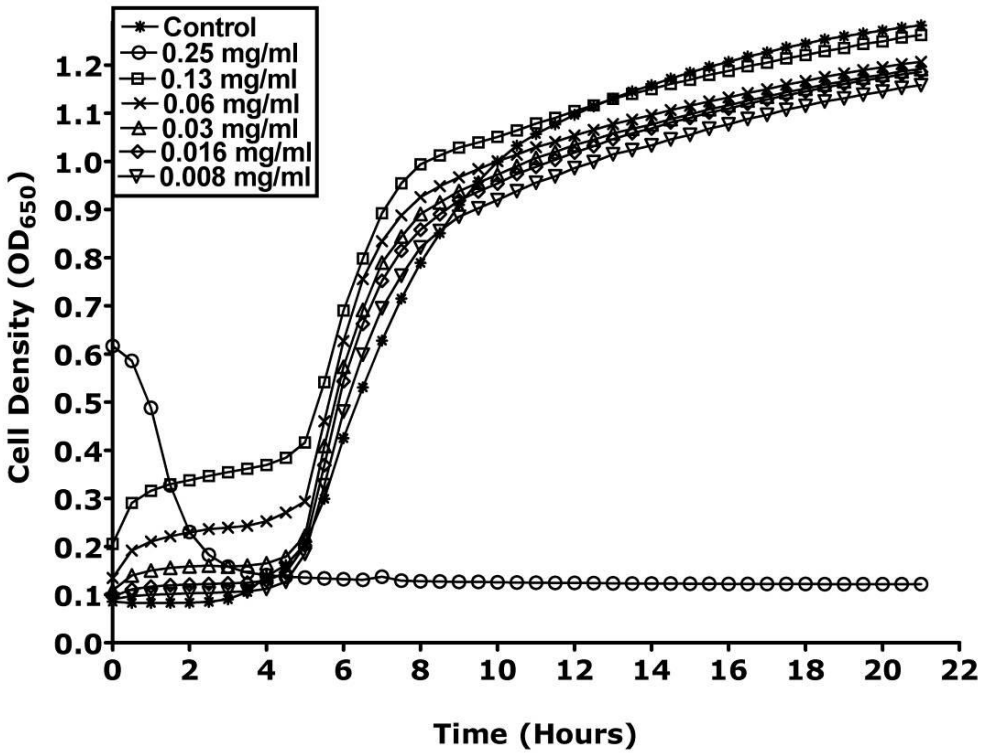

Figure 3.18 *S. aureus* $1x10^6$ cfu/ml incubated with 0.008–1.0 mg/ml NP101. MIC/MBC = 0.25 mg/ml NP101. N=6. S.E.M.

S. aureus 1x10^7 cfu/ml CAP incubated bacteria (Figure 3.19) displayed concentration dependent dual response of retarded onset of log phase bacterial growth and reduction of logarithmic bacterial growth of the 0.06 and 0.18 mg/ml NP101 cultures. The initial spike in optical density visible with the 0.031 mg/ml NP101 incubated bacteria resulted from a change in solubility of NP101 due to interaction with nutrient broth. The difference in the growth pattern of the *S. aureus* 1x10^7 cfu/ml CAP incubated bacteria compared to the 1x10^6 cfu/ml *S. aureus* CAP treated bacteria is that bacteria have now exhibited a struggle to overcome the effects of NP101 as visualised by a concentration dependent retardation in onset of logarithmic growth and reduction in final bacterial density.

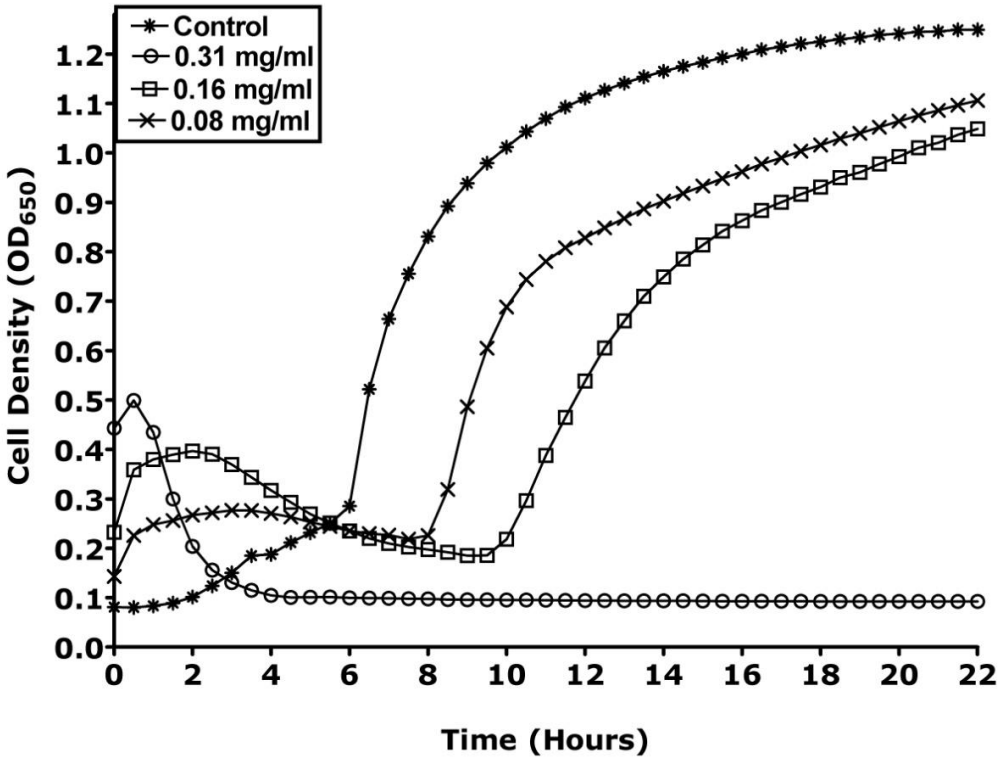

Figure 3.19 *S. aureus* 1x10^7 cfu/ml incubated with 0.08 – 10.0 mg/ml NP101. MIC/MBC = 0.31 mg/ml NP101. N=6. S.E.M.

Similarly, with 1x10^6 cfu/ml *S. aureus* incubated with NP101, the 1x10^7 cfu/ml CAP incubated bacteria did not display the growth pattern exhibited by the control

bacteria. However, the higher bacterial density resulted in a change in response of *S. aureus* to NP101 as witnessed by the bacterial struggle to survive in a higher NP101 concentration. A higher bacterial density offered no protection against the effects of NP101 and reversion to normal *S. aureus* growth did not occur.

c) *Pseudomonas aeruginosa*

NP101 sensitised bacterial growth of *P. aeruginosa* $1x10^6$ cfu/ml culture (Figures 3.20) was very similar to that of control over the 24-hour period, with equivalent final bacterial densities recorded for control and NP101 incubated bacteria. As with $1x10^6$ cfu/ml *S. aureus* and *E. coli* cultures, an all or nothing effect was also seen with the $1x10^6$ cfu/ml *P. aeruginosa* culture incubated with NP101.

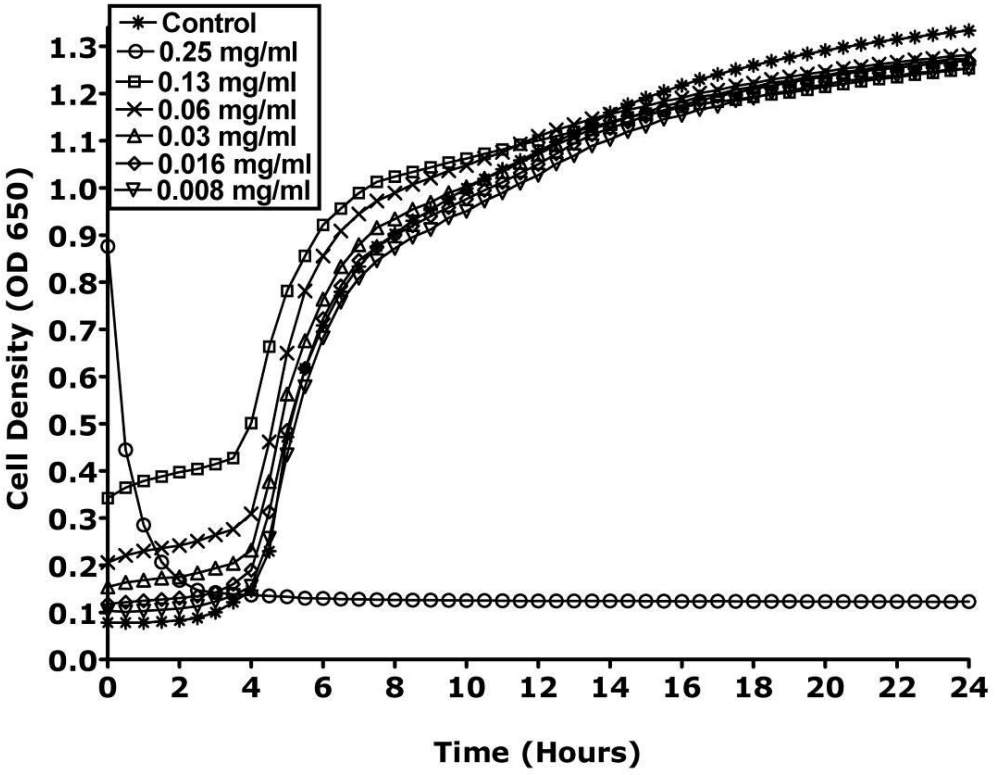

Figure 3.20 *P. aeruginosa* $1x10^6$ cfu/ml incubated with 0.008–1.0 mg/ml NP101. MIC/MBC = 0.25 mg/ml NP101. N=6. S.E.M.

P. aeruginosa $1x10^7$ cfu/ml (Figure 3.21) exhibited a struggle to withstand a higher concentration of NP101, in a similar manner to that displayed by NP101 *S. aureus*

$1x10^7$ cfu/ml incubated culture. What was recorded as initial bacterial growth in 0.16 mg/ml exposed cells was due to the interaction between NP101 and broth, and onset of actual bacterial growth commenced at 12 hours with a final bacterial density of 0.8, compared to onset of growth in control bacteria at 3 hours with a final bacterial density of 1.3. The dual effects of retardation of onset of bacterial growth and reduction in logarithmic growth of *P. aeruginosa* $1x10^7$ cfu/ml incubated with 0.16 mg/ml NP101 compared to control were exerted by the CAP.

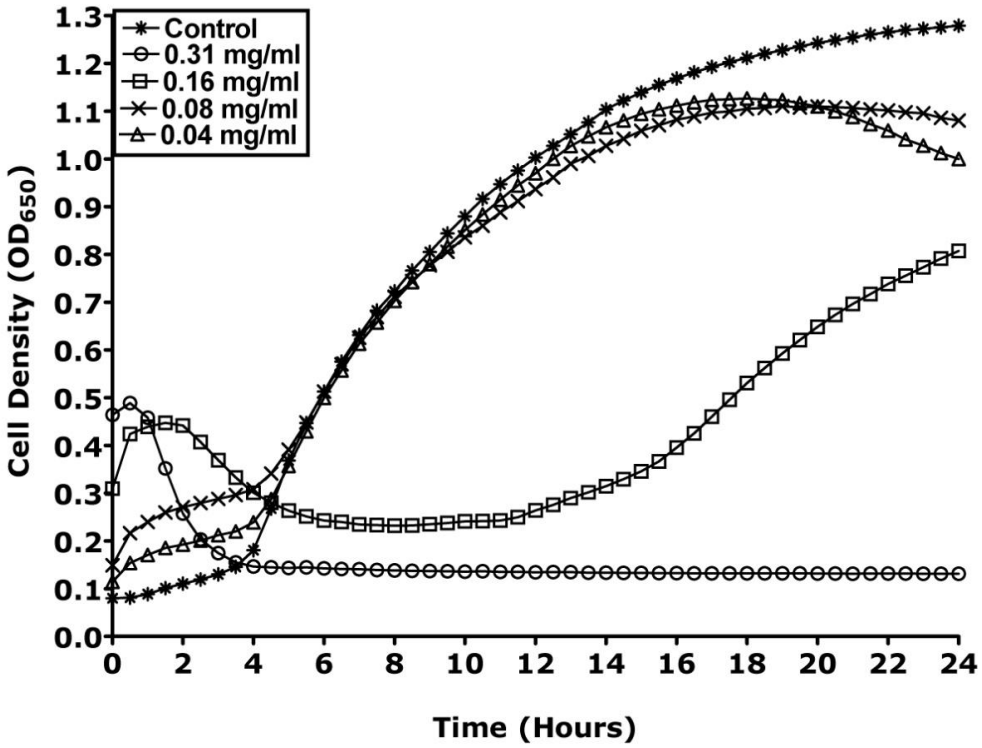

Figure 3.21 *P. aeruginosa* $1x10^7$ cfu/ml incubated with 0.04–5.0 mg/ml NP101. MIC/MBC = 0.31 mg/ml NP101. N=6. S.E.M.

3.3.3.4 NP108

a) *Escherichia coli*

E. coli $1x10^6$ cfu/ml incubated with all tolerated NP108 concentrations (Figure 3.22) displayed similar bacterial growth kinetics compared to control at all experimental time points. As noted previously with NP101, interaction between NP108 and

nutrient broth gave high optical density readings for the first two hours as a result of insolubility of the CAP at high concentration.

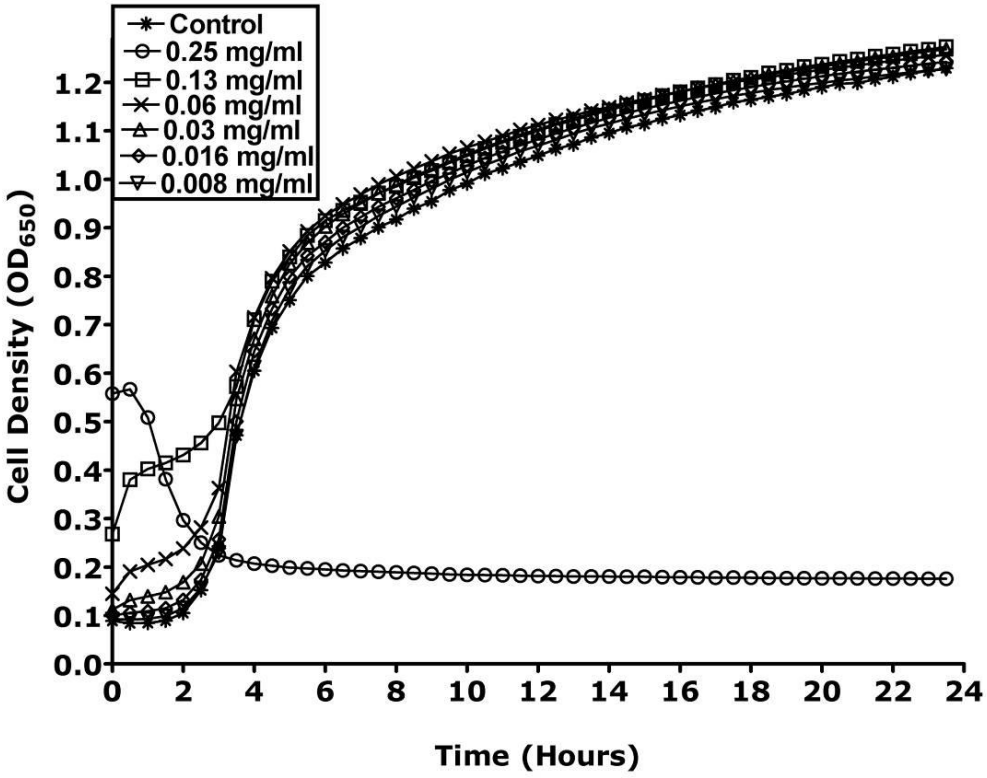

Figure 3.22 *E. coli* $1x10^6$ cfu/ml incubated with 0.008–1.0 mg/ml NP108. MIC/MBC = 0.25 mg/ml NP108. N=6. S.E.M.

NP108 at 0.25 mg/ml retarded onset of logarithmic bacterial growth of $1x10^7$ cfu/ml *E. coli* culture until 8 hours incubation whereupon bacterial growth began to increase exponentially and was equivalent to that of control at 24 hours (Figure 3.23). However the optical density value did not drop below 0.25 and at some point between 5 and 7 hours a crossover occurred where growth rather than insolubility was being measured. In contrast to the $1x10^7$ cfu/ml *E. coli* culture incubated with NP101, *E. coli* incubated with 0.25 mg/ml NP108 displayed marked retardation in onset of log phase bacterial growth but achieved a similar bacterial density to control at 24 hours. The all or nothing effect previously displayed by *E. coli* when incubated with a CAP was absent.

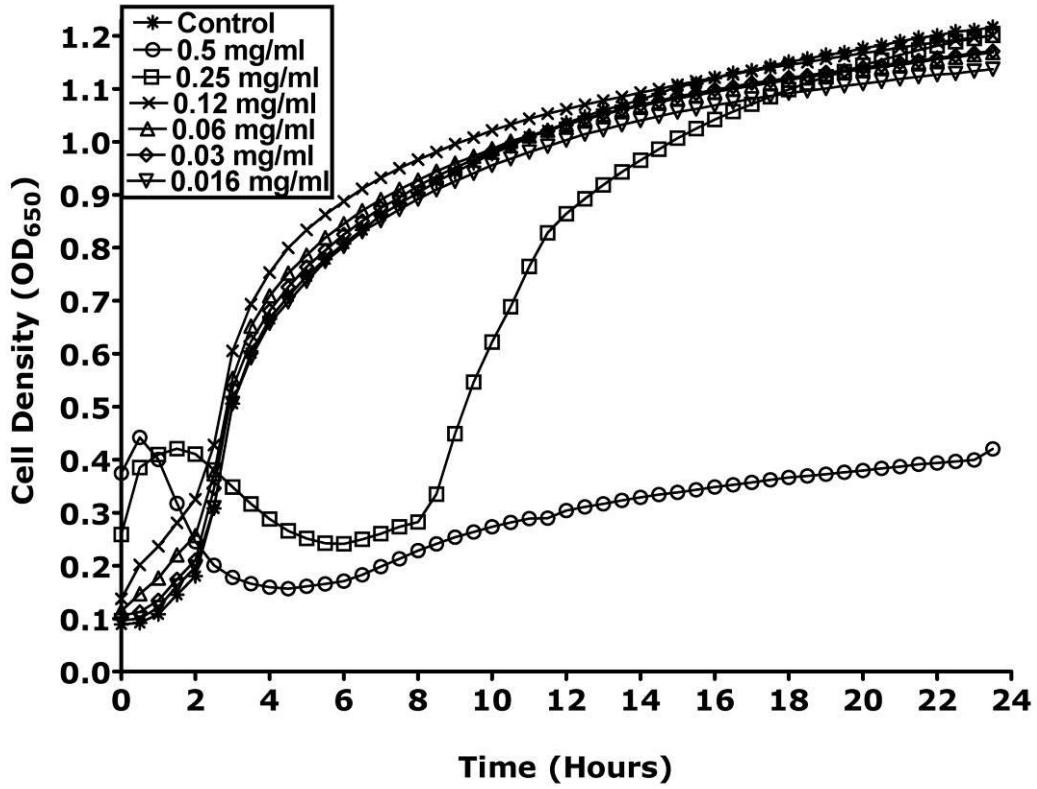

Figure 3.23 *E. coli* 1x10^7 cfu/ml incubated with 0.016–2.0 mg/ml NP108. MIC/MBC = 0.5 mg/ml NP108. N=6. S.E.M.

When incubated with 0.5 mg/ml NP108, *E. coli* displayed a slow rise in optical density after 5 hours incubation and a final bacterial density of 0.4 after 24 hours incubation. Though checking of bacterial viability through MBC analysis confirmed no viable bacteria, this slowing increasing bacterial density was most likely due to the presence of slowly growing persister bacterial cells. This was similar to what was observed in 1x10^7 cfu/ml *E. coli* culture incubated with 0.31 mg/ml NP101 (Figure 3.17).

b) *Staphylococcus aureus*

At all concentrations below recorded MIC for NP108 the growth of *S. aureus* 1x10^6 and 1x10^7 cfu/ml peptide-incubated cultures were similar to that of control at all time points (Figures 3.24 and 3.25).

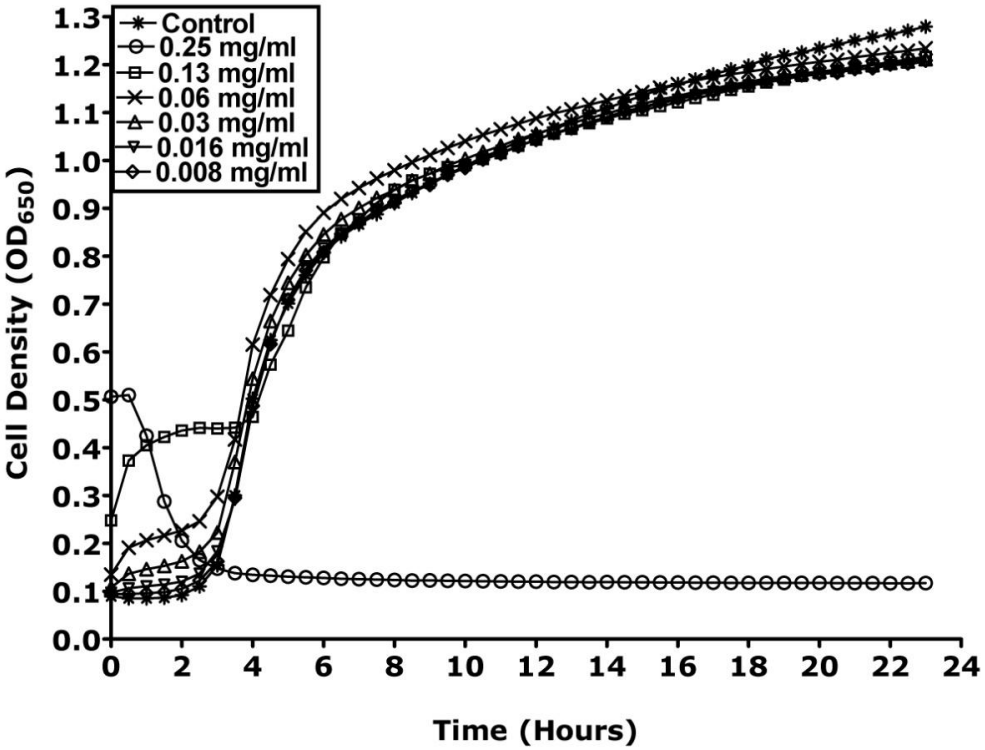

Figure 3.24 *S. aureus* 1x10^6 cfu/ml incubated with 0.008–1.0 mg/ml NP108. MIC/MBC = 0.25 mg/ml NP108. N=6. SDM.

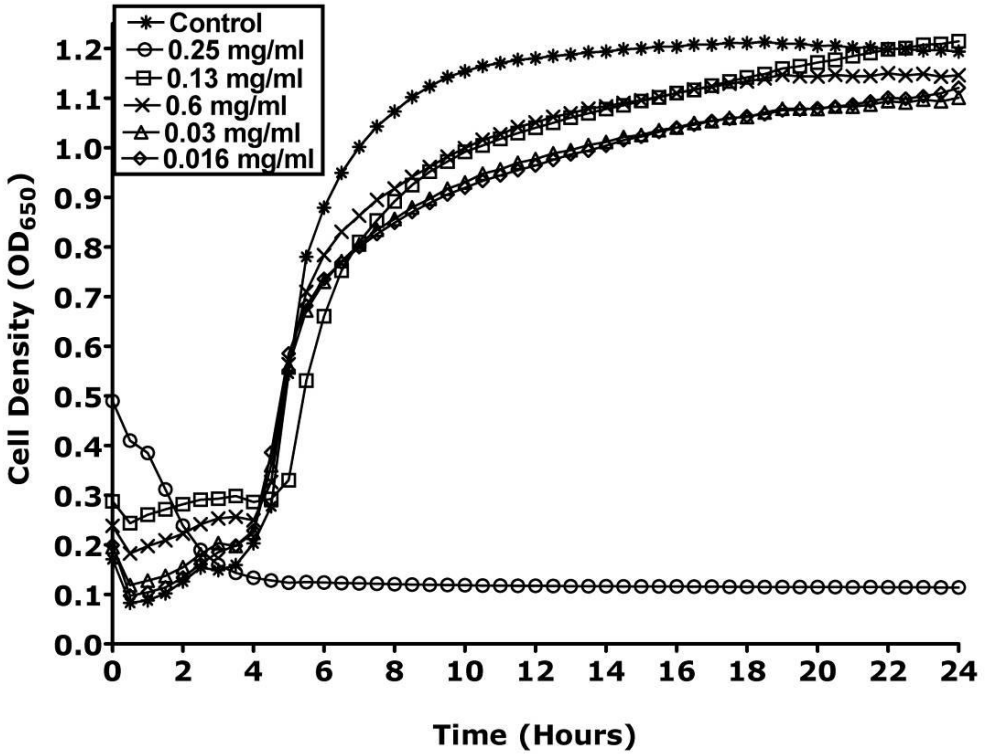

Figure 3.25 *S. aureus* 1x10^7 cfu/ml incubated with 0.016–2.0 mg/ml NP108. MIC/MBC = 0.25 mg/ml NP108. N=6. S.E.M.

The all or nothing effect previously seen with $1x10^6$ cfu/ml *S. aureus* incubated with NP101 was displayed by both $1x10^6$ and $1x10^7$ cfu/ml *S. aureus* incubated with NP108. Obviously the effects of NP108 exerted upon *S. aureus* were more tolerable and no struggle by the $1x10^7$ *S. aureus* culture was evidenced.

c) *Pseudomonas aeruginosa*

P. aeruginosa $1x10^6$ cfu/ml incubated with NP108 (Figures 3.26) displayed similar bacterial growth to control, except for bacteria incubated with 0.13 mg/ml NP108, which exhibited a marginal reduction in final cell density of bacterial growth compared to control. The all or nothing effect previously seen with $1x10^6$ cfu/ml *P. aeruginosa* incubated with NP101 was again displayed by $1x10^6$ cfu/ml *P. aeruginosa* incubated with NP108.

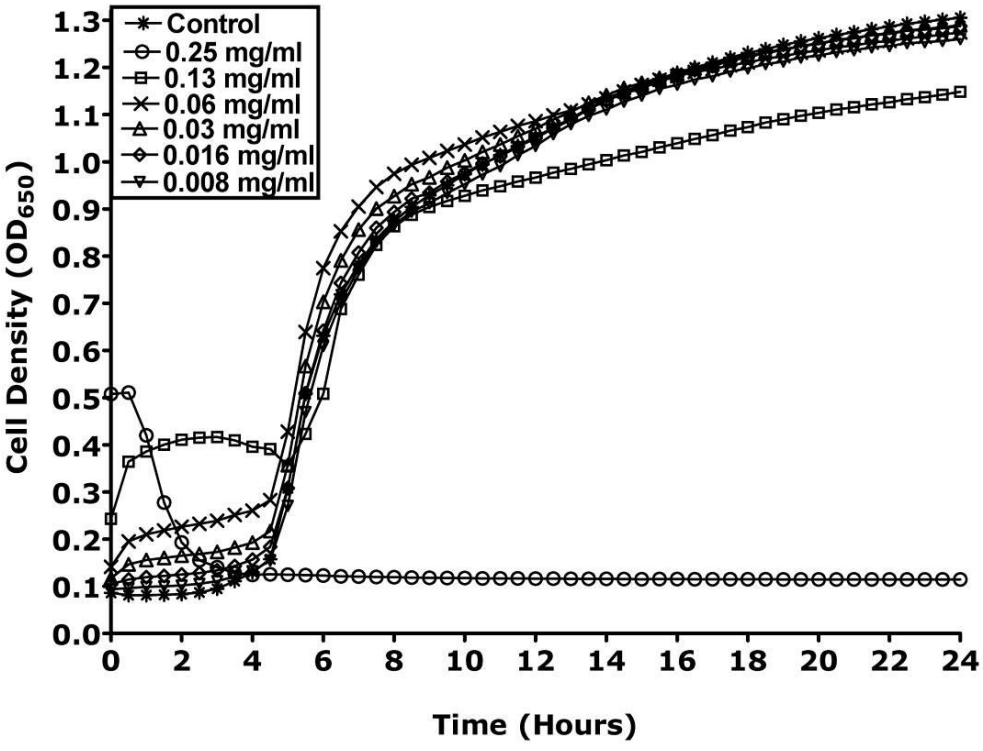

Figure 3.26 *P. aeruginosa* $1x10^6$ cfu/ml incubated with 0.008– 1.0 mg/ml NP108. MIC/MBC = 0.25 mg/ml NP108. N=6. S.E.M.

Equivalent growth to control was recorded for *P. aeruginosa* $1x10^7$ cfu/ml cultures incubated with all but the highest tolerated concentration of NP108 0.25mg/ml, which displayed combined retardation of onset of log phase with reduction in logarithmic bacterial growth (Figures 3.27). A similar growth pattern to that displayed by $1x10^7$ cfu/ml *P. aeruginosa* culture incubated with 0.16 mg/ml NP101 was displayed by the $1x10^7$ cfu/ml *P. aeruginosa* culture incubated with 0.25 mg/ml NP108, that of severely retarded onset of logarithmic growth and reduction in logarithmic growth. The presence of a higher bacterial density assisted the bacteria in tolerating a higher CAP concentration.

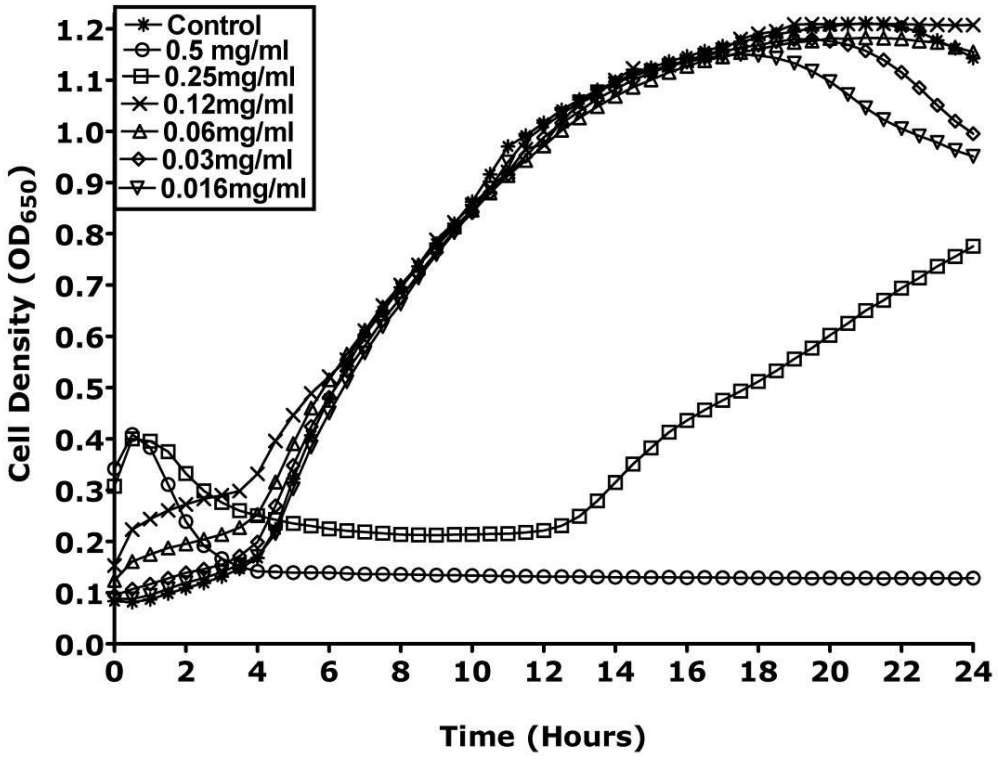

Figure 3.27 *P. aeruginosa* $1x10^7$ cfu/ml incubated with 0.016– 2.0 mg/ml NP108. MIC/MBC = 0.5 mg/ml NP108. N=6. S.E.M.

3.4 Discussion

3.4.1 Optimum bacterial growth

The final OD_{650} readings of bacterial growth under macro broth oxygenated and micro-titre plate conditions were similar at 24 hours. Higher bacterial growth was recorded with micro titre incubation due to the ratio of surface area to volume being six times higher (0.25) for a micro titre well containing 200 µl of culture compared to that of the 250 ml Erlenmeyer conical flask (0.0417) containing 100 ml of culture. This resulted in greater availability of oxygen to bacteria thus higher bacterial growth was recorded within the plate reader. Consequently, this automated analysis of bacterial growth was ideal for investigation of the effects of the test antimicrobials and strains to quantify activity.

3.4.2 Triclosan activity

MICs of triclosan against test bacteria correlated well with those in published literature: 128 µg/µl triclosan against *P. aeruginosa*, 0.09 µg/µl triclosan against *E. coli* and 0.01 µg/µl triclosan against *S. aureus.* (Chuanchuen, Karkhoff-Schweizer and Schweizer 2003)(Aiello et al. 2004)(Gomez- Escalada et al. 2005). De-sensitisation of *E. coli* to triclosan appeared to show a retained tolerance to triclosan, this is also in agreement with work previously undertaken by Russell *at al* (Russell 2004).

The effects of triclosan on the bacterial growth of all three test bacteria were revealed as concentration dependent retardation of onset of log phase bacterial growth and subsequent reduction in logarithmic bacterial growth compared to control. Retardation in onset of log phase bacterial growth was greatest in the $1x10^6$ cfu/ml *E. coli* and *S. aureus* incubated cultures (Figures 3.3 and 3.7), but

markedly reduced in the growth of the bisphenol incubated with either $1x10^6$ *P. aeruginosa* (Figure 3.9) or $1x10^8$ cfu/ml cultures of *E. coli* and *S. aureus* (Figures 3.4 and 3.8). However, the growth kinetics observed in these experiments demonstrated a marked impact upon both growth rate and final cell density achieved. These effects exerted on the test bacteria are attributable to the ability of triclosan to inhibit fatty acid synthesis and thus reduce bacterial growth (Escalada et al. 2005)(McMurray, Oethinger and Levy 1998)(Heath et al. 2000). Work published by Escalada *et al* on *E. coli* and *S. aureus* has also shown a concentration dependent retardation in onset of bacterial growth together with a non-concentration dependent reduction in logarithmic bacteria growth (Gomez- Escalada et al. 2005). This is not in agreement with the findings in this study where a concentration dependent inhibition in logarithmic growth has been shown in the $1x10^6$ and $1x10^8$ cfu/ml triclosan incubated cultures of *E. coli*. A concentration dependent inhibition in logarithmic growth has also been shown in the $1x10^6$ cfu/ml *S. aureus* culture incubated with triclosan (Figure 3.7). Conversely, *S. aureus* $1x10^8$ cfu/ml triclosan culture displayed a non-concentration dependent reduction in logarithmic bacterial growth. The concentration dependent reduction in log phase bacterial growth was most visible in *S. aureus* $1x10^6$ cfu/ml culture (Figure 3.5). This reduction in logarithmic bacterial growth was much less visible in triclosan incubated *E. coli* cultures, with the exception of bacteria incubated with the highest tolerated triclosan concentrations. (Figure 3.3) The final OD_{650} readings of all triclosan incubated cultures of *E. coli*, *S. aureus* and *P. aeruginosa* were significantly different from untreated cultures, which is also different to the findings of Gomez Escalada and colleagues which were also conducted over a 24 hour period (Gomez- Escalada et al. 2005).

The growth of *P. aeruginosa* $1x10^6$ cfu/ml culture, though incubated with a far higher range of triclosan concentrations than either *E. coli* or *S. aureus*, revealed the least retardation in bacterial growth. The non-concentration dependent reduction in final bacterial density of triclosan incubated *P. aeruginosa* compared to control was coupled with a concentration dependent reduction in log phase bacterial growth. Historically, *Ps. aeruginosa* has been accepted as resistant to triclosan through possession of a single multi-drug RND efflux pump (Chuanchuen, Karkhoff-Schweizer and Schweizer 2003). However the research presented here has revealed triclosan exerted the same effects on this bacterium as have been shown for *E. coli* and *S. aureus*. Triclosan incubated *E. coli* and *S. aureus* $1x10^8$ cfu/ml cultures, revealed a much-reduced retardation in logarithmic growth. This suggests that at higher bacterial inoculum, bacteria displayed a greater tolerance to the biocide.

E. coli that had been serially passaged in triclosan was investigated after 48 and 96 hours incubation with the bisphenol and though the MIC had risen dramatically, the effects of triclosan on retardation of onset of logarithmic bacterial growth and retardation in this growth were still visible. Long-term exposure to triclosan therefore does not appear to permit *E. coli* to develop an ability to completely withstand the effects of triclosan but exposure to the bisphenol does permit *E. coli* to develop tolerance to the biocide, which is manifested in higher MIC values.

The growth pattern of triclosan incubated *S. aureus* was also different to that displayed by control bacteria (Figures 3.7 and 3.8). Un-treated *S. aureus* displayed onset of a second phase of exponential logarithmic bacterial growth a number of hours after initiation of logarithmic growth. This bacterial growth pattern was absent from the growth of triclosan incubated $1x10^6$ and $1x10^7$ *S. aureus*. The inference that can be drawn from this is that a brake or restraint on *S. aureus*

growth had been removed and total bacterial numbers trebled within one hour. The inhibition of this dual phased bacterial growth in *S. aureus* by triclosan cannot be explained by inhibition of fatty acid synthesis, as exponential bacterial growth does occur in *S. aureus* triclosan incubated bacteria, once growth has commenced. Nor can it be explained by efflux of triclosan from *S. aureus*, as this would increase tolerance to the bisphenol by the bacterium. Perhaps triclosan interfered with quorum sensing in *S. aureus,* which resulted in the altered growth pattern of triclosan-incubated bacteria compared to control. Bacteria communicate for two purposes, to assist in conjugation and in adaptation to the environment (Lyon and Novick 2004). Gram-positive bacteria employ small peptides for both signalling purposes whereas Gram-negative bacteria employ homoserine lactones (Lyon and Novick 2004). The ability of bacteria to communicate with each other has resulted in the evolution of structured colonies which mutually co-operate to promote increased adaptation to environmental conditions (Ben Jacob et al. 2004). Synthesis changes in enzymes such as proteases and lipases involved with the spread and nutrition of *S. aureus* have been shown to occur in response to activation of the two-component *agr* system, which is activated by quorum sensing (Lyon and Novick 2004). Normal communication between un-treated *S. aureus* could be responsible for this dual phased logarithmic growth through stimulation of increased enzyme synthesis which resulted in the observed growth pattern of *S. aureus* control cells.

3.4.3 Colistin activity

Currently, colistin is used clinically as a last resort option in the treatment of multi drug resistant *Ps. aeruginosa* infections (Nation and Li 2009). Resistance to colistin is rare but reports of clinical isolates tolerant to colistin have been reported. One

resistance mechanism is the development of an adaptive tolerance by *P. aruginosa* to colistin, through aminoarabinose modified lipid A (Cummins et al. 2009). Colistin MIC values determined against Gram-negative bacteria compare favourably with those recorded by Li *et al* (Li et al. 2005)(Li et al. 2006). MIC values of 200 µg/ml were recorded for colistin against *S. aureus* NCTC 6571 in this investigation, while Alhanout *et al* reported an MIC > 128 µg/ml for *S. aureus* ATCC 25923 (Alhanout et al. 2010). The high MIC values can perhaps be explained by the imperviousness of the outer cell wall of the Gram-positive bacterium to colistin, given that colistin is predominantly reported in literature as being membrane active (Li et al. 2005). Cummins *et al* reported an MIC of 2.4 µg/ml for colistin against wild type *P. aeruginosa,* comparable to 1.5 µg/ml colistin reported in this work (Cummins et al. 2009). Growth of all three $1x10^6$ cfu/ml test bacterial cultures incubated with colistin (Figures 3.10, 3.12 and 3.14) also demonstrated the concentration dependent dual effects of retardation in onset of log phase bacterial growth, coupled with minimal reduction in final bacterial density compared to control. These dual effects were markedly reduced in the colistin incubated $1x10^7$ cfu/ml cultures of all test bacteria. (Figure 3.11, 3.13 and 3.15) This concurs with the triclosan findings, where the higher bacterial inoculum resulted in greater bacterial tolerance to the antibacterial employed. Colistin may affect the metabolic activities of the test bacteria in order to retard onset of logarithmic growth and reduce final bacterial density compared to that of control. Clauselle *et al* have suggested the mechanism of action of colistin at MIC concentration is through alteration of lipid regulation between the phospholipid interfaces bounding the periplasmic space (Clausell et al. 2003). Such effects on lipid regulation would certainly account for both the observed retardation in onset of log growth and reduction in final bacterial density.

Biphasic growth was also displayed by *S. aureus* control and colistin incubated bacteria (Figures 3.12 and 3.13). This biphasic growth exhibited by *S. aureus* control bacteria was absent from the growth of *S. aureus* triclosan incubated bacteria and this distinguishes the effects that colistin and triclosan exerted on the growth kinetics of *S. aureus.* Growth of untreated and colistin treated *S. aureus* displayed similar growth patterns; therefore no interference in the trigger that prompted onset of the dual phased logarithmic growth was exerted by colistin.

3.4.4 CAP activity

The MIC/MBC values recorded for all the CAPs tested correlated well with those determined by Novabiotics (D. Mercer, Personal communication, 2009). MICs and MBCs of all CAPs tested in this investigation coincided; several researchers have reported this phenomenon of identical MIC/MBC values for CAPs and there are many such reports in published literature (Marr, Gooderham and Hancock 2006)(Lai et al. 2008). Graphs of all three $1x10^6$ cfu/ml bacterial species incubated with NP101 and NP108 (Figures 3.16, 3.18, 3.20, 3.22, 3.24 and 3.26) displayed identical growth patterns equivalent to control at all time points. No dose dependent response to CAPs was shown by any of the test bacteria, suggesting a very fast bacteriostatic/ bactericidal onset of action, as has been attributed to CAPs in published literature (Brogden 2005). The bacterial growth of $1x10^6$ cfu/ml cultures of the test bacteria displayed an all or nothing effect, bacteria grew displaying the same onset of logarithmic growth and final bacterial densities as the control bacteria or no growth was evident. Growth at half the MIC concentrations was similar to growth displayed by control, this is substantially different to the growth patterns displayed by the test bacteria in half MIC concentrations of triclosan and colistin, where the bacteria revealed delayed onset of logarithmic

growth and reduced final density compared to control. CAPs therefore affect the test bacteria in a different manner to triclosan and colistin. CAPs, permitting onset of log growth and similar final densities to control, do not target the metabolic processes of the bacteria at this bacterial density. The reported bactericidal effects of CAPs include, inhibition of DNA and protein synthesis, interference with cell division and disruption of gene regulation (Hale and Hancock 2007)(Zhang and Falla 2006)(Zaiou 2007)(Reddy, Yedery and Aranha 2004). NP101 and NP108 could exert a bactericidal effect on the test bacteria through exertion of one of these CAP attributed mechanisms of action.

The response of the $1x10^7$ cfu/ml cultures to NP101 and NP108 were markedly different. *E. coli* incubated with sub MIC concentration of NP101 displayed growth patterns similar to control. (Figure 3.17) This was in contrast to *E. coli* $1x10^7$ cfu/ml culture incubated with 0.25 mg/ml NP108 (Figure 3.23), which displayed reduction in onset of logarithmic growth and retardation in log phase bacterial growth compared to control.

S. aureus $1x10^7$ cfu/ml culture incubated with NP101 displayed the dual effects of retardation in onset of log phase coupled with reduction in logarithmic bacterial growth. (Figure 3.19) *S. aureus* $1x10^7$ cfu/ml culture incubated with NP108 displayed similar growth to control. (Figure 3.25) However the concentration of NP108 in which both *S. aureus* densities displayed growth, was identical. *S. aureus* $1x10^7$ cfu/ml culture was not able to tolerate a higher CAP concentration at an increased bacterial density.

P. aeruginosa $1x10^7$ cfu/ml incubated with NP101 and NP108 (Figures 3.21 and 3.27) displayed a struggle with the CAPs similar to *E. coli* at higher CAP concentrations; a markedly delayed onset of logarithmic growth combined with reduced logarithmic bacterial growth. The growth of *S. aureus* and *P. aeruginosa*

$1x10^7$ cfu/m NP101 incubated cultures displayed a different effect exerted by the CAP on the increased bacterial densities; metabolic processes in *P. aeruginosa* are now being targeted as evidenced by the retarded onset of logarithmic bacterial growth and reduction in log growth. This effect was also seen in the growth of *E. coli* and *P. aeruginosa* $1x10^7$ cfu/ml NP108 incubated cultures; if metabolic processes were targeted this could account for the retarded onset of logarithmic bacterial growth and reduction in log growth. NP101 and 108 therefore exert different effects on bacterial cultures dependent on the density of bacteria present.

The biphasic growth pattern of *S. aureus* control was also absent in the growth of the CAP incubated bacteria (Figures 3.18, 3.19, 3.24 and 3.25) as has been previously shown with the triclosan incubated bacteria (Figures 3.17 and 3.18). This is in contrast to the growth of colistin incubated *S. aureus* (Figures 3.12 and 3.13) where the growth pattern of the un-treated and test bacteria was identical. The inference that can be drawn from these results is that triclosan, colistin and CAPs exert different and distinct effects to one another on the growth dynamics of *S. aureus.* This data suggests *S. aureus* was most affected by NP101 and NP108, followed by *P. aeruginosa* whilst *E. coli* appeared to tolerate the actions of the peptides best of the three test species.

3.5 Conclusion

In summary, dual effects of concentration dependent retardation in onset of logarithmic bacterial growth coupled with reduced logarithmic bacterial growth were visualised in all three test bacteria incubated with triclosan. This indicated that triclosan directly lengthened the replication time required by all test bacteria while also retarding the metabolic activity of each of the test bacterial species. Triclosan also affected the normal dual-phased growth pattern of *S. aureus* by abolishing the

presence of secondary logarithmic growth in triclosan incubated *S. aureus,* as displayed by control bacteria.

Colistin delayed onset of logarithmic growth in all test bacteria with slight reduction in final bacterial densities. The dual-phased growth of *S. aureus* was un-affected by incubation with colistin.

NP101 and NP108 exerted different actions on the test bacteria dependent on the bacterial densities present. An all or nothing effect was seen with all $1x10^6$ cfu/ml CAP incubated cultures, where either onset of bacterial growth and final bacterial density was equivalent to control or no growth was evident. This was markedly different to the delayed onset of logarithmic growth and reduced final bacterial densities displayed by the $1x10^7$ cfu/ml test bacterial cultures incubated with NP101 and NP108. As with triclosan incubated *S. aureus,* the growth pattern displayed by control bacteria was not displayed when *S. aureus* was incubated with NP101 and NP108.

Chapter Four

Detection of cytoplasmic membrane damage by measuring loss of internal potassium induced by cationic antibacterials

4.1 Introduction

In Chapter 3 it was established that triclosan, colistin, NP101 and NP108 display extensive antibacterial activity. The manner in which these compounds exert their antibacterial activity on the test species now has to be considered. An essential requirement of all living organisms is a fully functional selectively permeable biological membrane, such as the cytoplasmic membrane in bacterial cells (Xu, Tillman and Tang 2009)(Singleton 1999). Interaction of an antimicrobial with bacterial cell membranes could result in any or all of the following; partial leakage of intracellular solutes, disruption of membrane associated metabolic activity, specific or non-specific changes in membrane permeability and cell lysis (Denyer and Russell 2004)(Singleton 1999). Quantification of leaked intracellular solutes has been an effective means for the detection of membrane damage induced by antibacterial agents (Denyer and Russell 2004). As loss of intracellular potassium is known to be the first sign of membrane damage resulting in permeability (Denyer and Russell 2004), the quantification of potassium leakage from bacterial cells was selected as the method to examine membrane activity in the test antibacterial agents.

Normally potassium ions can be transported efficiently through bacterial membranes via the varied specific potassium ion channels such as KcsA and Trk (Chongsiriwatana and Barron 2010). Potassium plays a number of significant roles in bacterial cells, one being as a cytoplasmic-osmotic solute. Potassium influx into the bacterial cell occurs in response to osmotic up-shift, thereby permitting bacteria

to retain cell water in media with elevated osmolality, as occurs in *E. coli* through the Trk system (Epstein 2003)(Singleton 1999). Conversely, potassium efflux from the bacterial cell via for example the MscL channel in *E. coli* occurs when the osmolality of the media decreases (Epstein 2003)(Singleton 1999). Another significant role played by potassium is the activation or induction of enzymes and transport systems enabling cell adaptability to elevated osmolality: as in the Kdp transport system in *E. coli*, which is induced by potassium in conditions of high osmolality (Singleton 1999). A further role for potassium is to promote uptake or synthesis of compatible solutes; these are small molecules that can be accumulated at high concentrations within the cell without adversely affecting cell viability (Epstein 2003)(Singleton 1999)(Roosild et al. 2009). These compatible solutes replace some of the accumulated intracellular potassium ions, which are physiologically less friendly if present in high concentrations (Epstein 2003)(Singleton 1999). Potassium is also responsible for regulation of internal pH of bacterial cells, achieved by proton displacement from buffer anions within the cell, an example being phosphate groups of nucleic acids. This process requires a mono-valent cation and potassium, being the major intracellular cation, fulfils an important function in this process (Roosild et al. 2009)(Epstein 2003).

Historically it has been accepted and data supports the proposition that triclosan and colistin are membrane active agents, while many research groups have attributed membrane activity as one of several mechanisms of action of CAPs (Hale and Hancock 2007)(Reddy, Yedery and Aranha 2004). Several studies have shown that triclosan interacts with the bacterial cytoplasmic membrane and these research groups have suggested triclosan exerts antibacterial activity through damage to this structure (Villalaín et al. 2001)(Gomez- Escalada et al. 2005). Triclosan has also been shown to possess a slow, competitive, irreversible mechanism of action

by inhibition of the bacterial enoyl-acyl carrier protein (ACP) reductase (FabI) at low concentrations (Gomez- Escalada et al. 2005)(Levy et al. 1999).

Colistin is tightly bound to the lipid A component of LPS in the outer membrane of Gram-negative bacteria (Falagas, Rafailidis and Matthaiou 2010)(Falagas et al. 2010)(Denyer and Russell 2004). Distortion of the outer membrane leaflet occurs, segments of which are released and the permeability barrier destroyed (Falagas, Rafailidis and Matthaiou 2010)(Denyer and Russell 2004). Colistin then targets the cytoplasmic membrane, binding to phospholipids, disrupting membrane integrity and inducing irreversible leakage of cell components (Falagas, Rafailidis and Matthaiou 2010)(Falagas et al. 2010)(Denyer and Russell 2004). Colistin is much less active against Gram-positive species.

It was long considered that the sole antibacterial mechanism of action of CAPs was membrane disruption, however non-membrane bacterial targets have been reported either in addition or alternative to membrane activity (Hale and Hancock 2007)(Reddy, Yedery and Aranha 2004). These attributed mechanisms of action include interference with bacterial septation, inhibition of nucleic acid or protein synthesis, or disruption of cell wall synthesis and cell division (Hale and Hancock 2007)(Reddy, Yedery and Aranha 2004).

This phase of the work was therefore undertaken to examine the activity of test antimicrobial agents upon the cytoplasmic membrane of the selected bacteria, through quantification of potassium loss when exposed to the antimicrobials.

4.2 Methodologies

4.2.1 Detection and quantification of K^+ levels in extra pure de-ionised water and 1% SDS

The K^+ content of ultra pure de-ionised water and SDS was checked in triplicate prior to each experiment as described in Section 2.7.3.

4.2.2 Development of experimental protocol suitable for examination of K^+ loss from cationic antibacterial – treated bacteria

The purpose of the experimental work in this section was solely to refine the assay for measuring cationic antibacterial-induced K^+ loss. Samples were taken at times 0, 2, 5 and every 5 minutes thereafter until sixty minutes or at hourly intervals from time zero to eight hours and also at 24-hours. The effect of various parameters upon K^+ loss was investigated using the basic methodology described in Section 2.7.3. All glassware and plastic ware were steeped in ultra pure de-ionised water for 24 hours prior to the K^+ detection experiments to minimise the leeching of K^+ from the glass/plastic ware into the experimental media.

Glass flasks were used in addition to polymethylpentene flasks for K^+ detection in colistin and NP108 experiments, as both these compounds are known to bind to plastics. Experiments were performed in which different bacterial densities were employed, initially 1×10^7 cfu/ml and then 1×10^6 cfu/ml.

4.2.3 Quantification of total cytoplasmic K^+ present in *E. coli*, *S. aureus* and *P. aeruginosa*

Total intracellular bacterial K^+ was quantified using the sonication method as described in Section 2.7.2.

4.2.4 Examination of the effect of 1% SDS and 5% chlorhexidine on K^+ loss from *E. coli*, *S. aureus* and *P. aeruginosa*

Bacterial K^+ loss induced by 1% SDS and 5% chlorhexidine was undertaken as described in Section 2.7.3. The quantification of K^+ loss in the test bacteria induced by incubation with known membrane permeable agents (SDS and chlorhexidine) was undertaken to check the robustness of the optimised protocol and for comparison purposes with the K^+ loss induced by the test cationic antibacterial agents.

4.2.5 Examination of the effects of triclosan, colistin and NP108 on K^+ loss from cells of *E. coli*, *S. aureus* and *P. aeruginosa*

Bacterial K^+ loss induced by incubation with triclosan, colistin or NP108 was undertaken as described in Section 2.7.3.

4.3 Results

4.3.1 Detection and quantification of K^+ levels in extra pure de-ionised water and 1% SDS

The K^+ content of ultra pure de-ionised water was checked in triplicate prior to each experiment and recorded as zero on every occasion. The K^+ content of known

potassium standards was assessed before and after addition of 1% SDS. Samples containing only 1% SDS were also checked for K^+ content. The results obtained are displayed in Table 4.1.

K^+ standard (mg/L)	K^+ content measured (mg/L)	K^+ content measured after addition of 1% SDS (mg/L)	Difference in K^+ content measured (mg/L)
0.2	0.204	0.541	0.337
0.4	0.415	0.940	0.525
0.6	0.562	0.806	0.244
0.8	0.815	1.134	0.319
1.0	1.036	1.305	0.269
1% SDS	0.251	N/A	N/A

Table 4.1 Assessment of K^+ content (mg/L) in 1% SDS via flame photometer. Potassium concentrations shown represent the mean from three experiments. Sample volume was 10ml. N/A = Not applicable

1% SDS added 0.251 mg/L K^+ to 10 ml sample volume or 0.02 mg/L to each sample volume of 800 µl assayed for K^+ content in these experiments.

4.3.2 Detection and quantification of K^+ levels in 5% chlorhexidine

The K^+ content of ultra pure de-ionised water and known potassium standards were assessed before and after the addition of 5% chlorhexidine. Samples only containing 5% chlorhexidine were also checked for K^+ content. The results obtained are displayed in Table 4.2. 5% chlorhexidine added 0.066 mg/L K^+ to 10 ml sample volume or 0.0053 mg/L to each sample volume of 800 µl assayed for K^+ content in these experiments.

K^+ standard (mg/L)	K^+ content measured (mg/L)	K^+ content measured after addition of 5% chlorhexidine (mg/L)	Difference in K^+ content measured (mg/L)
0.1	0.104	0.175	0.071
0.2	0.205	0.280	0.075
0.3	0.310	0.398	0.088
0.4	0.415	0.485	0.07
0.5	0.516	0.585	0.069
5% chlorhexidine	0.066	N/A	N/A

Table 4.2 Assessment of K^+ content (mg/L) in 5% chlorhexidine via flame photometer. Potassium concentrations shown represent the mean from three experiments. Sample volume was 10ml. N/A = Not applicable

4.3.3 Development of an experimental protocol suitable for examination of K^+ loss from cationic antibacterial – treated bacteria

4.3.3.1 Comparison of the results obtained with ~1 x 10^6 cfu/ml and ~1 x 10^7 cfu/ml bacterial populations

Determination of K^+ content in samples taken from ~1 x 10^6 cfu/ml and ~1 x 10^7 cfu/ml bacterial populations, was the initial step in the development of an assay to quantify K^+ loss induced in bacteria incubated with triclosan, colistin or NP108. Results gained through experimental work demonstrated that K^+ leakage induced through incubation with an antimicrobial agent in a bacterial culture density of 1x10^6 cfu/ml for each test bacterial species was accurately quantifiable by flame photometer. Sample dilution was not required and this bacterial concentration was employed for all further K^+ assays.

4.3.4. Quantification of total K^+ present in *E. coli*, *S. aureus* and *P. aeruginosa*

The total K^+ content of *E. coli*, *S. aureus* and *P. aeruginosa* (re-suspended in ultra pure K^+ free de-ionised water) obtained through sonication, is shown in Table 4.3.

Bacterial species	Density (cfu/ml)	Concentration of K^+ (mg/L)	Bacterial viability after 24 hours (cfu/ml)
E. coli un-sonicated control	$1x10^6$	0.293	4.76×10^6
E. coli sonicated sample	$1x10^6$	3.20	< 10
E. coli un-sonicated control	$1x10^7$	0.422	8.7×10^7
E. coli sonicated sample	$1x10^7$	3.62	< 10
S. aureus un-sonicated control	$1x10^6$	0.096	5.2×10^6
S. aureus sonicated sample	$1x10^6$	2.80	< 10
S. aureus un-sonicated control	$1x10^7$	0.238	5.3×10^7
S. aureus sonicated sample	$1x10^7$	3.42	< 10
Ps. aeruginosa un-sonicated control	$1x10^6$	0.295	5.17×10^6
Ps. aeruginosa sonicated sample	$1x10^6$	3.20	< 10
Ps. aeruginosa un-sonicated control	$1x10^7$	0.42	$4.1x10^7$
Ps. aeruginosa sonicated sample	$1x10^7$	3.89	< 10

Table 4.3 Total K^+ content of bacterial cells. Data shown represented the mean from six experiments, each performed in triplicate. All cultures were prepared at time 0 to contain a cell density of $1x10^6$ cfu/ml

The total K^+ content of *E. coli* or *P. aeruginosa* $1x10^6$ cfu/ml culture obtained by sonication was identical at 3.2 mg/L, while slightly lower potassium content was recorded for *S. aureus* $1x10^6$ cfu/ml cells. Bacterial viability was checked after sonication for the three bacteria and recorded as <10 cfu/ml for all three bacterial species.

4.3.5 Quantification of loss of K^+ in *E. coli*, *S. aureus* and *P. aeruginosa* due to incubation with 1% SDS

K^+ loss in the test bacteria, induced by incubation with 1% SDS, is shown in Figure 4.1.

From Figure 4.1(a) it can be seen that 8% of total cell potassium was released from 1×10^6 cfu/ml *E. coli* bacteria within 5 minutes of being incubated with 1% SDS. Minimal further K^+ leakage was detected in *E. coli* control cells throughout the 7-hour experiment. Almost total K^+ loss was realised in *S. aureus* 1×10^6 cfu/ml bacteria (Figure 4.1b) within 5 minutes incubation with 1% SDS; though samples were assessed for potassium content for a further 415 minutes, the recorded K^+ content of samples remained constant. Partial leaching of K^+ from *S. aureus* control bacteria was detected after 2 hours, as might be anticipated given their re-suspension in ultra pure water. Approximately 11% of total potassium content was lost from *P. aeruginosa* 1×10^6 cfu/ml (Figure 4.1c) cells on incubation with 1% SDS; little leakage of K^+ was detected from the control cells over the 7 hour experimental period. Consequently it was deemed necessary to use an alternative membrane active agent to establish that full K^+ loss and complete loss of viability of the Gram-negative organisms could be achieved.

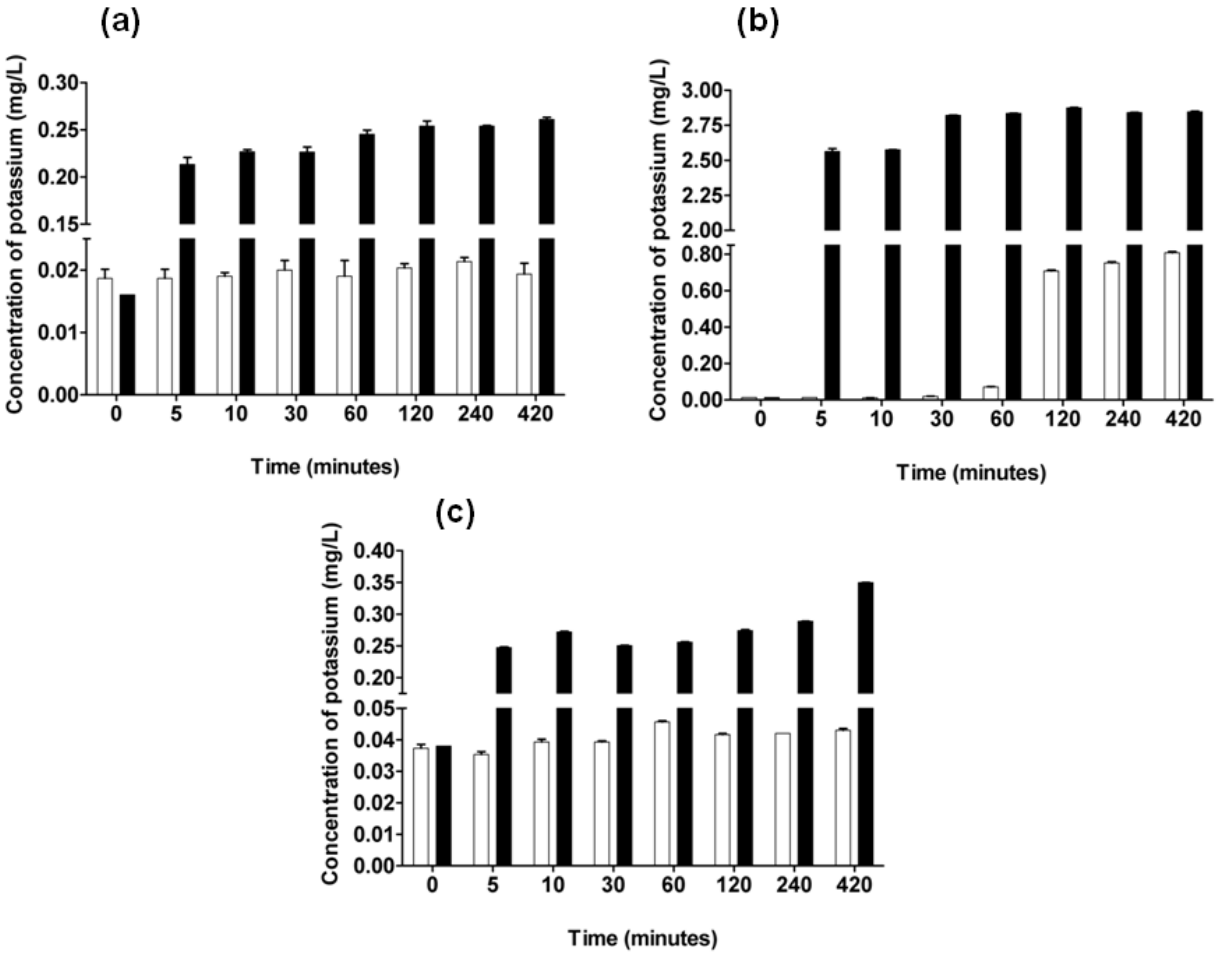

Figure 4.1 K^+ loss in bacteria induced by incubation with 1% SDS. N = 3. S.E.M. ☐ Control bacteria ■ Bacteria incubated with 1% SDS.

(a) *E. coli* $1x10^6$ cfu/ml culture: viability of *E. coli* control after 7 hours was 1.0×10^7 cfu/ml; viability of *E. coli* incubated with 1% SDS after 7 hours was < 10 cfu/ml. Total K^+ content of sonicated $1x10^6$ cfu/ml *E. coli* culture was 3.2 mg/L.

(b) *S. aureus* $1x10^6$ cfu/ml culture: viability of *S. aureus* control bacteria and *S. aureus* incubated with 1% SDS after 7 hours was < 10 cfu/ml. Total K^+ content of sonicated *S. aureus* $1x10^6$ cfu/ml culture was 2.8 mg/L.

(c) *P. aeruginosa* $1x10^6$cfu/ml culture: Viability of *P. aeruginosa* control bacteria after 7 hours was 5.0×10^6 cfu/ml; viability of *P. aeruginosa* incubated with 1% SDS after 7 hours was < 10 cfu/ml. Total K^+ content of sonicated $1x10^6$ cfu/ml *P. aeruginosa* culture was 3.2 mg/L.

4.3.6 Quantification of loss of K^+ in *E. coli*, *S. aureus* and *P. aeruginosa* due to incubation with 5% chlorhexidine

K^+ loss due to incubation with chlorhexidine is shown in Figure 4.2. Chlorhexidine is a biocide with a proven mechanism of action on bacterial membranes, leading to

loss of intracellular contents and it can be seen from Figure 4.2 that leakage of K^+ occurred in all three-test bacteria within 5 minutes incubation with chlorhexidine.

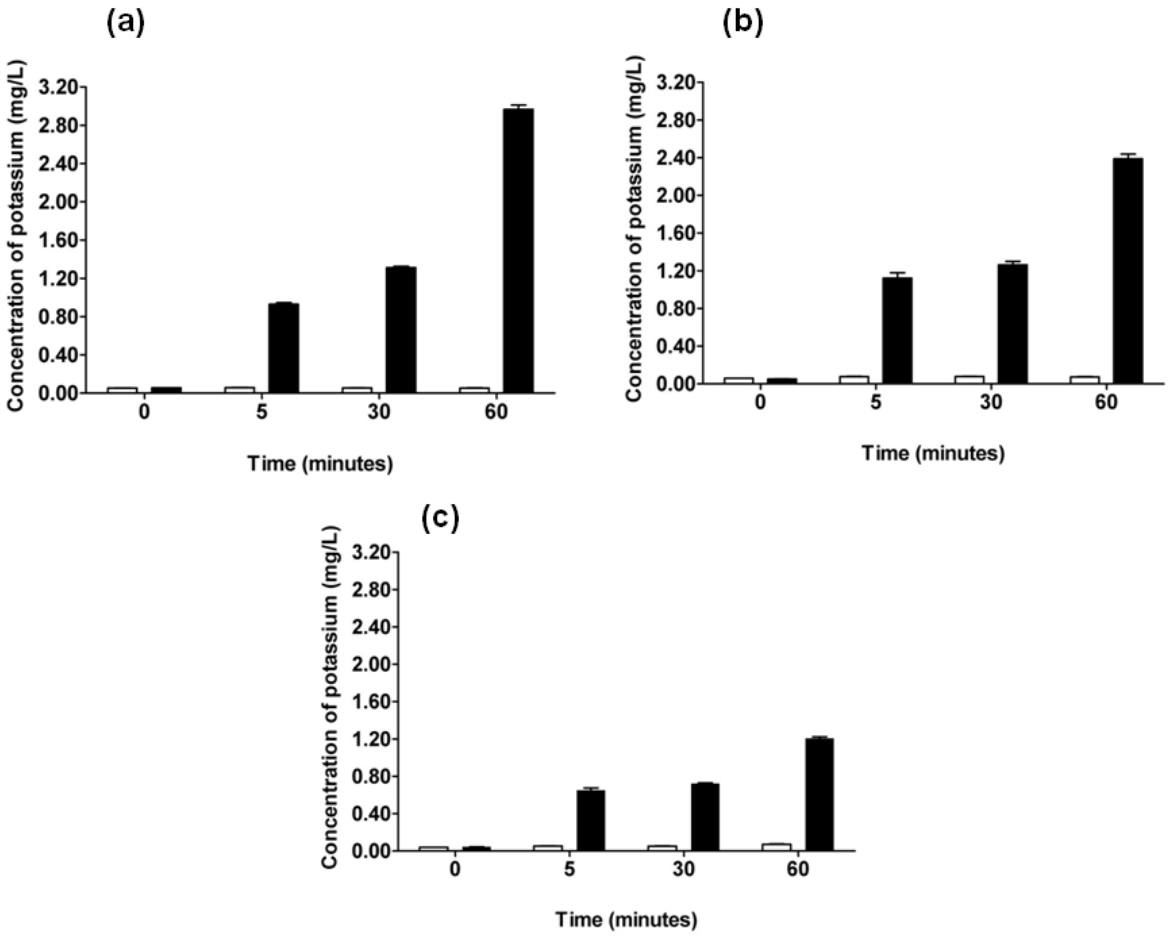

Figure 4.2 K^+ loss in bacteria induced by incubation with 5 % chlorhexidine. ☐ Control bacteria. ■ Bacteria incubated with 5 % chlorhexidine. N=3. S.E.M.
(a) *E. coli* $1x10^6$ cfu/ml culture: viability of *E. coli* control after 60 minutes was 4.3×10^5 cfu/ml; viability of *E. coli* incubated with 5 % chlorhexidine after 60 minutes was < 10 cfu/ml. Total K^+ content of sonicated $1x10^6$ cfu/ml *E. coli* culture was 3.2 mg/L.
(b) *S. aureus* $1x10^6$ cfu/ml culture: viability of *S. aureus* control bacteria after 60 minutes was $1.65x10^6$ cfu/ml; viability of *S. aureus* incubated with 5 % chlorhexidine after 60 minutes was < 10 cfu/ml. Total K^+ content of sonicated *S. aureus* $1x10^6$ cfu/ml culture was 2.8 mg/L.
(c) *P. aeruginosa* $1x10^6$ cfu/ml culture: Viability of *P. aeruginosa* control bacteria after 60 minutes was 2.4×10^4 cfu/ml; viability of *P. aeruginosa* incubated with 5 % chlorhexidine after 60 minutes was < 10 cfu/ml. Total K^+ content of sonicated $1x10^6$ cfu/ml *P. aeruginosa* culture was 3.2 mg/L.

Approximately 25% of total cell K^+ was lost from 1×10^6 cfu/ml *E. coli* (Figure 4.2a) within 5 minutes incubation with 5% chlorhexidine. The K^+ loss had risen to 40% total cell K^+ at 30 minutes and 93% loss of total intracellular K^+ at 60 minutes.

Minimal K^+ leakage was detected in *E. coli* control cells throughout the 60-minute experiment. K^+ release from 1 x 10^6 cfu/ml *S. aureus* (Figure 4.2b) incubated with 5% chlorhexidine was 40% of total cell K^+ within 5 minutes, with approximately 90% total K^+ lost from *S. aureus* cells after 60 minutes incubation with the biocide. Approximately 20% of total K^+ content was released from *P. aeruginosa* 1 x 10^6 cfu/ml (Figure 4.2c) cells within 5 minutes incubation with 5% chlorhexidine. At 60 minutes, the amount of intracellular K^+ that had bled from the bacterium had risen to 40%. Though total K^+ loss from *P. aeruginosa* incubated with 5% chlorhexidine was not recorded, no viable bacteria were produced when a viability check was performed after 60 minutes incubation in the biocide. These assays with SDS and chlorhexidine confirm that the protocol is sufficiently sensitive to accurately record the extent of K^+ lost from bacterial populations upon treatment with antimicrobials.

4.3.7 Quantification of K^+ loss in *E. coli*, *S. aureus* and *P. aeruginosa* upon incubation with cationic antibacterials

4.3.7.1 Quantification of K^+ loss from *E. coli* and *S. aureus* exposed to triclosan

K^+ loss over 24 hours from *E. coli* 1 x 10^6 cfu/ml cultures incubated with the MIC (0.07 μg/ml) and 10xMIC (0.7 μg/ml) of triclosan Figure 4.3(a) was quantified as 2 and 3% respectively. K^+ loss from the bacteria at 7 hours was statistically significant (p-value $<$ 0.001) between the control and 10xMIC triclosan incubated bacteria. At 24 hours a statistically significant difference in K^+ loss was recorded between the control and MIC incubated bacteria (p-value $<$ 0.01) and 10xMIC triclosan incubated cells (p-value $<$ 0.001). A statistically significant K^+ loss (p-value $<$ 0.001) was also seen between the treatment groups: MIC and 10xMIC concentrations at 7 and 24 hours.

(a)

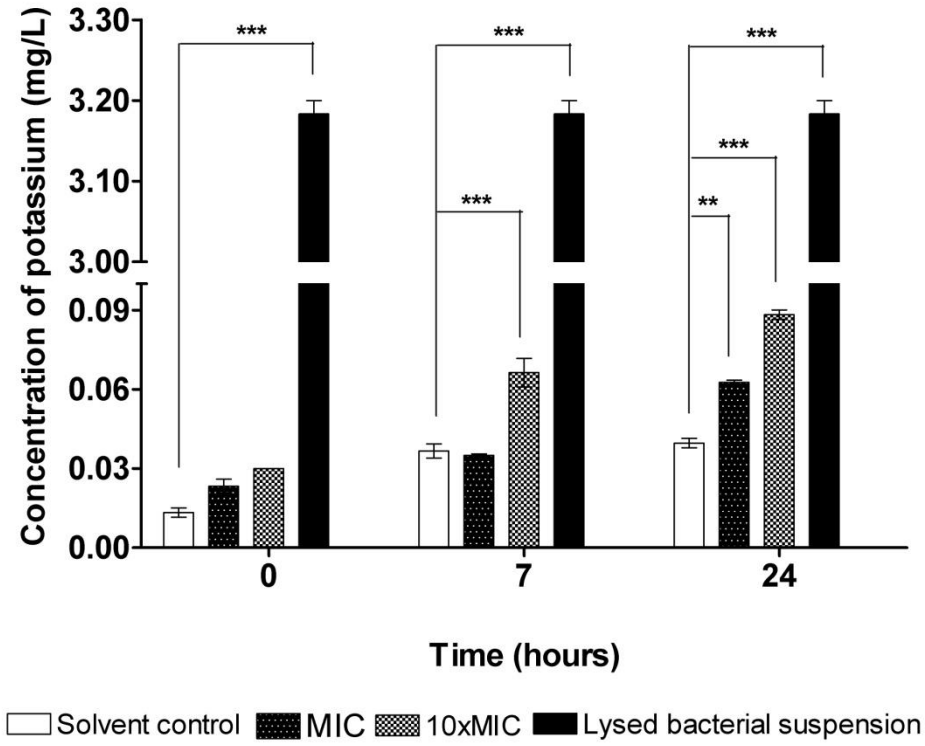

(b)

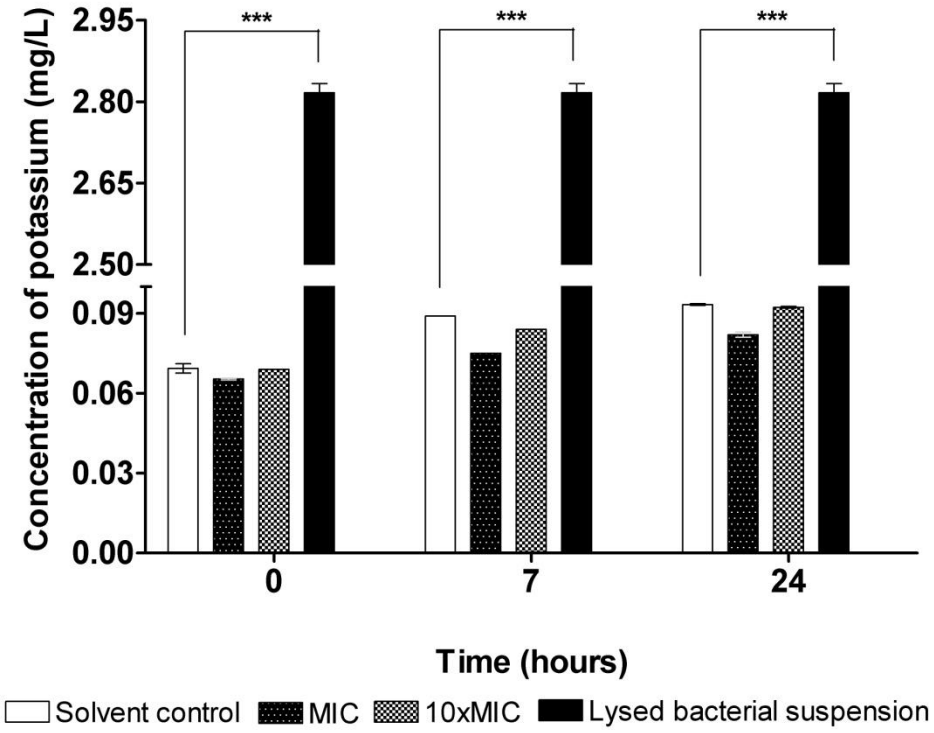

Figure 4.3 K^+ loss in bacteria induced by exposure to triclosan for 24 hours. Assessment of K^+ leakage was performed in triplicate on three occasions. (S.E.M.) * indicates *p*-value < 0.05, ** indicates *p*-values < 0.01, *** indicates *p*-value < 0.001

(a) *E. coli* $1x10^6$ cfu/ml culture: viability of *E. coli* control after 24 hours was 5.0×10^6 cfu/ml; viability of test bacteria after 24 hours was < 10 cfu/ml. Total K^+ content of

sonicated 1x10^6 cfu/ml *E. coli* culture was 3.2 mg/L. *E. coli* solvent control contained 3.44 μl DMSO.
(b) *S. aureus* 1x10^6 cfu/ml culture: viability of *S. aureus* control bacteria after 24 hours was 1.3 x 10^7 cfu/ml; viability of test bacteria after 24 hours was < 10 cfu/ml. Total K^+ content of sonicated *S. aureus* 1x10^6 cfu/ml culture was 2.8 mg/L. *S. aureus* solvent control contained 5.4 μl DMSO.

This means the quantity of K^+ lost by *E. coli* bacteria incubated with triclosan was dependent on the concentration of triclosan employed and the quantity of K^+ extruded from the test bacteria increased as the concentration and length of time the bacteria were exposed to triclosan increased compared to control bacteria. However, it must be noted that the total quantity of K^+ lost from *E. coli* due to incubation with triclosan was very low.

Partial leaching of K^+ from *S. aureus* control bacteria was noticed over the experimental period (Figure 4.3(b)), as might be anticipated given their re-suspension in ultra pure water. As with *E. coli* the loss of K^+ induced from *S. aureus* by exposure to triclosan was negligible and was equivalent to the 3% K^+ lost from control cells under experimental conditions. This means that leakage of K^+ from *S. aureus* cells was not solely dependent on the length of time or concentration of triclosan to which the test bacteria were exposed compared to control bacteria. However the extent of non-specific leaching was minimal, as can be seen in Figure 4.3(b). The very low level lost suggests triclosan does not induce K^+ loss, and by inference membrane disruption as a key mechanism of action in either *E. coli* or *S. aureus.*

4.3.7.2 Quantification of K^+ loss from *E. coli*, *S. aureus* and *P. aeruginosa* exposed to colistin

Loss of K^+ induced from *E. coli* 1 x 10^6 cfu/ml culture incubated with MIC (3 μg/ml) or 10xMIC (30 μg/ml) colistin for 24 hours is shown in Figure 4.4(a).

(a)

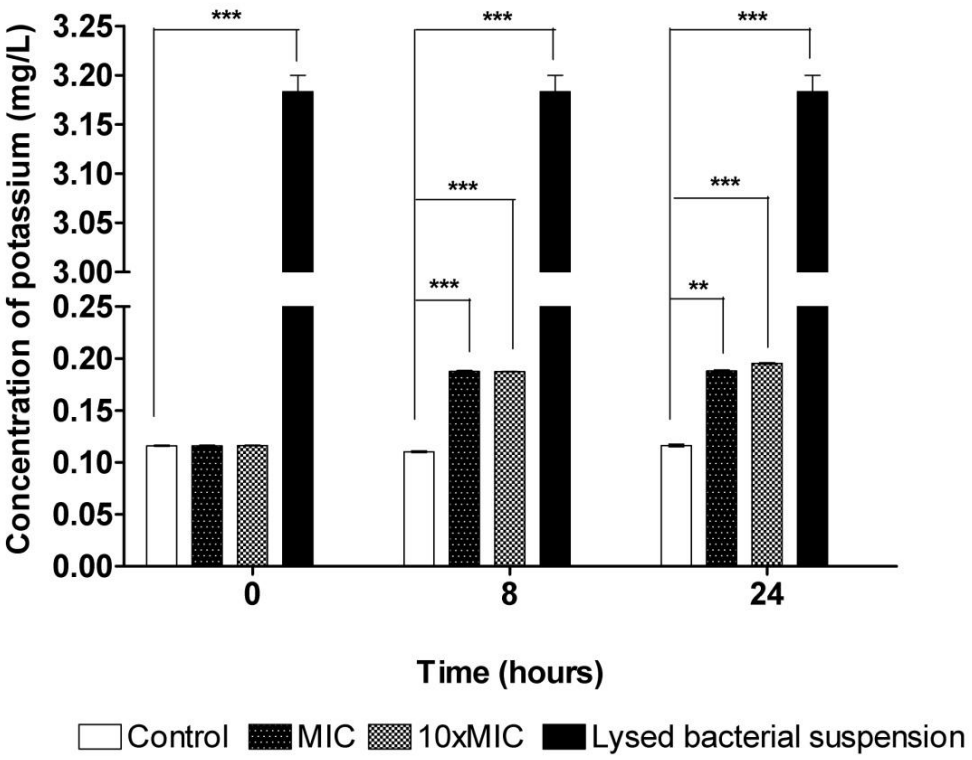

(b)

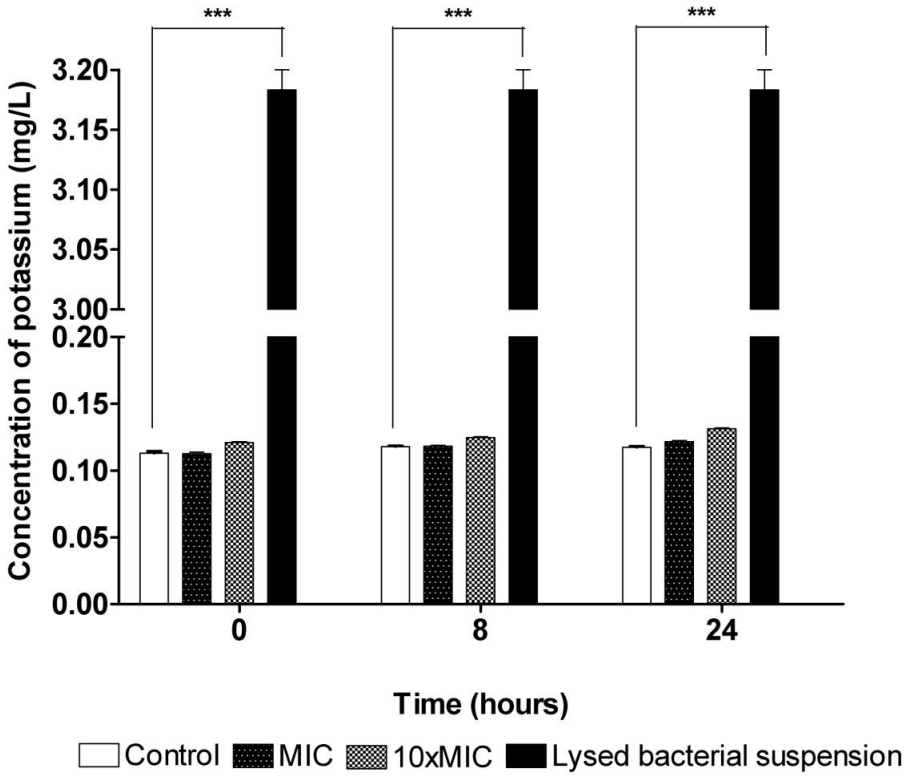

Figure 4.4 K^+ loss induced by incubation with colistin over 24-hours. Assessment of K^+ leakage was performed in triplicate on three occasions. S.E.M. * indicates *p*-value < 0.05, ** indicates *p*-values < 0.01, *** indicates *p*-value < 0.001.

(a) *E. coli* $1x10^6$ cfu/ml culture: viability of control bacteria after 24 hours was 7.0×10^6 cfu/ml; viability of test bacteria after 24 hours was < 10 cfu/ml. Total K^+ content of sonicated $1x10^6$ cfu/ml *E. coli* culture was 3.2 mg/L.
(b) *P. aeruginosa* $1x10^6$cfu/ml culture: Viability of control bacteria after 24 hours was 9.0×10^8 cfu/ml; viability MIC test bacteria after 24 hours was $1x10^7$ cfu/ml; viability 10xMIC test bacteria after 24 hours was $9x10^6$ cfu/ml. Total K^+ content of sonicated $1x10^6$ cfu/ml *P. aeruginosa* culture was 3.2 mg/L.

Colistin induced loss of approximately 6% of total K^+ content from *E. coli* cells incubated with either MIC or 10xMIC concentration, over 24 hours incubation. This statistically significant K^+ loss between control and test bacteria (p-value < 0.001) occurred within 5 minutes incubation with colistin (data not shown). Incubation of *E. coli* with colistin did not show any statistically significant difference in leakage of K^+ between MIC and 10xMIC test groups at 8 and 24 hours, meaning leakage of K^+ was not dependent on the length of time or concentration above a critical threshold of colistin to which *E. coli* was exposed. Minimal variation in the quantity of K^+ loss determined for samples over the 24-hour experimental period was recorded.

K^+ loss from *P. aeruginosa* 1×10^6 cfu/ml culture incubated with MIC (1.5 μg/ml) and 10xMIC (15 μg/ml) colistin for 24 hours is displayed in Figure 4.4 (b). *P. aeruginosa* incubated with MIC or 10xMIC colistin for 24 hours, resulted in loss of 4% of total K^+ content. This non-statistically significant K^+ loss (p-value > 0.05) from test compared to control cells was detected within 5 minutes incubation with the polymyxin (data not shown) and the recorded K^+ content of the samples remained constant thereafter. Incubation of *P. aeruginosa* with colistin did not show any statistically significant leakage of K^+ between test groups, meaning leakage of K^+ was not dependent on the length of time or concentration of colistin to which *P. aeruginosa* was exposed.

K^+ loss induced in the 1×10^6 cfu/ml *S. aureus* culture incubated with colistin for 60 minutes can be seen in Figure 4.5. A statically significant K^+ loss from test cells compared to control (p-value < 0.001) occurred within 5 minutes incubation of the

bacteria with colistin and the level of K^+ detected remained constant thereafter, even when assessed over 24 hours (data not shown). K^+ loss from *S. aureus* was also statistically significant between concentration groups of MIC (100 μg/ml) and 10xMIC (1 mg/ml) colistin incubated bacteria (*p*-value $<$ 0.001) at 5, 15 and 60 minutes. Approximately 36% of total K^+ content of 1 x 10^6 cfu/ml *S. aureus* cells was lost on incubation for 60 minutes with 10xMIC colistin, while the bacteria incubated with the MIC concentration lost approximately 7% of total bacterial K^+. A noteworthy point is that the MIC of colistin against *S. aureus* was recorded as 100 μg/ml, making 10xMIC concentration 1 mg/ml.

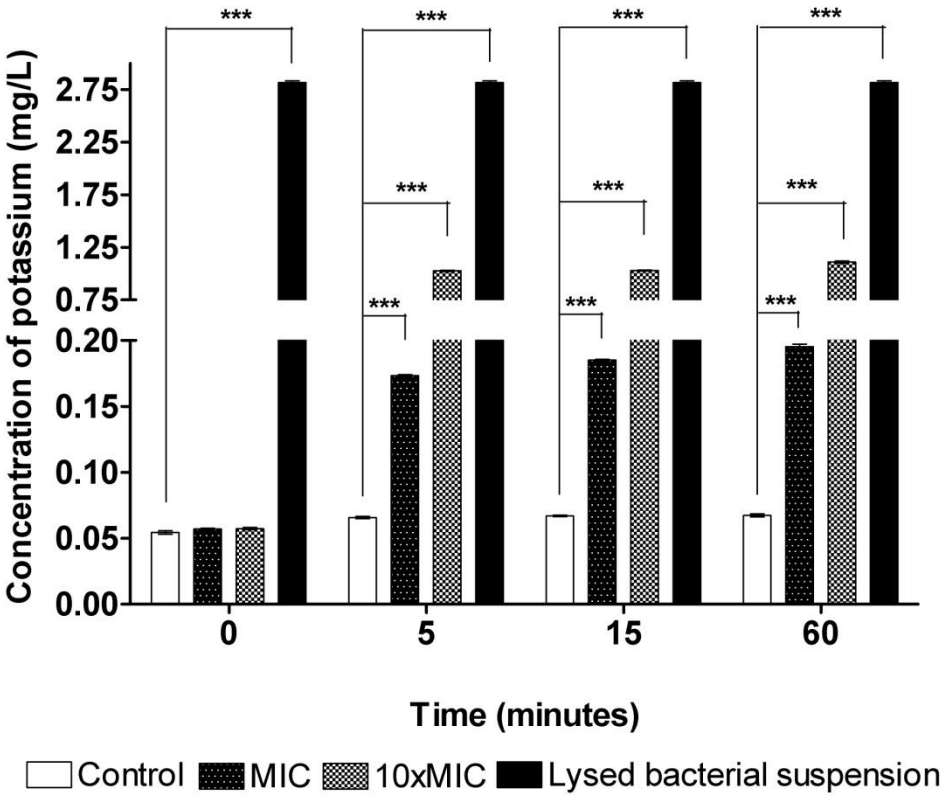

Figure 4.5 K^+ loss in 1 x 10^6 cfu/ml *S. aureus* induced by incubation with colistin for 60-minutes. Assessment of K^+ leakage was performed in triplicate on three occasions. S.E.M. * indicates *p*-value < 0.05, ** indicates *p*-values < 0.01, *** indicates *p*-value < 0.001. Viability of control bacteria after 24 hours was 6.3 x 10^6 cfu/ml; viability of test bacteria after 24 hours was < 10 cfu/ml. Total K^+ content of sonicated *S. aureus* 1x10^6 cfu/ml culture was 2.8 mg/L.

4.3.7.3 Quantification of K^+ loss in *E. coli*, *S. aureus* and *P. aeruginosa* due to NP108

K^+ loss induced in the 1 x 10^6 cfu/ml *E. coli* culture incubated with NP108 for 60 minutes can be seen in Figure 4.6. Approximately 38% of total K^+ content of 1 x 10^6 cfu/ml *E. coli* cells was lost on incubation with 2xMIC NP108, with 18% K^+ loss recorded for bacteria incubated with the MIC of NP108, while incubation with 1/20th MIC NP108 induced 7% K^+ loss from bacterial cells.

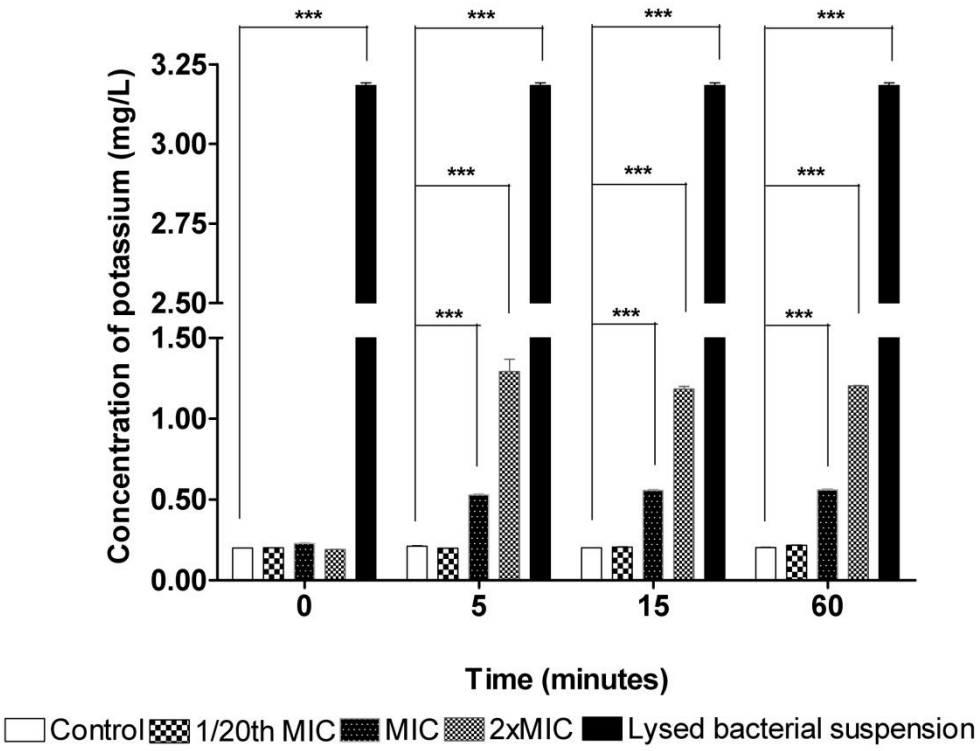

Figure 4.6 K^+ loss in 1 x 10^6 cfu/ml *E. coli* induced by incubation with NP108 for 60 minutes. Assessment of K^+ leakage was performed in triplicate on three occasions. S.E.M. * indicates *p*-value < 0.05, ** indicates *p*-values < 0.01, *** indicates *p*-value < 0.001. Viability of control bacteria after 24 hours was 5.0 x 10^6 cfu/ml; viability of 1/20th MIC test bacteria after 24 hours was 3.0 X 10^6 cfu/ml; viability of MIC test bacteria after 24 hours was 5.2 X 10^6 cfu/ml; viability of 2xMIC test bacteria after 24 hours was 6.6 X 10^5 cfu/ml. Total K^+ content of sonicated 1x10^6 cfu/ml *E. coli* culture was 3.2 mg/L.

A statistically significant K^+ loss (*p*-value $<$ 0.001) from test compared to control, occurred within 5 minutes incubation of the bacteria with NP108 and the level of K^+ detected thereafter remained constant, even when assessed over 24 hours (data not shown). A statistically significant K^+ loss (*p*-value $<$ 0.001) was also seen

between the treatment groups; 1/20th MIC (0.025 mg/ml) compared to MIC (0.5 mg/ml) and 2xMIC (1mg/ml) concentrations and between MIC and 2xMIC concentrations at 5 and 15 minutes and at 7 and 24 hours (data not shown). This means the quantity of K^+ lost by *E. coli* bacteria incubated with NP108 was dependent on the concentration of NP108 employed and the quantity of K^+ lost increased as the concentration and length of time the bacteria were exposed to NP108 compared to control bacteria.

Loss of K^+ induced from *S. aureus* and *P. aeruginosa* 1 x 10^6 cfu/ml cultures incubated with NP108 for 24 hours is shown in Figure 4.7 (a) and (b) respectively. K^+ loss induced in *S. aureus* on incubation with NP108 was statistically significant (p-value < 0.01 at 8 hours and < 0.001 at 24 hours) compared to control.

K^+ loss from these bacteria was also statistically significant between concentration groups; 1/20th MIC (0.013 mg/ml) bacteria compared to MIC (0.25 mg/ml) and 2xMIC (0.5 mg/ml) bacteria (p-value < 0.01) at 8 hours and (p-value < 0.001) at 24 hours and between MIC and 2xMIC bacteria (p-value < 0.05) at 24 hours.

As such the quantity of K^+ lost by *S. aureus* bacteria incubated with NP108 when compared to control bacteria was dependent on the concentration of NP108 employed and the quantity of K^+ released from bacterial cells increased as the concentration and length of time the bacteria were exposed to NP108.

(a)

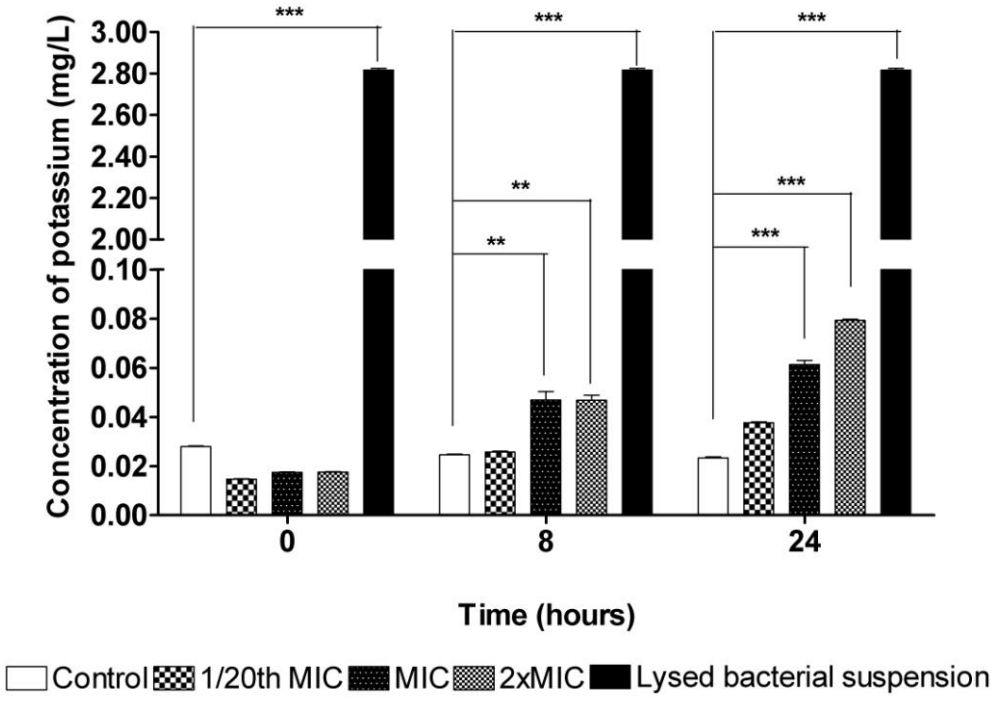

(b)

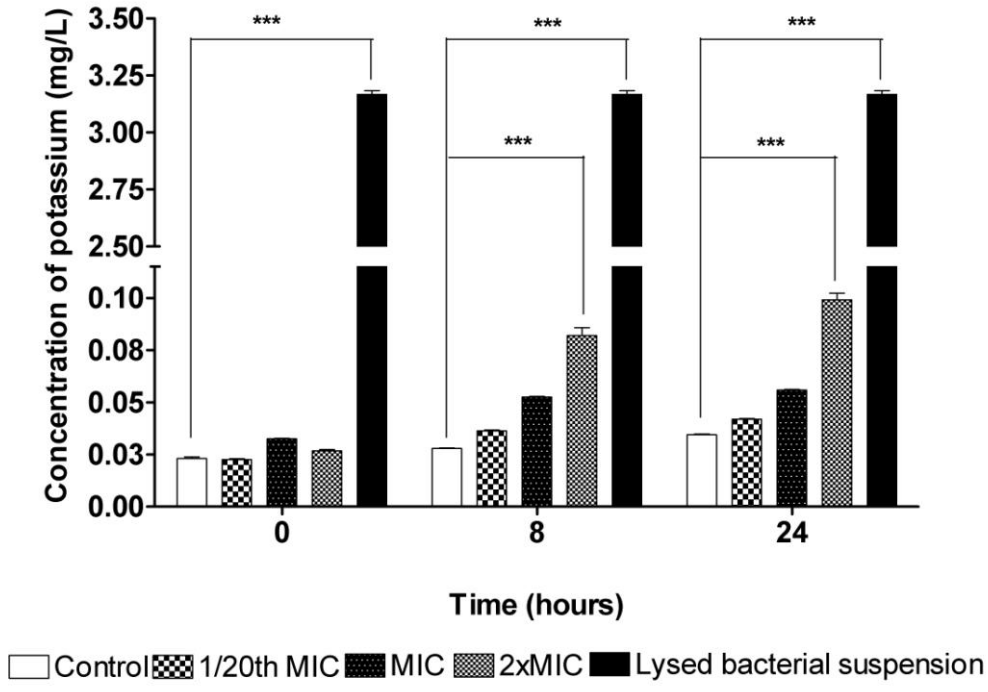

Figure 4.7 K^+ loss in bacteria incubated with NP108. Assessment of K^+ leakage was performed in triplicate on three occasions. S.E.M. * indicates *p*-value < 0.05, ** indicates *p*-values < 0.01, *** indicates *p*-value < 0.001.

(a) *S. aureus* 1x10^6 cfu/ml culture. Viability of control bacteria after 24 hours was 6.6 x 10^6 cfu/ml; viability of 1/20^{th} MIC test bacteria after 24 hours was 6.0 X 10^6 cfu/ml; viability of MIC test bacteria after 24 hours was 4.4 X 10^6 cfu/ml; viability of 2xMIC test bacteria after 24 hours was 4.1 X 10^4 cfu/ml. Total K^+ content of sonicated *S. aureus* 1x10^6 cfu/ml culture was 2.8 mg/L.

(b) *P. aeruginosa* $1x10^6$ cfu/ml culture. Viability of control bacteria after 24 hours was 2.23 x 10^{10} cfu/ml; viability of $1/20^{th}$ MIC test bacteria after 24 hours was 1.2 X 10^9 cfu/ml; viability of MIC test bacteria after 24 hours was 3.86 X 10^6 cfu/ml; viability of 2xMIC test bacteria after 24 hours was 3.5 X 10^6 cfu/ml. Total K^+ content of sonicated $1x10^6$ cfu/ml *P. aeruginosa* culture was 3.2 mg/L.

The K^+ loss induced from *P. aeruginosa* cells incubated with NP108 was also statistically significant (p-value < 0.001) compared to control at 8 and 24 hours. A statistically significant K^+ loss between concentration groups; $1/20^{th}$ MIC (0.025 mg/ml) compared to 2xMIC (1 mg/ml) (p-value < 0.01) at 8 hours and (p-value < 0.001) at 24 hours and between MIC (0.5 mg/ml) and 2xMIC bacteria (p-value < 0.01) at 24 hours was evident. As with both *E. coli* and *S. aureus*, the quantity of K^+ lost by *P. aeruginosa* bacteria incubated with NP108 was dependent on the concentration of NP108 employed and the quantity of K^+ lost increased with concentration and length of time the bacteria were exposed to NP108. However the maximum K^+ loss induced from either *S. aureus* or *P. aeruginosa* cells incubated with NP108 over a 24-hour experimental period was recorded as 2% for those bacteria incubated with 2xMIC concentrations. The K^+ loss that was induced occurred within 5 minutes (data not shown) and the K^+ content of samples tested up to 8 hours remained constant, with a further 1% increase in K^+ leakage recorded between 8 and 24-hours.

4.4 Discussion

4.4.1 K^+ content of bacterial cells

Sonication of bacterial suspensions of known density for each test species was carried out to ascertain the total potassium pool present within the culture. This gave an absolute reference value to which the quantified potassium, lost from bacterial cells due to incubation with cationic antibacterial agents, could be compared. Subsequent to this, potassium loss induced from the test bacteria by an agent with an acknowledged mechanism of action of membrane perturbation, leading to near loss of total intracellular K^+ content was performed. These assays confirmed the validity of the approach.

The biocide action of 1% SDS on bacterial cell walls and membranes and the consequence of this action is long documented as resulting in the progressive leakage of cell components such as potassium (Denyer 1995). Because of this SDS was selected to act as a reference compound quantifying the loss of potassium from bacterial cells. Total loss of potassium content from *S. aureus* bacteria compared to control, was seen within 5 minutes incubation with 1% SDS. Loss of potassium from *E. coli* and *P. aeruginosa* cells incubated with 1% SDS was 8 and 11% respectively after 7 hours incubation. That less potassium was lost from the Gram negative compared to the Gram positive bacterium can be explained by the presence of a double membrane structure that comprises the bacterial envelope of Gram-negative cells, whereas Gram-positive bacteria solely contain a peptidoglycan cell wall (Allison and Gilbert 2004). A second membrane active agent, chlorhexidine was employed to quantify K^+ loss from all three bacterial species. After 60 minutes incubation with 5% chlorhexidine, a loss of 90% of total intracellular K^+ was recorded for *E. coli* and *S. aureus* while a 40% K^+ loss was recorded for *P.*

aeruginosa. That there was a considerable difference in the quantity of K^+ leakage from *E. coli* and *P. aeruginosa* is not unexpected given that the cell wall in *P. aeruginosa* forms a more protective barrier than that possessed by *E. coli*.

4.4.2 Loss of intracellular K^+ induced by triclosan

E. coli incubated with MIC triclosan (0.07 μg/ml) for 24 hours and 10xMIC triclosan (0.7 μg/ml) for 7 and 24 hours, displayed K^+ loss that was statistically significant compared to control (Figure 4.3a)). K^+ loss was also statistically significant between MIC and 10xMIC triclosan incubated *E. coli* at 7 and 24 hours. The percentage of total intracellular K^+ lost from the MIC incubated *E. coli* cells was 2%, with 3% of total cell K^+ lost from 10xMIC bacteria; compared to approximately 1% of total K^+ cell content which leeched from control bacteria under experimental conditions. The conclusion that can be drawn from these results is that the slight K^+ loss induced from *E. coli* by triclosan is directly dependent on the concentration of triclosan employed. Support for this statement can be inferred from the fact that K^+ loss between control and 10xMIC treated bacteria and between MIC and 10xMIC triclosan incubated bacteria was seen at both time points analysed, whereas the K^+ loss induced from *E. coli* incubated with the MIC triclosan was not statistically significant at 7 hours when compared to control. K^+ loss from *E. coli* is also dependent on the length of time to which the bacteria were exposed to triclosan; as witnessed by the statistically significant loss of K^+ compared to control from *E. coli* incubated with the MIC of triclosan at 24 hours but not at 7 hours. The combined effects of a lower triclosan concentration linked with longer exposure to the bisphenol were required for this effect to be manifested.

The K^+ loss from *S. aureus* cells incubated with MIC (0.055 μg/ml) or 10xMIC triclosan (0.55 μg/ml) over 24-hour experimental periods conducted during this

research was not shown to be statistically significant compared to control (Figure 4.3b)) and was equivalent to the 3% K^+ content lost from the control cells under experimental conditions. Partial leaching of K^+ over the experimental duration was observed with *S. aureus* control populations, as might be anticipated given their re-suspension in ultra pure water. Therefore for this set of experiments, K^+ loss from *S. aureus* cells incubated with triclosan was not dependent on the length of exposure or the concentration of triclosan used.

Johnston *et al* reported little K^+ loss from *S. aureus* when treated with a single biocide – either chlorocresol or m-cresol. However rapid K^+ leakage was observed when the bacterium was exposed to a mixture of these two biocides (Johnston et al. 2003). Suller *et al* demonstrated no difference in K^+ leakage induced from 3 strains of *S. aureus* incubated with triclosan at concentrations of 2, 7.5 or 15 mg/L despite MICs of the three strains ranging from 0.025 – 1mg/L triclosan (Suller and Russell 2000). This study also recorded a maximum K^+ loss of 0.2 mg/L from a 1 x 10^7 cfu/ml suspension of *S. aureus* NCTC 6571 after incubation with 80xMIC triclosan (2 mg/L) over 60 minutes (Suller and Russell 2000). This ties in very well with the data presented in this study; 0.064 mg/L K^+ loss recorded from a $1x10^6$ cfu/ml suspension of *S. aureus* after 60 minutes incubation with 10xMIC (0.55 µg/ml) triclosan. Villalain *et al* reported no leakage of intracellular contents from *Streptococcus sobrinus* incubated with triclosan below 10xMIC concentration (Villalaín et al. 2001). Loss of amino acids from *Streptococcus sobrinus* was recorded at 0.3 mg/L (or 34xMIC) triclosan after 30 minutes exposure (Villalaín et al. 2001). The results from these previous studies concur with the results recorded in this study; that triclosan does not induce substantial levels of potassium loss from either *E. coli* or *S. aureus* and that membranotropic effects are slight and loss of membrane integrity may not be responsible even in part for the

bacteriostatic/bactericidal effects of triclosan. However these data do not rule out other membrane effects.

4.4.3 Loss of intracellular K^+ induced by colistin

The rapid K^+ loss from *E. coli (*data not shown) and *S. aureus* (Figure 4.5) incubated with colistin occurring within 5 minutes, proved statistically significant when compared to control. The quantity of K^+ lost from *S. aureus* cells was far more substantial than that lost from *E. coli*. However, the concentration of colistin used was also much higher (although these were MIC and 10xMIC concentrations); 1 mg/ml colistin for *S. aureus* compared to 30 µg/ml colistin for *E. coli*. The quantity of K^+ lost from both bacteria between the concentrations tested (MIC and 10xMIC), was also statistically significantly. *S. aureus* incubated with the MIC colistin lost 7% of total K^+ cell content, while 10xMIC incubated cells lost 36% of total intracellular K^+ over the experimental period. *E. coli* incubated with MIC and 10xMIC colistin lost 6% of total intracellular K^+ over 24 hours compared to the natural seepage of less than 4% of total intracellular K^+ from *E. coli* control cells re-suspended in ultra-pure water.

This proves K^+ loss induced from *E. coli* and *S. aureus* incubated with colistin was directly dependent on the concentration of colistin employed. Time was not a factor affecting K^+ loss induced by colistin from these bacteria; the levels of K^+ detected in samples taken over 24-hour periods from both *E. coli* (Figure 4.4(a)) and *S. aureus* (data not shown) incubated with MIC and 10xMIC colistin remained constant. K^+ loss detected from *P. aeruginosa* incubated with colistin during this investigation did not prove to be statistically significant when compared to control bacteria. Loss of K^+ from MIC (1.5 µg/ml) and 10xMIC (15 µg/ml) colistin incubated bacteria approximated the 4% K^+ lost from the untreated control bacteria under

experimental conditions. Length of time or concentration to which *P. aeruginosa* was exposed to colistin did not affect the quantity of K^+ lost.

The viabilities of $1x10^6$ cfu/ml *E. coli*, *S. aureus* and *P. aeruginosa* control and colistin incubated cells (MIC and 10xMIC) were checked by plating out on agar after every 24-hour incubation. All control cultures produced normal sized colonies in every instance, for all three test bacteria. Only the MIC and 10xMIC colistin incubated *P. aeruginosa* cultures revealed much, much smaller colonies or pinprick sized colonies after viability checks compared to the control colonies. Incubation with inhibitory and supra-inhibitory colistin concentrations subjected the bacteria to stresses, which resulted in small colony variants being produced by the incubated bacteria. Small colony variants are produced by bacteria as a result of energy deficiency and display a pleiotropic phenotype characterised by factors including slow growth (producing small sized colonies) and non-production of virulence factors (Seaman, Ochs and Day 2006). *P. aeruginosa* alone of the test bacteria in this study produced these small colony variants when incubated with colistin at MIC and 10xMIC concentrations in response to the presence of the antibacterial, probably to increase bacterial survival. The possession of a large genome bestows the metabolic capability and flexibility to survive under environmental conditions that prove in hospitable to other bacteria (El Solh and Alhajhusain 2009). The ability of *P. aeruginosa* to survive under conditions that would be lethal to other bacteria is due in part to the minimal nutritional requirements of the bacterium (El Solh and Alhajhusain 2009).

4.4.4 Colistin mechanisms of action

Peptide antibiotics can be categorised as non-ribosomally synthesised as part of secondary metabolism, which are mostly bacterial in origin, as for example colistin

produced by *Bacillus polymyxa* or ribosomally synthesised such as natural peptides produced by all living species as part of their immune system (Hancock and Chapple 1999)(Hancock and Sahl 2006). Colistin is a cationic antimicrobial agent with an overall positive charge of +5 (Clausell et al. 2003). Though colistin has been used clinically for several decades the mechanism of action through which colistin exerts its bactericidal effect is still not precisely known (Maviglia, Nestorini and Pennisi 2009)(Clausell et al. 2003). Zavascki *et al* report colistin's rapid bactericidal action as a result of a detergent-like mechanism of action (Zavascki et al. 2007). Many studies have suggested that colistin acts on bacterial membranes, however, the concentration of colistin employed in these studies was at high MIC multiples (Maviglia, Nestorini and Pennisi 2009)(Clausell et al. 2003). Clauselle et al have suggested the mechanism of action of colistin at MIC concentration alters lipid regulation between the phospholipid interfaces bounding the periplasmic space (Clausell et al. 2003). Bulitta *et al* in a recent study have shown that colistin exerted its bactericidal activity against *P. aeruginosa* within less than 2 minutes exposure of the bacterium to the polymyxin. Their hypothesis is that colistin, having 670 times greater affinity for lipid binding sites than Mg^{2+} or Ca^{2+} ions, rapidly displaces the divalent cations, binds to, and destabilizes the outer bacterial membrane, reaches its target site and swiftly kills the bacterium at 16xMIC concentration (Bulitta et al. 2010). However due to the very rapid bacterial killing speed of colistin, its exact mechanism of action is yet to be elucidated (Li et al. 2005)(Li et al. 2006). What has also been demonstrated for colistin is the ability of the polymyxin to bind to LPS, interact with lipid membranes, unbalance pressure forces and form transient pores in membranes (Ouberai et al. 2011). However, lack of K^+ loss in the current study would suggest such pores are not suitable for transport of this cation. Clauselle *et al* also demonstrated induction in changes in

membrane permeability at colistin concentrations many times higher than MIC values. A number of studies have discovered that colistin's bactericidal effect is not as a result of membrane activity, as colistin has been shown to exhibit lethal effects at concentrations far lower than those required for membrane permeabilisation (Mortensen et al. 2009)(Clausell et al. 2003). Mortensen *et al* speculate employing colistin at a concentration of 10 μg/ml as being too low to increase the permeability of bacterial cell membranes. This is in partial agreement with the experimental findings in this investigation, where colistin was employed at MIC concentrations of 1.5 and 3 μg/ml for *E. coli* and *P. aeruginosa* and K^+ loss of 6% and 4% respectively was detected. Leakage of 36% of total K^+ content occurred in *S. aureus* when incubated with an MIC of 100 μg/ml.

A recent study by Alhanout *et al* examined membrane disruption in *P. aeruginosa* and *E. coli* cells incubated with colistin at a concentration of 4 and 2 μg/ml respectively, through quantification of ATP release from these bacteria. The study revealed a loss of only 4% and 5% loss of total ATP content respectively, from these cells. Alhanout *et al* demonstrated that colistin creates electrically active lesions only 9.1 ± 1nm in diameter by interaction with the bacterial lipid bilayer, through which intracellular components are leaked to the external environment (Alhanout et al. 2010). The fact that ATP molecules have been shown to have leaked through lesions in the lipid bilayer of *P. aeruginosa* and *E. coli* caused by colistin at lower concentrations than were used in this investigation and yet leakage of the much smaller K^+ molecule was not recorded in this investigation was intriguing. This may be explained by the fact that K^+ is used by both these bacteria as an osmolarity regulator and is the first intracellular ion lost when the bacterial membrane is breached and is also the first ion which undergoes active influx into the bacterial cell on osmotic upshift; therefore a balance exists between the

quantity of K^+ lost and as quickly re-absorbed into the bacterial cell, which could account for the detection of minimal K^+ quantities. Whereas the re-absorption of ATP would require significantly greater expenditure of energy by the already stressed cell to re-acquire a currently non-essential molecule.

The same study examined ATP release by squalamine (an antimicrobial compound with similar activity to colistin) that created lesions in the lipid bilayer 33.5 nm in diameter, leading to loss of approximately 35% of total ATP content within 30 minutes (Alhanout et al. 2010). These data are not in agreement with the findings in this study where little leakage of intracellular contents was observed from bacteria incubated with colistin.

4.4.5 K^+ loss induced by NP108

E. coli incubated with NP108 displayed a rapid and substantial K^+ loss within 5 minutes incubation with the CAP (Figure 4.6). This statistically significant loss of 38% total intracellular K^+ occurred upon incubation with 2xMIC (0.5mg/ml) NP108 over 60 minutes. K^+ loss between *E. coli* cultures incubated with MIC (0.25 mg/ml) and 2xMIC NP108 was also statistically significant, demonstrating that concentration of NP108 alone was responsible for K^+ loss induced in these bacteria. Time was not a factor affecting induction of K^+ from *E. coli* cells as the levels of K^+ detected from MIC and 2xMIC concentrations remained constant over the 24-hour experiments (data not shown).

The statistically significant K^+ loss from *S. aureus* incubated with NP108 (Figure 4.7(a)) was also rapid, 3% loss of total K^+ intracellular pool with 2xMIC NP108 and 2% K^+ loss with MIC NP108 over 24 hours but clearly was less substantial than that displayed by *E. coli*. Whilst the slight loss of K^+ from *S. aureus* induced by incubation with MIC NP108 (0.25 mg/ml) was statistically significant when

compared to control. When *P. aeruginosa* was incubated with NP108, the slight K^+ loss observed from the test bacteria was only statistically significant between the 2xMIC (0.5 mg/ml) incubated bacteria (3%) and the control (1%). No statistically significant difference in K^+ loss from the bacterium was seen between the MIC (0.25 mg/ml) (2%) and 2xMIC NP108 concentrations. Concentration of NP108 alone was directly responsible for stimulating K^+ loss from *P. aeruginosa* cells, and this required a concentration of 0.5 µg/µl of NP108, twice the concentration that was required to induce a large K^+ loss from *E. coli*.

As the bacterial viability checks on MIC and 10xMIC colistin incubated *P. aeruginosa* revealed small colony variants at 24 hours in; these viability checks were extended to include 60 minute and 24-hour analysis of NP108 incubated bacteria. The test bacterial control or $1/20^{th}$ MIC NP108 incubated cells produced normal sized colonies at both 60 minutes and 24-hours. However, every bacterial species incubated with MIC or 2xMIC NP108 revealed small colony variants at both time periods. The appearances of small colony variants have been reported with equal frequency in planktonic cells and biofilms following antimicrobial exposure (Singh et al. 2009). The presence of small colony variants in bacterial cultures under stress is common and serves to ensure survival of the bacterial species (Singh et al. 2009). A *Bacillus* colony can collectively decide to sporulate if growth conditions become too stressful, once agreed by the majority of the bacteria present in the colony, induced through specific intracellular bacterial signalling (Ben Jacob et al. 2004). Bacteria use signal transduction systems to communicate with each other to promote adaptation of the bacterial colony to the environment and this process of communication is commonly termed quorum sensing (Lyon and Novick 2004). These signals are autoinducers and responses are dependent on the signal produced and population density (Lyon and Novick 2004). Signals in Gram-positive

bacteria attach as ligands to extracellular receptors of two component signal transduction modules which then internalize the signal (Lyon and Novick 2004)(Otto 2004). The homoserine lactone signals of Gram-negative bacteria enter the cell by diffusion and initiate responses upon binding to intracellular receptors (Lyon and Novick 2004)(Ben Jacob et al. 2004). Bacteria resistant to antibiotics send signals to other bacteria in the colony to announce this fact and bacteria lacking the resistance factor emit a response which is followed by conjugation. The rapid development of antimicrobial resistance in a bacterial community can therefore result from an initial small number of resistant cells. (Ben Jacob et al. 2004) CAPs have been shown to induce leakage from bacterial cells (Reddy, Yedery and Aranha 2004)(Shai 1999).

Though a consensus of opinion exists that CAPs exert their mechanism of action by selectively disrupting cell membranes, an exact mechanism of action for CAPs remains controversial (Reddy, Yedery and Aranha 2004). Four distinct methods have been suggested as the means through which CAPs interact with the bacterial cytoplasmic membrane and disrupt membrane integrity; these are termed the barrel stave, carpet, toroidal pore (Figures 1a) - c)) and aggregate models (Hale and Hancock 2007). The experimental results displayed here regarding K^+ loss from all three test bacteria incubated with the novel CAP NP108, where statistically significant K^+ loss compared to control was shown for all three bacteria, is in agreement with membrane disruption being caused by this CAP. That 0.5 µg/µl of NP108 was needed to induce K^+ loss of 3% in *P. aeruginosa* and *S. aureus* while causing 38% K^+ loss in *E. coli*, could be due to differences in the composition of the Gram-negative cell envelope of *E. coli* and *P. aeruginosa* and less binding of the peptide to the Gram-positive cell wall. However these data clearly point to different degrees of selectivity of action upon the test species.

4.5 Conclusion

Loss of K^+ induced by triclosan in *E. coli* was linked to the concentration of triclosan used and the length of time over which *E. coli* was exposed to the bisphenol. Neither increasing the concentration of triclosan or extending the length of exposure of *S. aureus* to triclosan, affected the quantity of K^+ loss that triclosan induced from this bacterium.

Incubation of *E. coli* and *S. aureus* with colistin induced K^+ loss that was solely dependent on the concentration used. No significant K^+ loss was exhibited by *P. aeruginosa* when exposed to colistin compared to control bacteria.

The effects of NP108 on the three test bacteria were varied; swift and statistically significant concentration dependent K^+ loss compared to control was induced in all three test bacterial species. The most substantial K^+ loss was seen in *E. coli* incubated with NP108, with *P. aeruginosa* requiring a higher concentration of the peptide for the induction of a statistically significant potassium loss compared to control. K^+ loss induced by NP108 was shown to be independent of the length of exposure of the bacteria to the peptide.

All three bacterial species produced small colony variants in response to incubation with MIC and 2xMIC NP108, while only *P. aeruginosa* produced small colony variants in response to incubation with MIC and 10xMIC colistin; probably a mechanism by the test bacteria to improve bacterial survival under the antimicrobial stress.

Overall, K^+ loss induced by triclosan was demonstrated to be a combination of concentration and exposure time, whereas K^+ loss induced by colistin and NP108 was shown to be dependent on concentration alone.

Chapter Five

Examination by flow cytometry growth dynamics and loss of bacterial viability upon incubation with cationic antimicrobial compounds

5.1 Introduction

5.1.1 Background

Until as recently as the late 1970's microscopy was the sole means available to scientists for examination and measurement of single microorganisms (Steen 2000). Today, it is possible to measure individual bacterial cells within a population at a rate of 1000 cells per second using a flow cytometer (Steen 2000). During World War II, the U.S. Army pioneered use of such an instrument in experiments designed to detect bacteria and spores, thus the application of flow cytometers to microbiology supersedes its use as a tool for studying mammalian cells by many years. The Cytoflurorograph was the first commercial laser based flow cytometer launched in 1970, while Becton Dickinson launched the Fluorescence-activated cell sorter (FACS) in 1974. Once a feature specific to their cell type has been selectively labelled, individual cells within a homogenous population can be identified using such instrumentation (Porter and Pickup 2000). In essence flow cytometry measures fluorescence per individual cell or particle.

5.1.2 Components of a flow cytometer

The internal structure of a flow cytometer can be seen in Figure 5.1.

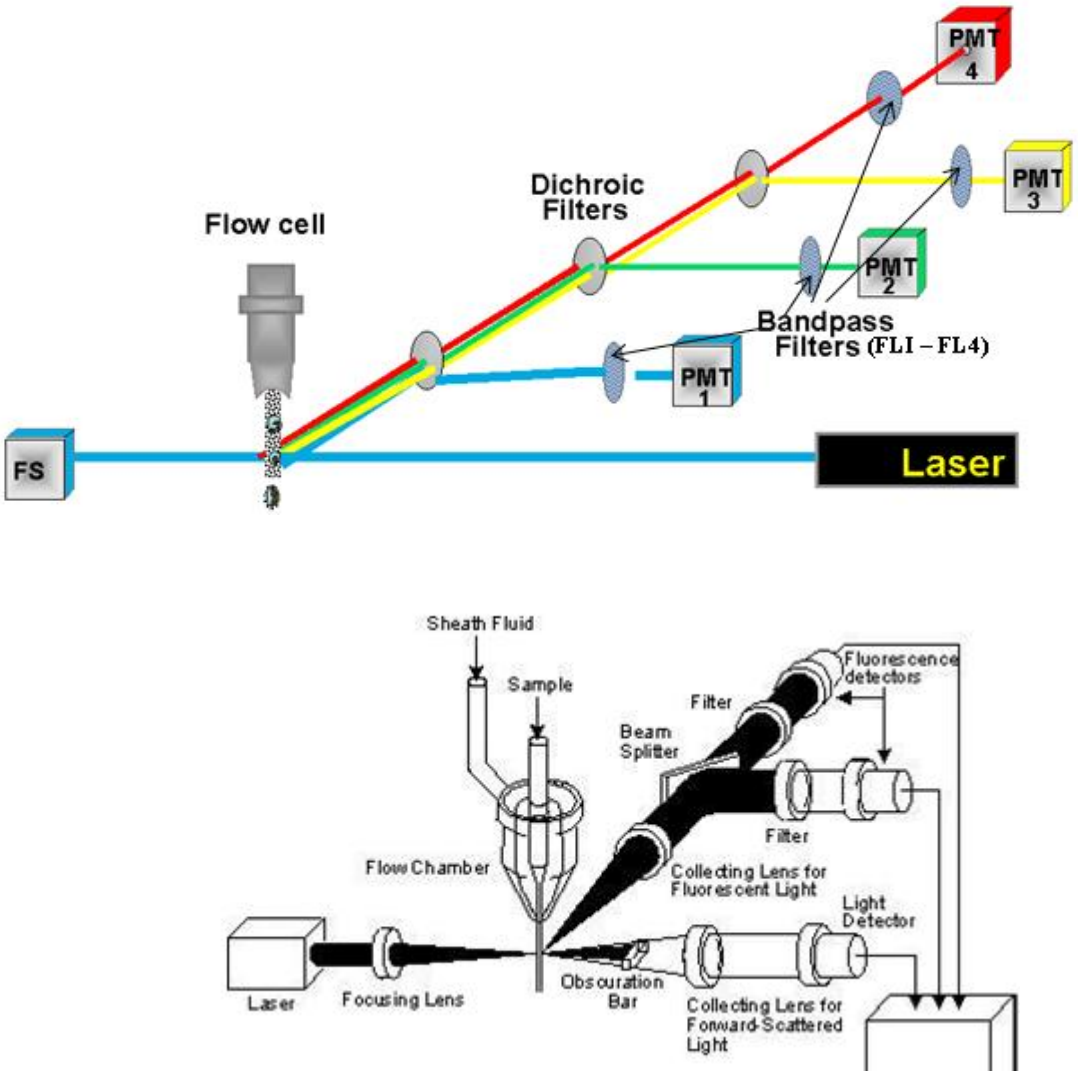

Figure 5.1 Internal structure and components of a functional flow cytometer. FS - forward scatter, PMT - Photo Multiplier Tube

The flow cytometer contains a laser capable of exciting fluorochromes; the fluorochrome absorbs energy in the form of light and emits this light at a different wavelength. The flow cytometer used in this investigation was an EPICS® XL™, which possesses an argon laser with an excitation wavelength of 488nm. There are four detectors in the EPICS® XL™ so depending upon the requirement up to four different dyes can be used simultaneously to stain a sample and these fluorescence signals are detected on separate filters; for example fluorescein at 525nm on FL1

and PE CYANINE 5 at 675nm on FL4. The instrument also utilises 2 light scatter parameters, known as forward scatter and side scatter. An obscuration bar blocks a substantial amount of fluorescence and scattered light but will allow sufficient of both to get into the collection system while preventing almost all of the light reflected from the stream from going into the collection system.

5.1.3 Hydrodynamic focussing

As the sample of bacterial cells from a planktonic population enters the flow chamber or flow cell, the sample core is focused in the centre of the faster flowing sheath fluid, which presents a single file of particles to the laser. This process is known as hydrodynamic focusing and is shown in Figure 5.2. For bacteria to properly intercept the single wavelength beam of light the fluids in the system must be properly pressurised and free of debris and air bubbles at all times. The sample pressure and the sheath fluid pressure are different, the sample pressure being greater. Sheath pressure is constant whereas sample pressure in the EPICS® XL™ can be low, medium or high, although all these are pressures above sheath pressure. A sample pressure regulator controls the sample flow rate, achieved by changing the sample pressure relative to the sheath pressure. Increasing the sample pressure increases the width of the sample core, which results in increased flow rate. The diameter of the core stream is critical for both the accurate positioning of the cells in the laser and for identifying when more than one cell is in the laser beam such as doublets or triplets. The diameter of the core stream should ideally be similar to the diameter of the bacteria being analysed.

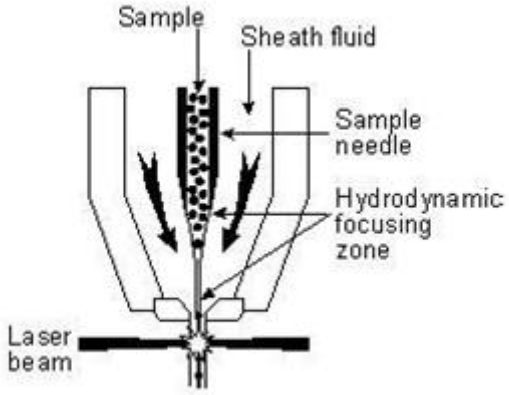

Figure 5.2 Hydrodynamic focussing in a flow cytometer

5.1.4 Analysing the fluid stream

When a particle enters the laser beam and starts to scatter light or fluoresce, a voltage pulse is created. When the amount of light scattered exceeds a threshold, a set period of time for signal detection commences. The threshold can be set on any parameter but in this investigation the threshold was set on forward scatter. When a particle is in the centre of the laser light where maximum amount of scatter or fluorescence is achieved, the highest level of the pulse is achieved. The pulse returns to the baseline as the particle leaves the laser beam. The intensity of light scatter or fluorescence determines the height of the peak pulse. The distribution of the fluorescence determines the width of the pulse. Therefore, the total fluorescence (intensity and distribution) determines the area under the pulse. Cells with the same amount of total fluorescence but with different fluorescence intensities produce different peak pulses.

A number of detectors are aligned at the point where the fluid stream passes through the beam of light, one detector is in line with the beam of light and several detectors are perpendicular to the beam of light. Light scatter is detected at two angles; forward scatter measures blue light scattered in the direction of the laser

path and gives information regarding bacterial size and shape. The amount of forward scatter is proportional to the size of the cell that scattered the laser light. A photodiode tube, which can convert light into either a current or a voltage, collects the forward scatter signal. Photodiodes are used for strong signals in cases where saturation is a potential problem as with forward scatter.

All side scatter and fluorescence measurements are made at a 90° angle relative to the laser beam and each of these is connected to a separate photomultiplier tube. Photomultiplier tubes are more sensitive than photodiodes and are used to detect small amounts of fluorescence emitted from fluorochromes. Photo detectors have a band pass filter in front of them, which only allow a specific bandwidth of light to reach the detector (Figure 5.1). Signals can be amplified by applying a voltage to the photomultiplier tube that collects or detects the light, or by increasing the amplification gain.

The laser light, which is directed to the side scatter and fluorescence detectors, passes through a series of dichroic filters. Dichroic filters can be either long pass of short pass and the photons of light which travel down channels are steered and split by these dichroic filters. A 488 nm dichroic long pass filter at a 45^0 angle to the incident light reflects light to the side scatter sensor but transmits fluorescent light of longer wavelengths. Some of the light is reflected at 90^0 to the incident light while part of the light is transmitted and continues on to the next dichroic filter. Side scatter measures blue light that is scattered off the internal components of the cell, such as the nucleolus and cytoplasmic granules, being a source of cell granularity. A short pass filter will transmit all wavelengths that are less than a specified wavelength, for example a 600 short pass filter will transmit all wavelengths less than 600 nm. The light the 488 nm long pass filter transmits, goes to a 488 nm laserblocking filter. The 488 nm laser blocking filter blocks any

remaining laser light and transmits only fluorescent light. The remaining optical filters separate the light for the four FL sensors and these are displayed in Table 5.1.

Dichroic long pass filter 45^0 angle	Reflected wavelength (nm)	Filter type	Transmitted wavelength (nm)	Sensor type	Detector name	Dye detected
None	488	Forward scatter	488	Photo diode	FS	None
488	488	Side scatter	N/A	PMT	SC	None
550	>550	525 Band Pass	505 - 545	FLI	FITC	Fluorescein isothyocyanate SYTO® dyes
600	555 - 600	575 Band Pass	560 – 590	FL2	PE	Phycoerythrin
645	605 - 645	620 Band Pass	605 - 635	FL3	ECD	Propidium iodide ECD (Energy coupled dye)
675	600 - 700	675 Band Pass	660 – 700	FL4	PC5	PE Cyanine 5

Table 5.1 EPICS® XL™ filters and detectors. FS; forward scatter. SC; side scatter. PMT; photomultiplier tube

Fluorescent chemicals attached to or within the bacterial cell are excited into emitting light of a longer wavelength than the light source and the fluorescent detectors pick up these signals. Filters designed to work at 90° to the incident light are placed in front of each detector. Light of a particular colour is separated from the light beam and directed to each detector using colour filters called dichroic filters that work at a 45° angle. These dichroic filters act in part like mirrors and are wavelength dependent; for example the first filter is a 488 nm dichroic long pass filter so any light up to and including 488 nm is blocked while light of a wavelength greater than 488 nm passes through the filter. The second filter is a 550 dichroic long pass filter therefore light between 489 and 550 nm is blocked and greater than

550nm passes through the filter. The third filter is a 600 nm dichroic long pass filter, so only light with a wavelength greater than 600 nm passes through this filter. Finally, light with a wavelength greater than 645 nm passes through the fourth dichroic long pass filter. The light from the dichroic filter is then directed through another filter, a band pass filter, which only permits passage of a very narrow beam of light (Table 5.1). There are four band pass filters in the EPICS® XL™ flow cytometer, termed FL1, FL2, FL3 and FL4. These bandpass filters are located in front of the photomultiplier tubes, or fluorescence detectors, to optimise the specificity of the detector for a particular fluorescent dye. This is achieved by only allowing a narrow range of wavelengths to reach the detector.

The photomultiplier tubes generate electrical impulses proportional to the amount of incident light striking the detectors. The light signals (photons) reach the photomultiplier tube from the band pass filter and side scatter detector or in the case of forward scatter a photodiode, and are converted into a proportional number of electrons. These electrons are multiplied, hence creating a greater electrical current, which travels to the amplifier and is converted to a voltage pulse. Next the signals undergo analogue to digital conversion before being transmitted to the computer. The voltage pulse is given a digital value by the analogue-to-digital converter. The resolution of the data is also dependent on the analogue to digital converter; in the EPICS® XL™ the 10-bit analogue to digital converter converts the lowest to highest voltage into numbers from 1 to 1024. These numbers are referred to as channels.

5.1.5 Fluorescent dyes

Various dyes are used in flow cytometry to stain bacterial cells thus allowing the examination of the stained bacteria by different detectors. These dyes absorb the

laser light energy and emit fluorescence of different colours. Dyes may be bound within or on the cell surface; for example, SYTO 9 has a spectrum of excitation at 420 nm and emission at 580 nm and enters living viable bacterium through specific pores and intercalates into DNA. Propidium iodide has an emission spectrum of excitation at 488 nm and emission at 640 nm, only diffuses across a damaged cell wall and intercalates into DNA (one molecule of propidium iodide binds per 4/5 base pairs of DNA). The differences in excitation and emission spectra means that SYTO 9 will be picked up on FL1 and propidium iodide on FL3.

When more than one dye is used to stain a bacterial population, colour compensation must be utilised. Colour compensation is an electronic subtraction method for correcting overlapping fluorescent signals. Each dye must be run independently first and parameters optimised before dual stained bacterial populations can be accurately separated. Once the colour compensation protocol is optimised, the flow cytometer can accurately identify and quantify the proportions of live and dead bacteria in a sample. In this investigation the use of both SYTO 9 and propidium iodide to stain all bacterial samples permitted the simultaneous detection of living and dead bacteria. SYTO 9 enters the living and damaged cells and intercalates with DNA, however propidium iodide crosses only damaged cell walls/cytoplasmic membranes and, due to possessing two positive charges, propidium iodide has a higher affinity for DNA and displaces SYTO 9. Propidium iodide is excluded from cells with structurally intact cytoplasmic membranes because of the size and charge of the propidium molecule.

5.1.6 Acquisition

The process by which data is collected from samples in a flow cytometer is termed acquisition. A computer is connected to the flow cytometer and the computer

software handles the digital interface with the flow cytometer. The discriminator on a flow cytometer is a size exclusion bar, which allows particles, debris or cells below a certain size to be excluded from the data collection. If the discriminator is set too high, viable cells will be excluded and if it is set too low, interference due to debris will show up on the plots. Once the protocol is optimised for a particular bacterial species, gating the population can isolate the majority of detected cells and only data from this gated population will be collected. Clicking an icon on the flow cytometer tool bar allows the operator to draw a gate or line around the bacteria of interest. Figure 5.3 (a) demonstrates a typical dot plot displaying 2 gated populations, A and B; this data was collected on a linear scale; side scatter versus forward scatter. A logarithmic scale was used to collect all other flow cytometry data in this study.

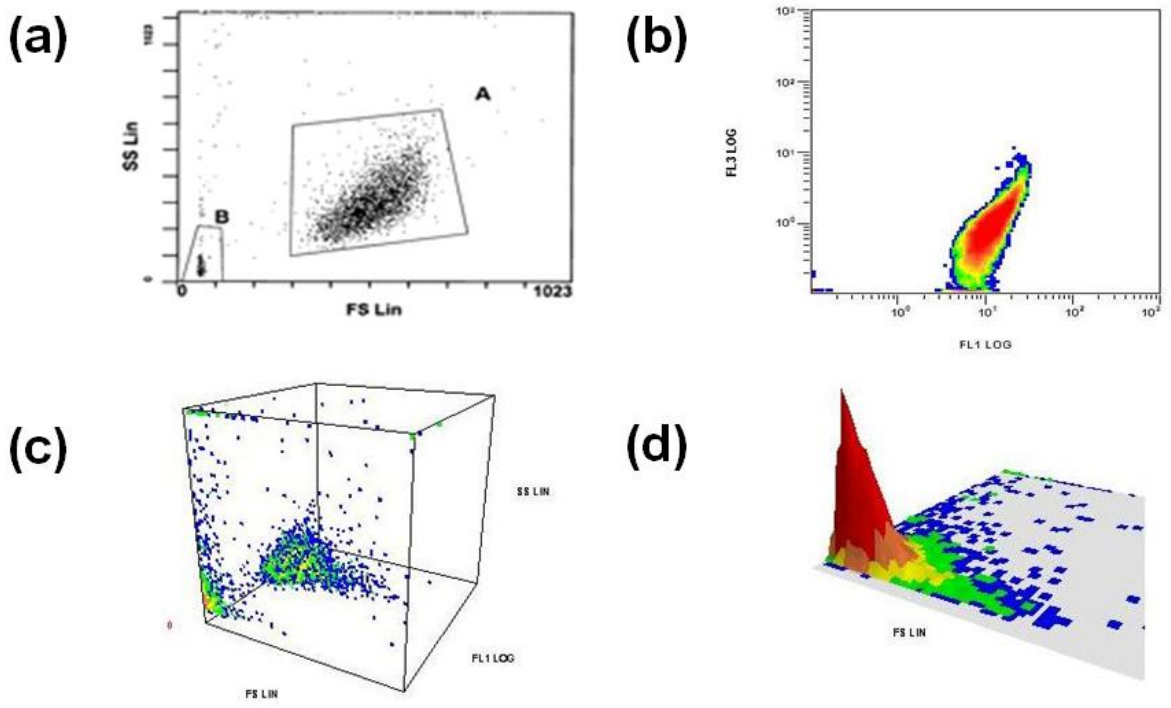

Figure 5.3 Several graphical representations of the same flow cytometry data: (a) dot plot displaying gated populations (b) density plot (c) tomogram plot (d) surface plot. SS Lin is Side Scatter Linear scale; FS Lin is Forward Scatter Linear scale

5.1.7 Aim of flow cytometry investigation

Antimicrobials have many different modes of action, some resulting in changes in bacterial structure post antimicrobial exposure. Also, changes in the growth dynamics of a bacterial culture can occur. Flow cytometry was undertaken on treated bacterial populations to give qualitative and quantitative information on bacteria once antimicrobial exposure had occurred. During this investigation data was collected from 10,000 cells for each test sample at a flow rate of approximately 500 cells per second.

5.2 Methodologies

5.2.1 Preparation of samples for analysis by flow cytometry

Samples of bacterial cultures incubated with either triclosan, colistin, NP101 or NP108 were prepared as described in Section 2.8.2

5.2.2 Calibration of flow cytometer

Prior to analysis of samples by flow cytometery, the instrument was calibrated as described in Section 2.8.1.

5.2.3 Data analysis

After completion of experiments, data analysis was performed using the EPICS® XL™ MCL on-board software provided by Beckman Coulter.

5.3 Results

5.3.1 Examination of the effects of triclosan on *E. coli* and *S. aureus*

Bacterial cultures containing 1 x 10^6 cfu/ml of either *E. coli* or *S. aureus* were incubated with control, 1/20^{th} MIC, MIC and 10xMIC triclosan and samples withdrawn for analysis at 24, 72 and 168 hours. Overlay histogram plots of data collected on FL1 (SYTO 9 fluorescence) by the flow cytometer of control and test bacteria and correlated culture viability are shown in Figures 5.4 and 5.6. For comparison purposes Figure 5.5 displays an overlay histogram plot of data collected on FL3 (propidium iodide fluorescence) with data gathered on FL1. All subsequent overlay histograms displayed in this Chapter will be based on data gathered on FL1 only.

a) *Escherichia coli*

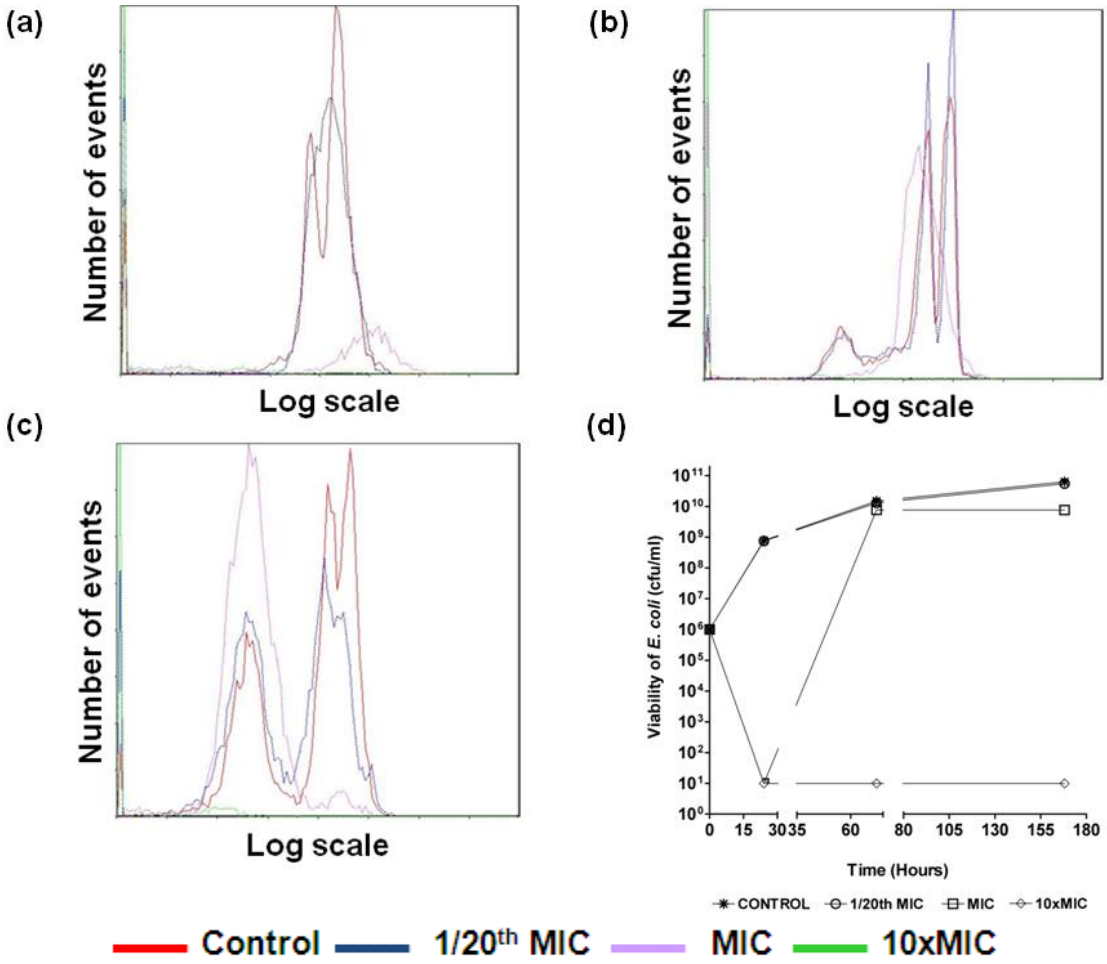

Figure 5.4 *E. coli* 1x10^6 cfu/ml cultures incubated with different concentrations of triclosan (control; 1/20th MIC – 0.0035 μg/ml; MIC - 0.07 μg/ml;10xMIC - 0.7μg/ml) and stained with Syto 9 were examined at (a) 24 (b) 72 and (c) 168 hours. Viability of *E. coli* cultures (d) post triclosan incubation at 24, 72 and 168 hours. Data are representative of flow cytometry experiments performed in triplicate on three occasions.

The control histogram portrays the normal bacterial size of an *E. coli* culture with bacterial cells continuously multiplying by binary fission, therefore two peaks in a control culture would represent the elongated cells prior to binary fission by the larger peak and the smaller peak representing the smaller just divided cells. From the data depicted in Figure 5.4 it is apparent that *E. coli* incubated with 10xMIC (0.7 μg/ml) triclosan could not withstand the effects of this concentration of the antibacterial, as witnessed by the absence of a peak at 24, 72 or 168 hours incubation. The culture viability data also support this finding, with the 10xMIC

culture showing no viable bacteria at any time point. When flow cytometry protocols are optimised for each bacterial species, these protocols are based on gated populations of untreated control bacteria. Bacterial populations that have been exposed to antimicrobials and have been physically altered as a consequence may not therefore be detected. For instance bacteria, which have reduced in size, may now be below the discriminator. This accounts for the fact that bacterial cells that comprise small colony variants (as detailed in Chapter 4), though detected by viability checks, do not appear in the flow cytometry histograms.

The matching overlay of the peaks for the control and 1/20th MIC cultures at all time points confirm very similar viability dynamics of these cultures. The presence of a single peak after 24 hours incubation indicates one homogenous sized group of bacteria within the sub-inhibitory culture with the control population displaying twin peaks; thus a heterogeneous bacterial population, with one bacterial group within the culture bigger than the other, possibly cells pre and post binary fission. This had changed at 72 hours to the appearance of three peaks, indicating the presence of three differently sized groups of bacteria within these populations; the minor peak closer to the y-axis representing bacteria much smaller in size to those in the two major peaks. The cultures at 168 hours incubation show two principal peaks therefore two bacterial groups, one larger than the other. That the histograms and viability of *E. coli* incubated with 1/20th MIC triclosan at 24, 72 and 168 hours were identical to control, which confirms the fitness cost or stress of incubation with 1/20th MIC triclosan over 168 hours was insufficient to induce changes in the growth dynamics of this culture. From Chapter 3 the exposure of *E. coli* to sub-lethal triclosan was shown to induce an additional tolerance to subsequent triclosan treatment. Therefore the 1/20th MIC culture would probably have a modified phenotype and would be worthwhile examining in future.

The MIC treated culture displayed no colonies that were viable after 24 hours incubation but had substantially recovered by 72 hours and displayed small colony variants as discussed in Chapter 4. The data gathered by the flow cytometer support this result, with a very small histogram peak for the MIC incubated bacteria visible at 24 hours but this had radically changed at 72 hours with the appearance of a much larger histogram equivalent to that of control and 1/20th MIC triclosan treated bacteria. The MIC histogram at 24 hours was further along the x-axis than the control and sub-inhibitory incubated bacteria, meaning the few detected bacteria were slightly larger than the bacteria in the other two cultures. This could be due to the detection of longer non-septated *E. coli* due to the effect of the inhibitory MIC concentration (which will be discussed and visualised in scanning electron micrographs in Chapter 6). The histogram for *E. coli* incubated with triclosan MIC at 72 hours was co-located with the control and 1/20th MIC peaks; therefore the bacteria in all three cultures were of a similar size. However, the MIC incubated bacteria at 168 hours, as shown by a very small broad histogram peak, identifies the bacteria in the MIC culture as a homogenous group of smaller bacteria compared to bacteria in the other cultures.

The data collected on FL3 and FL1 shows a different location of the histogram peaks for all cultures, the FL3 data being closer to the y-axis (Figure 5.4). Data collected on FL3 is based on propidium iodide fluorescence (Figure 5.5) and as this fluorescent dye stains dead or dying cells and is excluded from living cells, the data collected on control and 1/20th MIC cultures does not show the detail on bacterial size and culture diversity as shown in the FL1 data; thus, control and sub-inhibitory cultures are represented by triple peaks in the 72 hour plot in FL1 data compared to a single peak in FL3 data.

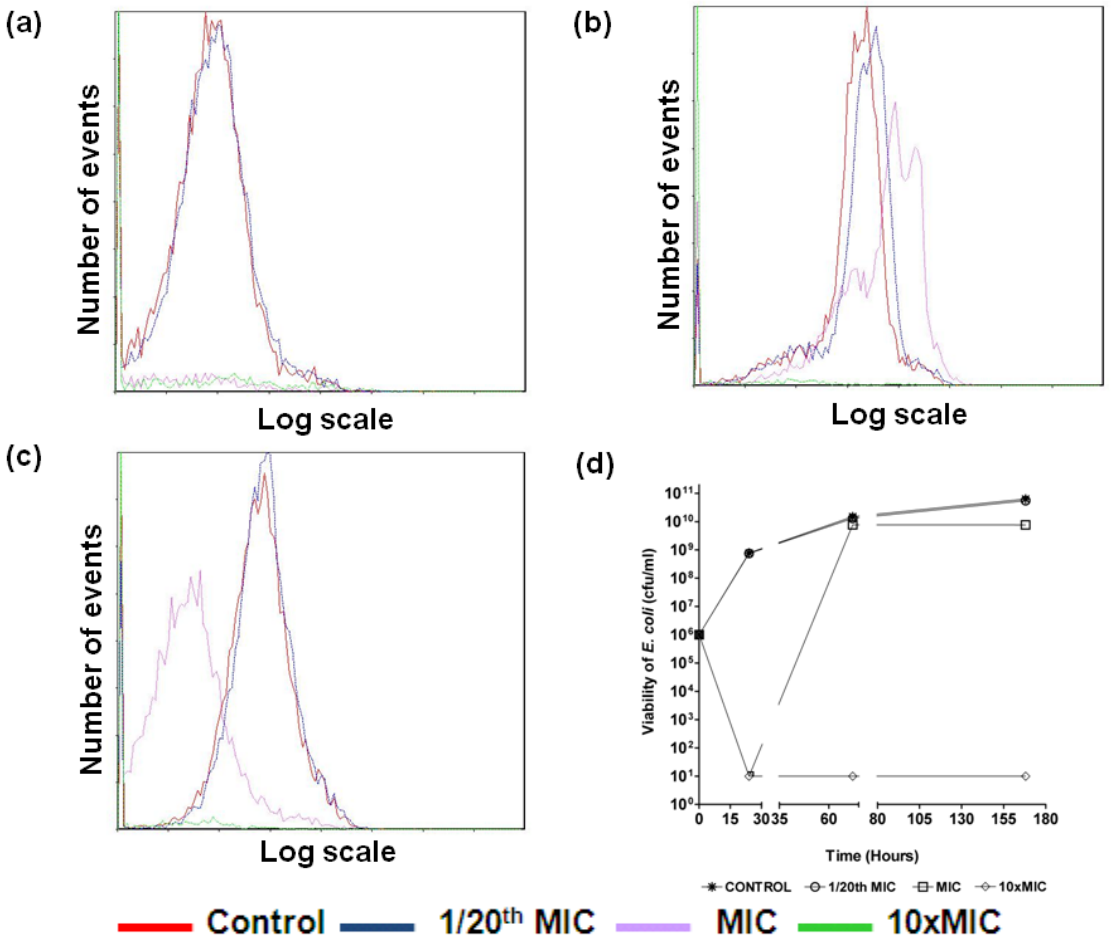

Figure 5.5 *E. coli* 1x10^6 cfu/ml cultures incubated with different concentrations of triclosan (control; 1/20th MIC – 0.0035 μg/ml; MIC - 0.07 μg/ml;10xMIC - 0.7μg/ml) and stained with propidium iodide were examined at (a) 24 (b) 72 and (c) 168 hours. Viability of *E. coli* cultures (d) post triclosan incubation at 24, 72 and 168 hours. Data are representative of flow cytometry experiments performed in triplicate on three occasions.

Conversely, the histogram peak for the MIC incubated bacteria is depicted as a single histogram peak at 72 hours in the FL1 data as opposed to a triple peaked histogram in the FL3 data.

b) *Staphylococcus aureus*

The overlay images of *S. aureus* incubated with triclosan (Figure 5.6) display single peaks representing control, 1/20th MIC (0.00275 μg/ml) and MIC (0.055 μg/ml) triclosan incubated bacteria. Very few bacteria were enumerated for 10xMIC (0.55 μg/ml) triclosan culture at all time points indicating the inability of *S. aureus* to withstand this treatment.

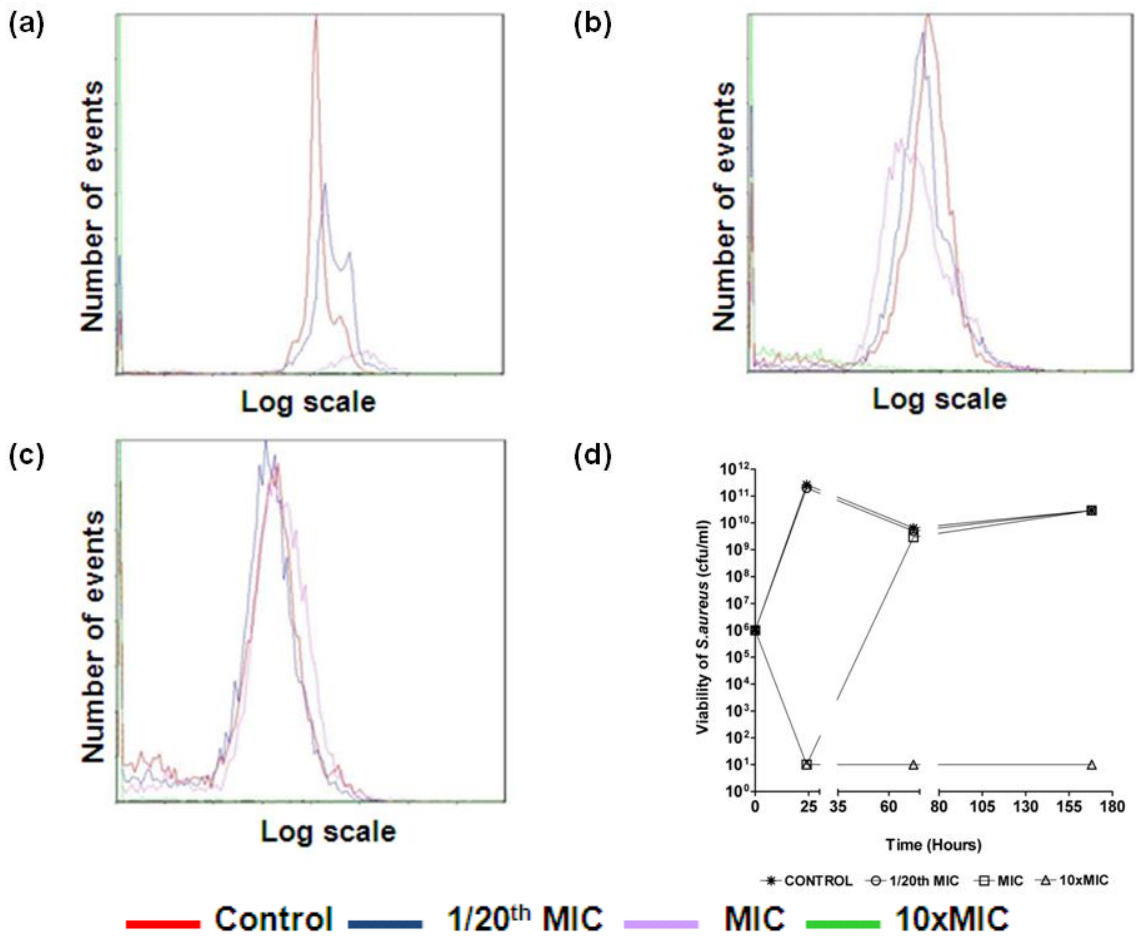

Figure 5.6 *S. aureus* 1x10^6 cfu/ml incubated with different concentrations of triclosan (control; 1/20th MIC – 0.00275 μg/ml; MIC - 0.055 μg/ml;10xMIC - 0.55μg/ml) and stained with Syto 9 were examined at (a) 24 (b) 72 and (c) 168 hours. Viability of *S. aureus* (d) cultures post triclosan incubation at 24, 72 and 168 hours. Data are representative of flow cytometry experiments performed in triplicate on three occasions.

The overlay histograms after 24 hours incubation reveal similarly placed peaks for control and 1/20th MIC triclosan cultures, however the histogram representing the sub inhibitory incubated bacteria was broader than control. These sub-inhibitory incubated bacteria therefore were similarly sized to control bacteria; however some of the sub-inhibitory bacterial cells were larger than those in the control population. Few bacteria were enumerated at the MIC concentration, as depicted by the appearance of a very small broad peak slightly further along the x-axis than control and 1/20th MIC histograms. The viability data after 24 hours triclosan incubation

support the flow cytometry data in that no viable cells were produced at this time point.

Histograms of *S. aureus* at 72 hours display very similar patterns between control and sub-inhibitory incubated bacteria, with a single peak representing each culture. This suggests that at 72 hours the control and 1/20th MIC incubated bacteria were very similar to each other; a single homogeneous sized group of bacteria in each culture. The histogram for the MIC culture reveals this culture has recovered substantially against triclosan at 72 hours. The single histogram peak for the MIC culture is broadly in the same position on the x-axis as the control and 1/20th MIC cultures; thus, *S. aureus* in all three cultures were similar in size to one another. The survival and subsequent division of a few persister cells in the culture was most likely responsible for the presence of a histogram peak for the MIC concentration at 72 hours. The 168 hour overlay plot reveals a similar situation with practically no variation in histogram breadth or location on the x-axis. Therefore bacteria from these three cultures possessed similar size and viability post 168 hour triclosan exposure relative to each other. This is supported by the viability data at 72 and 168 hours that shows little difference between control, 1/20th MIC and MIC triclosan *S. aureus* incubated bacterial populations.

5.3.2 Examination of the effects of colistin on *E. coli*, *S. aureus* and *P. aeruginosa*

a) *Escherichia coli*

The inability of *E. coli* to withstand the MIC and 10xMIC concentrations of colistin (Figure 5.7) is evidenced by the absence of a histogram peak at any experimental time point. The viability data show the 10xMIC colistin incubated bacteria produced no viable bacteria over the experimental period. The MIC incubated bacteria

viability had increased substantially at 72 hours but showed a four-log difference to control at 168 hours.

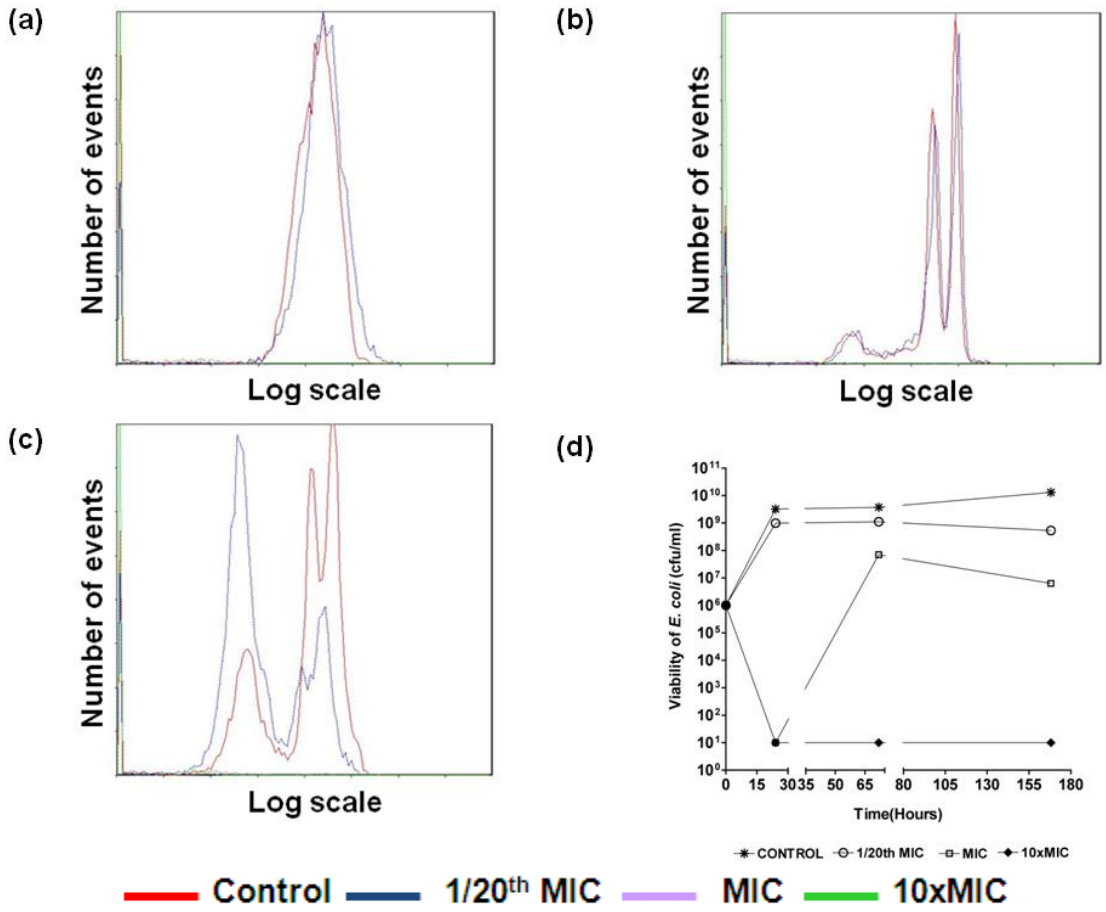

Figure 5.7 *E. coli* cultures inoculated with 1x10^6 cfu/ml, incubated with different concentrations of colistin (control; 1/20^{th} MIC – 0.15 μg/ml; MIC - 3 μg/ml;10xMIC - 30 μg/ml) and stained with Syto 9 were examined at (a) 24 (b) 72 and (c) 168 hours. Viability of *E. coli* cultures (d) inoculated with 1 x 10^6 cfu/ml, post colistin incubation at 24, 72 and 168 hours. Data are representative of flow cytometry experiments performed in triplicate on three occasions.

The control and 1/20^{th} MIC cultures displayed histograms remarkably similar to each other at 24 and 72 hours, each displaying a homogenously sized population at 24 hours and two differently sized bacterial groups at 72 hours. The control histogram at 168 hours showed a triple peaked histogram depicting a population of smaller bacteria co-existing with two groups of larger bacteria within the culture. Twin histograms were also depicted for the 1/20^{th} MIC culture with small cells comprising the majority of bacteria in the culture that also contained a second

group of larger bacteria. The viability data also showed a difference between the control and sub-inhibitory bacteria, with more than one log-scale difference in viability between these two cultures at 168 hours.

b) *Staphylococcus aureus*

The lack of a detectable peak for the 10xMIC colistin incubated *S. aureus* (Figure 5.8) verified the inability of the bacterium to withstand this concentration of the antibacterial, as confirmed by the viability data.

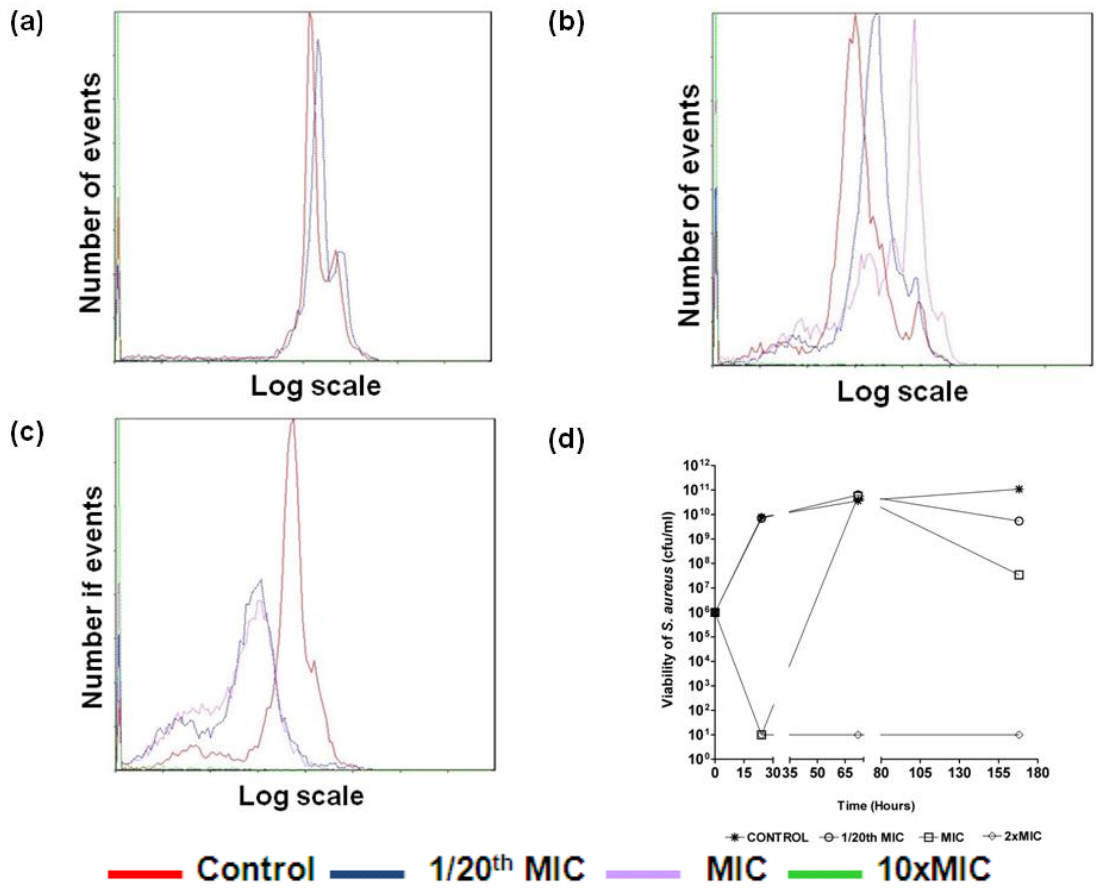

Figure 5.8 *S. aureus* cultures inoculated with $1x10^6$ cfu/ml, incubated with different concentrations of colistin (control; $1/20^{th}$ MIC – 5 μg/ml; MIC – 100 μg/ml;10xMIC – 1 mg/ml) and stained with Syto 9 were examined at (a) 24 (b) 72 and (c) 168 hours. Viability of *S. aureus* cultures (d) inoculated with 1 x 10^6 cfu/ml, post colistin incubation at 24, 72 and 168 hours. Data are representative of flow cytometry experiments performed in triplicate on three occasions.

The absence of a histogram peak for the MIC incubated bacteria at 24 hours is also verified by the viability data, as is the appearance of a peak for this culture at 72

and 168 hours. The triple peaked MIC histogram at 72 hours appeared further along the x-axis than the control and 1/20th MIC histograms, which indicated three differently sized groups of bacteria within the culture, the smaller group similarly sized to the control and sub-inhibitory bacteria, with the bigger group within the MIC culture larger in size compared to the bacteria in the other two cultures.

The broad MIC histogram peak at 168 hours spanned the 1/20th and control histograms; this indicated a great diversity in bacterial size within the MIC culture. The histograms representing control and sub-inhibitory treatment were very similar at 24 hours, by 72 hours both histograms displayed broad bases indicating diversity in the size of bacteria within the cultures, with slightly bigger bacteria present in the sub-inhibitory compared to control culture. This situation had reversed at 168 hours with the control bacteria now larger in size than the 1/20th MIC bacteria.

c) *Pseudomonas aeruginosa*

The data confirm that *P. aeruginosa* when incubated with 10xMIC colistin was unable to withstand exposure to that concentration of colistin due to the lack of a histogram peak (Figure 5.9). This is supported by the viability data which shows no viable bacteria were produced by *P. aeruginosa* incubated with 10xMIC colistin at 24, 72 or 168 hours. *P. aeruginosa* incubated with MIC colistin displayed no histogram at 24 hours but the bacterium had recovered sufficiently by 72 hours to produce a single peaked narrow based histogram further along the x-axis than the control, indicating the MIC incubated bacteria were a single homogenous group larger in size than control or 1/20th MIC incubated bacteria. The MIC culture displayed a triple peaked histogram at 168 hours, indicating the presence of a large group of very small bacteria (peak close to the y-axis) and two other groups of larger bacteria, similar in profile to control and 1/20th MIC bacteria.

The broad spread of the control histogram base and twin peaks at 24 hours identified diverse bacterial sizes within this culture. The single histogram peak representing the 24 hour 1/20th MIC culture was similarly located with the main body of the control histogram but without the broad spreading histogram tail which reached the y-axis, indicating bacteria within the 1/20th MIC culture were equal in size to the majority of the control bacteria.

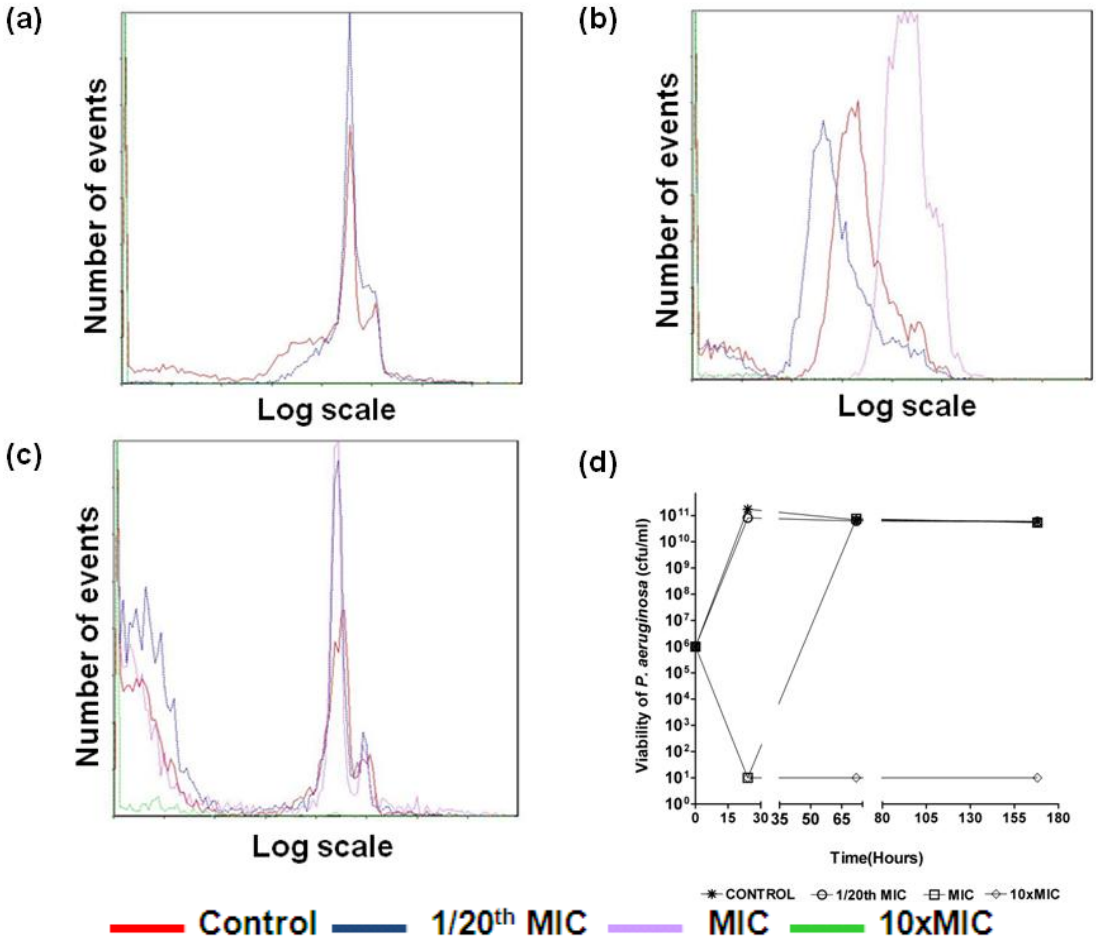

Figure 5.9 *P. aeruginosa* cultures inoculated with 1x10^6 cfu/ml, incubated with different concentrations of colistin (control; 1/20th MIC – 0.075 μg/ml; MIC – 1.5 μg/ml;10xMIC – 15 μg/ml) and stained with Syto 9 were examined at (a) 24 (b) 72 and (c) 168 hours. Viability of *P. aeruginosa* cultures (d) inoculated with 1 x 10^6 cfu/ml, post colistin incubation at 24, 72 and 168 hours. Data are representative of flow cytometry experiments performed in triplicate on three occasions.

At 72 hours *P. aeruginosa* incubated with the sub-inhibitory colistin concentration exhibited a histogram that was closer to the y-axis than control, which indicated the bacteria were smaller in size than control bacteria.

The 168 hour histograms for control and 1/20th MIC cultures all displayed triple peaked histograms, similarly located on the x-axis, therefore both cultures possessed two differently sized groups of bacteria, very small bacteria (very close to the y-axis) and much larger bacteria further along the x-axis.

5.3.3 Effects of NP101 on *E. coli*, *S. aureus* and *P. aeruginosa*

a) *Escherichia coli*

E. coli incubated with MIC and 2xMIC of NP101 were not detected by flow cytometry at 24 and 72 hours (Figure 5.10), which indicated the inability of the bacterium to tolerate the effects of the CAP.

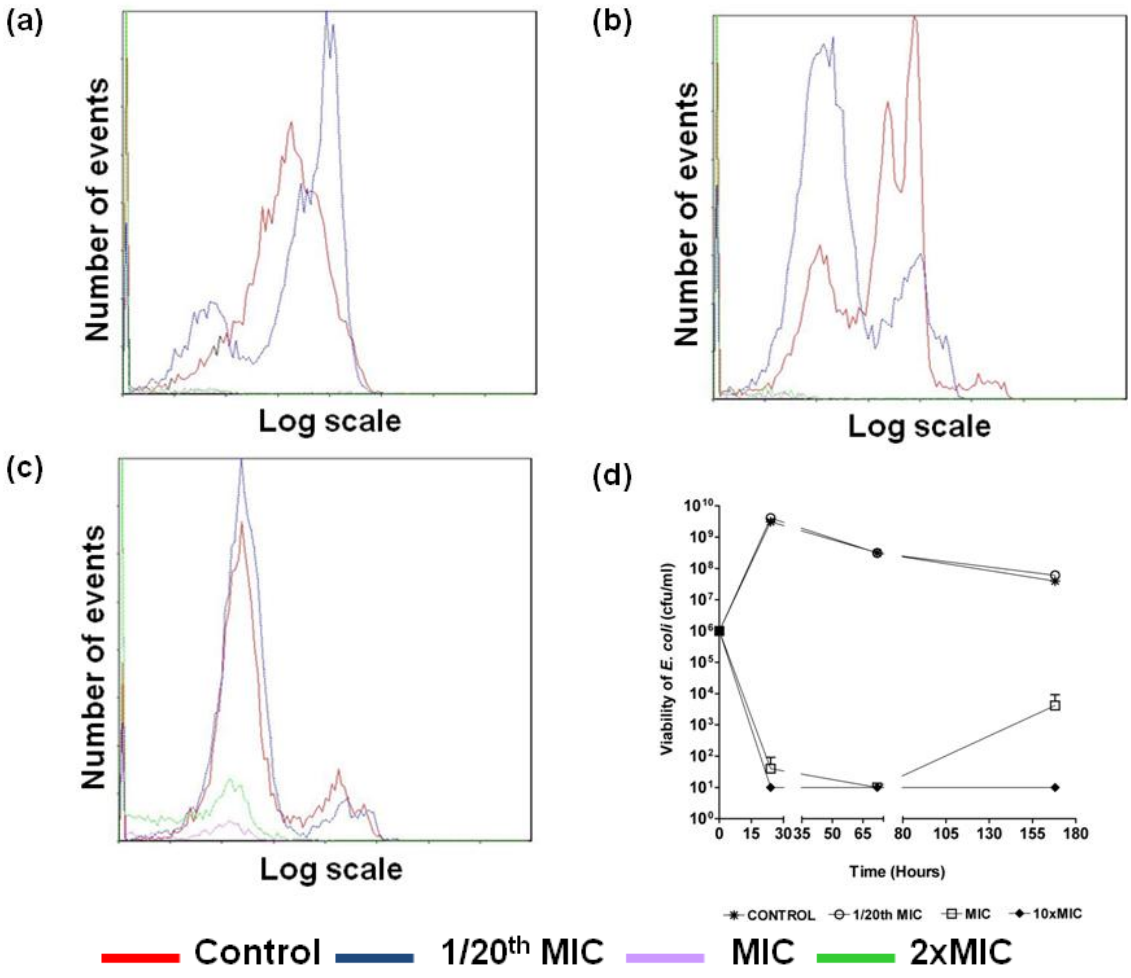

Figure 5.10 *E. coli* cultures inoculated with 1x10^6 cfu/ml, incubated with different concentrations of NP101 (control; 1/20th MIC – 0.025 mg/ml; MIC - 0.5 mg/ml;10xMIC – 5 mg/ml) and stained with Syto 9 were examined at (a) 24 (b) 72 and (c) 168 hours. Viability of *E. coli* cultures (d) inoculated with 1 x 10^6 cfu/ml, post NP101 incubation at 24, 72 and

168 hours. Data are representative of flow cytometry experiments performed in triplicate on three occasions.

At 168 hours a small peak from the MIC culture had appeared, most likely the result of tolerance developed by a very small number of *E. coli* cells to the presence of NP101. The viability data support the flow cytometry findings; with a small viable population produced by the 168 hour MIC incubated *E. coli*. The control histogram at 24 hours covered more than one log scale in width that revealed one heterogeneous population of bacteria of differing sizes. At 72 hours three separate peaks appeared on the control histogram, therefore a wide range of bacterial sizes were present in the culture. The 1/20th MIC histogram displayed two peaks at both 24 and 72 hours, but these display a different profile. By 168 hours both control and 1/20th MIC cultures displayed very similar twin peaked histograms.

b) *Staphylococcus aureus*

Neither the MIC or 2xMIC *S. aureus* cultures were able to withstand incubation with NP101 as revealed by flow cytometry assessment over the experimental period. The viability data revealed the recovery of the MIC culture from 72 hours but these persister cells were not detected by the flow cytometry assay, probably due to size limitation.

The control and sub-inhibitory concentrations displayed very similar peak profiles at 24 hours indicating three groups of differently sized bacteria within the population. This changed to a single peak at 72 hours suggesting these bacterial populations were matched and similar in size. By 168 hours the control culture histogram was spread over several log scales and displayed two separate peaks, so the diversity of sizes within this culture was substantial. The sub-inhibitory culture at 168 hours also displayed a twin peaked histogram spread over several log scales, with the larger histogram peak closer to the y-axis, therefore the greater proportion of bacteria in this culture were smaller in size than control bacteria.

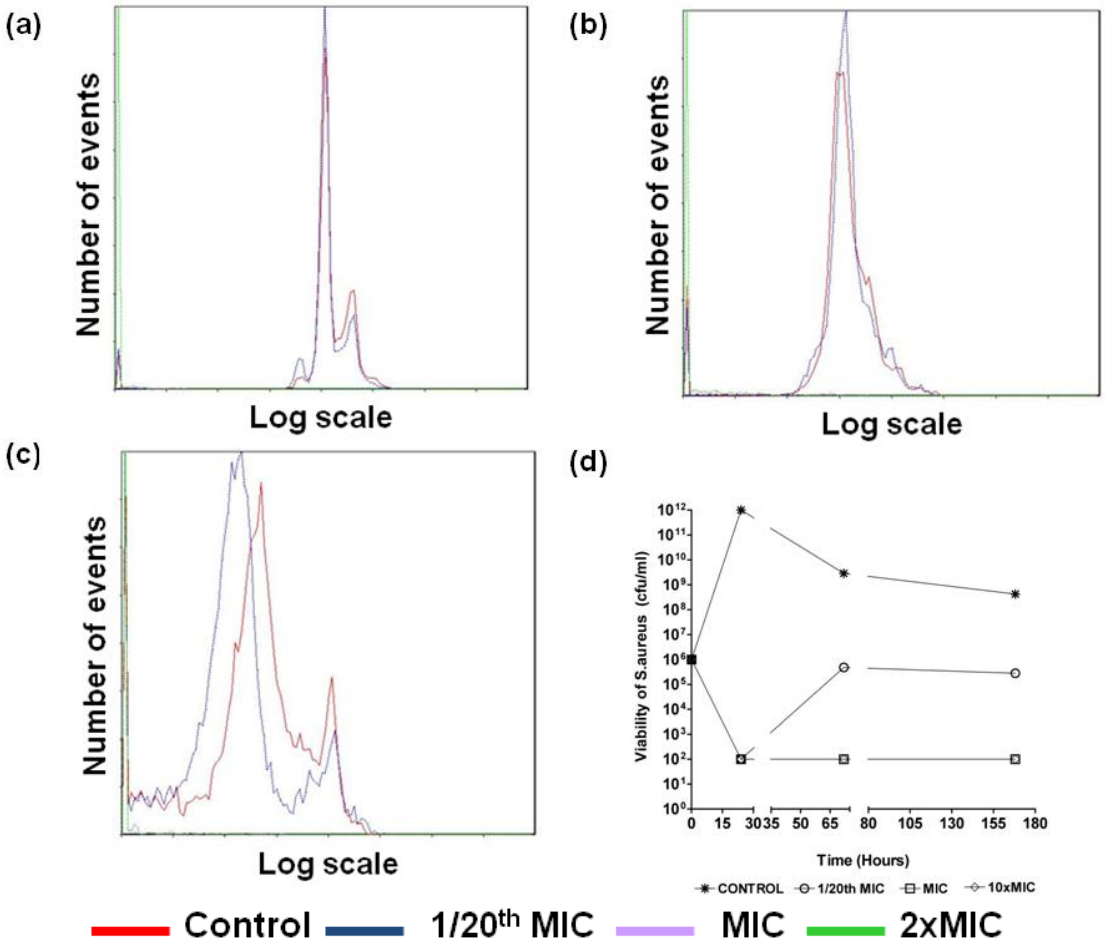

Figure 5.11 *S. aureus* cultures inoculated with 1x10^6 cfu/ml, incubated with different concentrations of NP101 (control; 1/20th MIC – 0.0125 mg/ml; MIC - 0.25 mg/ml;10xMIC – 2.5 mg/ml) and stained with Syto 9 were examined at (a) 24 (b) 72 and (c) 168 hours. Viability of *S. aureus* cultures (d) inoculated with 1 x 10^6 cfu/ml, post NP101 incubation at 24, 72 and 168 hours. Data are representative of flow cytometry experiments performed in triplicate on three occasions.

Though the viability data revealed a four-log difference between control and 1/20th MIC incubated bacteria at 72 and 168 hours, the bacterial size was substantially similar between these two cultures.

c) *Pseudomonas aeruginosa*

The 2xMIC incubated bacteria were not able to withstand the effects of NP101 and no histogram was recorded for this culture at any time point. The MIC incubated bacteria were recorded at 24 hours as a small peak but no histograms were recorded for the 72 hour and 168 hour cultures. The viability data also supported

this evidence while neither the MIC or 2xMIC cultures produced viable bacteria at 24, 72 or 168 hours.

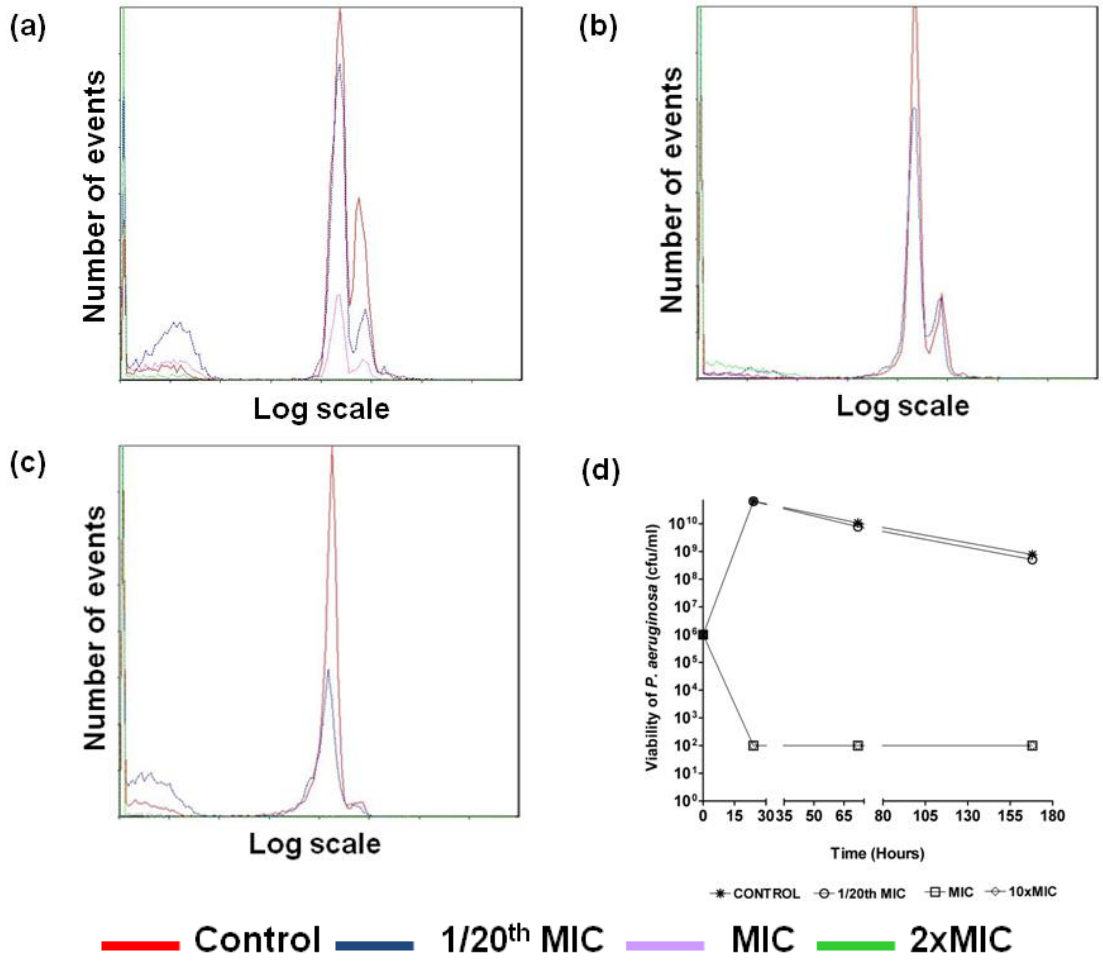

Figure 5.12 *P. aeruginosa* cultures inoculated with $1x10^6$ cfu/ml, incubated with different concentrations of NP101 (control; $1/20^{th}$ MIC – 0.0125 mg/ml; MIC - 0.25 mg/ml;10xMIC – 2.5 mg/ml) and stained with Syto 9 were examined at (a) 24 (b) 72 and (c) 168 hours. Viability of *S. aureus* cultures (d) inoculated with 1 x 10^6 cfu/ml, post NP101 incubation at 24, 72 and 168 hours. Data are representative of flow cytometry experiments performed in triplicate on three occasions.

Control and $1/20^{th}$ MIC histograms were very similar to each other over the experimental period. The peak representing a population of small cells had disappeared by 72 hours and only two larger groups of bacteria existed within each culture. The histograms for control and sub-inhibitory concentrations at 168 hours also exhibited two peaks, one peak very close to the y-axis and the other much

further along the y-axis, so the dynamics of the bacterial response varied substantially under the effect of NP101 over the experimental period.

5.3.4 Examination of the effects of NP108 on *E. coli*, *S. aureus* and *P. aeruginosa*

a) *Escherichia coli*

The absence of histogram peaks for *E. coli* incubated with MIC and 2xMIC NP108 indicated the inability of *E. coli* to tolerate the effects of NP108.

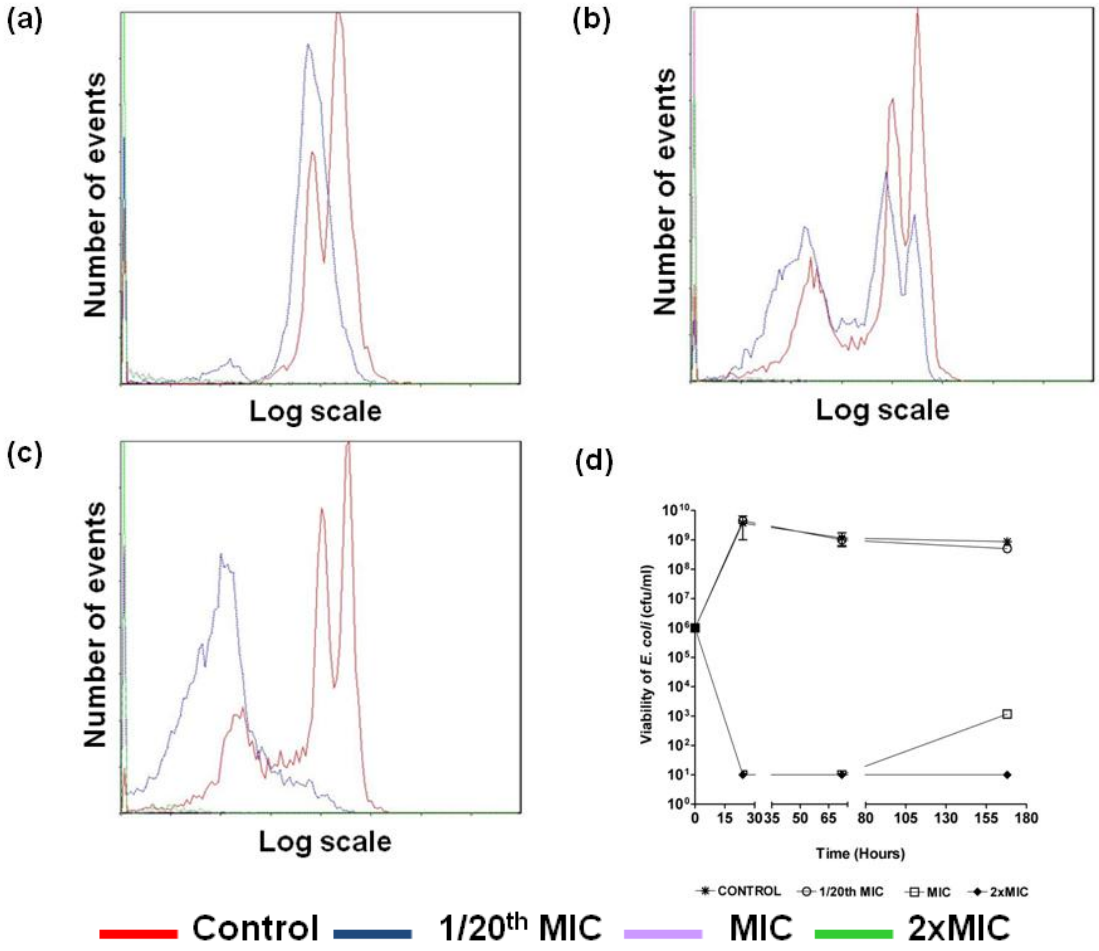

Figure 5.13 *E. coli* cultures inoculated with $1x10^6$ cfu/ml, incubated with different concentrations of NP108 (control; $1/20^{th}$ MIC – 0.0125 mg/ml; MIC - 0.25 mg/ml;10xMIC – 2.5 mg/ml) and stained with Syto 9 were examined at (a) 24 (b) 72 and (c) 168 hours. Viability of *E. coli* cultures (d) inoculated with 1 x 10^6 cfu/ml, post NP108 incubation at 24, 72 and 168 hours. Data are representative of flow cytometry experiments performed in triplicate on three occasions.

This is also supported by the viability data at all time points. At 24 hours the control histogram revealed two groups of different sized bacteria within the culture. Triple peaks on both control and 1/20th MIC histograms at 72 hours revealed a range of bacterial sizes in both cultures, however the sub-inhibitory incubated bacterial groups were smaller in size compared to control. The control histogram at 168 hours was practically identical to the 72 hour profile whereas the 1/20th MIC histogram, possessed one peak and a base extending over several log scales down to the y-axis, therefore the majority of these bacteria were substantially smaller than the control bacteria.

b) *Staphylococcus aureus*

S. aureus did not withstand the effects of MIC or 2xMIC NP108 at any time point (Figure 5.14), as indicated by the absence of histogram peaks for either of these two concentrations, the viability data generally support this finding.

The histograms of control and 1/20th MIC cultures were very similar to each other at all time points assessed. Both cultures displayed single histogram peaks at 24 hours. At 72 hours the histograms had moved closer to the y-axis, indicating the bacteria had decreased in size and each histogram exhibited a second small histogram peak further along the x-axis; therefore a small population of larger bacteria co-existed within the culture composed mainly of smaller bacteria.

The control and sub-inhibitory histograms had bases extending down to the y-axis at 168 hours and two histogram peaks, so these cultures contained varying sizes of small bacterial cells, similarly sized with each other.

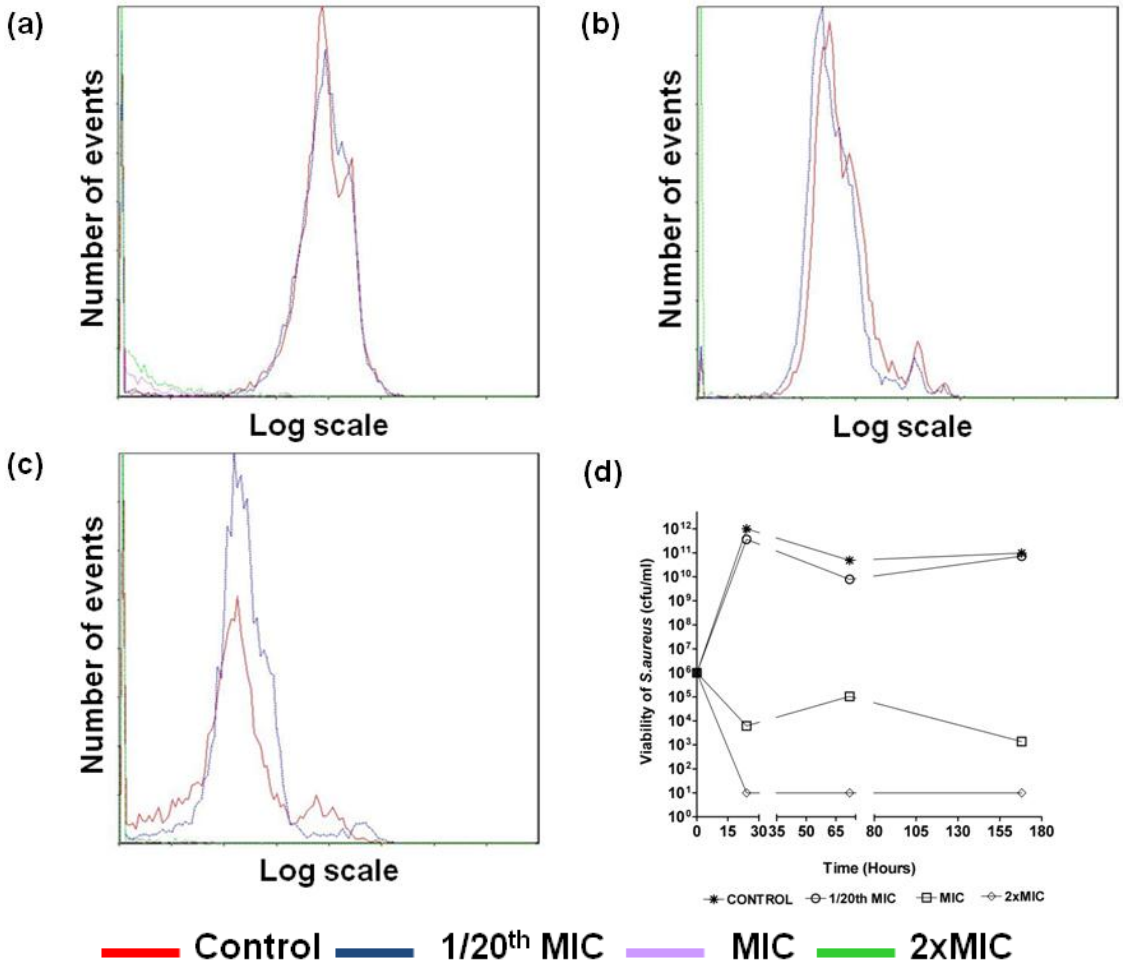

Figure 5.14 *S. aureus* cultures inoculated with 1x10^6 cfu/ml, incubated with different concentrations of NP108 (control; 1/20th MIC – 0.0125 mg/ml; MIC - 0.25 mg/ml;10xMIC – 2.5 mg/ml) and stained with Syto 9 were examined at (a) 24 (b) 72 and (c) 168 hours. Viability of *S. aureus* cultures (d) inoculated with 1 x 10^6 cfu/ml, post NP108 incubation at 24, 72 and 168 hours. Data are representative of flow cytometry experiments performed in triplicate on three occasions.

c) *Pseudomonas aeruginosa*

As previously seen with NP101, *P. aeruginosa* was unable to tolerate the effects of NP108 at either MIC or 2xMIC concentrations, as supported by the viability data. The control and 1/20th MIC plots were very similar at 24 hours, with two differently sized groups of bacteria within each culture. At 72 hours the histograms that represented each culture were very broad and extended right to the y-axis, which revealed a wide range of bacterial sizes. Control and sub-inhibitory histograms at 168 hours both revealed twin histogram peaks very similar in size and location to

one another, one peak beside the y-axis and the other histogram peak further along the x-axis.

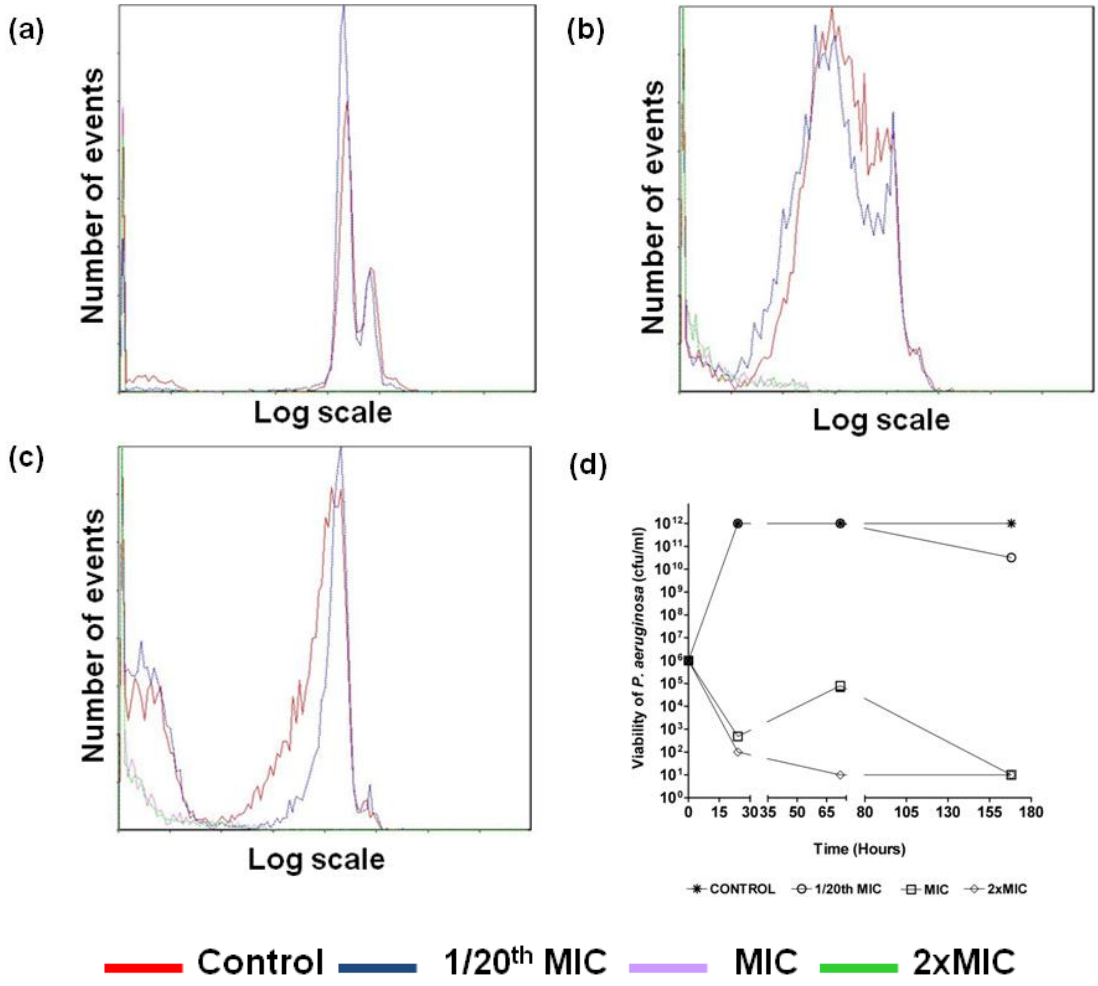

Figure 5.15 *P. aeruginosa* cultures inoculated with $1x10^6$ cfu/ml, incubated with different concentrations of NP108 (control; $1/20^{th}$ MIC – 0.0125 mg/ml; MIC - 0.25 mg/ml;10xMIC – 2.5 mg/ml) and stained with Syto 9 were examined at (a) 24 (b) 72 and (c) 168 hours. Viability of *P. aeruginosa* cultures (d) inoculated with 1 x 10^6 cfu/ml, post NP108 incubation at 24, 72 and 168 hours. Data are representative of flow cytometry experiments performed in triplicate on three occasions.

The lesser histogram peak represented small bacteria with the presence of the larger histogram peak further along the x-axis revealed the presence of a group of much larger bacteria within each of these cultures.

5.4 Discussion

5.4.1 Flow cytometry for analysing antimicrobial activity

The multiparameter measurements obtained from flow cytometer analysis of a bacterial population can be used to measure microbial diversity (Koch, Robertson and Button 1996). The flow cytometer permits the individual physical and fluorescence properties of each bacterial cell within a sample containing tens of thousands bacterial cells to be recorded (Valdivia and Falkow 1998). Early flow cytometry studies have shown that the growth of bacterial cells within a culture differs substantially from one another (Broger et al. 2011). This lack of growth homogeneity may be due to various reasons such as phenotypic changes during the cell cycle, spontaneous genetic mutations in some bacteria or differences in bacterial microenvironments (Broger et al. 2011)(Hall 1995)(Dien and Srienc 1991). Flow cytometry however permits the measurement of population distributions within bacterial cultures (Broger et al. 2011)(Rieseberg et al. 2001). Changes in bacterial cultures exposed to antimicrobials can also be measured to analyse the bacterial reactions to stresses induced by incubation with these agents. These bacterial responses to antimicrobial exposure can be diverse, ranging from morphological and size changes, alteration in bacterial growth rates, to bacterial death (Gant, Warnes and Phillips, I. and Savidge, G.F. 1993).

However there are drawbacks associated with flow cytometry use. Analysis of bacterial viability through the utilisation of dyes requires caution as it has been shown that the viability of a propidium iodide labelled, heat treated *S. aureus* population detected by flow cytometry was lower than the viability recorded by plate count, due to the ability of some bacteria retaining sufficient membrane

integrity to exclude propidium iodide despite being non-culturable (Comas and Vives-Rego 1998).

Also, optimised flow cytometry protocols are based on control bacteria with the discriminator set to exclude background noise and small sub-cellular particles or debris. However when analysing samples incubated with either MIC or supra-inhibitory concentrations of an antimicrobial, the monitor at the time of data acquisition, showed a large component of detected events fell below the discriminator level set on forward scatter. Consequently these events representing material below 0.2 μm were excluded from analysis and are not included in the overlay histograms presented in this investigation. Whether these were whole cells substantially smaller than those normally found or pieces of sub-cellular debris were un-clear.

Longer acquisition times were also necessary for all MIC and 2/10xMIC cultures due to the smaller number of cells present. The maximum acquisition time and level of detected events were set at 100 seconds and 10,000 events respectively and while data acquisition for the control and 1/20th MIC cultures took 20 seconds to record this number of events for every test species analysed, neither the MIC or 2/10xMIC cultures, except for *E. coli* and *S. aureus* incubated with triclosan MIC (Figure 5.4 and 5.5) and *S. aureus* and *P. aeruginosa* incubated with colistin MIC, (Figures 5.8 and 5.9) had 10,000 events recorded within the time period set on the flow cytometer. While the rate of bacterial viability in these cultures is directly attributable to exposure to the cationic antibacterials, analysis of these cultures was limited by the detection parameters of the flow cytometer to accurately analyse particles below 0.2 μm.

5.4.2 Effect of triclosan upon *E. coli* and *S. aureus*

a) *Escherichia coli*

Homogeneity in viability patterns were not displayed by *E.coli* control and triclosan incubated cultures. The control histograms display fluorescence associated with normal healthy bacterial cells to which the triclosan incubated cultures can be compared. The presence of viable cells in MIC and 10xMIC incubated bacteria was severely retarded through incubation with the bisphenol at 24 hours, resulting in insufficient numbers of bacteria being detected. At 72 and 168 hours the MIC culture had recovered sufficiently to be measured, but the 10xMIC culture was unable to tolerate exposure to triclosan at this concentration over the experimental period. This was also demonstrated in Chapter 3 (Figure 3.3) where severe retardation in onset of logarithmic growth coupled with reduction in logarithmic growth was shown for the MIC (0.07 μg/ml) bacteria and no growth was recorded at 10xMIC (0.7 μg/ml) triclosan.

The presence of viable bacteria in the MIC culture at 72 hours could be attributed to the development of tolerance by *E. coli* to triclosan that has been demonstrated in this investigation (Chapter 3) and by other investigators (Russell 2004). The substantial increase in the number of bacteria in the MIC culture could also be explained by the reduction in triclosan available for interaction with the bacteria at 72 hours, possibly through binding of the bisphenol to older bacteria within the culture, thus allowing cells composing the small colony variants to replicate and grow without the restraining influence of triclosan (Levy et al. 1999). The susceptibility of *E. coli* to triclosan concentrations of 0.07 μg/ml (MIC) displayed by the reduced growth rate of the bacterium is attributable to the ability of triclosan to inhibit fatty acid synthesis, subsequently reducing bacterial growth (Escalada et al. 2005)(Heath et al. 2000). Up-regulation of efflux pumps in *E. coli* has also been

proposed as a mechanism of decreased susceptibility to triclosan, permitting the bacterial cell to expel the bisphenol from within the bacterium as quickly as it enters (Suller and Russell 2000). Thus given time, *E. coli* is far better able to tolerate the presence of triclosan. Exposure to the antibacterial results in increased production or increased activity of these efflux pumps in the exposed bacteria than normal.

Another factor to be considered in recovery of the MIC culture is that as the incubation time increases and the availability of nutrients is reduced, susceptibility to antimicrobials decreases due to bacterial gene expression altering the bacterial envelope, which either reduces the permeability of the cell to the antimicrobial or the availability of fewer binding sites in the bacterium reducing the attachment of the agent to the bacterium and subsequent reduced antimicrobial effects (Gant, Warnes and Phillips, I. and Savidge, G.F. 1993)(Delcour 2009).

The result of exposure to triclosan MIC over 168 hours resulted in size reduction in *E. coli* i.e. the MIC culture was composed of small bacteria, compared to normal sized bacteria forming the bulk of the control culture.

b) *Staphylococcus aureus*

As with *E. coli* the 10xMIC triclosan incubated *S. aureus* was unable to tolerate the effects of that concentration of the biocide and the culture did not grow; therefore no histograms were recorded for these cultures. Similarly with the MIC incubated *E. coli* culture, the growth at 24 hours had been sufficiently inhibited that only a small histogram was registered for this culture. The MIC culture had significantly recovered at 72 and 168 hours for histograms to be recorded at these time points, most likely as a result of the similar responses observed for *E. coli*.

The MIC histogram at 72 and 168 hours were similarly located on the x-axis as the control histogram, therefore the MIC culture tolerated the effects of triclosan well

and the bacteria were similar in size and number to control. This was possibly due to *S. aureus* altering the permeability of its outer envelope to triclosan and up-regulation of efflux pumps (Suller and Russell 2000). The effects of the sub-inhibitory triclosan concentrations were well tolerated by *S. aureus* and the viability dynamics of these bacterial cultures substantially correlated to those of control culture. No fitness cost was placed on *S. aureus* as a result of incubation with the $1/20^{th}$ MIC triclosan.

5.4.3 Effects of colistin on *E. coli*, *S. aureus* and *P. aeruginosa*

a) *Escherichia coli*

Incubation with MIC and 10xMIC colistin exerted a bactericidal effect on *E. coli* over the experimental period and *E. coli* did not develop tolerance as a result of exposure to colistin. The viability of MIC incubated bacteria was sufficiently inhibited that not enough bacteria were detected at 24, 72 or 168 hour assays to be detected. The reputed mode of action of colistin, as described in Chapter 3, is by diffusion through bacterial walls to undertake intracellular activity. Unlike the irreversible binding of triclosan to bacterial targets reducing the concentration of triclosan within the incubated cultures, the concentration of colistin over the experimental period appeared to remain constant and *E. coli* was un-able to develop tolerance or acquire resistance to either the MIC or 10xMIC colistin concentrations.

Though the viability data revealed the MIC culture displayed small colony variants at 72 and 168 hours, any bacteria detected were too small to be registered as events and were registered as sub-cellular particles by the discriminator. The growth of the sub-inhibitory incubated bacteria was very similar to control at 24 and 72 hours so these bacteria matched the control culture for size and rate of

growth. The bulk of the 168 hour 1/20th MIC culture however was composed of smaller bacteria than the control culture, which indicated this concentration of colistin caused a size reduction in *E. coli* at longer exposure times.

b) *Staphylococcus aureus*

The most significant finding from the exposure of *S. aureus* to colistin was the concentration tolerated by the Gram-positive bacterium. Colistin is a cyclic CAP that was first isolated from the Gram positive *Bacillus polymyxa* (El Solh and Alhajhusain 2009) which is not used clinically in the treatment of Gram positive infections (Maviglia, Nestorini and Pennisi 2009). This colistin MIC was 33 times greater than that tolerated by *E. coli* and 67 times greater than the concentration tolerated by *P. aeruginosa.* Though bacteria in the 24 hour MIC colistin culture were not detected, sufficient bacterial numbers were enumerated in the 72 and 168 hour cultures for these cultures to be represented in histogram form. This suggests the development of a tolerance by *S. aureus* to colistin or an alteration of a colistin target by *S. aureus* resulting in decreased susceptibility to the antibacterial. The location of the 72 hour MIC histogram registered these bacteria as being larger in size than control bacteria. From this data it is perhaps a result of doublets or triplets being registered as single large events rather than colistin causing an increase in *S. aureus* size for which some evidence is available (Chapter 6). The sub-inhibitory concentration was well tolerated by *S. aureus* and matched the control at 24 hours with slightly larger bacteria registered by the 72 hour culture compared to control, probably as a result of the aggregatory effect of colistin on *S. aureus*. Both sub-inhibitory and inhibitory colistin concentrations at 168 hours revealed similarly placed histograms closer to the y-axis than the control histogram. Therefore as previously seen with *E. coli* the effect of long term

exposure on *S. aureus* by colistin at these concentrations resulted in a decrease in bacterial size compared to control.

c) *Pseudomonas aeruginosa*

Exposure of *P. aeruginosa* to 10xMIC colistin recorded a bactericidal effect at all assay times, as was previously shown in Chapter 3 (Figure 3.14). As described for *S. aureus*, the inhibitory effects of the MIC concentration on *P. aeruginosa* resulted in a loss of a detectable population after 24 hours exposure, although the organism was detected at 72 and 168 hours. As such *P. aeruginosa* is more able to deal with colistin than *E. coli*, as evidenced by the presence of detectable cells by flow cytometry. The 72 hour histogram was further along the x-axis compared to control but as with *S. aureus* it is plausible to suggest that doublet or triplet cells were recorded as large singlet events rather than colistin causing a size increase in *P. aeruginosa*.

The sub-inhibitory concentration was very similar to control at 24 hours but the viability dynamics had changed by 72 hours to reveal smaller bacteria within this culture. The data from control, sub-inhibitory and inhibitory concentrations were similar by 168 hours, revealing two group sizes of bacteria within each culture. However, as the un-treated control depicted the normal viability of this bacterium, neither of these colistin concentrations at this time point exerted a fitness cost on *P. aeruginosa* as both bacterial size and growth rate matched that of the untreated control.

5.4.4 Effects of NP101 on *E. coli*, *S. aureus* and *P. aeruginosa*

Exposure of *E. coli* to 2xMIC NP101 exerted a bactericidal effect on the bacterium, as previously revealed in Chapter 3 (Figure 3.16). The growth of MIC incubated bacteria was sufficiently inhibited that no cells were detected at either 24 or 72

hour assays; however, by 168 hours *E. coli* survivors had either developed a tolerance to or alteration of a target site such that a small histogram peak was recorded at this time point. Further investigation to elucidate whether this tolerance was stable or reversible upon de-sensitisation to NP101 would be worthwhile, as this would have serious implications as to whether CAPs could be used as therapeutic agents. Incubation with sub-inhibitory concentrations of NP101 caused changes in bacterial size over the experimental period, with bacterial size at 24 hours similar to control, changing to smaller bacteria at 72 hours and reverting to normal bacterial size, as depicted by the control culture, by 168 hours.

b) *Staphylococcus aureus*

Both MIC and 2xMIC NP101 concentrations affected bacterial viability to such an extent that no histograms were recorded for either of these cultures at any time point. However, viability data showed a limited presence of some small colony variants in the MIC culture.

Incubation of *S. aureus* with $1/20^{th}$ MIC NP101 revealed histograms similar to control at 24 and 72 hours, while the viability data at 24 hours revealed viability of this culture being less than $1x10^2$ cfu/ml. This could be due to variations experienced in cultivating *S. aureus* colonies on agar plates from planktonic cultures, as sufficient bacteria were present in this culture for enumeration in flow cytometry samples i.e. viable but not culturable (Trevors 2011). The 168 hour histogram revealed NP101 caused a reduction in size of the majority of the sub-inhibitory incubated bacteria compared to control.

c) *Pseudomonas aeruginosa*

Tolerance to NP101 was not developed by *P. aeruginosa* to the MIC or 2xMIC concentration. A small histogram was displayed by the MIC culture at 24 hours, but by 72 hours insufficient bacteria were detected in this culture for a histogram to be

displayed. The 1/20th MIC culture revealed viability and bacterial size similar to control with no reduction in size after extended exposure to the CAP.

5.4.5 Effects of NP108 on *E. coli*, *S. aureus* and *P. aeruginosa*

Incubation with MIC and 2xMIC concentration of NP108 did not result in the development of tolerance by *E. coli*, *S. aureus* or *P. aeruginosa* to the antibacterial. Insufficient bacterial numbers were detected in all three bacterial species for peaks to be present in overlay histograms.

As seen with NP101 exposure to the sub-inhibitory concentration of NP108 resulted in a reduction in bacterial size of *E. coli* over long term exposure to this peptide. However no size reduction was detected in *Staphylococcus aureus* after extended exposure to the sub-inhibitory concentration of NP108, whereas extended exposure of *Pseudomonas aeruginosa* to 1/20th MIC NP108 concentration resulted in slightly larger bacteria compared to control.

5.5 Conclusion

The sub-inhibitory triclosan concentration was well tolerated by both *E. coli* and *S. aureus* with neither culture exhibiting any apparent physiological stress. As with triclosan the supra-inhibitory 10xMIC colistin concentration was bactericidal against all three test species. *E. coli* alone of the test species did not develop a tolerance to the effects of the MIC colistin concentration. The reduction in size of *S. aureus* after prolonged exposure to the inhibitory colistin concentration was not detected in *P. aeruginosa*; however the colistin concentration tolerated by *S. aureus* was 67 times higher than that withstood by *P. aeruginosa*.

Exposure of *E. coli* to the inhibitory concentration of NP101 resulted in what appeared to be tolerance to the CAP by 168 hours, requiring further investigation.

Tolerance to either MIC or 2xMIC NP108 did not develop in *E. coli*, *S. aureus* or *P. aeruginosa* over the experimental period.

Chapter Six

Examination of the influence of cationic antibacterials upon test bacteria using scanning electron microscopy

6.1 Introduction

Scanning electron microscopy was used to examine any morphological or population changes in *E. coli*, *S. aureus* and *P. aeruginosa* incubated with sub-inhibitory, inhibitory and supra-inhibitory concentrations of four antimicrobial agents; triclosan, colistin, NP101 and NP108.

6.1.1 Electron Microscope

The prototype of the electron microscope was developed in 1931 by Ernst Ruska and Max Knoll with the capacity for a 400 fold magnification. Instruments today are capable of magnifications in excess of one million fold and Figure 6.1 shows the internal components of a scanning electron microscope.

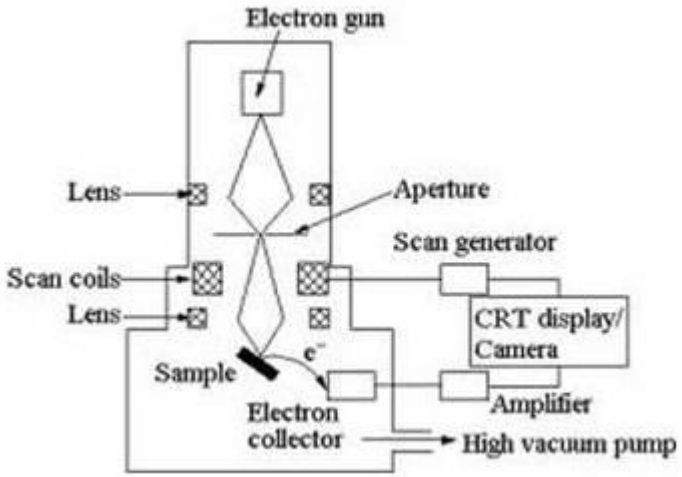

Figure 6.1 Components of a scanning electron microscope

An electron microscope uses a particle beam of electrons to illuminate a sample and obtain a magnified image. Within the electron microscope, electrostatic and electromagnetic lenses are used to control the electron beam and focus them to

form an image. The 50 picometre resolution of the electron microscope is due to electrons possessing wavelengths approximately 100,000 times shorter than visible light, permitting sample magnification by up to 10,000,000 times.

6.1.2 Scanning Electron Microscope

The scanning electron microscope (SEM) produces an image by scanning a very small spot on a sample with a focussed electron beam. This electron beam is in turn moved over every part of the sample being examined. At each point on the specimen, the incident electron beam loses some energy and this energy is converted into the emission of low-energy secondary electrons and heat. The electron current leaving the sample is collected and amplified and is then used to modulate the brightness of a cathode-ray tube (CRT). The movement of the CRT on the display screen exactly corresponds to the motion of the electron beam over the object. Any feature on a sample causing the electron current to change from point to point upon leaving, is recorded on the picture generated by the CRT. Thus variations in any property of the scanned area of the sample are recorded.

6.1.3 Bacterial responses to incubation with antibacterial agents

Investigation of bacterial responses to incubation with various concentrations of test antibacterials was undertaken via SEM. All test agents were cationic antibacterials with reputed known effects on bacterial membranes. However CAPs are reported to have several mechanisms of action (Hale and Hancock 2007)(Zhang and Falla 2006) and the exact mode of colistin activity remains to be identified (Clausell et al. 2003), while many groups have attributed direct activity on lipid synthesis by triclosan (Escalada et al. 2005)(McMurray, Oethinger and Levy 1998).

Therefore the effect of incubation with antibacterials possessing varied modes of action on the gross morphology of each test bacterium was undertaken in this investigation.

Bacterial responses to incubation with increasing antibacterial concentrations were also investigated. Sub-inhibitory antibacterial concentrations can inhibit normal cellular functions without death ensuing (Dynes et al. 2009) so investigations were undertaken to determine whether bacterial morphology displayed by such treated bacteria proved different to that of bacteria incubated with growth inhibitory MIC or multiples of the MIC concentration.

The response of bacteria reported to be resistant to or unaffected by some of the selected antimicrobials; such as *P. aeruginosa* to triclosan (Chuanchuen, Karkhoff-Schweizer and Schweizer 2003) and *S. aureus* to colistin (Clausell et al. 2003), were also examined and results obtained compared with the effects displayed by susceptible bacteria.

6.1.4 Morphology of test species

Escherichia coli, family Enterobacteriaceae, is reported as being a blunt ended rod shaped Gram-negative bacterium 0.3-1 x 1–6 μm in length, peritrichously flagellate, naturally existing as a pair of two bacteria or as single cells (Furchtgott, Wingreen and Huang 2011)(Singleton 1999). *Staphylococcus aureus (*Genus *Staphylococcus)* is a round or ellipsoidal non-motile Gram positive bacterium, approximately 1 μm in diameter, naturally occurring as irregular clusters of bacteria, resembling bunches of grapes, from whence their name is derived. (Salton and Kim 1996)(Singleton 1999). *Pseudomonas aeruginosa* is a Gram-negative rod shaped bacterium 0.5-1 x 1.5 - 5 μm in length, belonging to the family Pseudomonadacaea, occurring as single cells or groups of two/three cells, with

one/several un-sheathed typically polar flagella per bacterium (El Solh and Alhajhusain 2009)(Singleton 1999).

6.2 Methodologies

6.2.1 Preparation of bacterial cultures for Scanning Electron Microscopy analysis

All bacterial cultures were prepared for SEM examination as described in Section 2.9. The images presented are representative of several similar images obtained across the field of view. Attempts have been made to ensure that operator subjectivity have been minimised.

6.2.2 Scanning Electron Microscope data collection

SEM micrographs in this investigation were collected at a magnification of 20,000 and 50/100,000 and at a working distance of 7 - 8 mm. As triclosan incubated bacteria were the first to be examined, the magnification employed to capture these SEM images are not consistent as protocols were being optimised. However, the magnifications at which subsequent SEM images of colistin and CAP incubated bacteria were recorded, are identical.

6.2.3 Selection of suitable bacterial density

Initial SEM experiments employed a density of $1x10^6$ cfu/ml, which proved a sufficient initial bacterial density for experiments of 24-hours duration and longer. However this bacterial density was insufficient when SEM analysis of cultures incubated for less than 24 hours was undertaken and as triclosan was examined initially, a cell density of $1x10^8$ cfu/ml was selected. However, this concentration was revised downwards to $1x10^7$ cfu/ml for all subsequent bacterial analysis when examination of this bacterial density proved suitable. The SEM images of NP101

and NP108 displayed here were prepared from the same bacterial cultures used for the flow cytometry experiments described in Chapter 5, Sections 5.3.3 and 5.3.4.

6.3 Results

6.3.1 SEM images of *E. coli*, *S. aureus* and *P. aeruginosa* incubated with triclosan

a) *Escherichia coli*

The morphology of *E. coli* control and triclosan incubated bacteria can be seen in Figure 6.2. The control micrographs revealed a normal morphological pattern; bacterial length being 2-3 μm and rod shaped cells of an *E. coli* culture under optimum conditions. This served as a reference to which triclosan incubated bacteria could be compared. It can be clearly seen from the SEM images below that the reaction of *E. coli* to the presence of triclosan was swift. Within one hour's incubation with sub, MIC and supra-inhibitory triclosan concentrations, the effect of triclosan was manifest by the rounding of individual cells and inhibition of normal septation in the bacterium at all three triclosan concentrations.

Bacterial size in the sub-inhibitory triclosan concentration was 1.5 μm in length; the non-septated chain in the MIC culture was 11.8 μm in length, with individual bacteria measuring just over 1 μm in length. The reduction in bacterial size due to incubation of *E. coli* with triclosan is inversely proportional to the increasing triclosan concentrations.

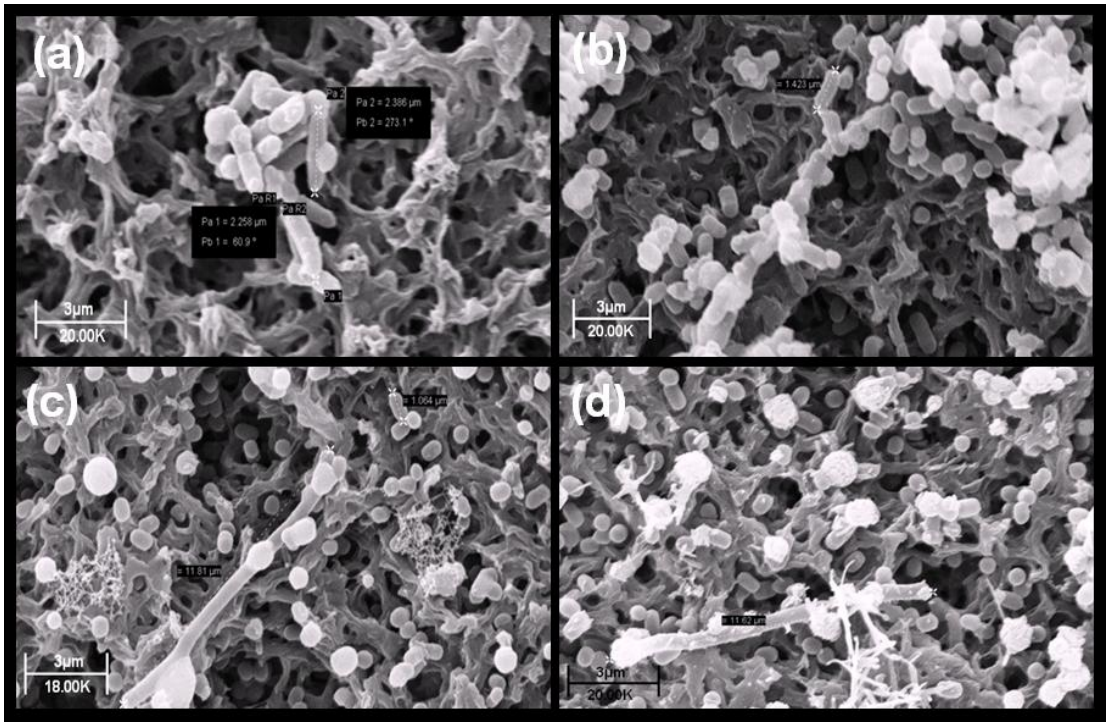

Figure 6.2 Scanning electron micrograph of $1x10^8$ cfu/ml *E. coli* exposed to triclosan for 1 hour: (a) control (b) 0.9 µg/ml (1/20th MIC) (c) 18 µg/ml (MIC) and (d) 180 µg/ml (10xMIC)

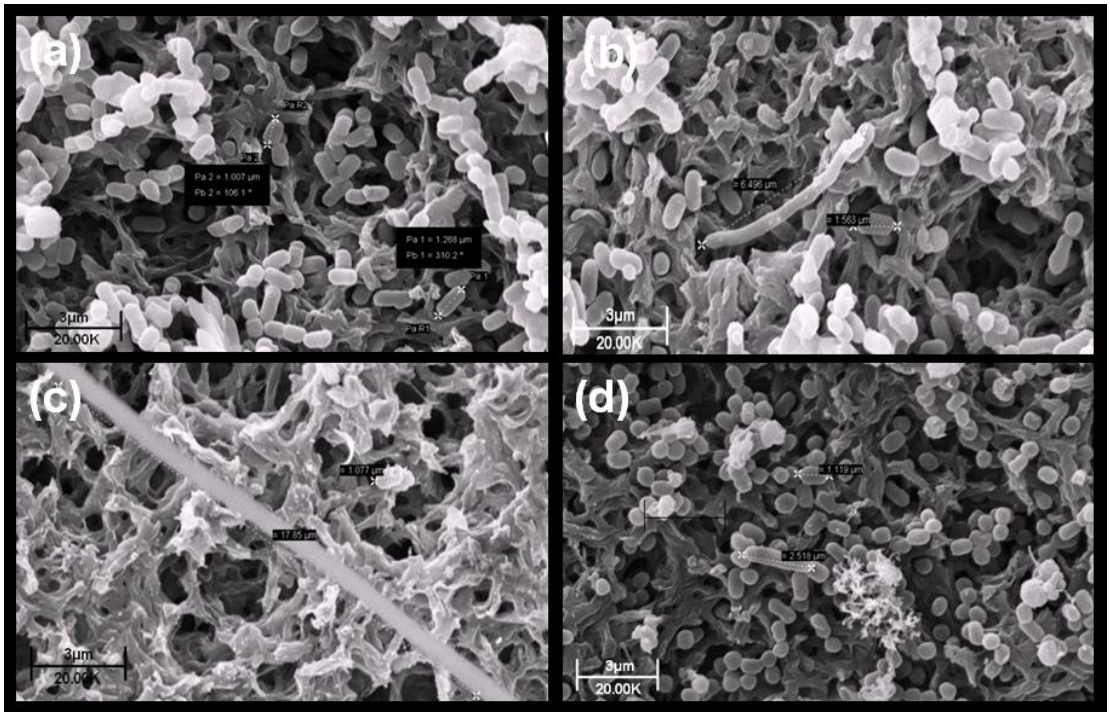

Figure 6.3 Scanning electron micrograph of $1x10^8$ cfu/ml *E. coli* exposed to triclosan for 3 hours: (a) control (b) 0.9 µg/ml (1/20th MIC) (c) 18 µg/ml (MIC) and (d) 180 µg/ml (10xMIC).

At three hours incubation (Figure 6.3) with the agent, the long co-joined *E. coli* were more apparent especially at MIC concentration, where few single bacteria were now visible. Control bacteria were 1.3 μm in length, with 1/20th MIC bacteria measuring 6.5 μm for non-septated bacteria and 1.6 μm for individual bacteria. The visualized co-joined bacterial chain in the MIC culture was 18 μm long, while the bacteria visualised in the 10xMIC micrograph measured 1.2 μm and 2.5 μm respectively.

Control bacteria were 1μm long at 6 hours (Figure 6.4) compared to 0.9μm for 1/20th MIC bacteria.

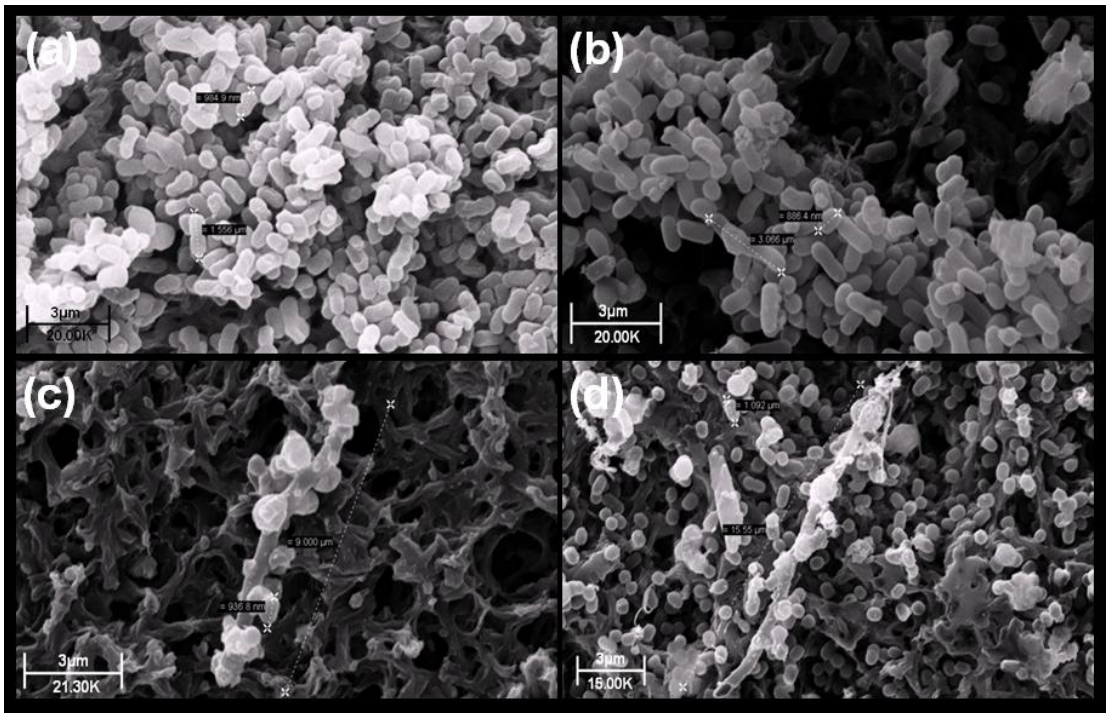

Figure 6.4 Scanning electron micrograph of 1x10^{8} cfu/ml *E. coli* exposed to triclosan for 6 hours: (a) control (b) 0.9 μg/ml (1/20th MIC) (c) 18 μg/ml (MIC) and (d) 180 μg/ml (10xMIC). Viability after 6 hours; *E. coli* control 1.55x10^{11} cfu/ml; *E. coli* incubated with 1/20th MIC triclosan 4.5x10^{9} cfu/ml; MIC and 10xMIC triclosan incubated bacteria was < 10 cfu/ml

The inhibitory triclosan concentration still displayed aberrant septation behaviour with the presence of long chains of attached bacteria 9 μm in length, which also displayed a budding propensity (Figure 6.4 (c)). This budding effect suggested growth in *E. coli* was now occurring not only longitudinally but also in other

dimensions to the co-joined chain. The supra-inhibitory concentration continued to reveal co-joined bacteria.

Incubation at 24 hours (Figure 6.5) revealed the normal size and typical blunt ended shape of *E. coli* control bacteria. A clumping effect of the sub-inhibitory triclosan concentration was more apparent at 24 hours; however bacterial length was equivalent to control. Flow cytometry data presented in Chapter 5 (Figure 5.4 (a)) revealed control and 1/20th MIC bacteria were very similarly sized to one another, while the MIC treated bacteria that were detected were larger in size than these two cultures. The inhibition of normal bacterial septation was now displayed by the entire MIC incubated culture with cross-linked bacteria visible throughout this culture, which would account for the identification of larger bacteria in this culture by flow cytometry.

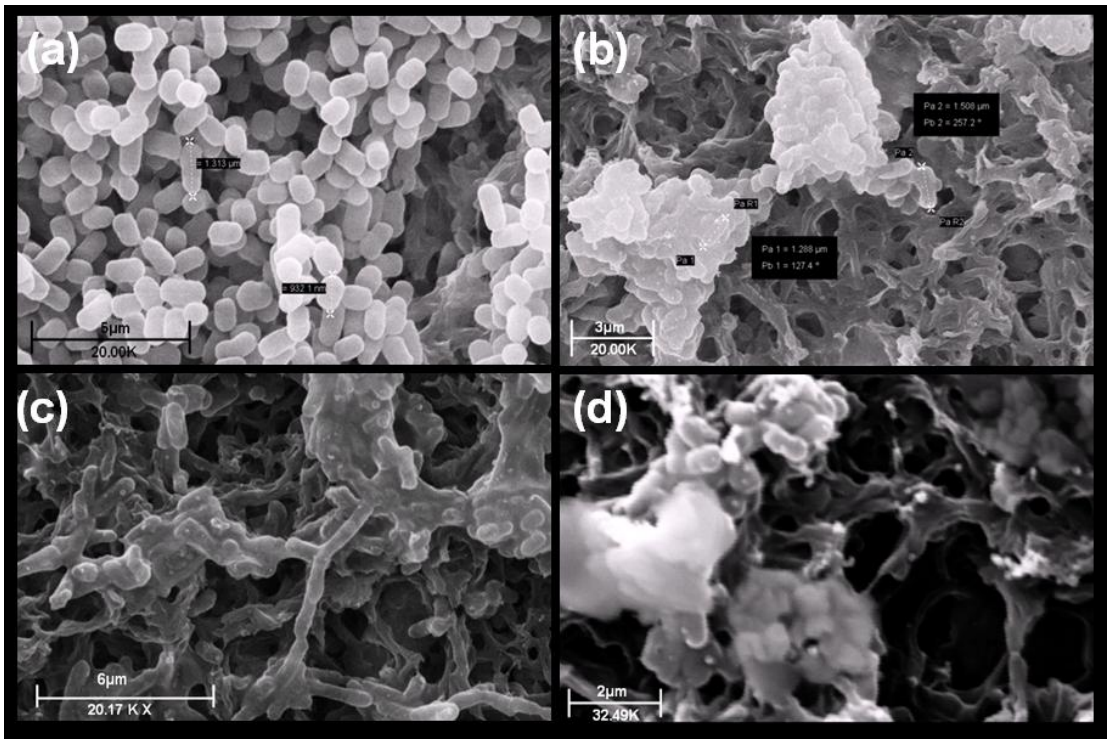

Figure 6.5 Scanning electron micrograph of 1x10^6 cfu/ml *E. coli* exposed to triclosan for 24 hours: (a) control (b) 0.0035 µg/ml (1/20th MIC) (c) 0.07 µg/ml (MIC) and (d) 0.7 µg/ml (10xMIC). Viability after 24 hours; *E. coli* control 7.75x10^8 cfu/ml; *E. coli* incubated with 1/20th MIC triclosan 7.5x10^8 cfu/ml; MIC and 10xMIC triclosan incubated bacteria was < 10 cfu/ml

The 10xMIC culture was now displaying a gelling effect, previously reported for biocides on bacteria by other researchers (Barrett-Bee, Newboult and Edwards 1994). This would explain why insufficient bacteria were detected by flow cytometry in the supra-inhibitory culture, as bacterial features employed in flow cytometry to identify bacteria within a culture, include forward scatter for size and bacterial shape and side scatter for granularity.

The varied effects of triclosan on *E. coli* revealed in the 24 hour SEM images had intensified by 72 hours (Figure 6.6); namely aggregation in the sub-inhibitory concentration, non-septation at inhibitory concentration and gelling at the supra-inhibitory concentration.

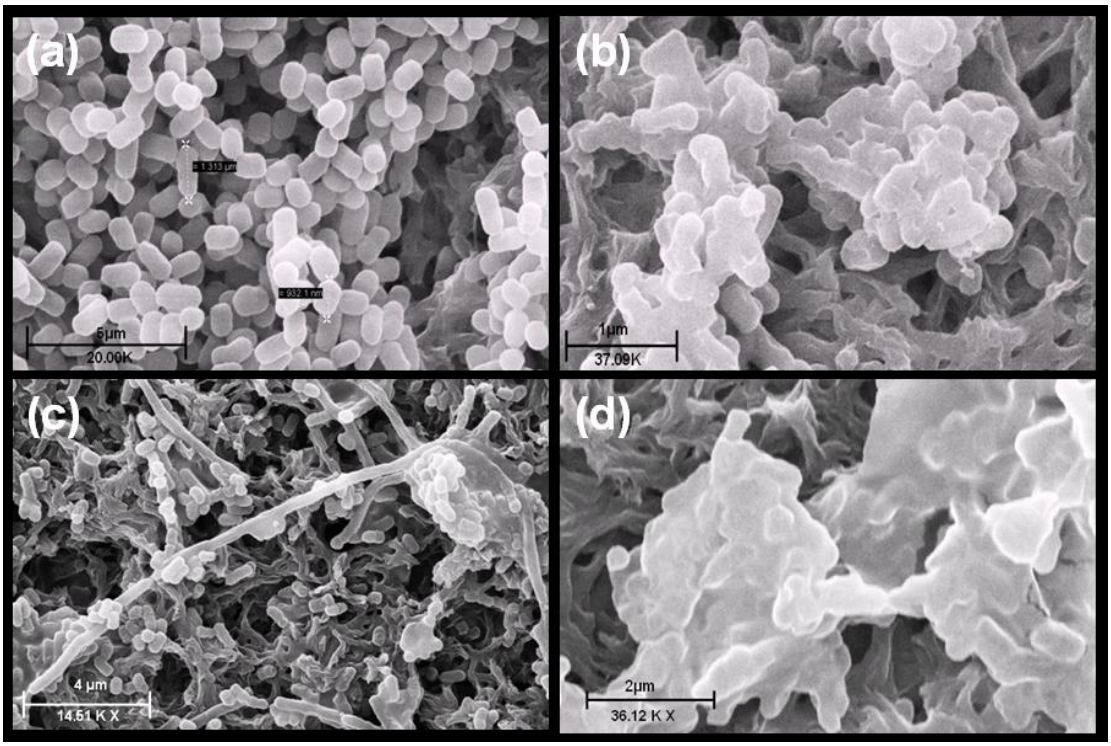

Figure 6.6 Scanning electron micrograph of $1x10^6$ cfu/ml *E. coli* exposed to triclosan for 72 hours: (a) control (b) 0.0035 µg/ml (1/20th MIC) (c) 0.07 µg/ml (MIC) and (d) 0.7 µg/ml (10xMIC). Viability after 72 hours; *E. coli* control $1.5x10^{10}$ cfu/ml; *E. coli* incubated with 1/20th MIC triclosan $1.3x10^{10}$ cfu/ml; *E. coli* incubated with MIC triclosan $7.7x10^9$ cfu/ml ; 10xMIC triclosan incubated bacteria was < 10 cfu/ml

The inhibitory concentration revealed the re-appearance of single bacteria, co-existing with the non-septated bacteria. Flow cytometry data in (Figure 5.4 (b))

revealed the re-appearance of normal sized cells in the MIC culture in the 72-hour overlay plot, which were absent from the overlay plot describing the 24-hour cultures. The viability of *E. coli* exposed to the inhibitory triclosan concentration had recovered substantially (Figure 5.4 (D)) and the bacteria were exhibiting a tolerance to triclosan gained through exposure to the bisphenol for 72 hours.

After 168 hours incubation normal *E. coli* bacteria 1 μm long can be seen in the control culture (Figure 6.7 (a)).

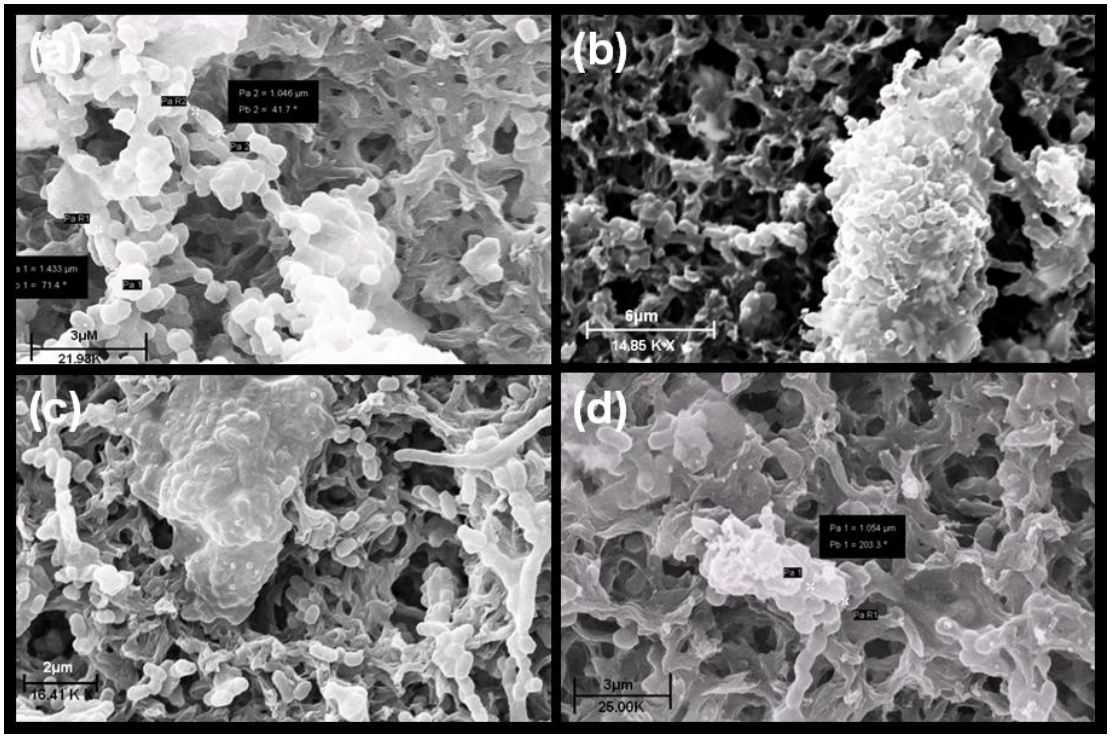

Figure 6.7 Scanning electron micrograph of $1x10^6$ cfu/ml *E. coli* exposed to triclosan for 168 hours: (a) control (b) 0.0035 μg/ml (1/20th MIC) (c) 0.07 μg/ml (MIC) and (d) 0.7 μg/ml (10xMIC). Viability after 168 hours; *E. coli* control $6.3x10^{10}$ cfu/ml; *E. coli* incubated with 1/20th MIC triclosan $5.5x10^{10}$ cfu/ml; *E. coli* incubated with MIC triclosan $7.6x10^9$ cfu/ml ; 10xMIC triclosan incubated bacteria was < 10 cfu/ml

The 1/20th MIC incubated culture revealed large aggregated bodies of bacterial cells. Whilst bacterial viability was not affected by 1/20th MIC triclosan, the degree of bacterial aggregation was. Incubation with the MIC concentration for 168 hours, revealed co-joined *E. coli* as well as individual bacterial cells, smaller in size than

control cells. It is important to note that after both 72 and 168 hours incubation with triclosan, the MIC treated culture displayed a viable population.

At 168 hours the bacteria in the 10xMIC culture revealed barely discernible bacterial outlines clumped in a gelled mass, in keeping with the loss of a viable population. This is supported by flow cytometry data (Figure 5.4 (c)) where the MIC culture revealed bacteria smaller in size than control cells and few bacteria were acquired in the 10xMIC culture.

b) *Staphylococcus aureus*

S. aureus cultures were examined after incubation with triclosan for one hour (Figure 6.8).

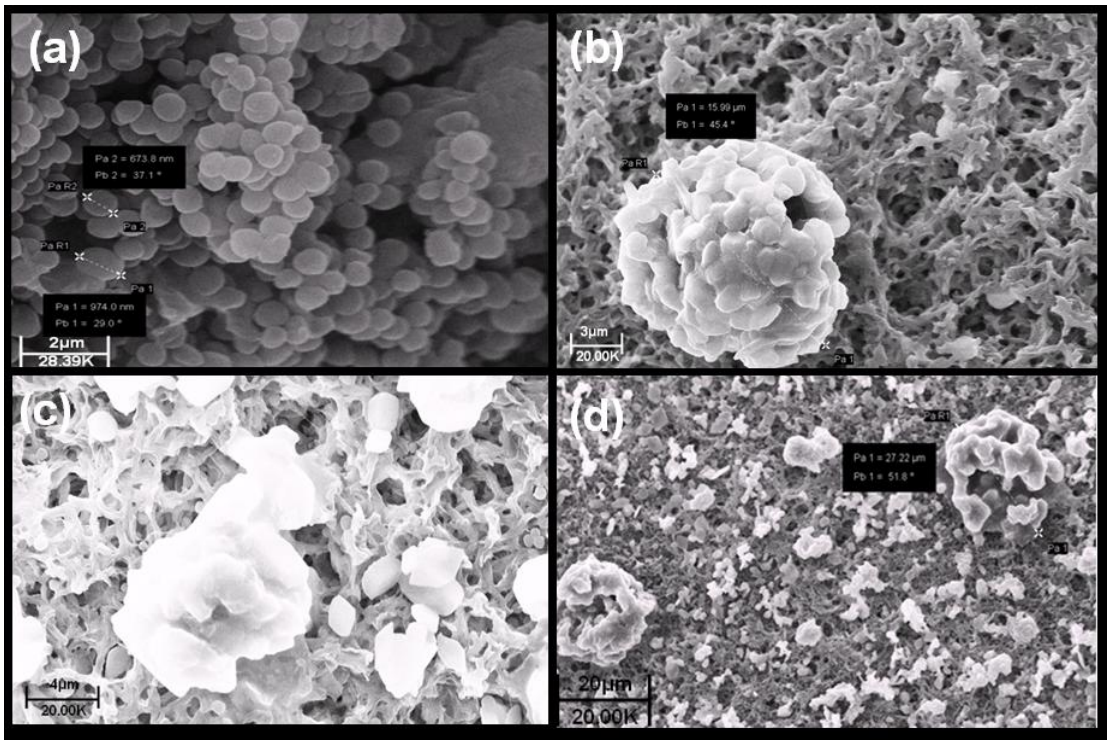

Figure 6.8 Scanning electron micrograph of $1x10^8$ cfu/ml *S. aureus* exposed to triclosan for 1 hour: (a) control (b) 0.7 µg/ml ($1/20^{th}$ MIC) (c) 14 µg/ml (MIC) and (d) 140 µg/ml (10xMIC) (b) *S. aureus* $1x10^6$ cfu/ml culture.

The control culture displayed clusters of bacteria between 0.7 – 1 µm in diameter. Incubation in the sub-inhibitory triclosan concentration caused *S. aureus* cells to form spherical aggregates approximately 16 µm in diameter. Spherical aggregates

were also observed in the MIC and 10xMIC culture but were imperfectly formed in the 10xMIC culture.

Images obtained for 3 hours exposure (Figure 6.9) revealed bacteria of a normal size in the control culture, whilst single and aggregated bacteria were visualised in the 1/20th MIC culture, although the larger spherical entities from one hour were missing. The MIC and 10xMIC cultures continued to display spherical cellular aggregates, with larger aggregates observed in the MIC culture, and no normal clusters of two to three bacterial cells.

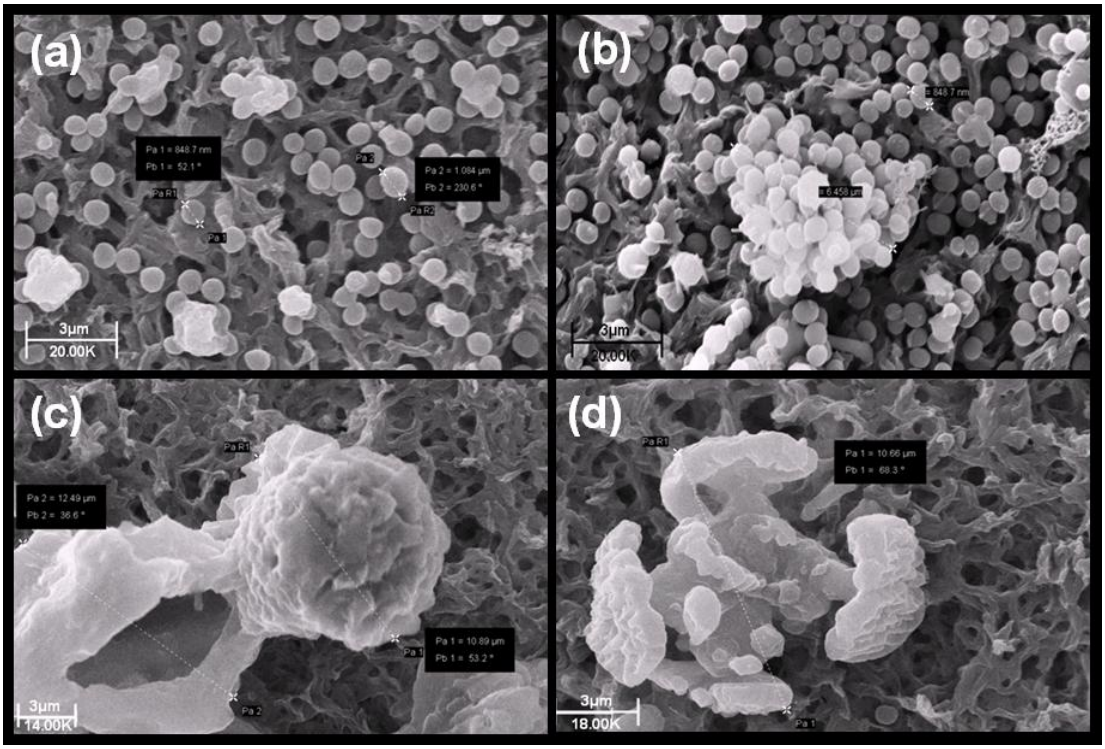

Figure 6.9 Scanning electron micrograph of 1x10^{8} cfu/ml *S. aureus* exposed to triclosan for 3 hours: (a) control (b) 0.7 µg/ml (1/20th MIC) (c) 14 µg/ml (MIC) and (d) 140 µg/ml (10xMIC).

By 6 hours incubation (Figure 6.10) bacterial sizes in all the cultures were similarly sized and the aggregatory effect of triclosan on *S. aureus* was more apparent as the concentration of triclosan increased. However in both MIC and 10xMIC populations there was a lack of the larger spherical structures observed at one and three hours. These must have disassembled.

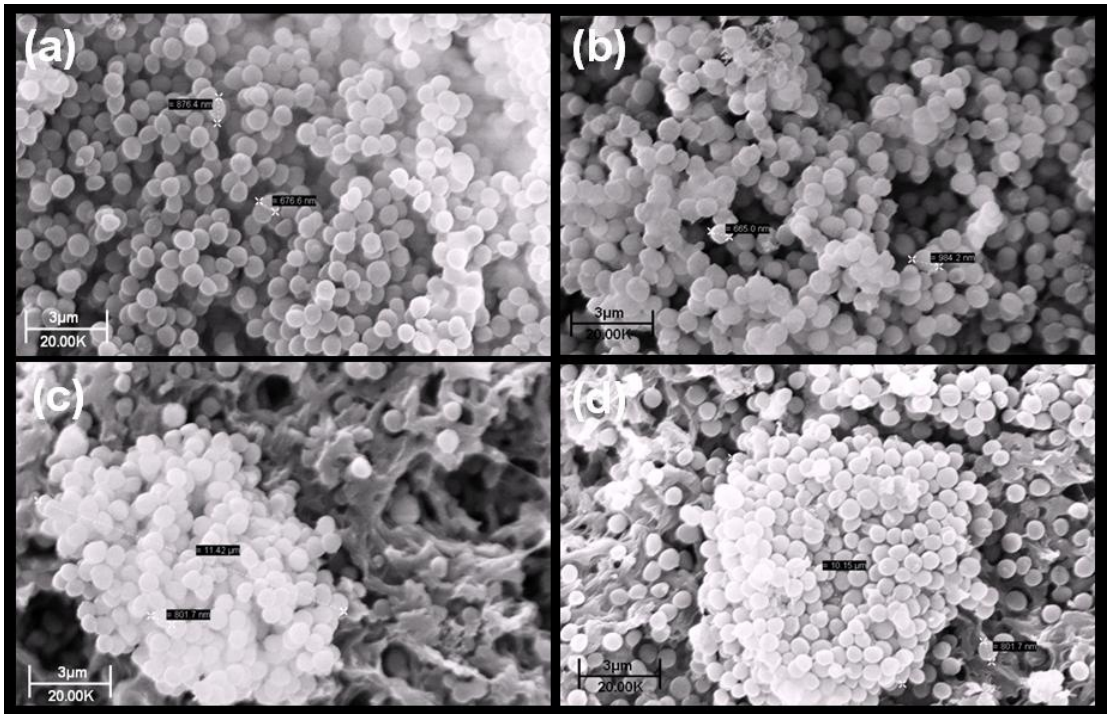

Figure 6.10 Scanning electron micrograph of $1x10^8$ cfu/ml *S. aureus* exposed to triclosan for 6 hours: (a) control (b) 0.7 µg/ml ($1/20^{th}$ MIC) (c) 14 µg/ml (MIC) and (d) 140 µg/ml (10xMIC). Viability after 6 hours; *S. aureus* control $5.6x10^9$ cfu/ml; *S. aureus* incubated with $1/20^{th}$ MIC triclosan $3.8x10^8$ cfu/ml; MIC and 10xMIC triclosan incubated bacteria was < 10 cfu/ml

After 24 hours incubation (Figure 6.11) the control culture revealed the normal staphylococcal morphology and size. The presence of aggregates in the sub-inhibitory culture was universal on the sample surface, which also revealed single cells. Large, well formed and regular spherical structures of dimensions varying from 2 – 19 µm were observed in both MIC and 10xMIC cultures with no single cells visible in either culture. Results presented in Figure 5.6 (a) after 24 hours incubation with triclosan, revealed the absence of cells in the MIC and 10xMIC cultures at this time point; examination of the SEM data for both these cultures revealed the presence of far fewer bacteria (single or aggregated), compared to control and sub-inhibitory cultures.

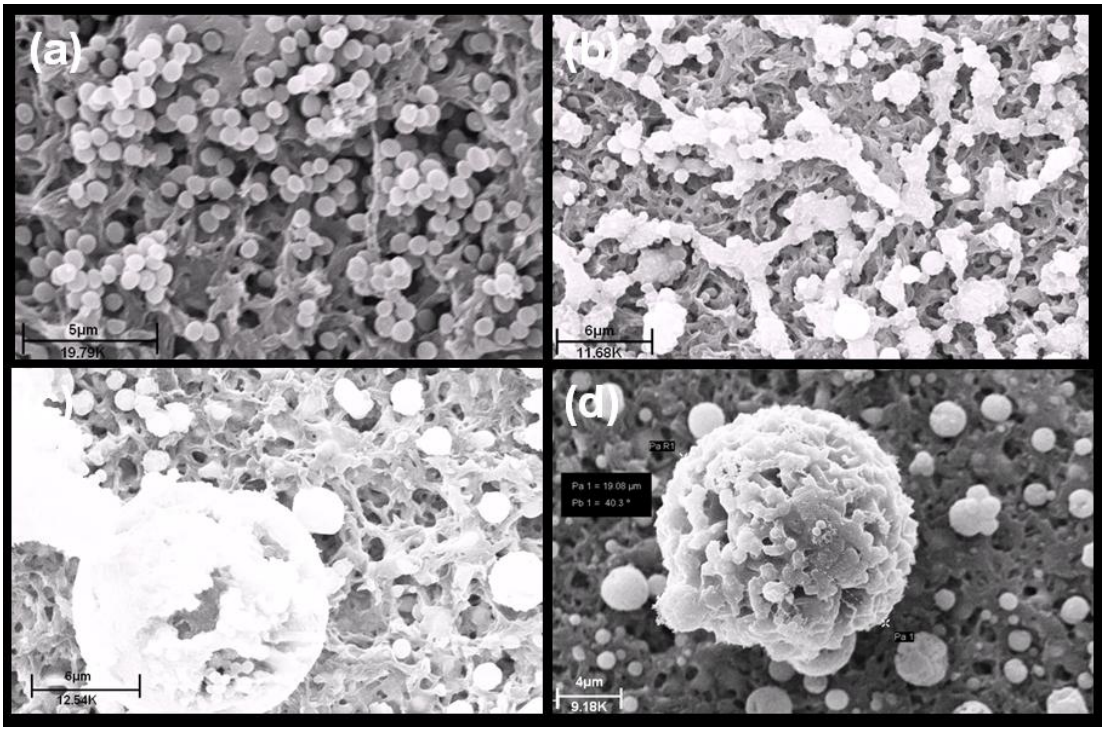

Figure 6.11 Scanning electron micrograph of $1x10^6$ cfu/ml *S. aureus* exposed to triclosan for 24 hours: (a) control (b) 0.7 µg/ml (1/20th MIC) (c) 14 µg/ml (MIC) and (d) 140 µg/ml (10xMIC). Viability after 24 hours; *S. aureus* control $1.4x10^9$ cfu/ml; *S. aureus* incubated with 1/20th MIC triclosan $1.4x10^9$ cfu/ml; MIC and 10xMIC triclosan incubated bacteria was < 10 cfu/ml

It is worth noting at this stage that SEM samples were prepared by concentrating a 10 ml culture sample to 2.5 ml final volume by brief centrigugation, with one ml passed through a 0.2 µm filter; whereas samples for flow cytometry analysis employed 10 µl of culture. Therefore while the quantities of bacterial aggregates would suggest the both these cultures possessed enough bacteria at 24 hours to be observed in flow cytometry, in reality there was a 1000-fold difference in the volume of culture employed to prepare samples for SEM and flow cytometry. This being the case, density of cells on the SEM samples is important; there are far more bacteria present on control and 1/20th MIC samples than on MIC and 10xMIC samples. Thus enumeration of too few bacterial cells for these cultures resulted in their non-representation in the 24-hour overlay images in flow cytometry.

By 72 hours (Figure 6.12), the presence of spherical aggregates were still apparent at all three triclosan concentrations, however the MIC culture now revealed both

individual and spherical aggregated cells, which correlated with the data presented in Chapter 5 (Figure 5.6 (b)) where the viability of *S. aureus* incubated with MIC of triclosan had recovered by 72 hours. The individual cells were probably viable, with the aggregates containing non-viable cell remnants.

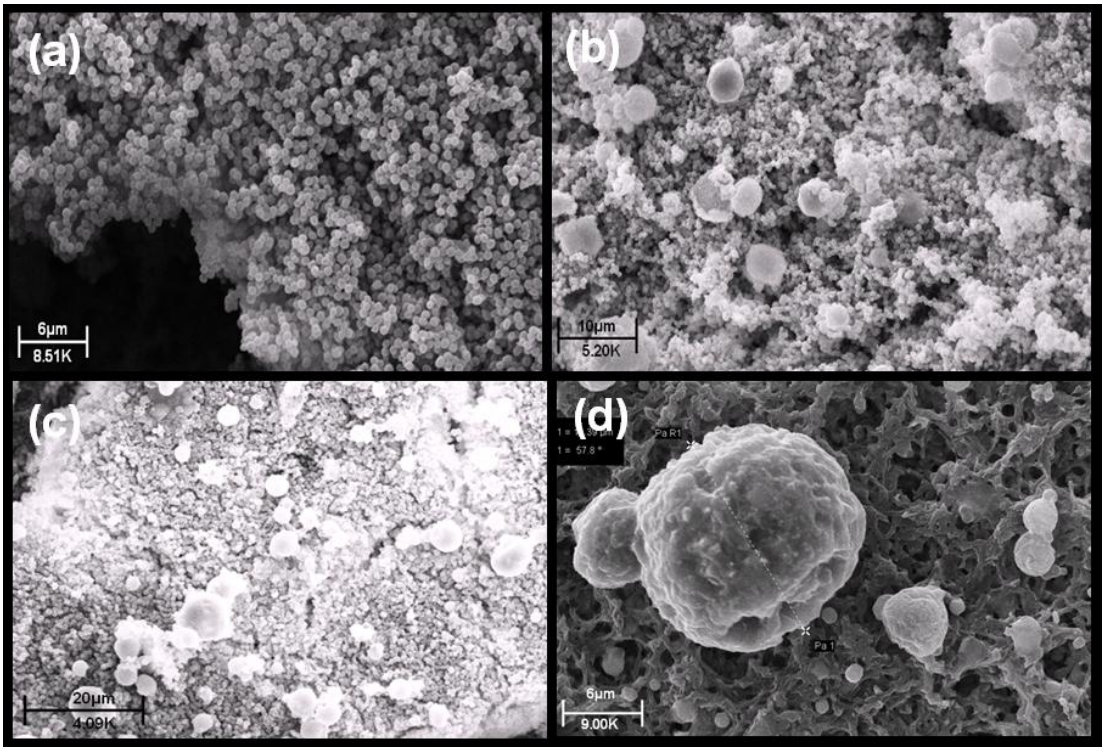

Figure 6.12 Scanning electron micrograph of $1x10^6$ cfu/ml *S. aureus* exposed to triclosan for 72 hours: (a) control (b) 0.7 µg/ml (1/20th MIC) (c) 14 µg/ml (MIC) and (d) 140 µg/ml (10xMIC). Viability after 72 hours; *S. aureus* control $6.5x10^9$ cfu/ml; *S. aureus* incubated with 1/20th MIC triclosan $5.0x10^9$ cfu/ml; *S. aureus* incubated with triclosan MIC $2.95x10^{10}$ cfu/ml; 10xMIC triclosan incubated bacteria was < 10 cfu/ml

This recovery of the MIC culture by 72-hours meant the re-appearance of cells in the inhibitory culture, with bacterial size similar to control, as revealed by the SEM micrographs.

Investigation of all bacterial cultures at 168 hours (Figure 6.13) showed the normal size and shape of *S. aureus,* whilst the aggregatory effect of triclosan on the bacterium was still visible in all three test triclosan concentrations. Both sub-inhibitory and inhibitory concentrations also possessed individual cells co-existing with aggregated spherical entities, which indicated *S. aureus* developed a tolerance

or resistance to triclosan, manifested as the de-aggregation of the majority of the visualised bacterial cells.

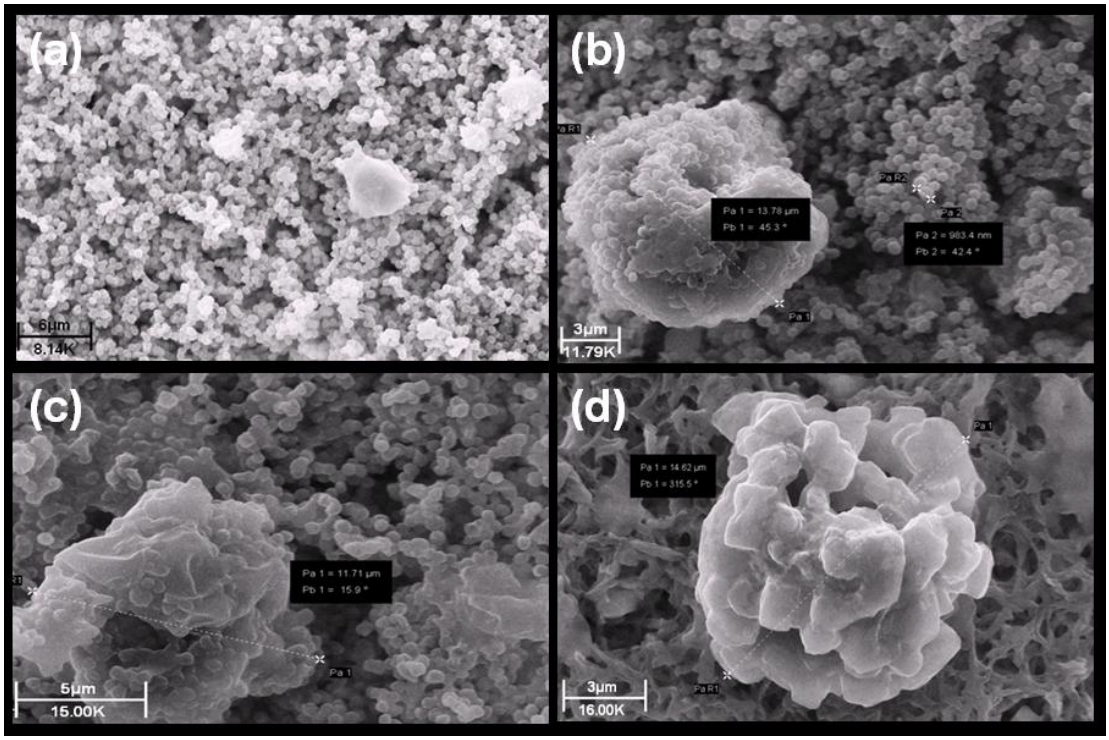

Figure 6.13 Scanning electron micrograph of $1x10^6$ cfu/ml *S. aureus* exposed to triclosan for 168 hours: (a) control (b) 0.7 µg/ml ($1/20^{th}$ MIC) (c) 14 µg/ml (MIC) and (d) 140 µg/ml (10xMIC). Viability after 168 hours; *S. aureus* control $2.9x10^{10}$ cfu/ml; *S. aureus* incubated with $1/20^{th}$ MIC triclosan $5.9x10^{10}$ cfu/ml; *S. aureus* incubated with triclosan MIC $2.9x10^{10}$ cfu/ml; 10xMIC triclosan incubated bacteria was < 10 cfu/ml

c) *Pseudomonas aeruginosa*

Flow cytometry was not performed on *P. aeruginosa* as the bacterium was reported to be resistant to triclosan and determination of an MIC for triclosan against *P. aeruginosa* in this investigation (Figure 3.9) only resulted in an MIC being determined for a time period of 32 hours. This time period permitted the monitoring of morphological responses by *P. aeruginosa* to the presence of triclosan.

Different time points were selected for SEM analysis compared to *E. coli* and *S. aureus* as preliminary experiments revealed longer exposure times to triclosan were necessary for effects of the antibacterial on the bacterium to be visualised.

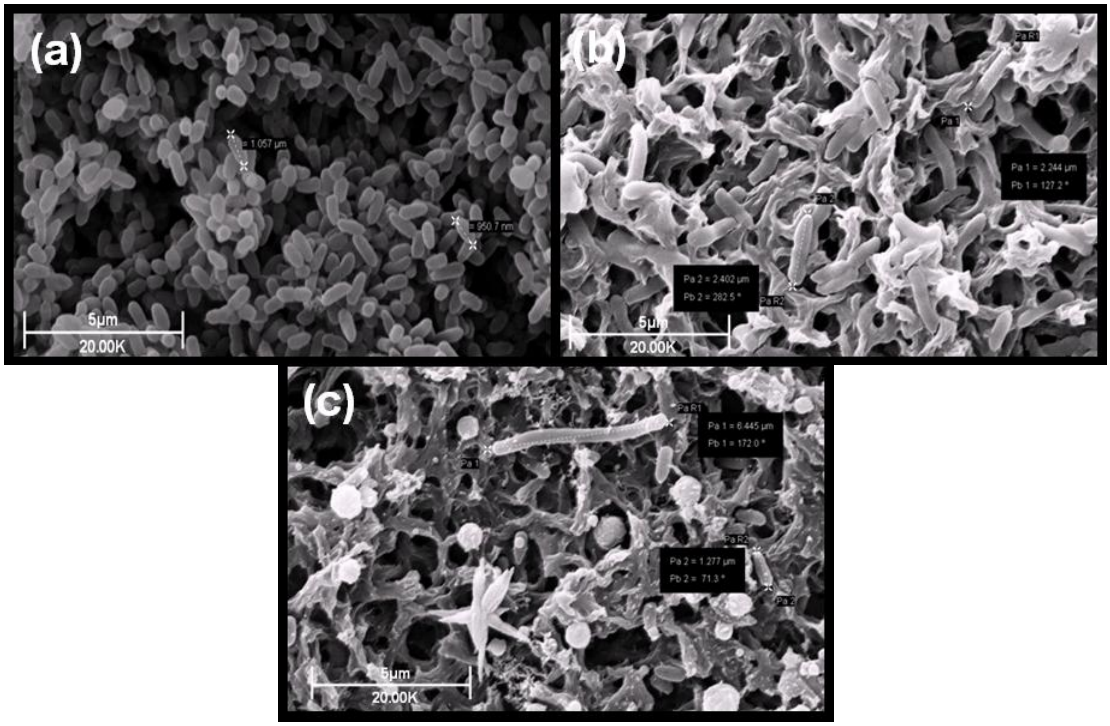

Figure 6.14 Scanning electron micrograph of $1x10^6$ cfu/ml *P. aeruginosa* exposed to triclosan for 4 hours: (a) control (b) 18 µg/ml ($1/20^{th}$ MIC) and (c) 360 µg/ml (MIC). Viability after 4 hours; *P. aeruginosa* control $1.2x10^8$ cfu/ml; *P. aeruginosa* incubated with $1/20^{th}$ MIC triclosan $8.5x10^7$ cfu/ml; *P. aeruginosa* incubated with triclosan MIC < 10cfu/ml

After four hours incubation (Figure 6.14) control bacteria displayed bacteria of normal shape and size. *P. aeruginosa* incubated with $1/20^{th}$ MIC triclosan were longer at 2.5 µm, while the inhibitory concentration contained bacteria from 1.3 to 7 µm long. A number of spherical shaped entities were also visualised in the MIC culture.

After eight hours incubation (Figure 6.15) the control sample revealed normal bacteria, with the sub-inhibitory culture containing bacteria ranging in size from 1.3 to 7.3 µm in length. The spherical shaped entities had disappeared from the inhibitory culture but the length of single bacteria varied in size from 1.3 –5 µm. The sparse number of bacteria visualised in the MIC sample was in stark contrast to the control and $1/20^{th}$ MIC cultures.

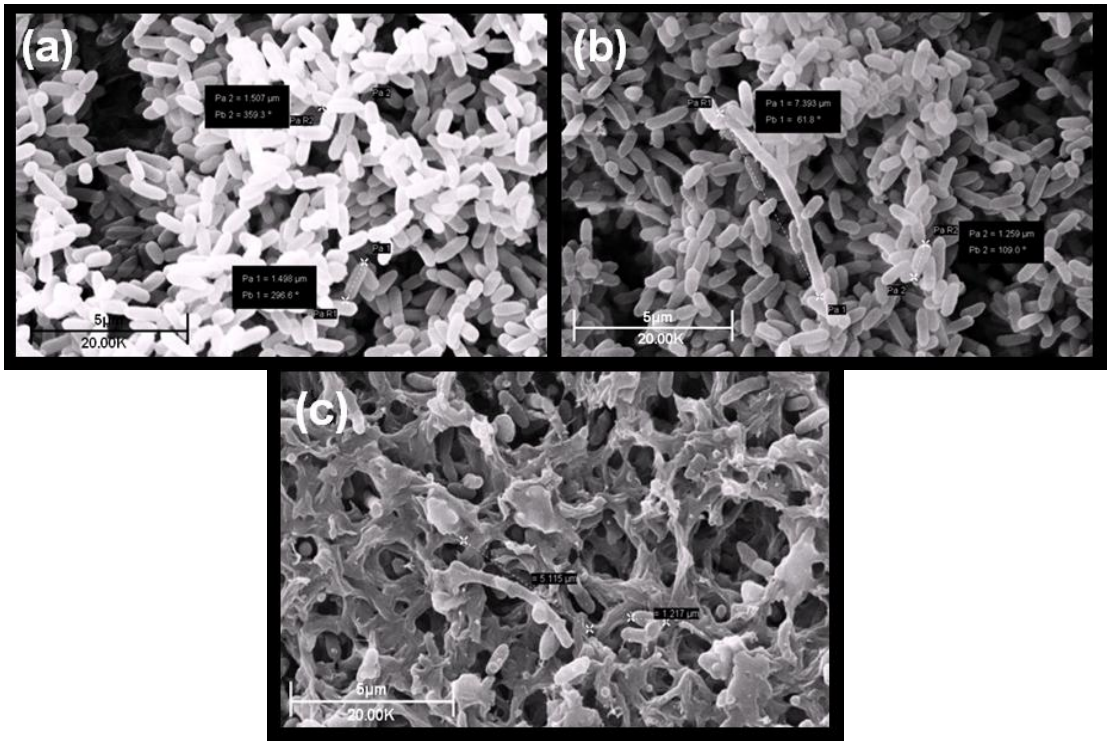

Figure 6.15 Scanning electron micrograph of $1x10^6$ cfu/ml *P. aeruginosa* exposed to triclosan for 8 hours: (a) control (b) 18 µg/ml ($1/20^{th}$ MIC) and (c) 360 µg/ml (MIC). Viability after 8 hours; *P. aeruginosa* control $1.2x10^9$ cfu/ml; *P. aeruginosa* incubated with $1/20^{th}$ MIC triclosan $9.2x10^8$ cfu/ml; *P. aeruginosa* incubated with triclosan MIC < 10cfu/ml

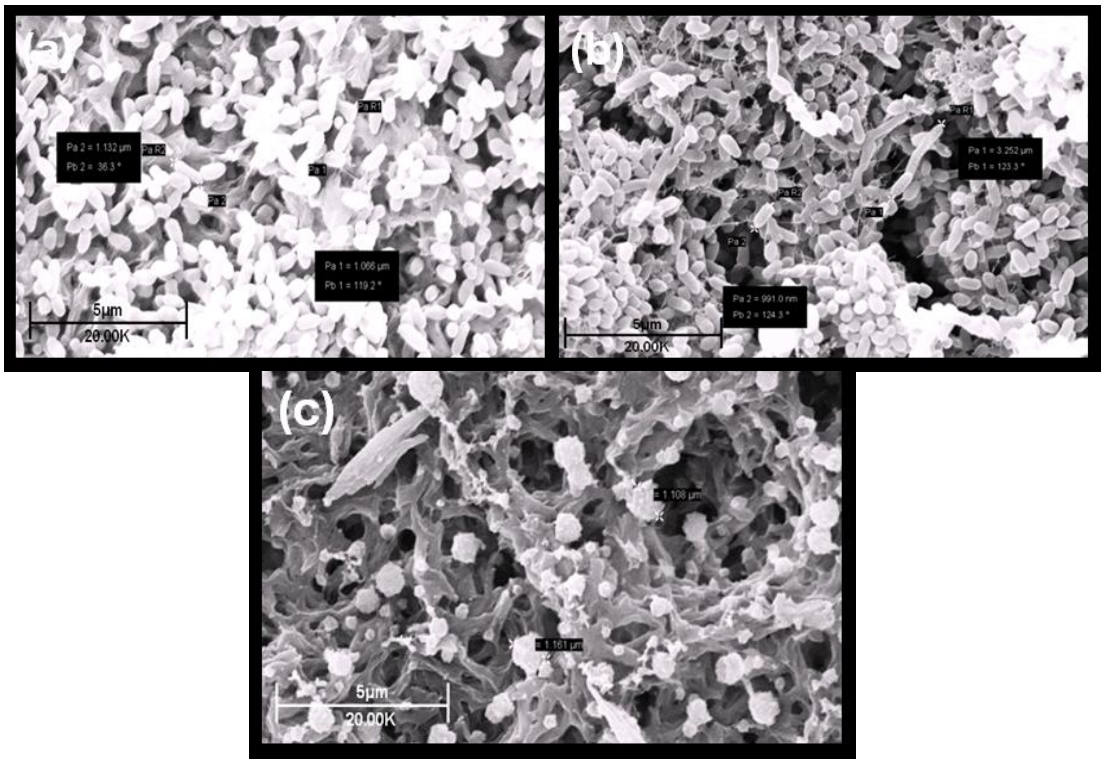

Figure 6.16 Scanning electron micrograph of $1x10^6$ cfu/ml *P. aeruginosa* exposed to triclosan for 24 hours: (a) control (b) 18 µg/ml ($1/20^{th}$ MIC) and (c) 360 µg/ml (MIC). Viability after 24 hours; *P. aeruginosa* control $5.6x10^{10}$ cfu/ml; *P. aeruginosa* incubated with $1/20^{th}$ MIC triclosan $3.5x10^{10}$ cfu/ml; *P. aeruginosa* incubated with triclosan MIC < 10cfu/ml

After 24 hours incubation (Figure 6.16) the difference between the control and triclosan incubated bacteria was substantial. Sub-inhibitory incubated bacteria displayed a variety of bacterial sizes that appeared to be interconnected by a fine thread like substance, possibly fimbriae. This culture also demonstrated some aggregation of the bacteria compared to control cells. The MIC culture displayed no familiar rod-shaped bacteria but had transformed into spherical shaped entities bearing a roughened exterior in response to exposure to this concentration of triclosan.

The last time point sampled was 32 hours (Figure 6.17) as *P. aeruginosa* had developed sufficient tolerance to triclosan after this time, most likely due to the up-regulation of MDR efflux pumps (Chuanchuen, Karkhoff-Schweizer and Schweizer 2003), that an MIC could not be determined, due to the limitations of the solubility of triclosan.

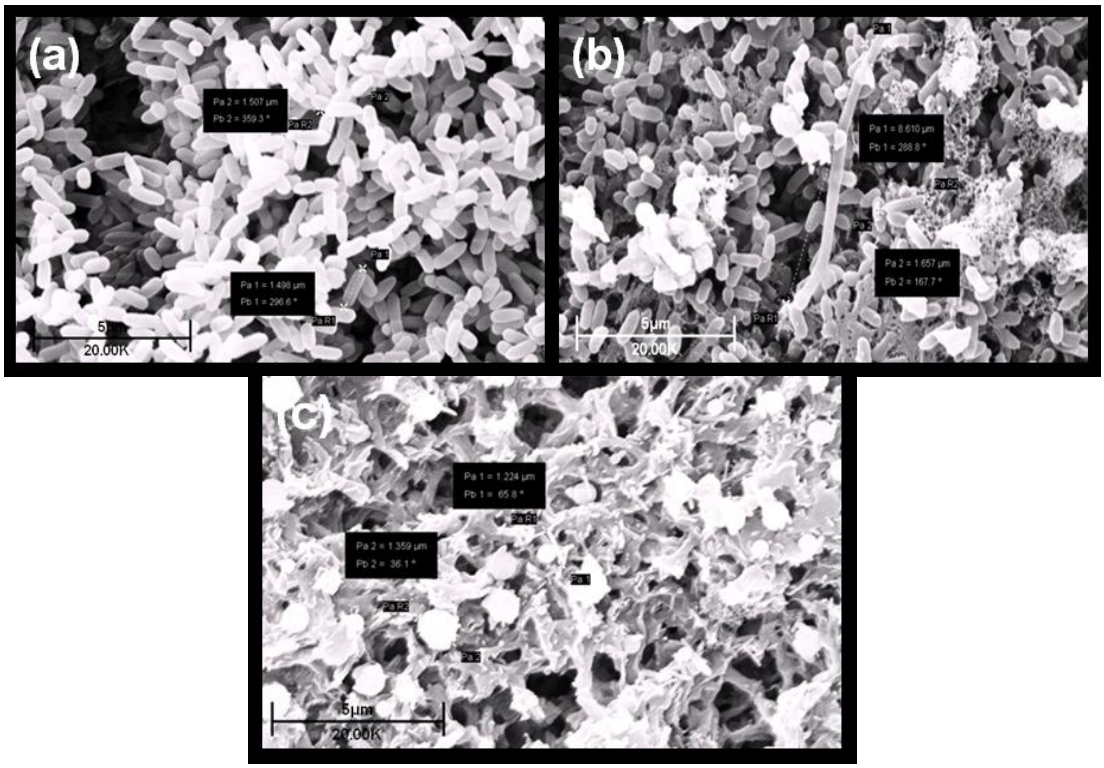

Figure 6.17 Scanning electron micrograph of $1x10^6$ cfu/ml *P. aeruginosa* exposed to triclosan for 32 hours: (a) control (b) 18 μg/ml ($1/20^{th}$ MIC) and (c) 360 μg/ml (MIC). Viability after 32 hours; *P. aeruginosa* control $7.8x10^{10}$ cfu/ml; *P. aeruginosa* incubated with $1/20^{th}$ MIC triclosan $6.3x10^{10}$ cfu/ml; *P. aeruginosa* incubated with triclosan MIC < 10cfu/ml

P. aeruginosa incubated with 1/20th MIC triclosan displayed bacterial sizes from 1.7 to 9 µm in length and some of the extracellular material interconnecting the bacteria was still evident. The MIC culture displayed spherical shapes approximately 1.5 µm in diameter. Thus *P. aeruginosa* displayed a number of morphological changes in response to triclosan exposure. The sub-inhibitory concentration revealed no visible effects at four hours exposure; that had changed to non-septated bacterial cells co-existing with bacteria of normal length after eight hours triclosan exposure. Incubation of 24 hours and longer revealed fine strands of cellular material were interconnecting the bacteria, with the 24 and 32 hour incubated cultures revealing aggregation of cells compared to control.

6.3.2 SEM images of *E. coli*, *S. aureus* and *P. aeruginosa* incubated with colistin

a) *Escherichia coli*

The control bacteria after one hour incubation (Figure 6.18) exhibited cells of normal shape and size between 1.5 – 2.5 µm. Large, spherical cellular aggregates were present throughout the sub-inhibitory culture, with clearly visible *E. coli* cells approximately 1.3 µm in length on the aggregate surface. Single cells were also visible in the sub-inhibitory, inhibitory and supra-inhibitory concentrations, similarly sized to control bacteria. Aggregated cells were seen in the MIC and 10xMIC concentrations, however, the structures in the 10xMIC concentration were half the size of those visualised in the MIC culture.

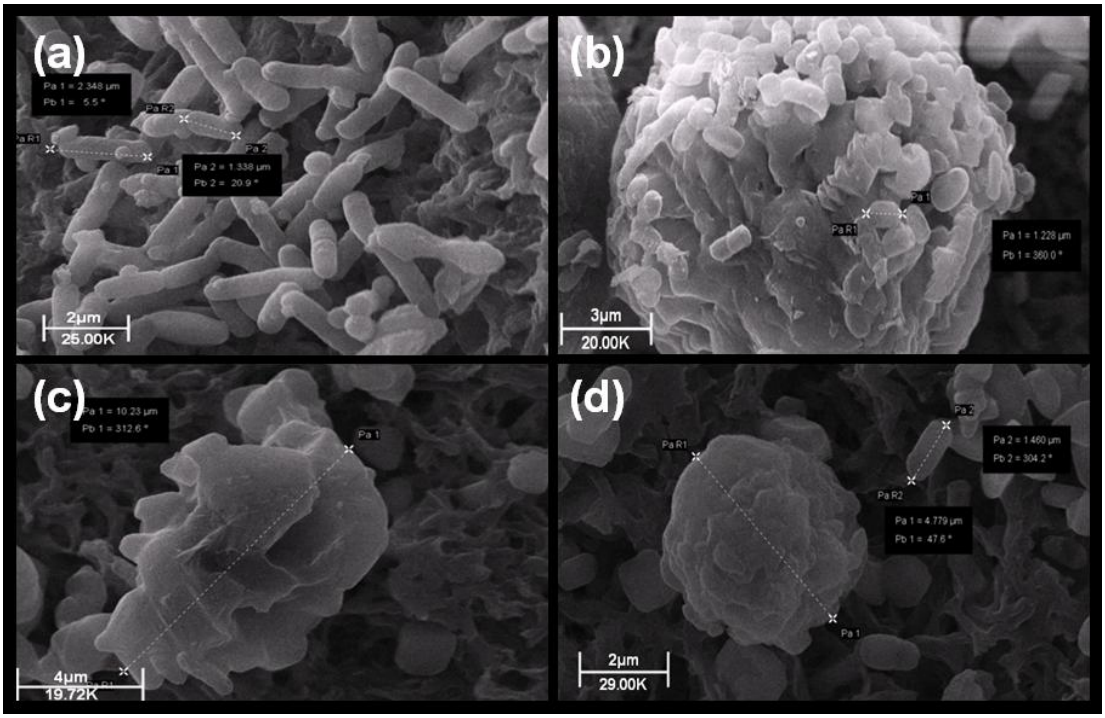

Figure 6.18 Scanning electron micrograph of $1x10^7$ cfu/ml *E. coli* exposed to colistin for 1 hour: (a) control (b) 0.49 µg/ml ($1/20^{th}$ MIC), (c) 9.8 µg/ml (MIC) and (d) 98 µg/ml (10xMIC)

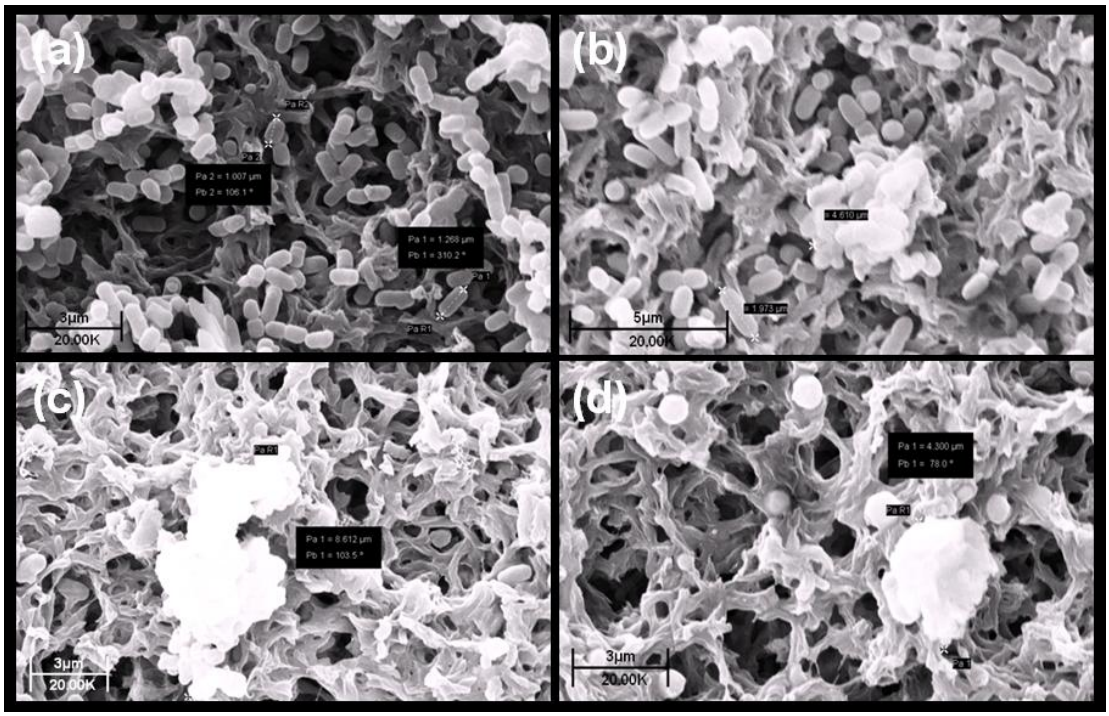

Figure 6.19 Scanning electron micrograph of $1x10^7$ cfu/ml *E. coli* exposed to colistin for 3 hours: (a) control (b) 0.49 µg/ml ($1/20^{th}$ MIC), (c) 9.8 µg/ml (MIC) and (d) 98 µg/ml (10xMIC)

After three hours incubation with colistin (Figure 6.19) the 1/20th MIC incubated bacteria resembled the control culture far more than at 1 hour, with single cells co-existing with aggregated cells. The MIC culture also displayed single misshapen bacteria and spherical structures. No single rod shaped *E. coli* were visible in the 10xMIC sample, which contained variously sized spherical structures.

The appearance of un-treated *E. coli* bacteria (Figure 6.20) was substantially different to exposed bacteria at 6 hours. The sub-inhibitory and inhibitory concentrations displayed large and small spherical structures with only large spherical structures approximately 15 µm in diameter observed in the 10xMIC sample.

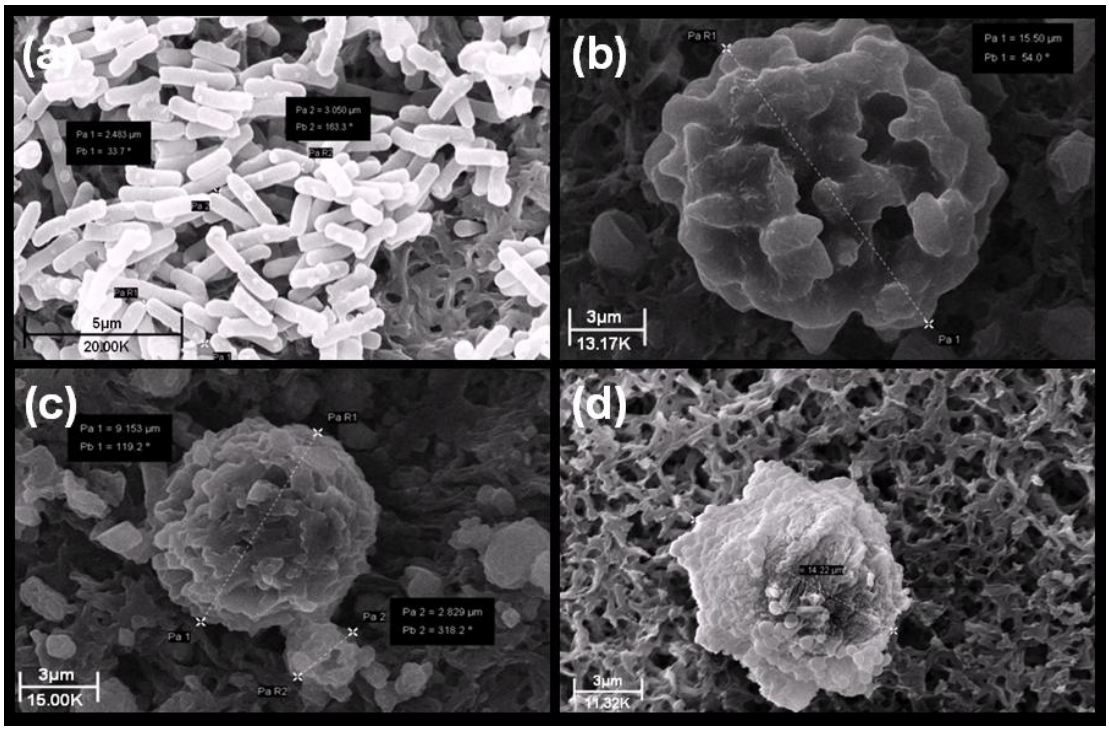

Figure 6.20 Scanning electron micrograph of 1x10^7 cfu/ml *E. coli* exposed to colistin for 6 hours: (a) control (b) 0.49 µg/ml (1/20th MIC), (c) 9.8 µg/ml (MIC) and (d) 98 µg/ml (10xMIC). Viability after 6 hours; *E. coli* control 3.2x10^9 cfu/ml; *E. coli* incubated with 1/20th MIC colistin 1.1x10^9 cfu/ml; *E. coli* incubated with colistin MIC and 10xMIC < 10cfu/ml

After 24 hours incubation (Figure 6.21), *E. coli* control exhibited shape and sizes typical of the bacterium. The micrographs of bacteria in all three colistin incubated cultures continued to reveal spherical aggregates. The outline of *E. coli* cells can be

detected as the component parts of these spherical structures. The composition of the material connecting these cells appears to have been extruded from within the bacterial interiors as a defence mechanism in the formation of spherical entities to improve bacterial survival due to incubation with colistin.

Results from flow cytometry (Figure 5.7 (a)) revealed control and sub-inhibitory cultures were similar in size to one another, which agree with the SEM micrographs. Insufficient numbers of bacteria were enumerated – limit was set for 10,000 bacteria within 100 seconds - for the MIC and 10xMIC cultures to be represented by flow cytometry.

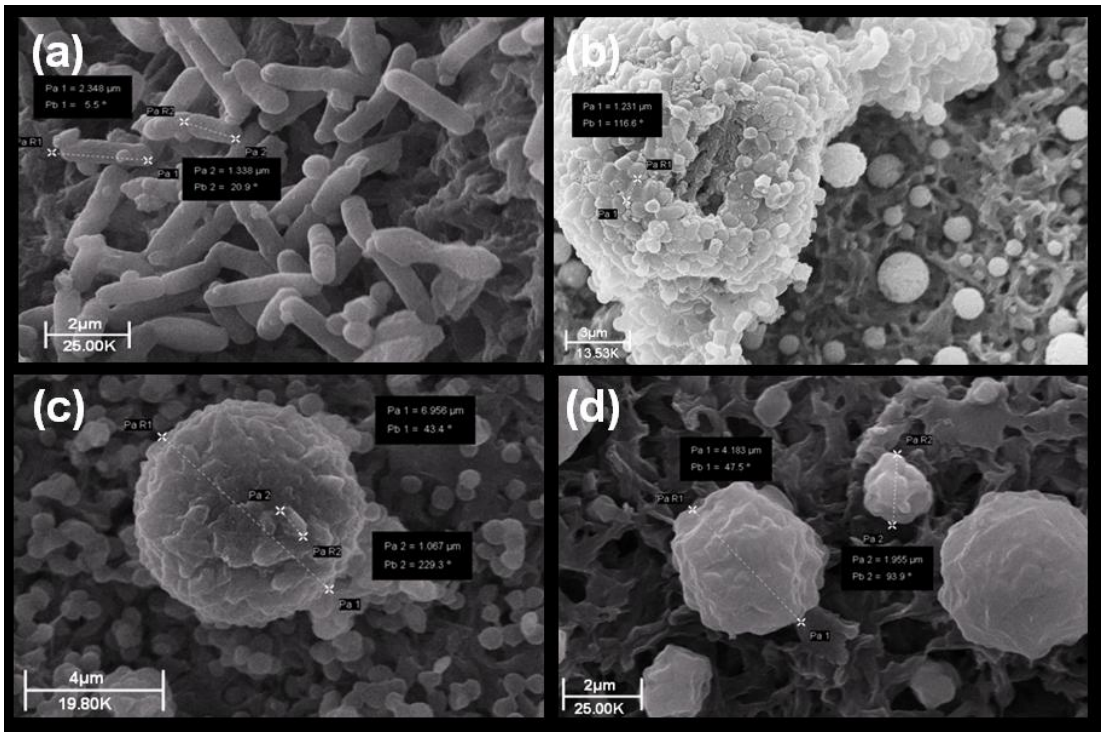

Figure 6.21 Scanning electron micrograph of $1x10^7$ cfu/ml *E. coli* exposed to colistin for 24 hours: (a) control (b) 0.49 µg/ml ($1/20^{th}$ MIC), (c) 9.8 µg/ml (MIC) and (d) 98 µg/ml (10xMIC). Viability after 24 hours; *E. coli* control $3.6x10^{10}$ cfu/ml; *E. coli* incubated with $1/20^{th}$ MIC colistin $1.13x10^{10}$ cfu/ml; *E. coli* incubated with colistin MIC and 10xMIC < 10cfu/ml

SEM images of colistin incubated bacteria at 72 hours, displayed the de-aggregation of the sub-inhibitory incubated *E. coli,* though morphological distortion of bacterial cells from rod to round shaped cells was apparent. The MIC and 10xMIC samples

only contained spherical structures, the density of which was very low compared to control and 1/20th MIC samples.

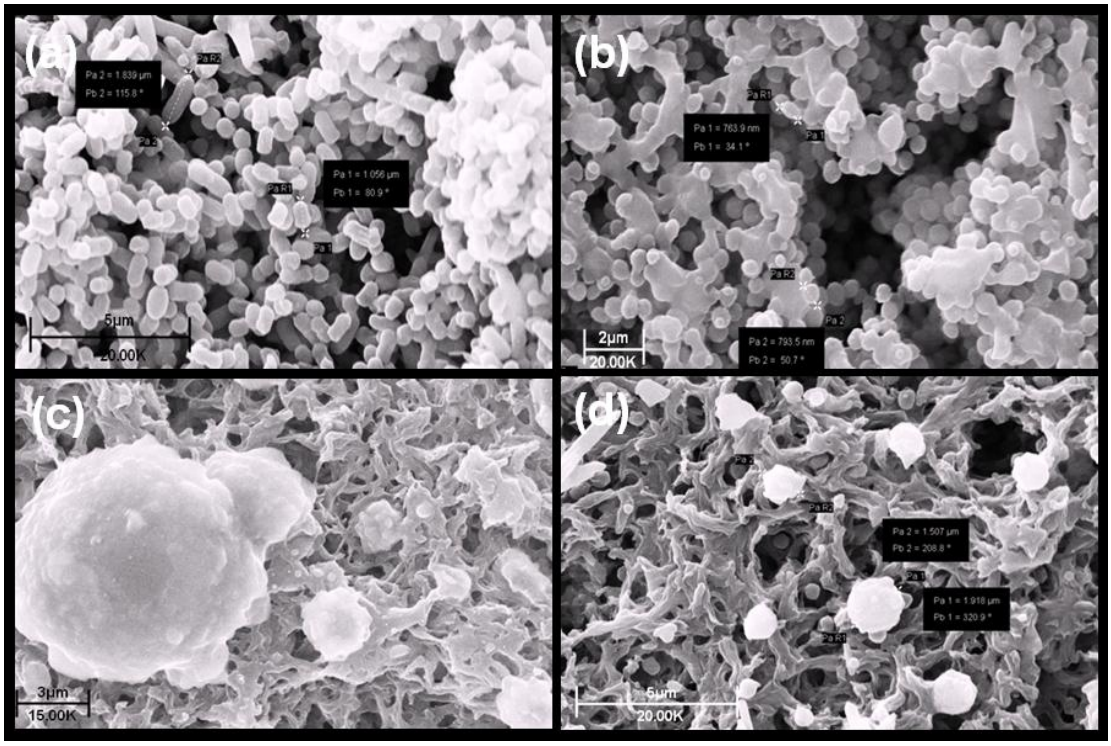

Figure 6.22 Scanning electron micrograph of 1x10^{7} cfu/ml *E. coli* exposed to colistin for 72 hours: (a) control (b) 0.49 µg/ml (1/20th MIC), (c) 9.8 µg/ml (MIC) and (d) 98 µg/ml (10xMIC). Viability after 72 hours; *E. coli* control 3.7x10^{9} cfu/ml; *E. coli* incubated with 1/20th MIC colistin 1.1x10^{9} cfu/ml; *E. coli* incubated with colistin MIC 7.0x10^{7} cfu/ml; *E. coli* incubated with 10xMIC colistin < 10cfu/ml

Incubation of *E. coli* for 168 hours (Figure 6.23) revealed rod shaped control bacteria approximately 2 µm in length, with the 1/20th MIC culture displayed both single as well as bacterial aggregates. The exposure to the sub-inhibitory colistin concentration had not only caused a rounding in *E. coli* cells, they were substantially smaller than control bacteria. Flow cytometry data (Figure 5.7 (c)) had previously revealed a smaller bacterial size in the 1/20th MIC culture compared to control. Sparse clusters of aggregated cells were visualised in the MIC and 10xMIC samples, explaining the absence of histograms in the flow cytometry overlay images due to insufficient bacterial numbers in these cultures. Bacterial replication through binary fission was visible over the experimental period in un-

treated bacteria. This phenomenon was also identified in the 1/20th MIC incubated bacteria but was not observed at any point in either the MIC or 10xMIC incubated bacteria.

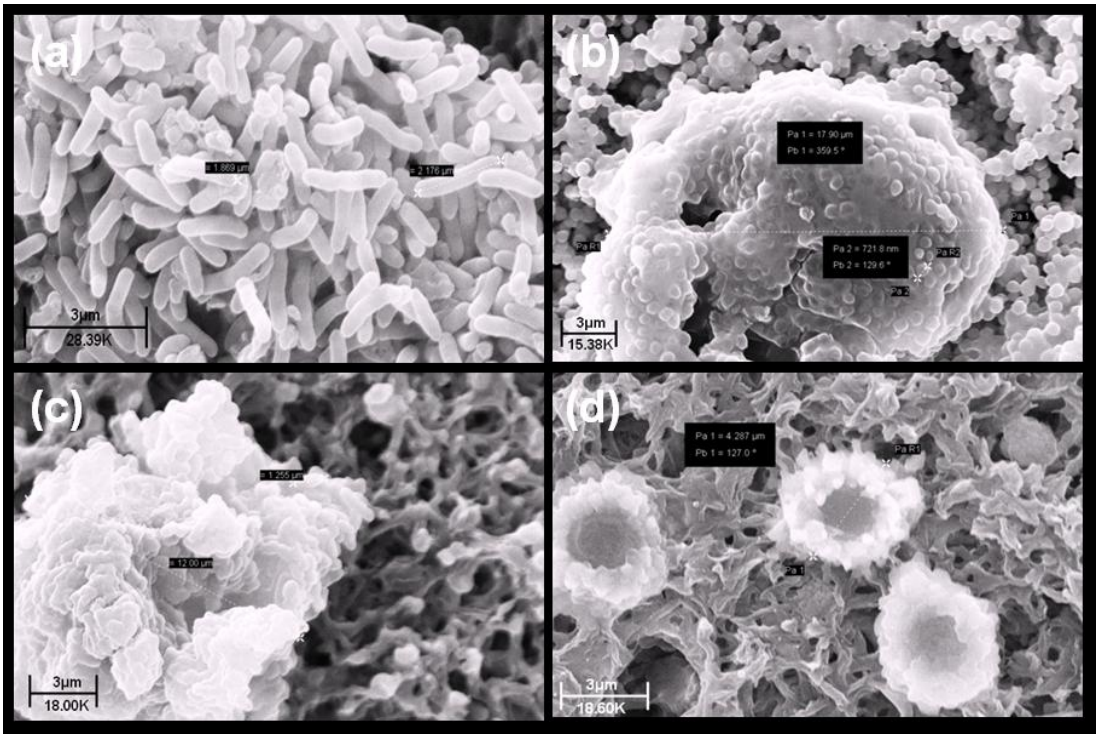

Figure 6.23 Scanning electron micrograph of 1x10^{7} cfu/ml *E. coli* exposed to colistin for 168 hours: (a) control (b) 0.49 µg/ml (1/20th MIC), (c) 9.8 µg/ml (MIC) and (d) 98 µg/ml (10xMIC). Viability after 168 hours; *E. coli* control 1.3x10^{10} cfu/ml; *E. coli* incubated with 1/20th MIC colistin 5.3x10^{8} cfu/ml; *E. coli* incubated with colistin MIC 6.3x10^{6} cfu/ml; *E. coli* incubated with 10xMIC colistin < 10cfu/ml

b) *Staphylococcus aureus*

A different time scale was selected for the *S. aureus* SEM micrographs (Figure 6.24 a)), to highlight the incredibly swift reaction of this bacterium when incubated with a very high colistin concentration of 156 µm/ml. Colistin is not used clinically in the treatment of Gram-positive infections. Control bacteria at 30 minutes were ellipsoidal in shape and approximately 1 µm in diameter. Incubation with the sub-inhibitory, inhibitory and supra-inhibitory colistin concentrations for merely 30 minutes (Figure 6.24) resulted in the formation of cellular spheres. The structure of

the spheres became more developed as the concentration of colistin increased; with the least well-developed spherical aggregates in the 1/20th MIC culture.

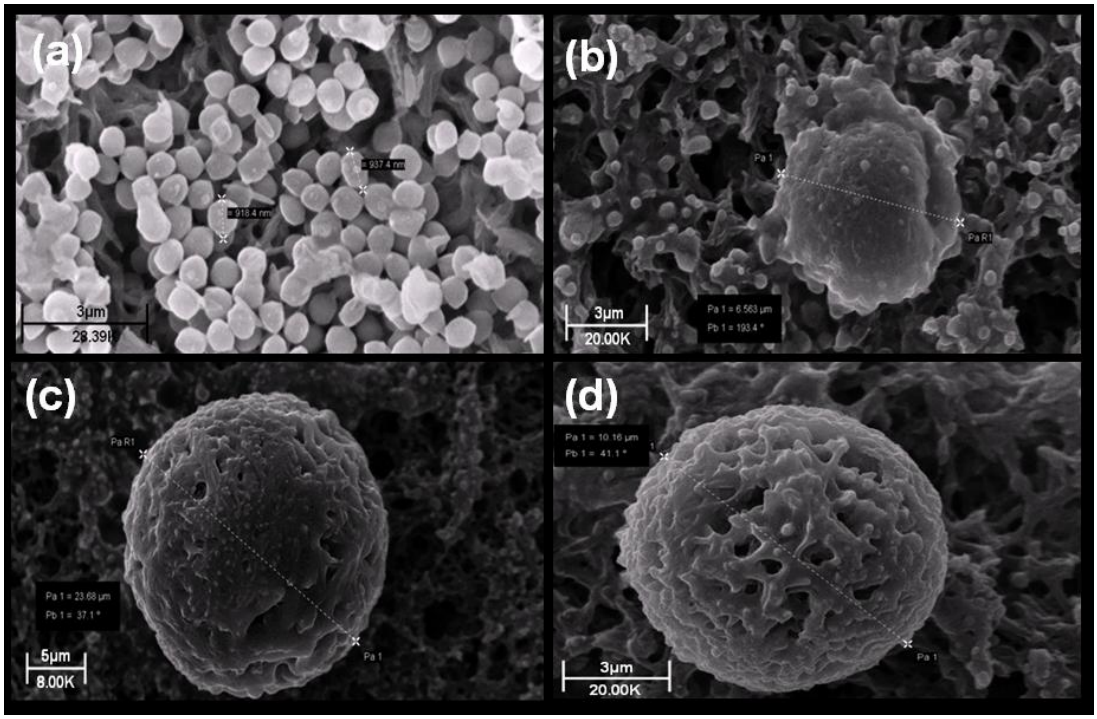

Figure 6.24 Scanning electron micrograph of 1x10^{7} cfu/ml *S. aureus* exposed to colistin for 30 minutes: (a) control (b) 7.8125 µg/ml (1/20th MIC) (c) 156 µg/ml (MIC) and (d) 1560 µg/ml (10xMIC)

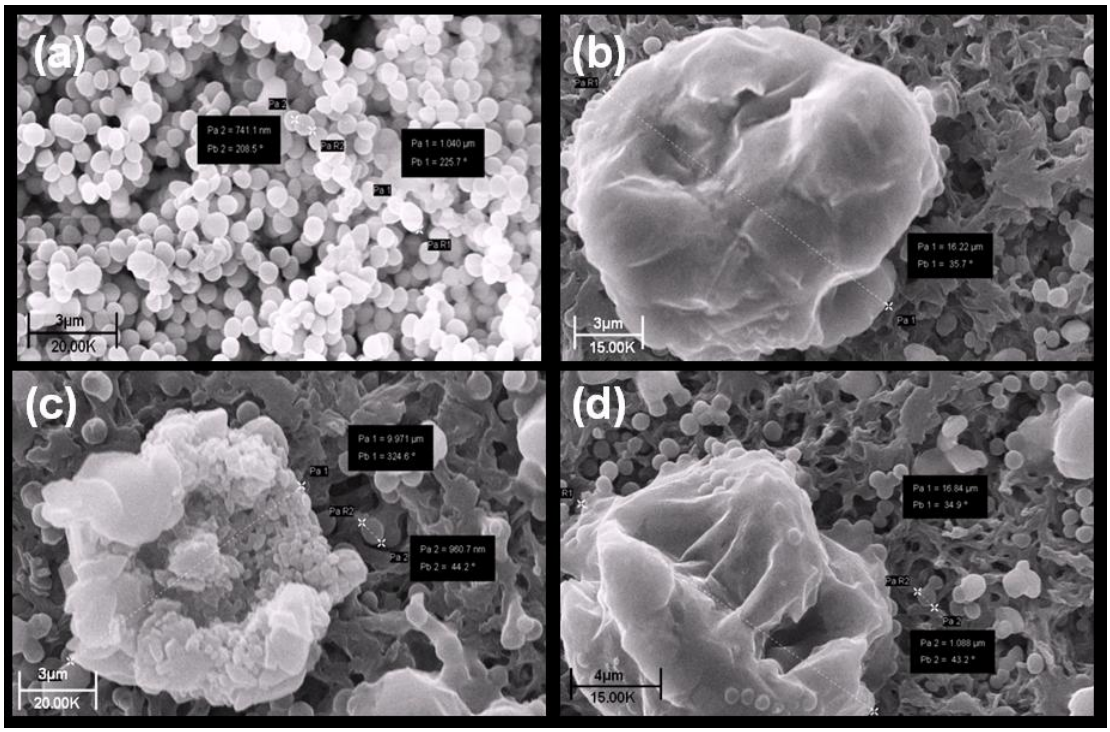

Figure 6.25 Scanning electron micrograph of 1x10^{7} cfu/ml *S. aureus* exposed to colistin for 1 hour: (a) control (b) 7.8125 µg/ml (1/20th MIC) (c) 156 µg/ml (MIC) and (d) 1560 µg/ml (10xMIC)

The micrographs at one hour (Figure 6.25) exhibited the substantial difference between the control and exposed bacteria. A great proportion of bacteria in the three colistin incubated cultures had formed large spherical structures with few single bacteria visible.

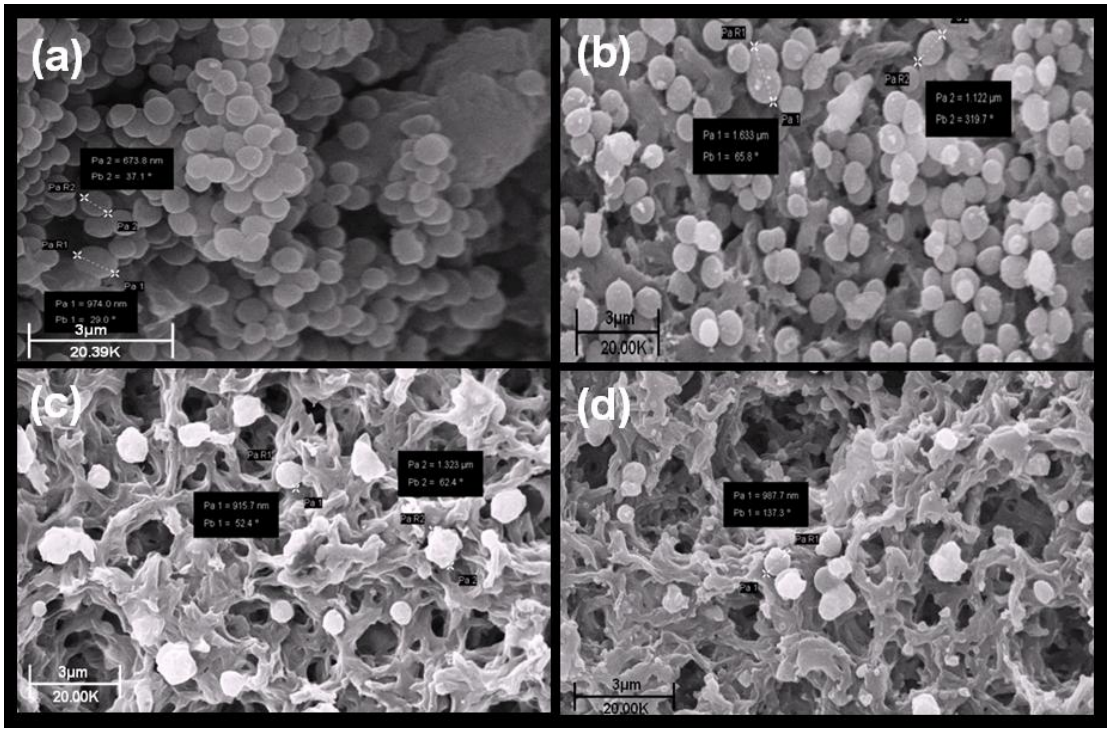

Figure 6.26 Scanning electron micrograph of $1x10^7$ cfu/ml *S. aureus* exposed to colistin for 3 hours: (a) control (b) 7.8125 µg/ml ($1/20^{th}$ MIC) (c) 156 µg/ml (MIC) and (d) 1560 µg/ml (10xMIC)

Micrographs of *S. aureus* incubated with colistin for three hours (Figure 6.26) revealed control and sub-inhibitory bacteria similar in size and shape. However the $1/20^{th}$ MIC incubated bacteria displayed blebbed bacterial membranes. Spheres populated the MIC and 10xMIC sample surface, with a higher density present on the inhibitory sample compared to 10xMIC sample surface.

Incubation for 24 hours resulted in the un-treated and sub-inhibitory incubated bacteria substantially similar in size and shape (Figure 6.27). Few bacteria were present in the MIC micrograph, however the clusters of bacteria present resembled

normal *S. aureus* groupings compared to structures visualised at earlier time points.

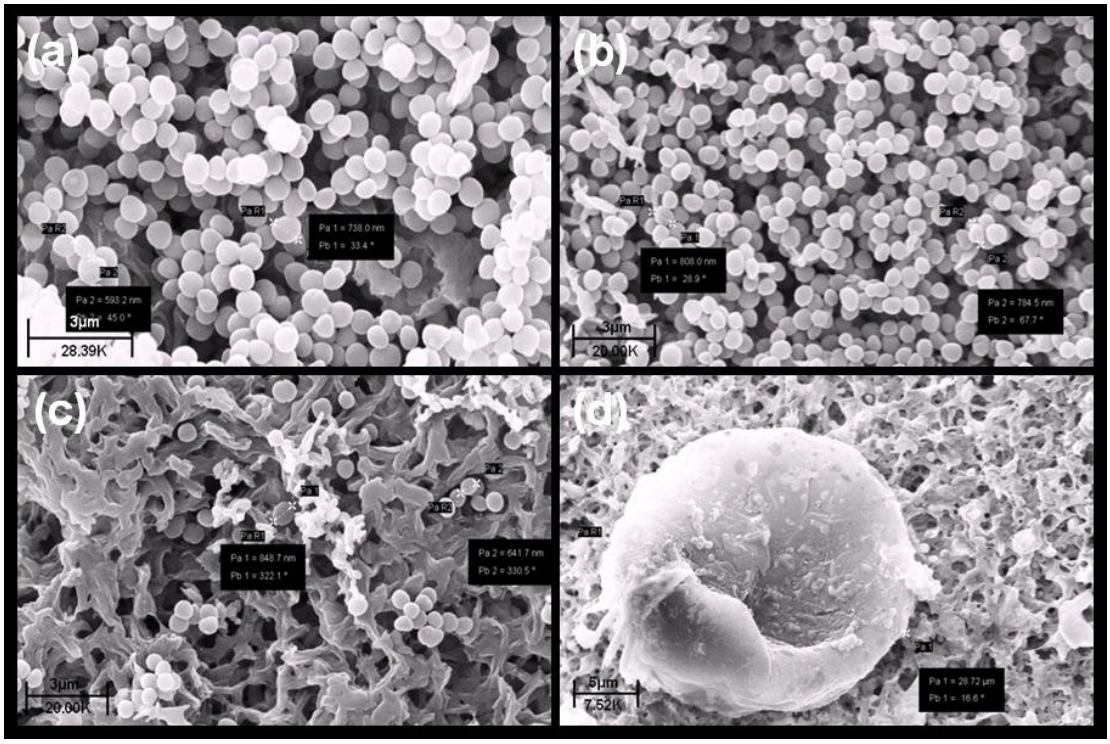

Figure 6.27 Scanning electron micrograph of $1x10^7$ cfu/ml *S. aureus* exposed to colistin for 24 hours: (a) control (b) 7.8125 µg/ml ($1/20^{th}$ MIC) (c) 156 µg/ml (MIC) and (d) 1560 µg/ml (10xMIC). Viability after 24 hours; *S. aureus* control $7.8x10^9$ cfu/ml; *S. aureus* incubated with $1/20^{th}$ MIC colistin $7.0x10^9$ cfu/ml; MIC and 10xMIC colistin incubated bacteria was < 10 cfu/ml

Micrographs of the 10xMIC culture revealed sparse spherical entities. Examination of *S. aureus* incubated with colistin by flow cytometry (Figure 5.8 (a)) support what is shown in the SEM images; control and sub-inhibitory cultures similar to each other, while neither MIC nor 10xMIC colistin cultures were detected due to insufficient bacterial numbers detected in these cultures.

S. aureus control and $1/20^{th}$ MIC cultures bore great similarity to each other at 72 hours (Figure 6.28). Normal size and shaped bacteria were also visualised in the MIC culture, which also contained some larger spherical cellular aggregates. Few bacteria were identified in the 10xMIC micrograph, the majority of which appeared as spherical structures.

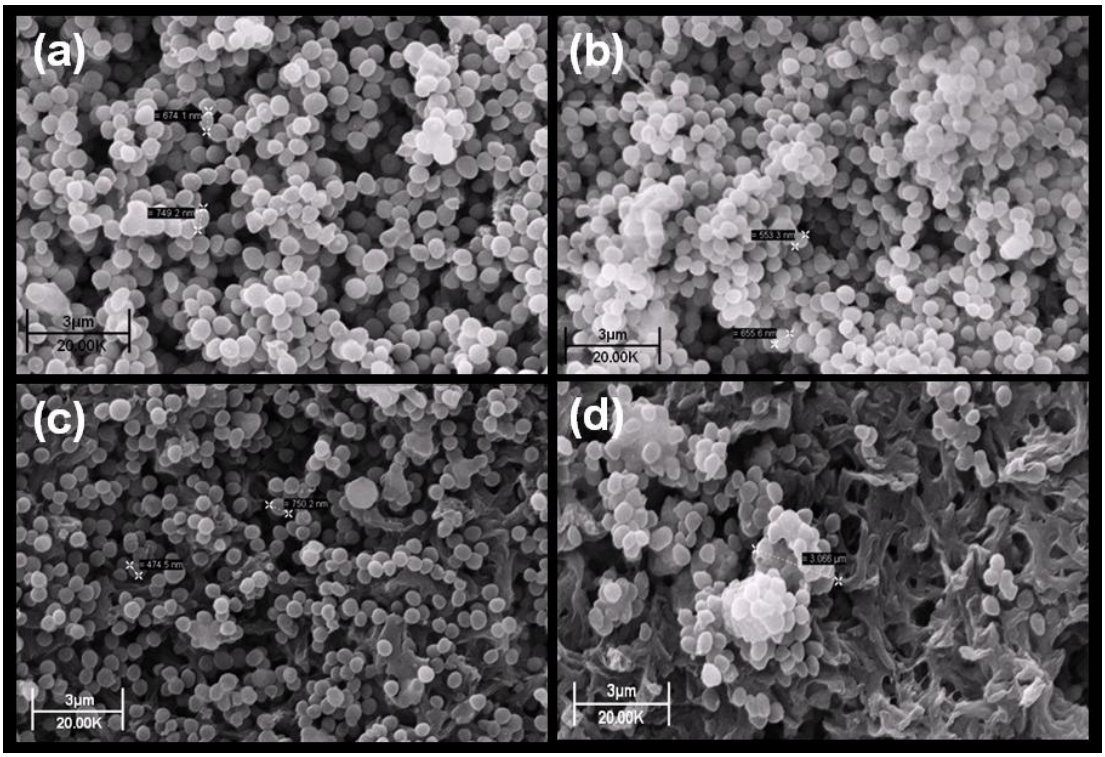

Figure 6.28 Scanning electron micrograph of $1x10^7$ cfu/ml *S. aureus* exposed to colistin for 72 hours: (a) control (b) 7.8125 µg/ml ($1/20^{th}$ MIC) (c) 156 µg/ml (MIC) and (d) 1560 µg/ml (10xMIC). Viability after 72 hours; *S. aureus* control $3.6x10^{10}$ cfu/ml; *S. aureus* incubated with $1/20^{th}$ MIC colistin $6.3x10^{10}$ cfu/ml; *S. aureus* incubated with MIC colistin $5.6x10^{10}$ cfu/ml and 10xMIC colistin incubated bacteria was < 10 cfu/ml

Data presented in Figure 5.8 (b) revealed bacterial size in control and $1/20^{th}$ MIC cultures very similar to each other, while bacteria incubated with MIC colistin appeared larger in size. The presence of some aggregated cellular structures in conjunction with the normal *S. aureus* clusters depicted in the SEM images could explain this result.

Bacteria in $1/20^{th}$ MIC and MIC cultures at 168 hours (Figure 6.29) were smaller in size compared to control. The MIC incubated bacteria, while not aggregated were different in appearance to that of control, while the 10xMIC culture continued to display a few aggregated structures. Overlay flow cytometry data support the SEM data (Figure 5.8 (c)); with histograms for sub-inhibitory and inhibitory cultures

smaller in size compared to control bacteria and a lack of bacteria in the 10xMIC colistin incubated culture.

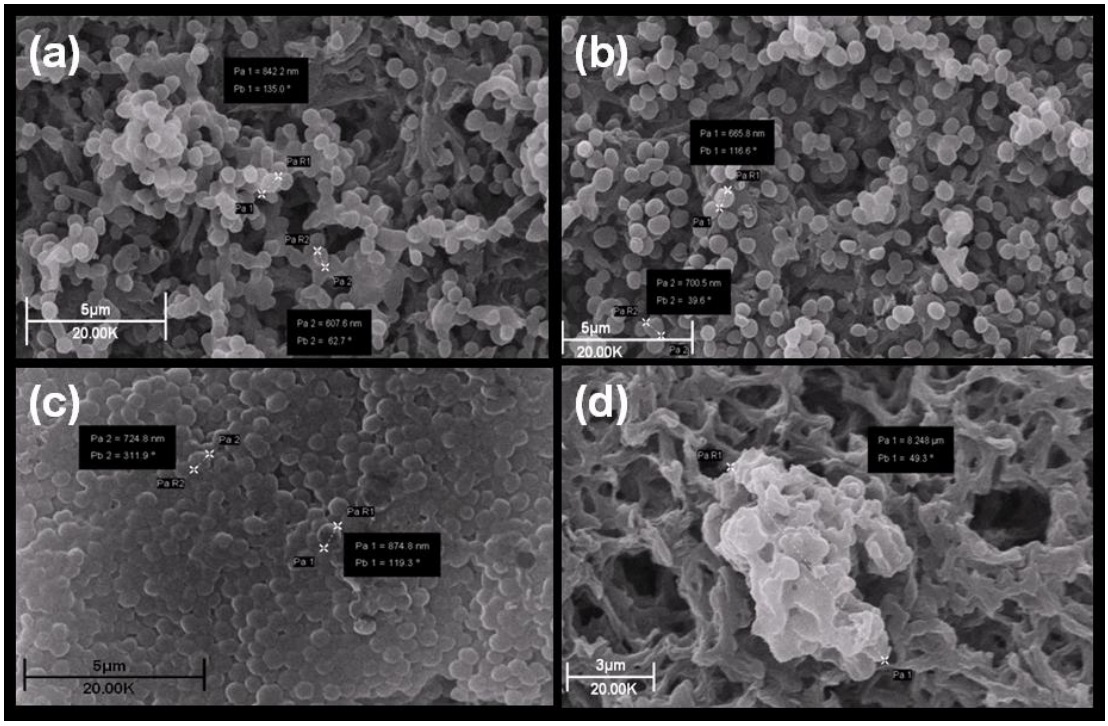

Figure 6.29 Scanning electron micrograph of $1x10^7$ cfu/ml *S. aureus* exposed to colistin for 168 hours: (a) control (b) 7.8125 µg/ml ($1/20^{th}$ MIC) (c) 156 µg/ml (MIC) and (d) 1560 µg/ml (10xMIC). Viability after 168 hours; *S. aureus* control $1.7x10^{10}$ cfu/ml; *S. aureus* incubated with $1/20^{th}$ MIC colistin $2.3x10^{10}$ cfu/ml; *S. aureus* incubated with MIC colistin $2.1x10^{10}$ cfu/ml and 10xMIC colistin incubated bacteria was < 10 cfu/ml

Actively dividing bacteria were observed in all cultures over the experimental period except the 10xMIC culture. It is likely that the bactericidal ability of colistin is due in part to inhibition of bacterial reproduction.

c) *Pseudomonas aeruginosa*

Incubation with colistin produced no effect on the morphology of *P. aeruginosa* at or less than 90 minutes; therefore the SEM images presented here were taken at different time intervals to *E. coli* and *S. aureus.* SEM micrographs of *P. aeruginosa* incubated with colistin for two hours (Figure 6.30) revealed aggregation in the incubated bacteria proportional to the concentration of colistin present.

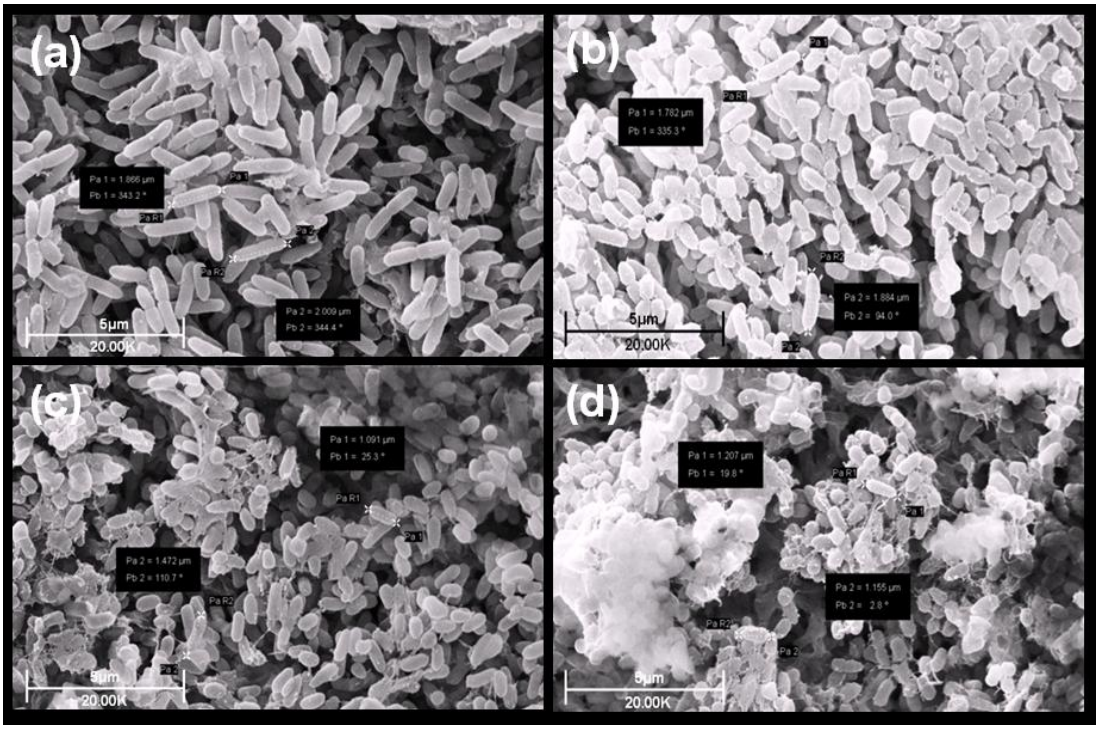

Figure 6.30 Scanning electron micrograph of $1x10^7$ cfu/ml *P. aeruginosa* exposed to colistin for 2 hours: (a) control (b) 0.245 µg/ml ($1/20^{th}$ MIC), (c) 4.9 µg/ml (MIC) and (d) 49 µg/ml (10xMIC) colistin

The aggregation did not result in spherical cellular structures as seen with *E. coli* and *S. aureus* but in the formation of layers of attached bacteria, interlinked by strands of extracellular material. Changes in *P. aeruginosa* shape were observed at all colistin concentrations at this time point.

Four hours incubation of *P. aeruginosa* with colistin (Figure 6.31) resulted in substantial differences between the appearances of un-treated and treated bacteria. The sub-inhibitory incubated bacteria were rod-shaped in appearance, with some long *P. aeruginosa* cells visualised in the aggregated bacterial layers. The MIC incubated bacteria were more tightly interwoven into layers, with the supra-inhibitory culture displaying a more spherical than rod-shaped appearance of individual cells. Also, a clear presence of an extracellular matrix of what appeared to be thin fibres is seen in all the treated cultures.

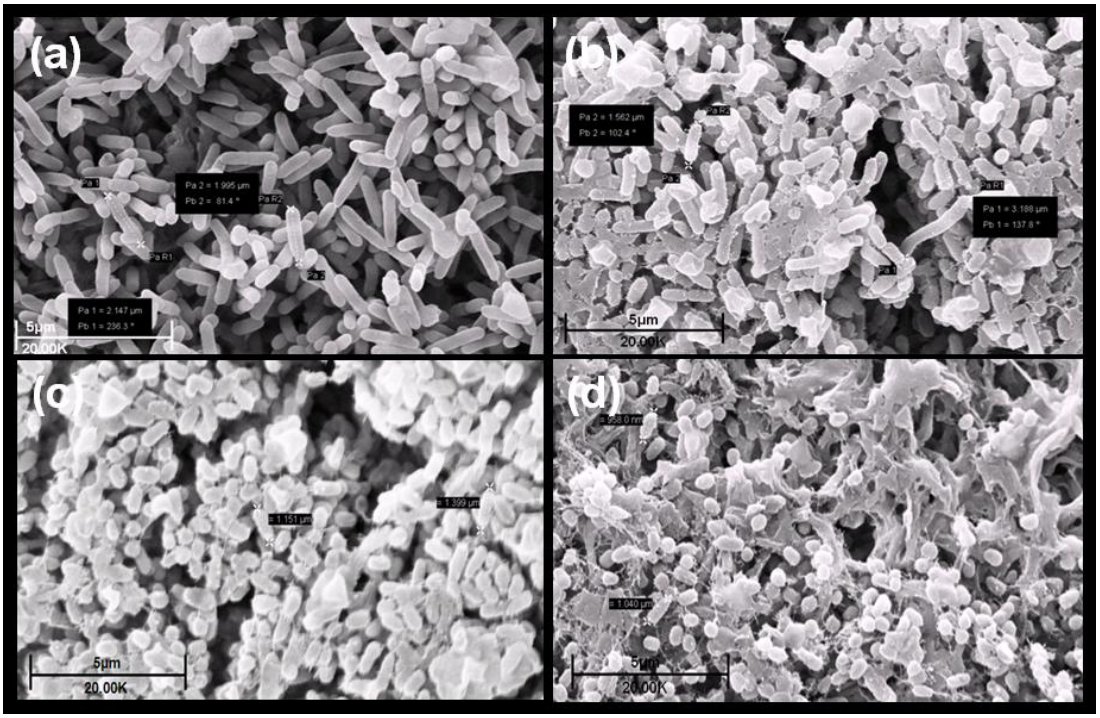

Figure 6.31 Scanning electron micrograph of $1x10^7$ cfu/ml *P. aeruginosa* exposed to colistin for 4 hours: (a) control (b) 0.245 µg/ml ($1/20^{th}$ MIC), (c) 4.9 µg/ml (MIC) and (d) 49 µg/ml (10xMIC) colistin

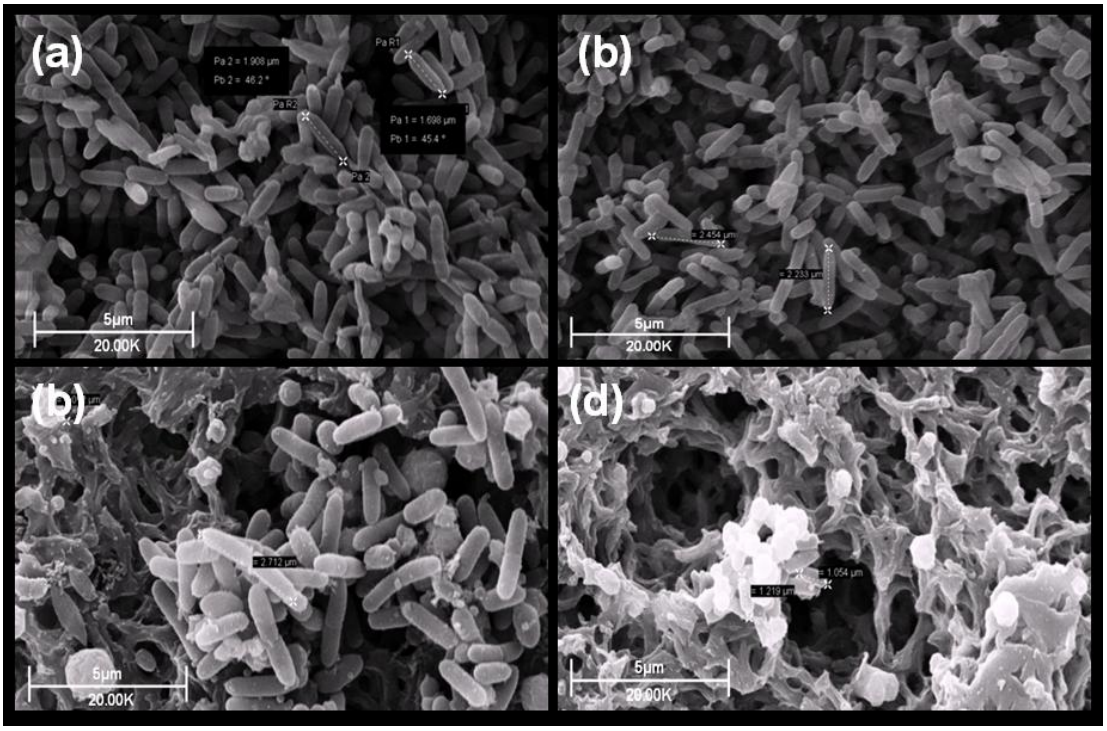

Figure 6.32 Scanning electron micrograph of $1x10^7$ cfu/ml *P. aeruginosa* exposed to colistin for 8 hours: (a) control (b) 0.245 µg/ml ($1/20^{th}$ MIC), (c) 4.9 µg/ml (MIC) and (d) 49 µg/ml (10xMIC) colistin. Viability after 8 hours; *P. aeruginosa* control $3.1x10^9$ cfu/ml; *P. aeruginosa* incubated with $1/20^{th}$ MIC colistin $3.1x10^9$ cfu/ml; *P. aeruginosa* incubated with MIC colistin $1.5x10^{11}$ cfu/ml; *P. aeruginosa* incubated with 10xMIC colistin < 10 cfu/ml

P. aeruginosa appeared to have developed a tolerance to the antimicrobial, after eight hours incubation (Figure 6.32) with 1/20th MIC colistin. These sub- inhibitory exposed bacteria had reverted from the aggregated bacterial layers seen at 4 hours and now closely resembled the control bacteria in size, shape and bacterial groupings. The MIC incubated bacteria had also abandoned the layered bacterial structures at eight hours incubation and were beginning to assemble spherical cellular structures. Blebs were apparent on the surface of MIC incubated bacteria as were distorted bacterial shapes. Few bacteria incubated with 10xMIC colistin were visualised in the eight-hour micrograph, with these bacteria also spherical in shape.

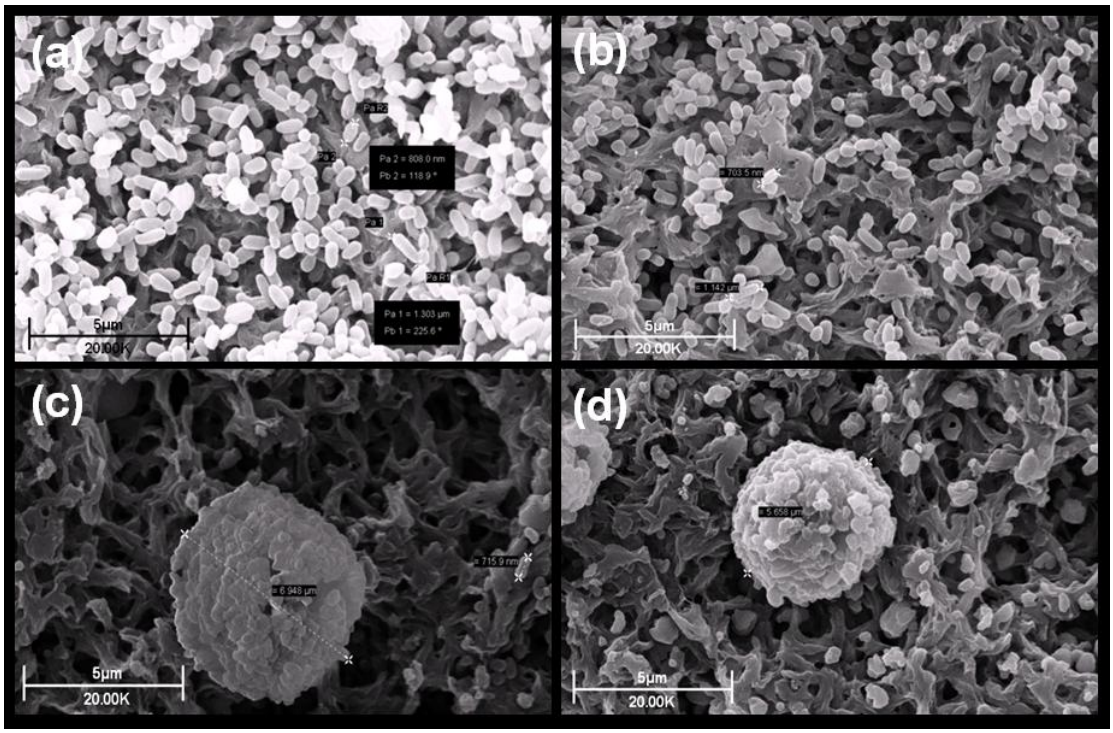

Figure 6.33 Scanning electron micrograph of 1x10^{7} cfu/ml *P. aeruginosa* exposed to colistin for 24 hours: (a) control (b) 0.245 µg/ml (1/20th MIC), (c) 4.9 µg/ml (MIC) and (d) 49 µg/ml (10xMIC) colistin. Viability after 24 hours; *P. aeruginosa* control 6.8x10^{10} cfu/ml; *P. aeruginosa* incubated with 1/20th MIC colistin 6.2x10^{10} cfu/ml; *P. aeruginosa* incubated with MIC 7.6x10^{10} cfu/ml; *P. aeruginosa* incubated with 10xMIC colistin < 10 cfu/ml

After 24-hours incubation *P. aeruginosa* control and 1/20th MIC cells were similar in size and structure. Bacteria in the MIC and 10xMIC incubated cultures had formed spherical aggregates, slightly larger in the MIC culture than the 10xMIC culture. Very few of these aggregated structures were visualised on the MIC sample surface

but considerable cellular debris was present on the surface of the 10xMIC sample. Flow cytometry results in Figure 5.9 (a) revealed the control and sub-inhibitory bacteria at 24 hours being very similar to each other, with insufficient bacteria enumerated in the MIC and 10xMIC cultures to be analysed at this time point, all of which is supported by the SEM images.

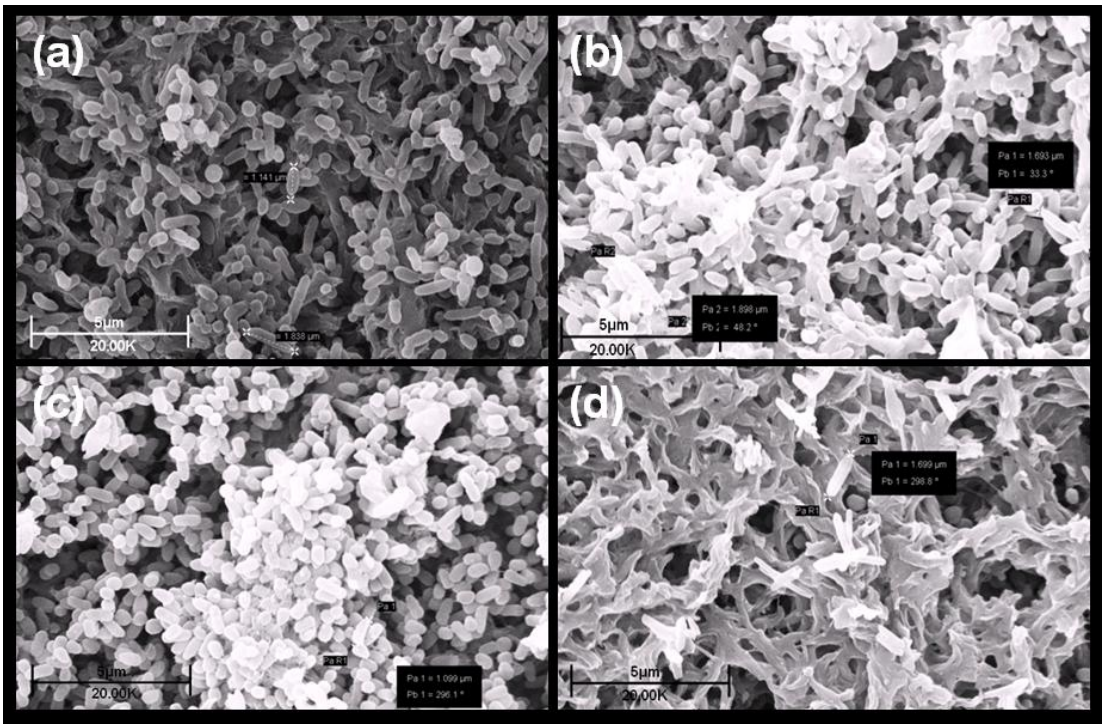

Figure 6.34 Scanning electron micrograph of $1x10^7$ cfu/ml *P. aeruginosa* exposed to colistin for 72 hours: (a) control (b) 0.245 µg/ml ($1/20^{th}$ MIC), (c) 4.9 µg/ml (MIC) and (d) 49 µg/ml (10xMIC) colistin. Viability after 72 hours; *P. aeruginosa* control $6.8x10^{10}$ cfu/ml; *P. aeruginosa* incubated with $1/20^{th}$ MIC colistin $6.2x10^{10}$ cfu/ml; *P. aeruginosa* incubated with MIC $7.6x10^{10}$ cfu/ml; *P. aeruginosa* incubated with 10xMIC colistin < 10 cfu/ml

P. aeruginosa incubated with $1/20^{th}$ MIC colistin for 72 hours were similar in size to control bacteria (Figure 6.34). The bacterial density in the MIC culture had improved substantially in keeping with the viability data, with some of the visualised bacteria in clusters. Very few bacteria were captured on the 10xMIC sample, with those present bearing altered shapes. Flow cytometry results at 72 hours (Figure 5.9 (b)) identified that the MIC culture had recovered substantially at this time point and was represented by a histogram peak indicating bacteria larger

than control. This could be as a result of aggregates visualised in the MIC SEM images.

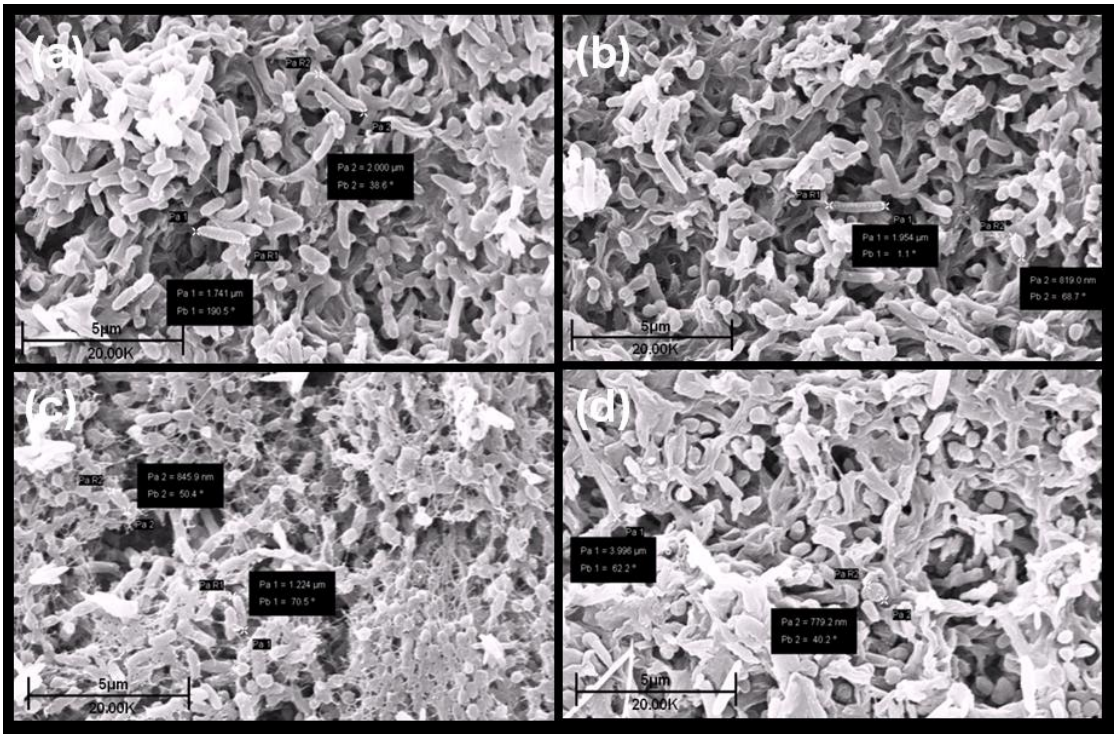

Figure 6.35 (a) Scanning electron micrograph of $1x10^7$ cfu/ml *P. aeruginosa* exposed to colistin for 168 hours: (a) control (b) 0.245 µg/ml ($1/20^{th}$ MIC), (c) 4.9 µg/ml (MIC) and (d) 49 µg/ml (10xMIC) colistin. Viability after 168 hours; *P. aeruginosa* control $4.5x10^9$ cfu/ml; *P. aeruginosa* incubated with $1/20^{th}$ MIC colistin $3.2x10^9$ cfu/ml; *P. aeruginosa* incubated with MIC $3.0x10^9$ cfu/ml; *P. aeruginosa* incubated with 10xMIC colistin < 10 cfu/ml

Incubation for 168 hours (Figure 6.35 a)) displayed control, $1/20^{th}$ MIC and MIC incubated bacteria all similar in size and shape. However the MIC culture has once again started to reveal extracellular strands or fibres connecting the bacteria into layers (Figure 6.35 b)). Some bacteria were visualised in the 10xMIC culture, with misshapen exteriors. Flow cytometry data in (5.9 (c)) supports the SEM findings with control, $1/20^{th}$ MIC and MIC cultures revealed as similar in size to each other, with no detection of the 10xMIC culture due to lack of normal bacterial cells in this culture.

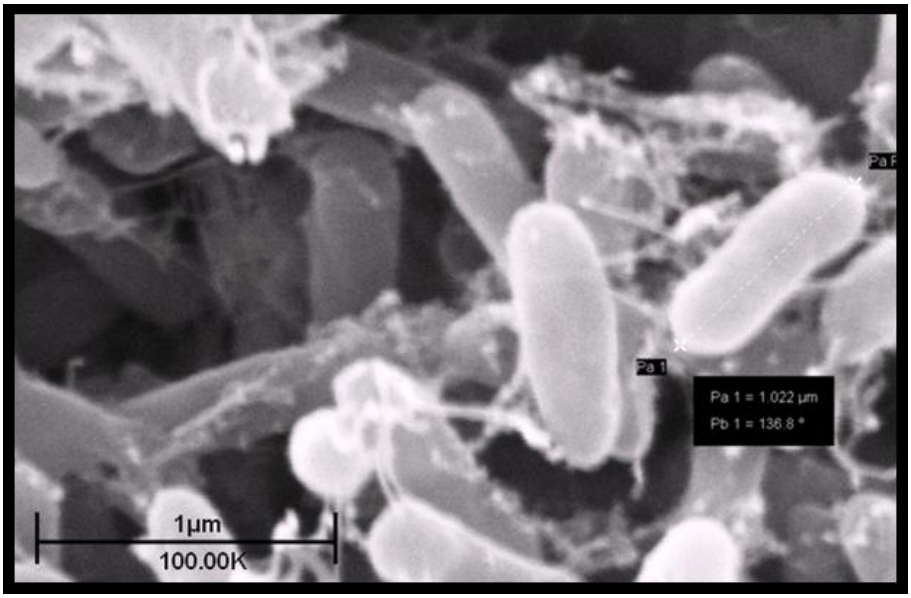

Figure 6.35 (b) High magnification scanning electron micrograph of $1x10^6$ cfu/ml *P. aeruginosa* exposed to MIC colistin for 168 hours

6.3.3 SEM images of *E. coli*, *S. aureus* and *P. aeruginosa* incubated with NP101

a) *Escherichia coli*

Incubation of *E. coli* with increasing concentrations of NP101 (Figure 6.36) resulted in substantial changes to bacterial size and shape after exposure to the CAP for one hour, when compared to the normal size and shape of the un-treated bacteria. Non-septated *E. coli* cells were visualised in the sub-inhibitory and inhibitory concentrations, while shorter and rounder cells were visible in the supra-inhibitory concentration. What appears to be extrusion of cellular contents and presence of extracellular fibres forming a matrix can also be seen in the $1/20^{th}$, MIC and 2xMIC images.

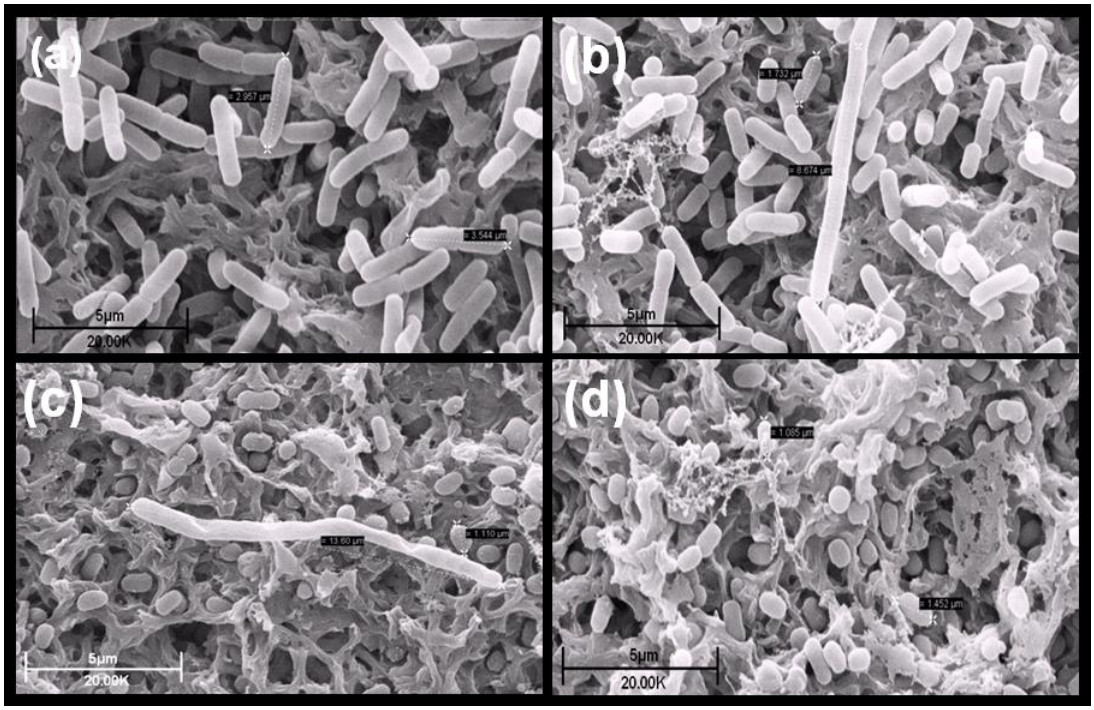

Figure 6.36 Scanning electron micrograph of $1x10^7$ cfu/ml *E. coli* exposed to NP101 for 1 hour: (a) control (b) 0.0155 mg/ml ($1/20^{th}$ MIC) (c) 0.31 mg/ml (MIC) and (d) 0.62 mg/ml (2xMIC)

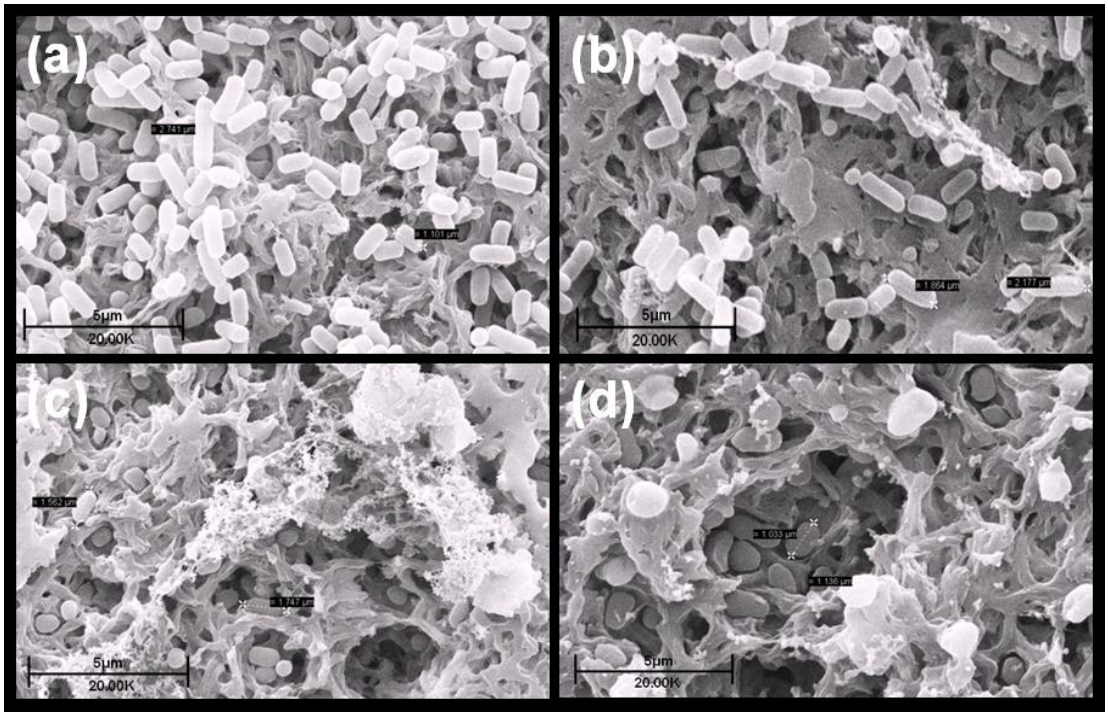

Figure 6.37 Scanning electron micrograph of $1x10^7$ cfu/ml *E. coli* exposed to NP101 for 3 hours: (a) control (b) 0.0155 mg/ml ($1/20^{th}$ MIC) (c) 0.31 mg/ml (MIC) and (d) 0.62 mg/ml (2xMIC).

Three hours incubation with NP101 (Figure 6.37) revealed bacteria in the $1/20^{th}$ MIC culture appeared to be linked to each other. Extrusion of fibrous material from

bacterial cells was also visible. Bacteria in the inhibitory culture displayed misshapen exteriors in some cells, extrusion of what appeared to be intracellular contents from some bacteria, as well as spherical cellular aggregates. Grossly deformed bacterial exteriors were exhibited by cells incubated with 2xMIC NP101 in conjunction with misshapen spherical bacterial cells or their remnants.

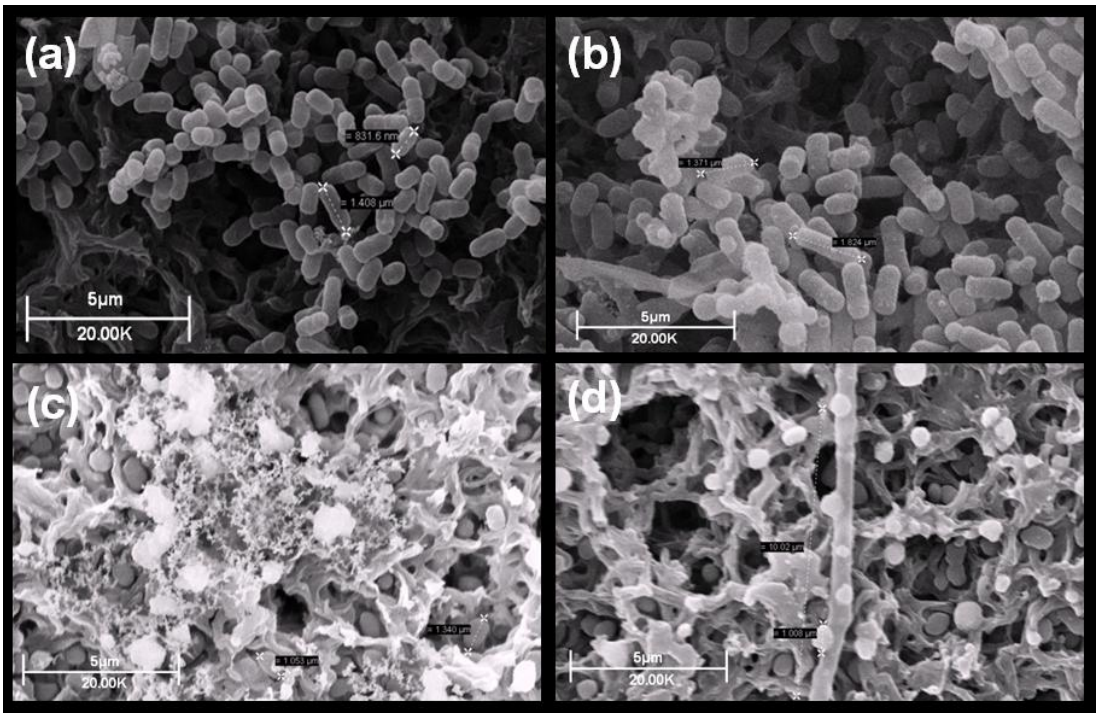

Figure 6.38 a) Scanning electron micrograph of $1x10^7$ cfu/ml *E. coli* exposed to NP101 for 6 hours: (a) control (b) 0.0155 mg/ml ($1/20^{th}$ MIC) (c) 0.31 mg/ml (MIC) and (d) 0.62 mg/ml (2xMIC). Viability after 6 hours; *E. coli* control $6.6x10^8$ cfu/ml; *E. coli* incubated with $1/20^{th}$ MIC NP101 $7.8x10^6$ cfu/ml; MIC and 2xMIC NP101 incubated bacteria was < 10 cfu/ml

By six hours incubation with NP101 (Figure 6.38 a)) *E. coli* incubated with $1/20^{th}$ MIC were reverting to the size and shape displayed by the control bacteria. Bacteria with deformed exteriors were visible in the MIC culture, together with spherical structures that appeared to be linked by extruded cellular contents. An SEM image at higher magnification of the spherical structures and connecting material is shown in Figure 6.38 b). The 10xMIC incubated bacteria revealed non-septation, blebbing, spheronisation and deformation of gross morphology of bacterial cells.

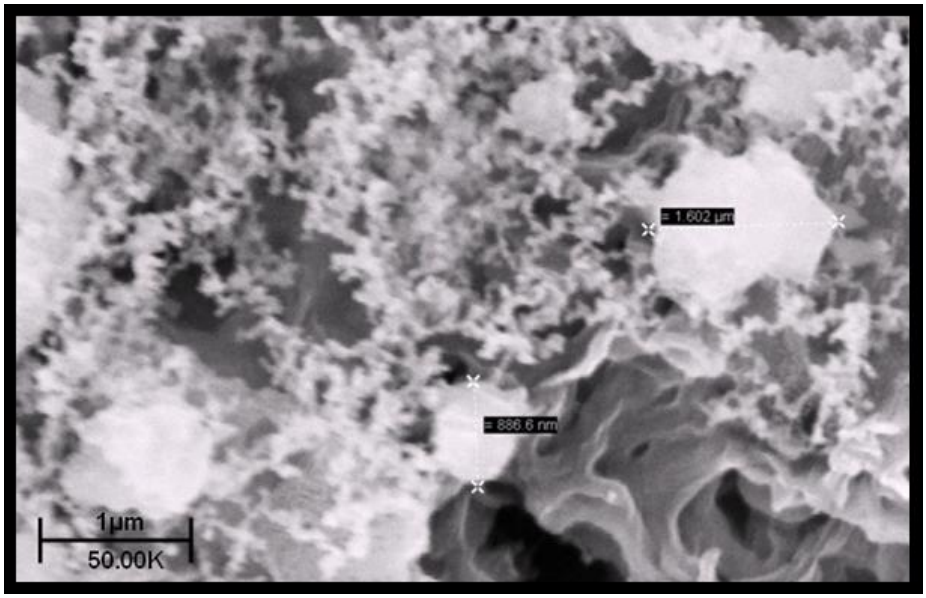

Figure 6.38 b) High magnification scanning electron micrograph of $1x10^7$ cfu/ml *E. coli* exposed to MIC NP101 for 6 hours

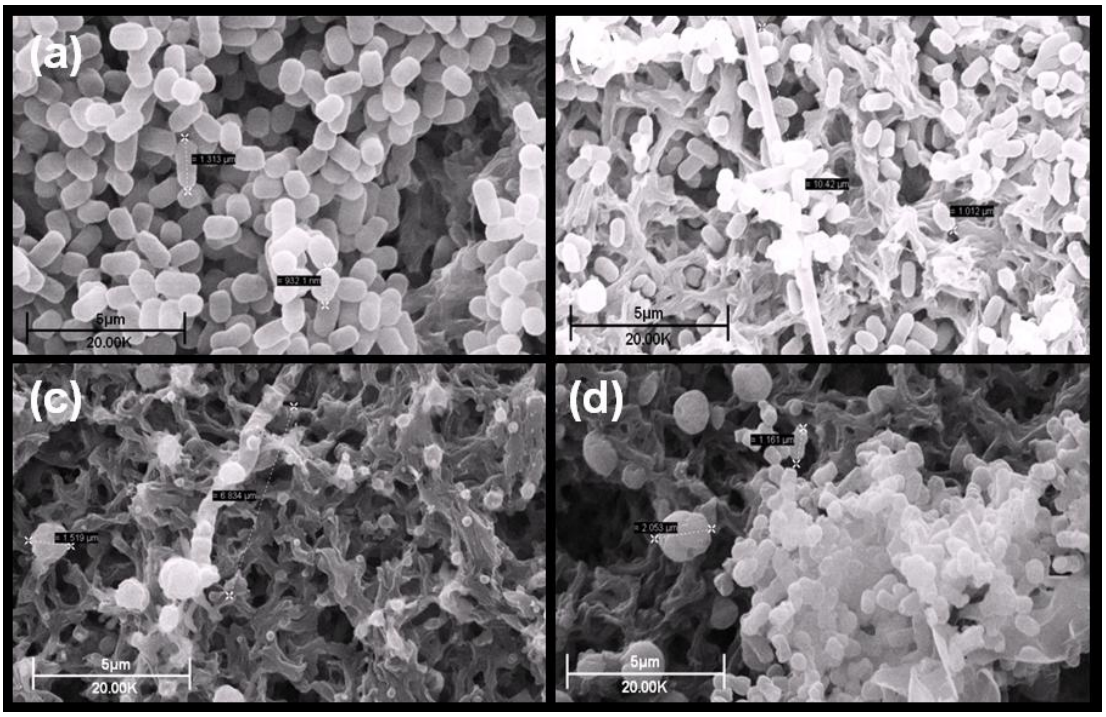

Figure 6.39 Scanning electron micrograph of $1x10^6$ cfu/ml *E. coli* exposed to NP101 for 24 hours: (a) control (b) 0.025 mg/ml ($1/20^{th}$ MIC) (c) 0.5 mg/ml (MIC) and (d) 1.0 mg/ml (2xMIC). Viability after 24 hours; *E. coli* control $3.5x10^9$ cfu/ml; *E. coli* incubated with $1/20^{th}$ MIC NP101 $4.9x10^9$ cfu/ml and *E. coli* incubated with MIC and 2xMIC NP101 was < 10 cfu/ml

Typical blunt ended bacteria comprised the control culture at 24 hours (Figure 6.39). Some non-septated bacteria were present in the $1/20^{th}$ MIC culture, co-existing with *E. coli* of normal shape and size. This could account for the flow

cytometry data (Figure 5.10) revealing the 1/20th MIC incubated bacteria being larger than control at 24 hours. Very few cells were visualised in the MIC culture, those present revealed non-septation and cell spheronisation. *E. coli* incubated with 2xMIC NP101 only displayed one cluster of aggregated cells on the entire sample surface as well as some spherical entities.

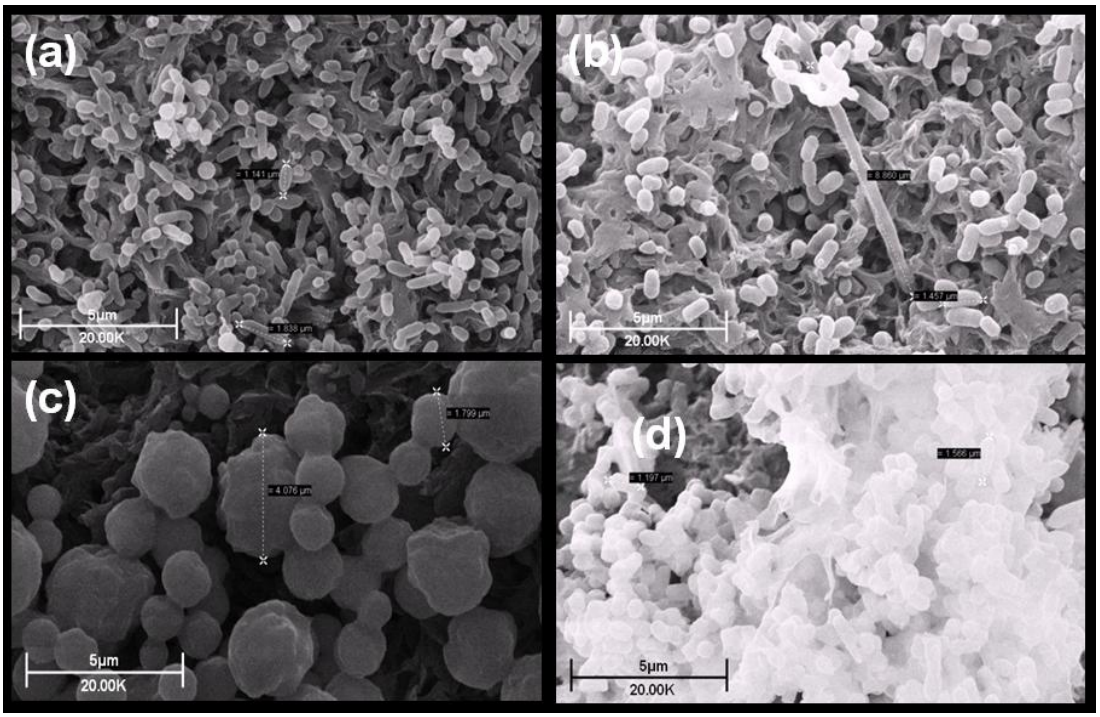

Figure 6.40 Scanning electron micrograph of 1x10^6 cfu/ml *E. coli* exposed to NP101 for 72 hours: (a) control (b) 0.025 mg/ml (1/20th MIC) (c) 0.5 mg/ml (MIC) and (d) 1.0 mg/ml (2xMIC). Viability after 72 hours; *E. coli* control 3.1x10^8 cfu/ml; *E. coli* incubated with 1/20th MIC NP101 3.2x10^8 cfu/ml and *E. coli* incubated with MIC and 2xMIC NP101 was < 10 cfu/ml

After seventy two hours incubation (Figure 6.40), NP101 continued to inhibit proper septation of bacterial cells in the sub-inhibitory concentration. Single bacterial cells in this culture were smaller in size than control cells. The inhibitory concentration produced spherical cellular structures up to 4 µm in diameter, with the 2xMIC culture revealed a gelling of bacterial cells similar to that previously seen with *E. coli* incubated with 10xMIC triclosan (Figure 6.5 (d)). Flow cytometry data at 72 hours (Figure 5.10 (b)) showed the greater proportion of control bacteria slightly larger in size to 1/20th MIC incubated bacteria.

Incubation with NP101 for 168 hours resulted in substantial changes to the size and shape of the incubated bacteria (Figure 6.41 a)).

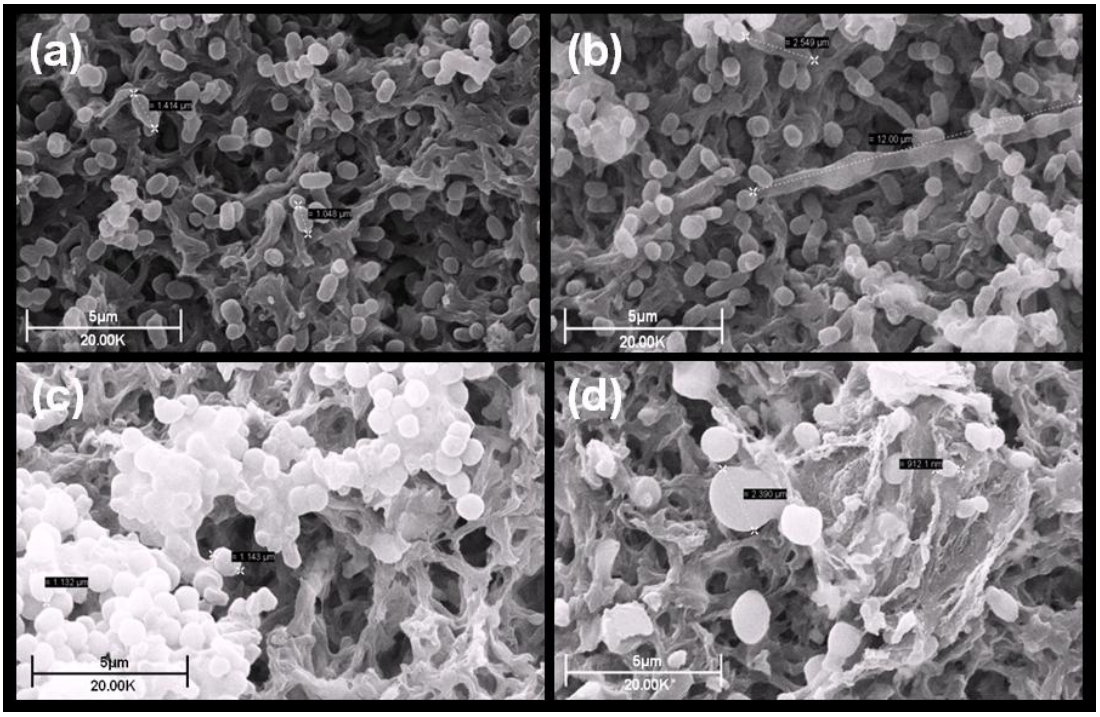

Figure 6.41 a) Scanning electron micrograph of $1x10^6$ cfu/ml *E. coli* exposed to NP101 for 168 hours: (a) control (b) 0.025 mg/ml ($1/20^{th}$ MIC) (c) 0.5 mg/ml (MIC) and (d) 1.0 mg/ml (2xMIC). Viability after 168 hours; *E. coli* control $3.1x10^8$ cfu/ml; *E. coli* incubated with $1/20^{th}$ MIC NP101 $6.7x10^7$ cfu/ml and *E. coli* incubated with MIC and 2xMIC NP101 was < 10 cfu/ml

Non-septated bacteria were present in the sub-inhibitory culture, a higher magnification SEM micrograph showing the unusual elongation in cell length can be seen in Figure 6.41 b). However, the majority of bacteria in the $1/20^{th}$ MIC and MIC cultures were similar in size and shape to control bacteria. The inhibitory culture also revealed a degree of cellular aggregation but single cells were also visible. The density of cells in the MIC culture had also increased significantly by 168 hours although no viable cells were detected by plate counts. The supra-inhibitory culture revealed irregular spherical cellular structures of varying sizes, which appeared to be interconnected by cellular debris. Results presented in Figure 5.10 displayed what appeared to be the development of tolerance to the effects of NP101 by *E.*

coli, in the re-appearance of cellular peaks for both MIC and 2xMIC cultures at 168 hours, having been absent from both 24 and 72 hour histograms.

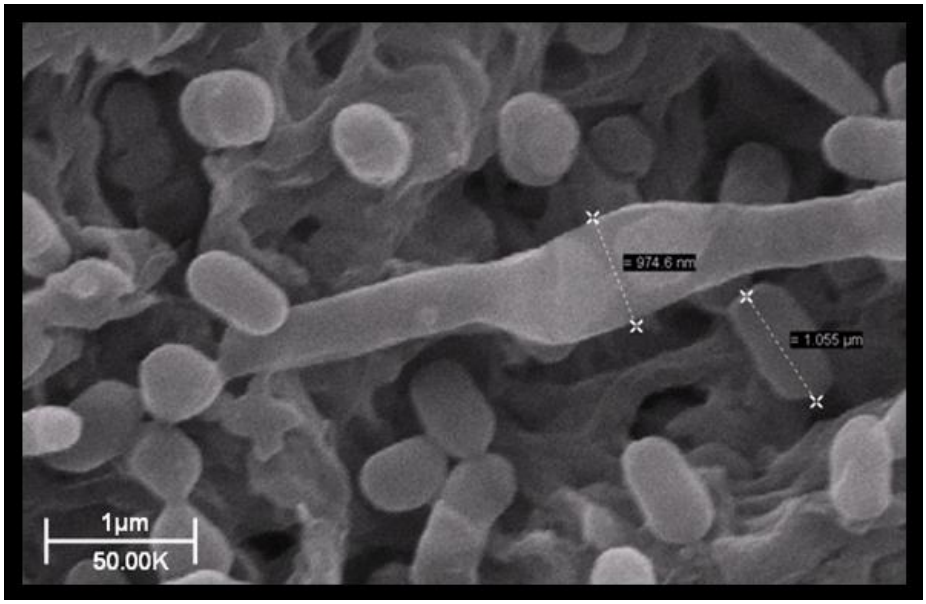

Figure 6.41 b) High magnification scanning electron micrograph of $1x10^6$ cfu/ml *E. coli* exposed to MIC NP101 for 168 hours

b) *Staphylococcus aureus*

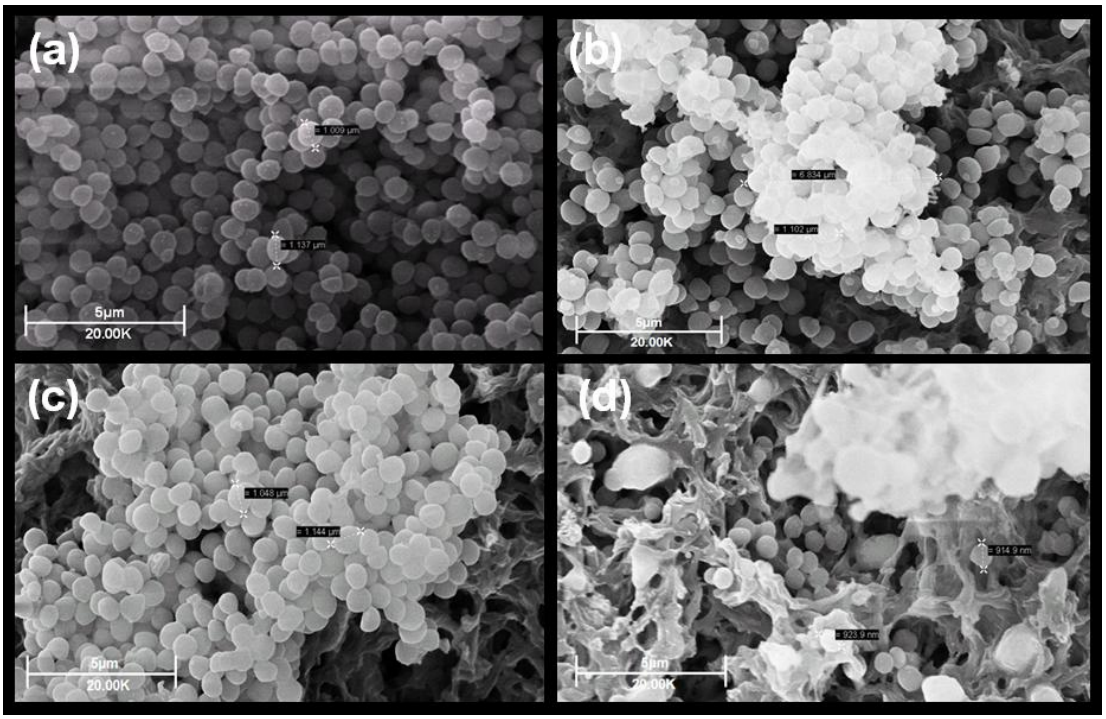

Figure 6.42 Scanning electron micrograph of $1x10^7$ cfu/ml *S. aureus* exposed to NP101 for 1 hour: (a) control (b) 0.0155 mg/ml ($1/20^{th}$ MIC) (c) 0.31 mg/ml (MIC) and (d) 0.62 mg/ml (2xMIC)

The effects of incubation with NP101 for one hour on *S. aureus* are revealed in Figure 6.42. Aggregation of cells was visible in all three treated cultures. Bacteria in the control, 1/20th MIC and MIC culture were similar in size and shape, whereas slightly smaller bacteria were visualised in the 2xMIC culture.

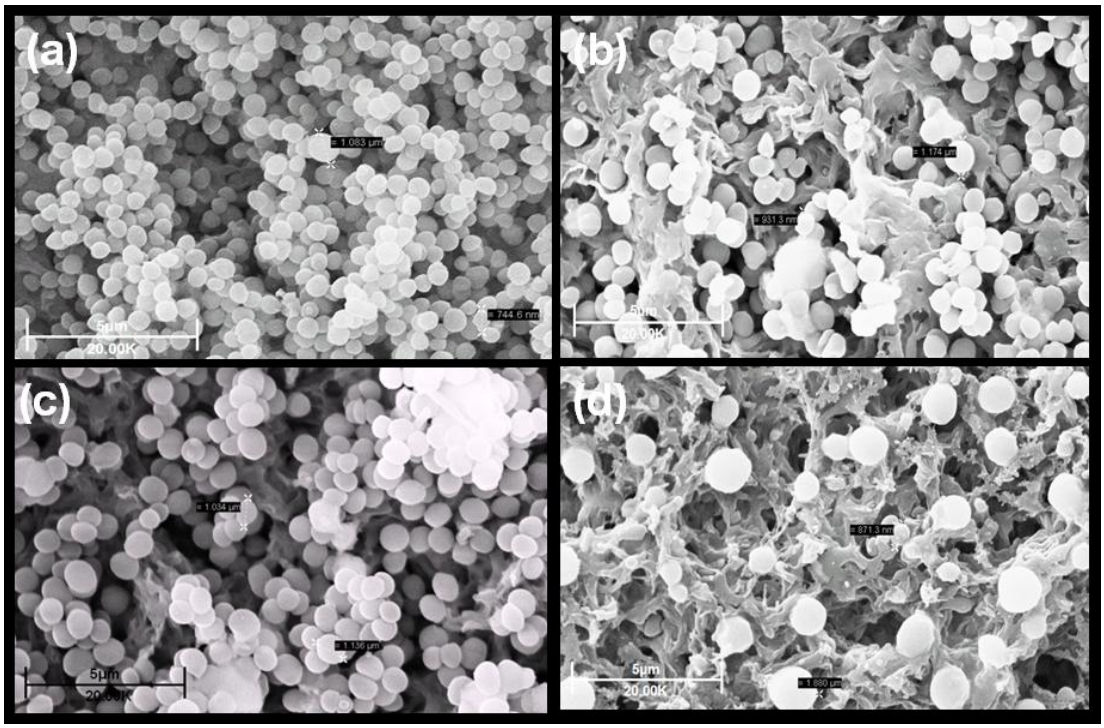

Figure 6.43 Scanning electron micrograph of 1x10^{7} cfu/ml *S. aureus* exposed to NP101 for 3 hours: (a) control (b) 0.0155 mg/ml (1/20th MIC) (c) 0.31 mg/ml (MIC) and (d) 0.62 mg/ml (2xMIC)

Cell aggregation could be seen in the sub and inhibitory cultures at 3 hours (Figure 6.43), while spherical structures of varying diameter were visualised in the 2xMIC culture, different in appearance to control bacteria. NP101 appeared to have lost its aggregatory effect on *S. aureus* at the sub-inhibitory concentration after 6 hours incubation (Figure 6.44). A low bacterial density was revealed in the MIC and 2xMIC samples, with both cultures displaying spherical cellular aggregates as well as single cells.

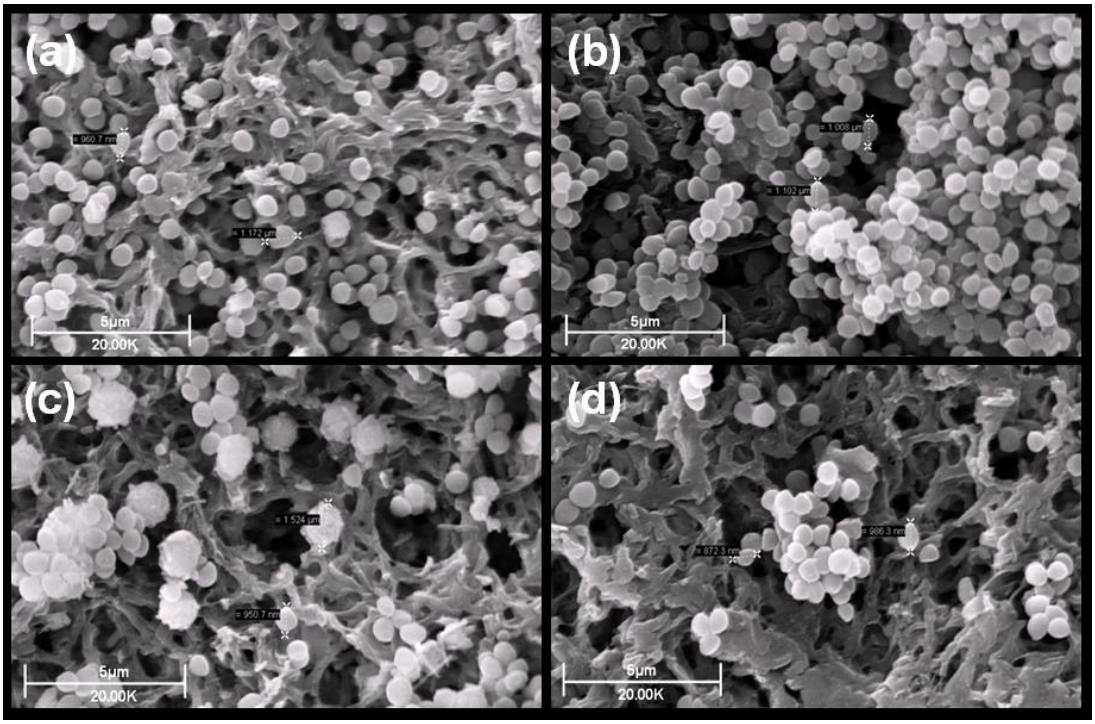

Figure 6.44 Scanning electron micrograph of $1x10^7$ cfu/ml *S. aureus* exposed to NP101 for 6 hours: (a) control (b) 0.0155 mg/ml ($1/20^{th}$ MIC) (c) 0.31 mg/ml (MIC) and (d) 0.62 mg/ml (2xMIC). Viability after 6 hours; *S. aureus* control $1.5x10^9$ cfu/ml; *S. aureus* incubated with $1/20^{th}$ MIC NP101 $1.17x10^9$ cfu/ml; *S. aureus* incubated with MIC and 2xMIC was < 10 cfu/ml

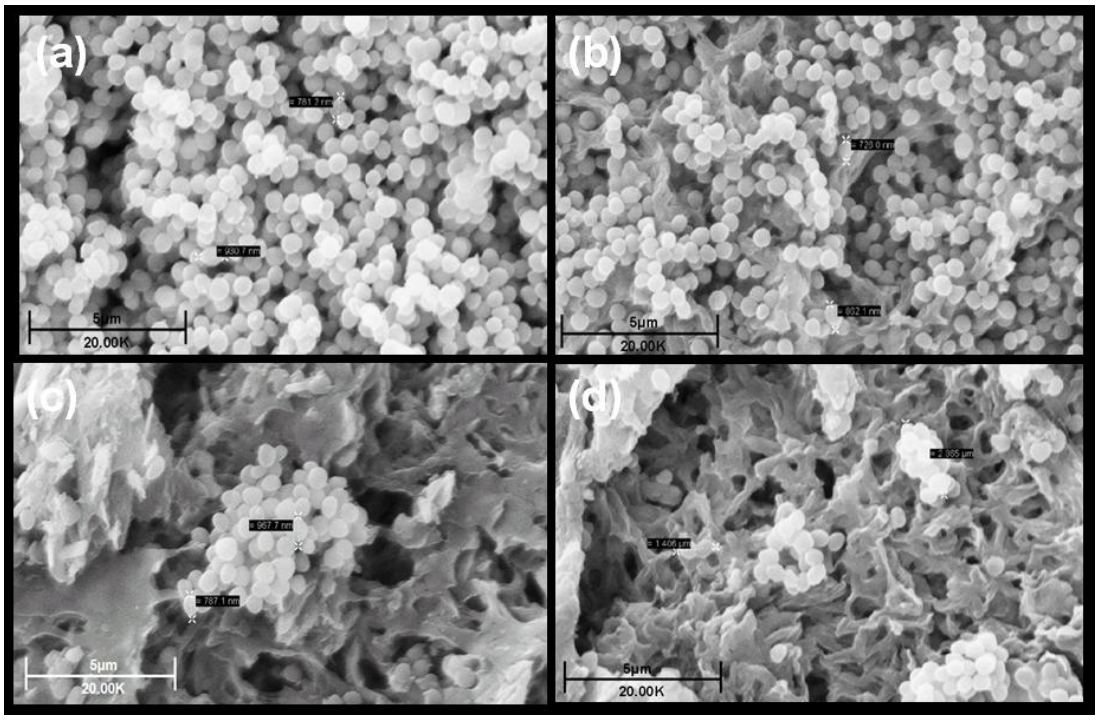

Figure 6.45 Scanning electron micrograph of $1x10^6$ cfu/ml *S. aureus* exposed to NP101 for 24 hours: (a) control (b) 0.0125 mg/ml ($1/20^{th}$ MIC) (c) 0.25 mg/ml (MIC) and (d) 0.5 mg/ml (2xMIC). Viability after 24 hours; *S. aureus* control $5.6x10^{11}$ cfu/ml; *S. aureus* incubated with $1/20^{th}$ MIC NP101 $5.6x10^{11}$ cfu/ml; *S. aureus* incubated with MIC NP101 $1.0x10^2$ cfu/ml; *S. aureus* incubated with 2xMIC NP101 $1.0x10^2$ cfu/ml

Great similarity in size and shape of control and sub-inhibitory bacteria existed at 24 hours (Figure 6.45). Clearly visible bacterial aggregates were present in the MIC and 2xMIC samples, which also revealed a much reduced bacterial density compared to control.

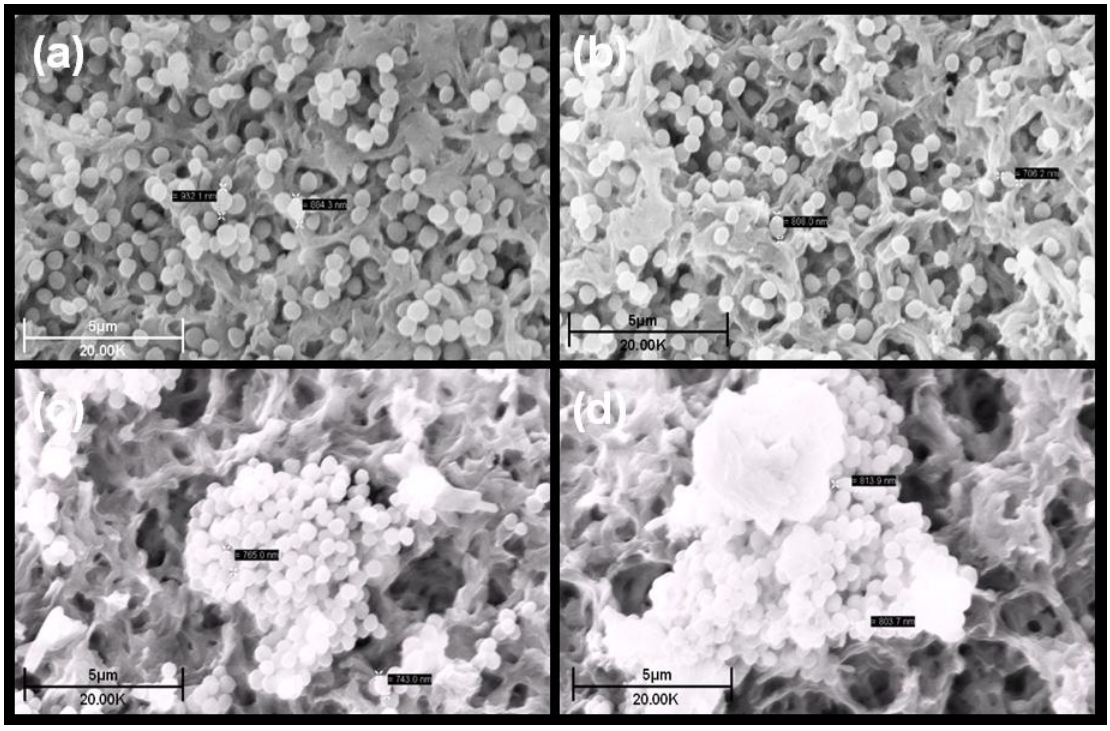

Figure 6.46 Scanning electron micrograph of $1x10^6$ cfu/ml *S. aureus* exposed to NP101 for 72 hours: (a) control (b) 0.0125 mg/ml ($1/20^{th}$ MIC) (c) 0.25 mg/ml (MIC) and (d) 0.5 mg/ml (2xMIC). Viability after 72 hours; *S. aureus* control $2.9x10^9$ cfu/ml; *S. aureus* incubated with $1/20^{th}$ MIC NP101 $5.6x10^5$ cfu/ml; *S. aureus* incubated with MIC NP101 $1.0x10^2$ cfu/ml; *S. aureus* incubated with 2xMIC NP101 $1.0x10^2$ cfu/ml

Micrographs of *S. aureus* after 72 hours incubation (Figure 6.46) disclosed similar bacterial size and shaped cells in the control and sub-inhibitory cultures. Large spherical bacterial aggregates or clusters were visible in the MIC and 2xMIC NP101 cultures.

Control bacteria were slightly larger than sub-inhibitory incubated bacteria after 168 hours incubation with NP101 (Figure 6.47). A single cluster of slightly gelled looking aggregated cells was present on the MIC sample surface. Bacteria present on the 2xMIC sample, were slightly smaller in size than control cells. Low bacterial

density of the MIC and 2xMIC cultures was most probably responsible for the absence of detectable cells from both these cultures at any sampled time point in the flow cytometry experiments (Figure 5.11). Control and 1/20th MIC incubated bacteria were identified as similar in size and shape by flow cytometry and confirmed by the SEM images.

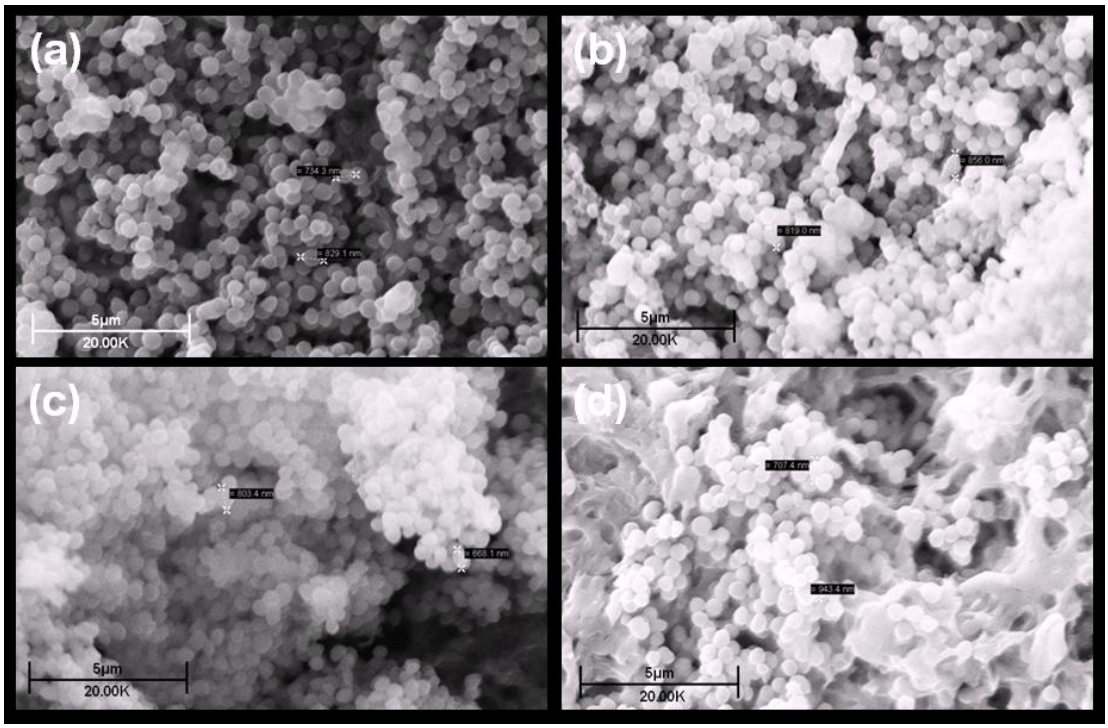

Figure 6.47 Scanning electron micrograph of 1x10^{6} cfu/ml *S. aureus* exposed to NP101 for 168 hours: (a) control (b) 0.0125 mg/ml (1/20th MIC) (c) 0.25 mg/ml (MIC) and (d) 0.5 mg/ml (2xMIC). Viability after 168 hours; *S. aureus* control 4.5x10^{8} cfu/ml; *S. aureus* incubated with 1/20th MIC NP101 2.1x10^{5} cfu/ml; *S. aureus* incubated with MIC NP101 1.0x10^{2} cfu/ml; *S. aureus* incubated with 2xMIC NP101 1.0x10^{2} cfu/ml

c) *Pseudomonas aeruginosa*

Spherical structures were present in the sub-inhibitory culture, though bacterial size and shape were similar to control after incubation for one hour with NP101 (Figure 6.48). The reaction of *P. aeruginosa* to incubation with the MIC and 2xMIC concentration was to form bacterial layers interconnected with what appeared to be extruded fibrous cellular material; similar to the response of *P. aeruginosa* to incubation with colistin at both two and four hours (Figure 6.30/6.31). As with the

sub-inhibitory culture, spherical structures were also apparent in the inhibitory and supra-inhibitory cultures.

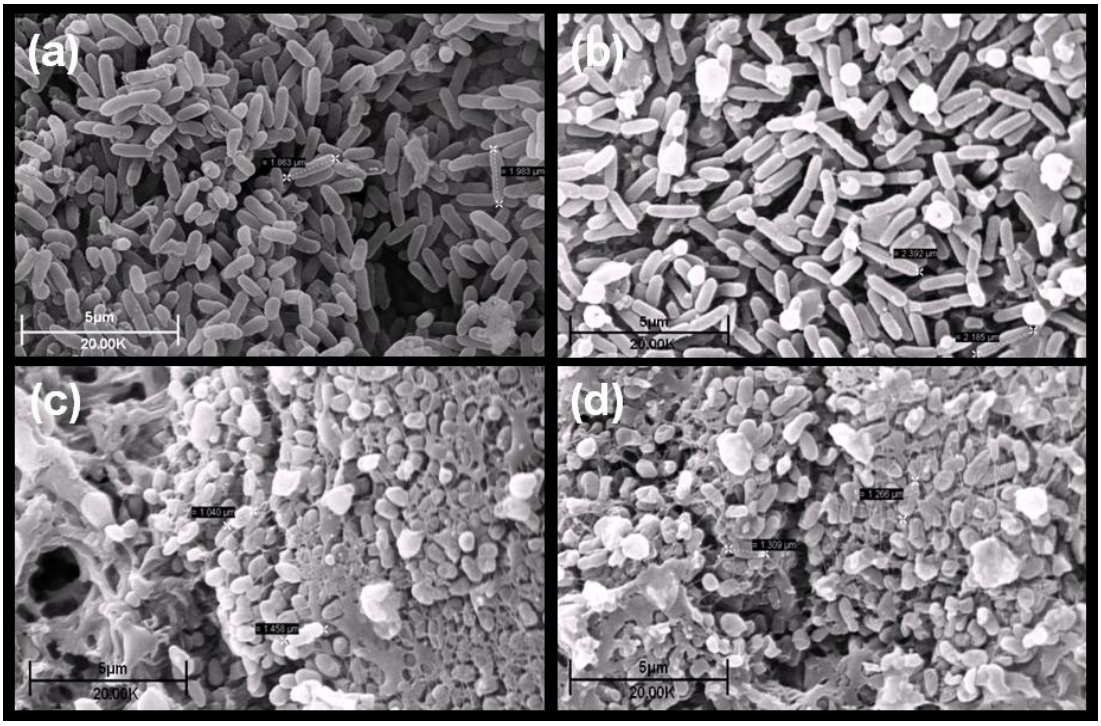

Figure 6.48 Scanning electron micrograph of $1x10^7$ cfu/ml *P. aeruginosa* exposed to NP101 for 1 hour: (a) control (b) 0.0155 mg/ml ($1/20^{th}$ MIC), (c) 0.31 mg/ml (MIC) and (d) 0.62 mg/ml (2xMIC) NP101

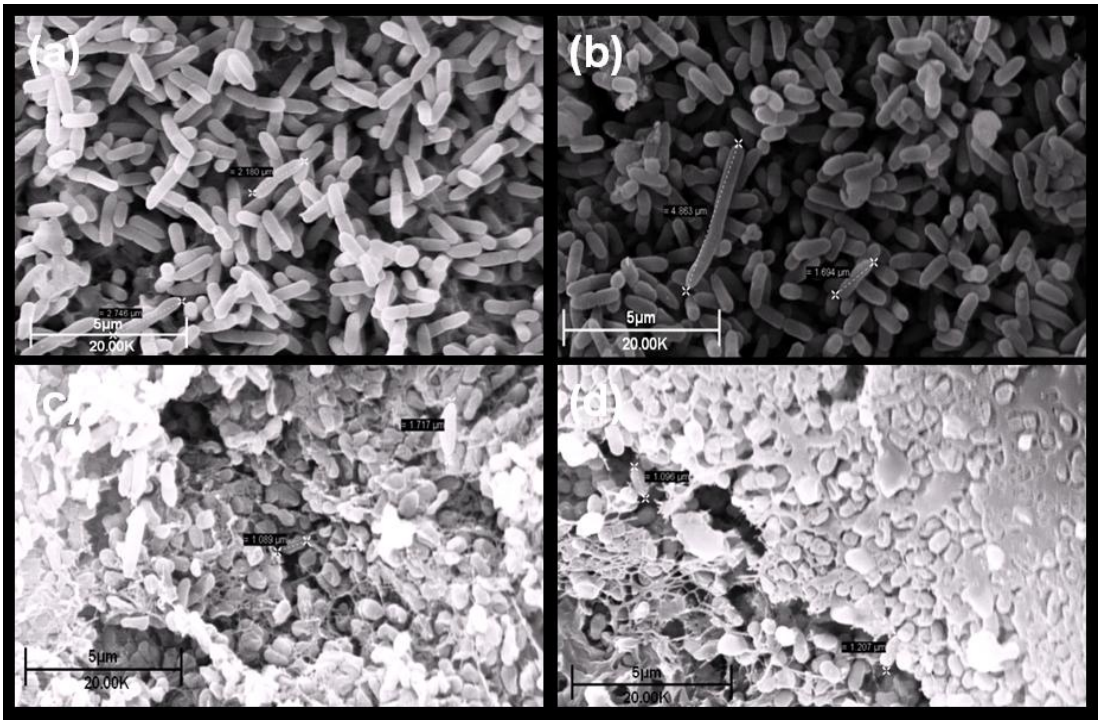

Figure 6.49 Scanning electron micrograph of $1x10^7$ cfu/ml *P. aeruginosa* exposed to NP101 for 3 hours: (a) control (b) 0.0155 mg/ml ($1/20^{th}$ MIC), (c) 0.31 mg/ml (MIC) and (d) 0.62 mg/ml (2xMIC) NP101

Three hours incubation with NP101 (Figure 6.49) resulted in the appearance of non-septated bacteria in the sub-inhibitory culture, while the formation of bacterial sheets in the MIC and 2xMIC incubated cultures was even more pronounced than when visualised after incubation for one hour with these NP101 concentrations.

SEM images revealing the effects of six hours incubation with NP101 (Figure 6.50) on *P. aeruginosa* disclosed inhibition of normal bacterial septation in the 1/20th MIC culture. However, layered bacterial aggregation was absent from the MIC and 2xMIC cultures at six hours, though some aggregated bacterial clumps were visible in both these cultures. Gelling of some bacteria was also visualised in bacteria in the MIC sample.

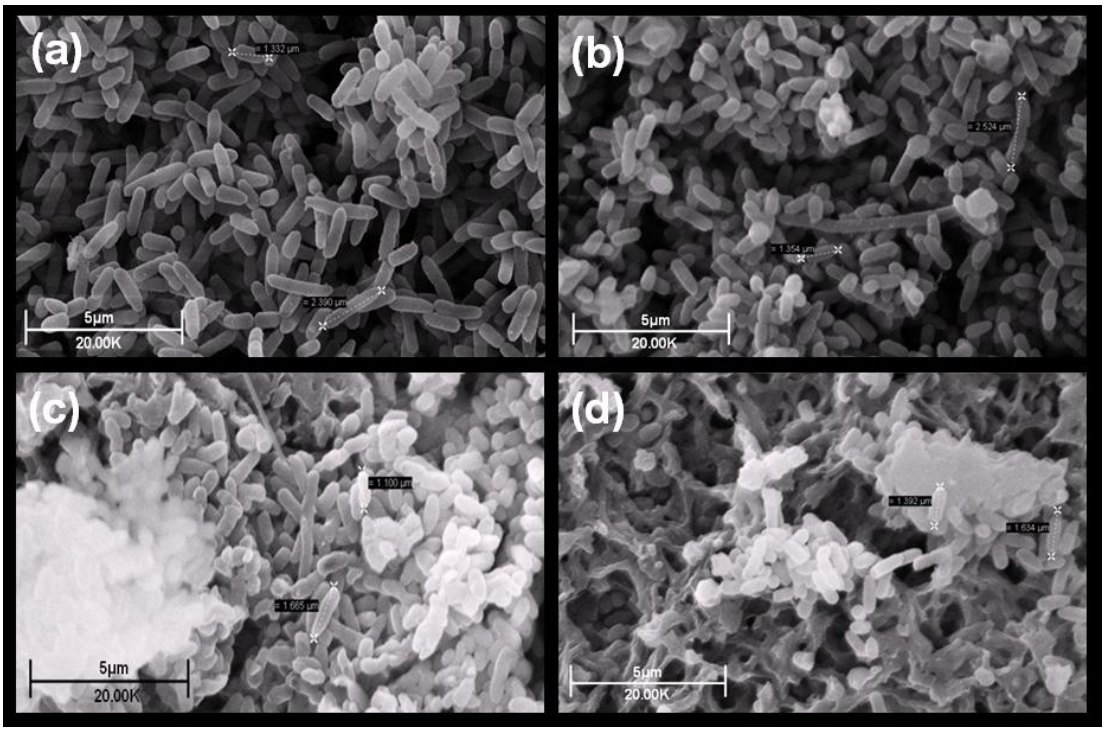

Figure 6.50 Scanning electron micrograph of 1x10^{7} cfu/ml *P. aeruginosa* exposed to NP101 for 6 hours: (a) control (b) 0.0155 mg/ml (1/20th MIC), (c) 0.31 mg/ml (MIC) and (d) 0.62 mg/ml (2xMIC) NP101. Viability after 6 hours; *P. aeruginosa* control 5.1x10^{10} cfu/ml; *P. aeruginosa* incubated with 1/20th MIC NP101 5.0x10^{10} cfu/ml; *P. aeruginosa* incubated with MIC NP101 2.0x10^{3} cfu/ml; *P. aeruginosa* incubated with 2xMIC NP101 1.0x10^{2} cfu/ml

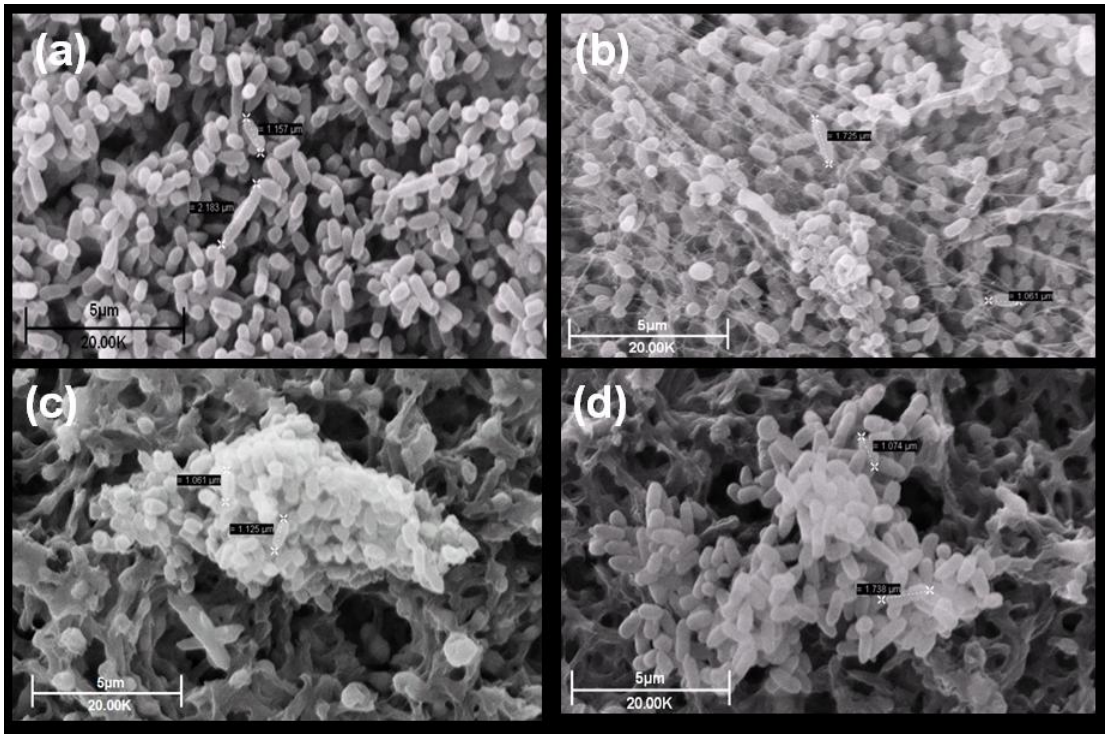

Figure 6.51 a) Scanning electron micrograph of $1x10^6$ cfu/ml *P. aeruginosa* exposed to NP101 for 24 hours: (a) control (b) 0.0125 mg/ml ($1/20^{th}$ MIC), (c) 0.25 mg/ml (MIC) and (d) 0.5 mg/ml (2xMIC) NP101. Viability after 24 hours; *P. aeruginosa* control $6.6x10^{10}$ cfu/ml; *P. aeruginosa* incubated with $1/20^{th}$ MIC NP101 $6.6x10^{10}$ cfu/ml; *P. aeruginosa* incubated with MIC NP101 $1.0x10^2$ cfu/ml; *P. aeruginosa* incubated with 2xMIC NP101 $1.0x10^2$ cfu/ml

The appearances of the three NP101 cultures were very different to control at 24 hours (Figure 6.51 a)). Though size and bacterial shape of control and $1/20^{th}$ MIC cultures was very similar, the sub-inhibitory incubated bacteria were interconnected by what appeared to be thin filaments of an extracellular nature (Figure 6.51 b)). Bacterial clumping in the inhibitory and supra-inhibitory cultures was visualised, with some gelling of bacteria in the MIC culture. The flow cytometry data (Figure 5.12) revealed both control and $1/20^{th}$ MIC cultures were similar is size. The MIC and 2xMIC cultures were not detected at any time point due to reduced bacterial density, which is apparent from the SEM micrographs. The examination of viability demonstrated 99.99% reduction at six hours and non-viability of *P. aeruginosa* in both MIC and 2xMIC cultures at 24, 72 and 168 hours.

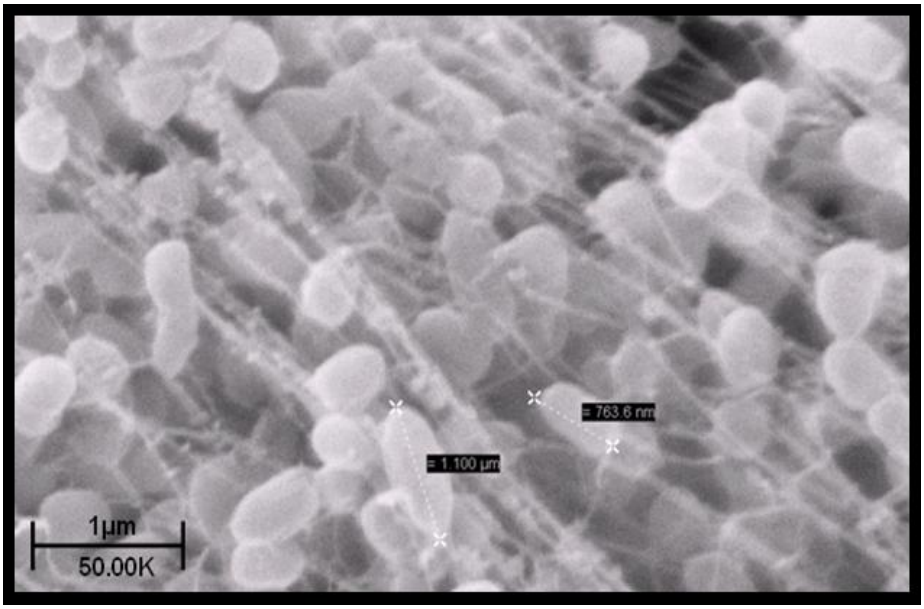

Figure 6.51 b) High magnification scanning electron micrograph of $1x10^6$ cfu/ml *P. aeruginosa* exposed to $1/20^{th}$ MIC NP101 for 24 hours

SEM images of *P. aeruginosa* incubated with NP101 for seventy two hours (Figure 6.52) revealed similar size and shaped control and sub-inhibitory bacteria. The density of bacteria in the inhibitory and supra-inhibitory cultures was very low, with the visualised bacteria forming aggregated clumps.

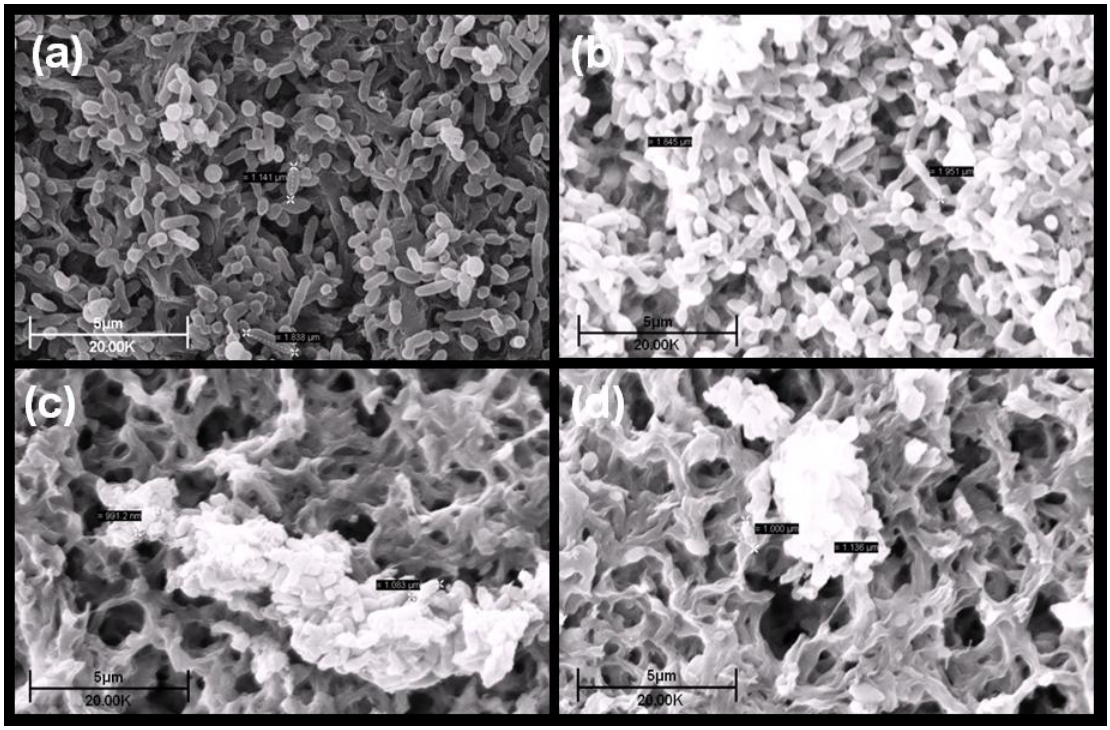

Figure 6.52 Scanning electron micrograph of $1x10^6$ cfu/ml *P. aeruginosa* exposed to NP101 for 72 hours: (a) control (b) 0.0125 mg/ml ($1/20^{th}$ MIC), (c) 0.25 mg/ml (MIC) and (d) 0.5

mg/ml (2xMIC) NP101. Viability after 72 hours; *P. aeruginosa* control $1.2x10^{10}$ cfu/ml; *P. aeruginosa* incubated with $1/20^{th}$ MIC colistin $7.9x10^{9}$ cfu/ml; *P. aeruginosa* incubated with MIC NP101 $1.0x10^{2}$ cfu/ml; *P. aeruginosa* incubated with 2xMIC NP101 $1.0x10^{2}$ cfu/ml

After 168 hours incubation (Figure 6.53) bacteria incubated with $1/20^{th}$ MIC NP101 displayed inhibition of normal bacterial septation. Bacterial density in MIC and 2xMIC cultures was again very low, with these bacteria forming spherical cellular aggregated structures with some gelling in 2xMIC apparent.

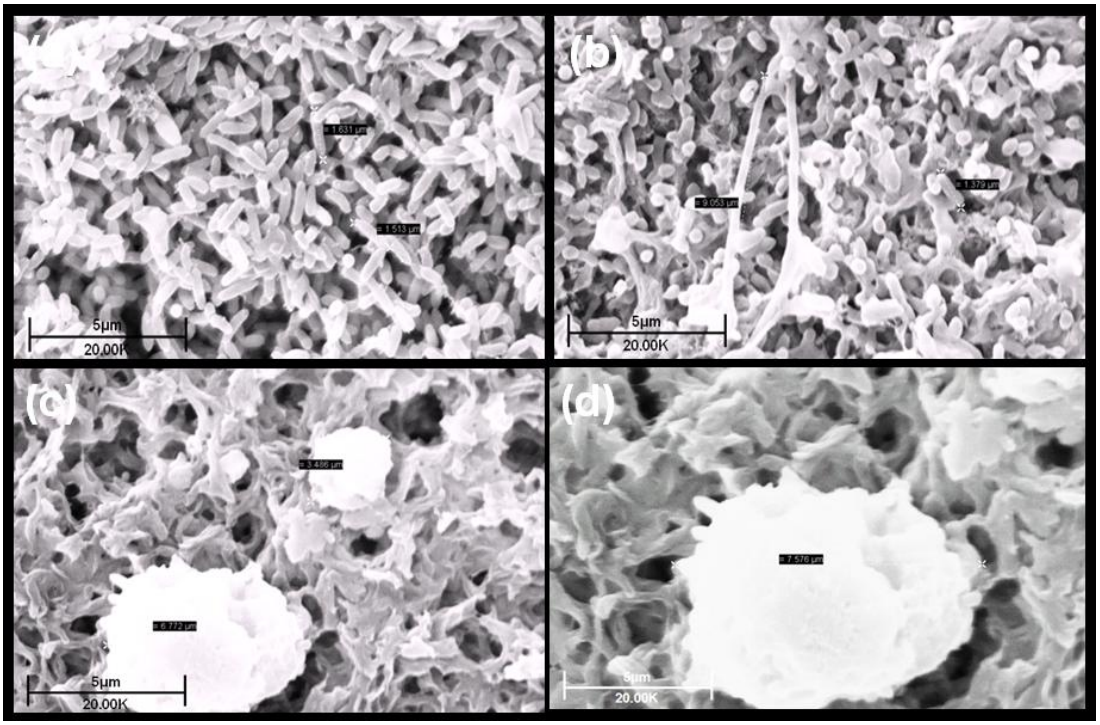

Figure 6.53 Scanning electron micrograph of $1x10^{6}$ cfu/ml *P. aeruginosa* exposed to NP101 for 168 hours: (a) control (b) 0.0125 mg/ml ($1/20^{th}$ MIC), (c) 0.25 mg/ml (MIC) and (d) 0.5 mg/ml (2xMIC) NP101. Viability after 168 hours; *P. aeruginosa* control $7.8x10^{8}$ cfu/ml; *P. aeruginosa* incubated with $1/20^{th}$ MIC colistin $5.6x10^{8}$ cfu/ml; *P. aeruginosa* incubated with MIC NP101 $1.0x10^{2}$ cfu/ml; *P. aeruginosa* incubated with 2xMIC NP101 $1.0x10^{2}$ cfu/ml

6.3.4 SEM images of *E. coli*, *S. aureus* and *P. aeruginosa* incubated with NP108

a) *Escherichia coli*

Incubation of *E. coli* with NP108 for one hour (Figure 6.54) led to dramatic differences in the appearance of all incubated cultures compared to control. *E. coli* incubated with $1/20^{th}$ MIC NP108 revealed bacteria similar in size and shape to

control, as well as bacteria with clearly visible blebbed exteriors. The sample also contained a wide film of material to which spherical and normal bacterial cells were attached. This film was probably formed from extruded cellular material. The MIC culture revealed a number of spherical cellular entities of varying dimensions. The 2xMIC culture revealed a similar film of material to that observed in the sub-inhibitory sample; to which the cells were attached. Some of the bacteria in the sample also exhibited blebbed outer membranes as well as distorted external morphologies.

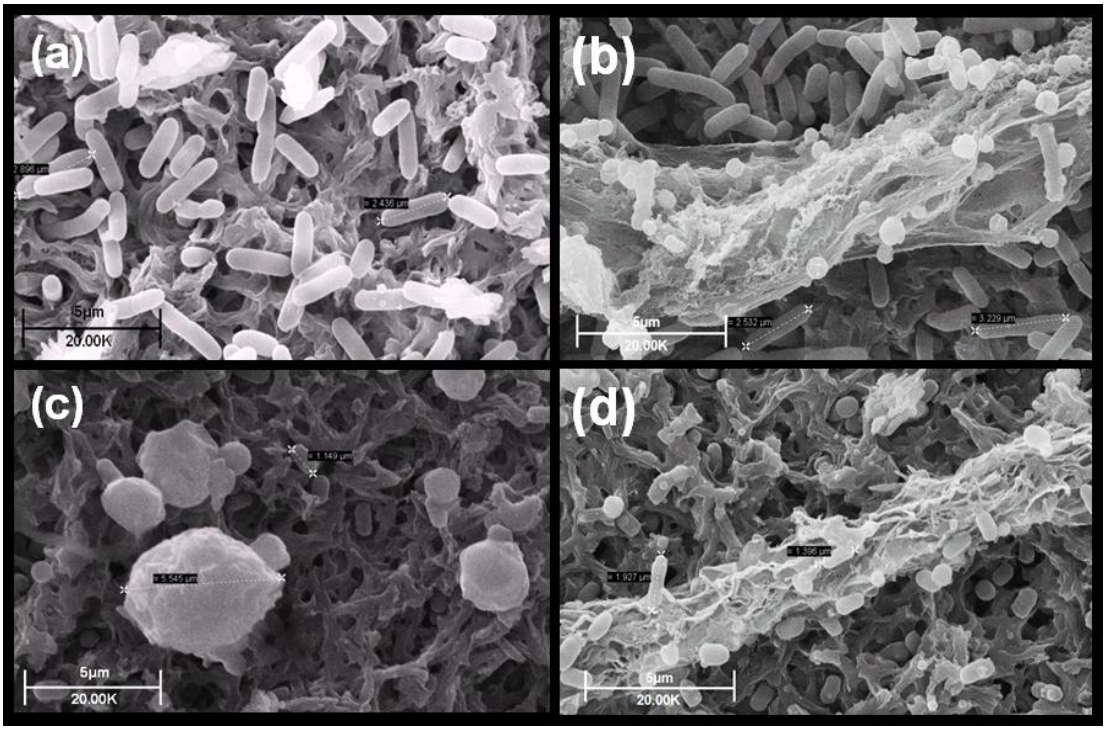

Figure 6.54 Scanning electron micrograph of $1x10^7$ cfu/ml *E. coli* exposed to NP108 for 1 hour: (a) control (b) 0.025 mg/ml ($1/20^{th}$ MIC) (c) 0.5 mg/ml (MIC) and (d) 1.0 mg/ml (2xMIC)

Incubation for three hours incubation with NP108 resulted in the sub-inhibitory incubated bacteria displaying inhibition of normal septation, and bacterial aggregation. Bacterial aggregation was also visible in the MIC culture, while the supra-inhibitory bacteria revealed distorted and blebbed cellular exteriors.

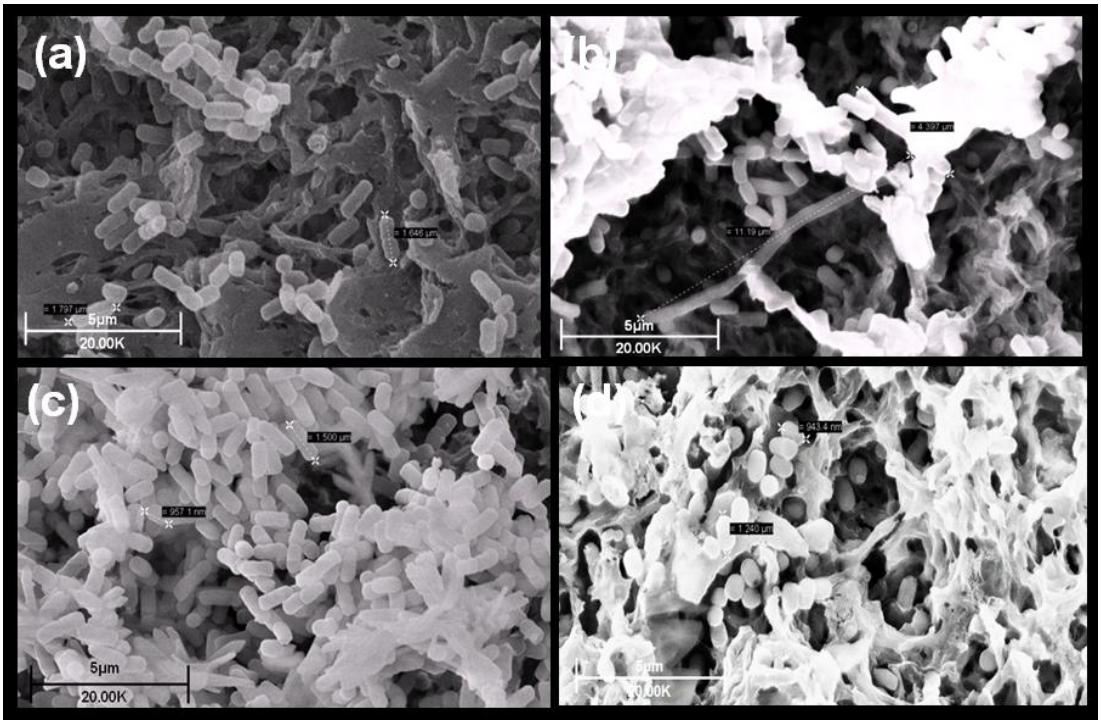

Figure 6.55 Scanning electron micrograph of $1x10^7$ cfu/ml *E. coli* exposed to NP108 for 3 hours: (a) control (b) 0.025 mg/ml ($1/20^{th}$ MIC) (c) 0.5 mg/ml (MIC) and (d) 1.0 mg/ml (2xMIC)

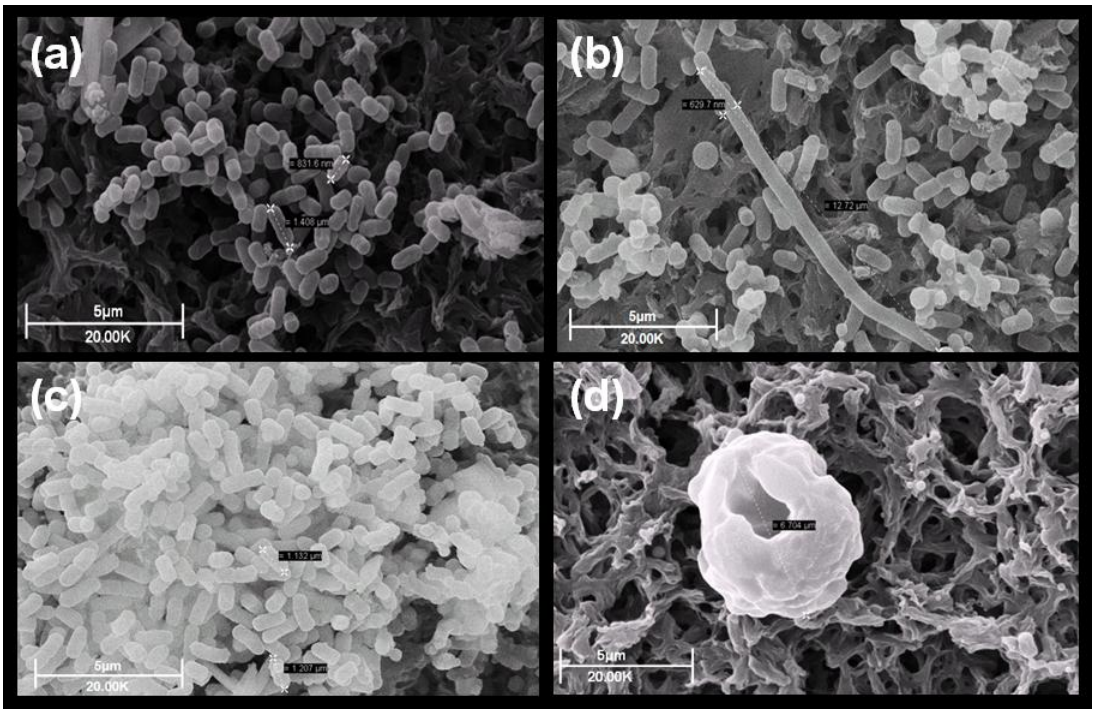

Figure 6.56 Scanning electron micrograph of $1x10^7$ cfu/ml *E. coli* exposed to NP108 for 6 hours: (a) control (b) 0.025 mg/ml ($1/20^{th}$ MIC) (c) 0.5 mg/ml (MIC) and (d) 1.0 mg/ml (2xMIC). Viability after 6 hours; *E. coli* control $4.0x10^{10}$ cfu/ml; *E. coli* incubated with $1/20^{th}$ MIC NP101 $3.6x10^9$ cfu/ml; *E. coli* incubated with MIC and 2xMIC NP101 was < 10 cfu/ml

Six hours incubation (Figure 6.56) with 1/20th MIC NP108 continued to disrupt normal bacterial septation and cause bacterial aggregation. The bacteria visualised in the MIC sample were aggregated into one large cluster, which was slightly gelled in appearance. Nothing could be seen on the very clean 2xMIC sample surface except for a few spherical structures, most probably of cellular debris.

Sub-inhibitory and inhibitory concentrations after 24-hours incubation with NP108 (Figure 6.57) revealed non-septated *E. coli.* Small spherical structures, probably cellular remnants, were also visualised in the MIC sample along with bacteria displaying blebbed and distorted exteriors.

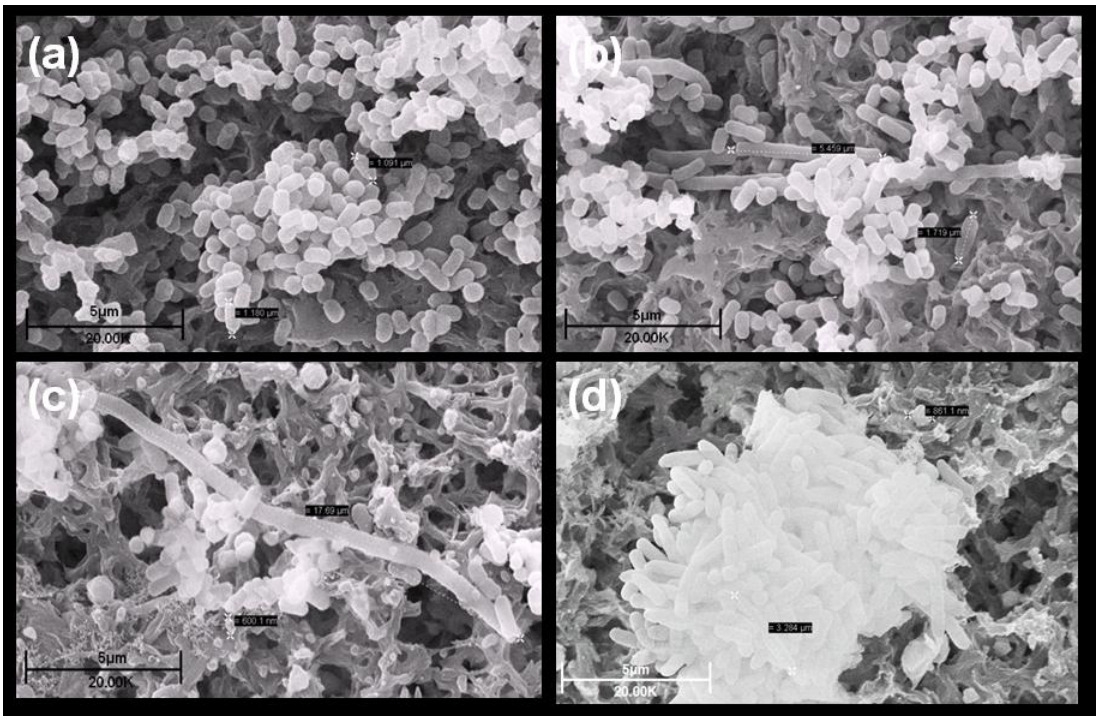

Figure 6.57 Scanning electron micrograph of 1x10^{6} cfu/ml *E. coli* exposed to NP108 for 24 hours: (a) control (b) 0.0125 mg/ml (1/20th MIC) (c) 0.25 mg/ml (MIC) and (d) 0.5 mg/ml (2xMIC). Viability after 24 hours; *E. coli* control 5.1x10^{9} cfu/ml; *E. coli* incubated with 1/20th MIC NP101 5.0x10^{9} cfu/ml; *E. coli* incubated with MIC and 2xMIC NP101 was < 10 cfu/ml

A single aggregated bacterial group, slightly gelled in appearance was revealed in the SEM micrograph for the 2xMIC culture. Data presented in Figure 5.13 demonstrated the 1/20th MIC bacteria as being larger than control bacteria, this can now be explained by the non-septated bacterial cells co-existing with single

bacteria. Neither the MIC nor 2xMIC treated cultures were detected by flow cytometry as insufficient bacteria were present in these cultures at all the time points assayed. The low bacterial density in both MIC and 2xMIC cultures visualised by SEM is the most likely explanation for this occurrence.

The 1/20th MIC treated bacteria were still exhibiting long, non-septated cells after 72 hours incubation with NP108 (Figure 6.58).

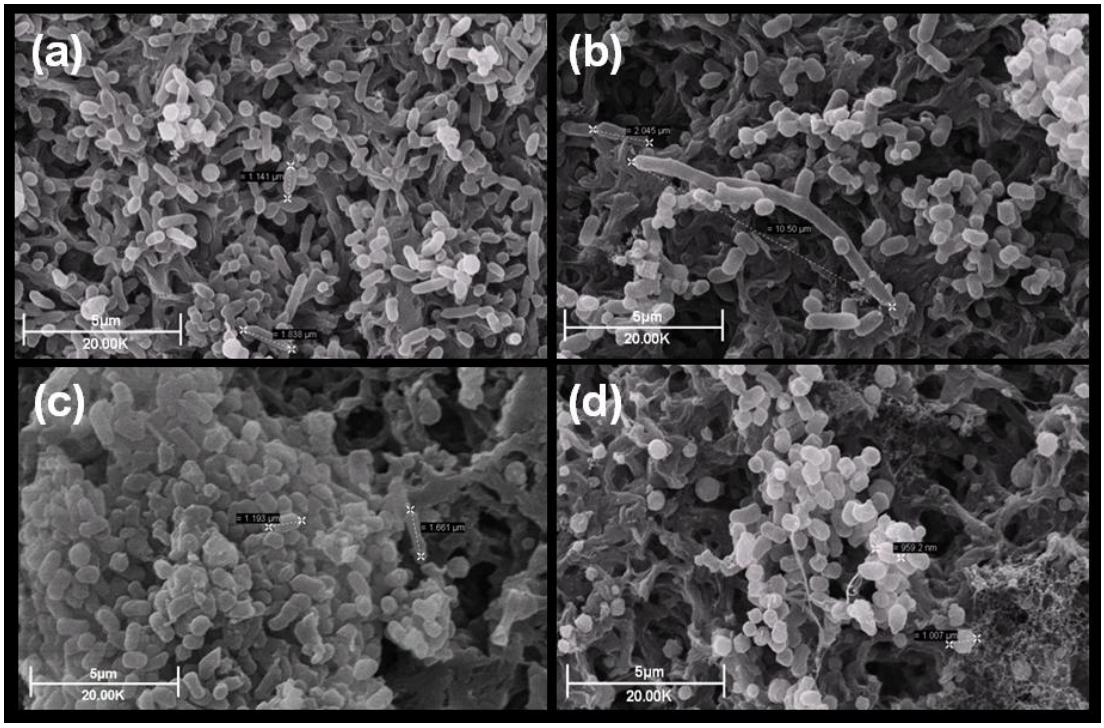

Figure 6.58 Scanning electron micrograph of 1x10^{6} cfu/ml *E. coli* exposed to NP108 for 72 hours: (a) control (b) 0.0125 mg/ml (1/20th MIC) (c) 0.25 mg/ml (MIC) and (d) 0.5 mg/ml (2xMIC). Viability after 72 hours; *E. coli* control 1.8x10^{9} cfu/ml; *E. coli* incubated with 1/20th MIC NP101 1.4x10^{9} cfu/ml; *E. coli* incubated with MIC and 2xMIC NP101 incubated bacteria was < 10 cfu/ml

The sub-inhibitory culture contained a variety of bacterial sizes at this time point; however, this was not un-usual as the control sample also contained bacterial cells ranging from less than 1 µm up to nearly 3 µm at this time. The MIC culture contained only one aggregated clump of distorted *E. coli* bacteria. The 2xMIC culture sample revealed an aggregated clump of small, distorted cells that appeared to have extruded some cellular material. Smaller spherical entities were also visualised in the 2xMIC sample. Sub-inhibitory incubated cells were revealed

as larger than control bacteria by flow cytometry (Figure 6.58), which is supported by the SEM data with the presence of long co-joined bacteria in this culture.

The inhibitory effect of NP108 on normal bacterial septation in *E. coli* was still visible in the sub-inhibitory incubated bacteria at 168 hours (Figure 6.59 a)).

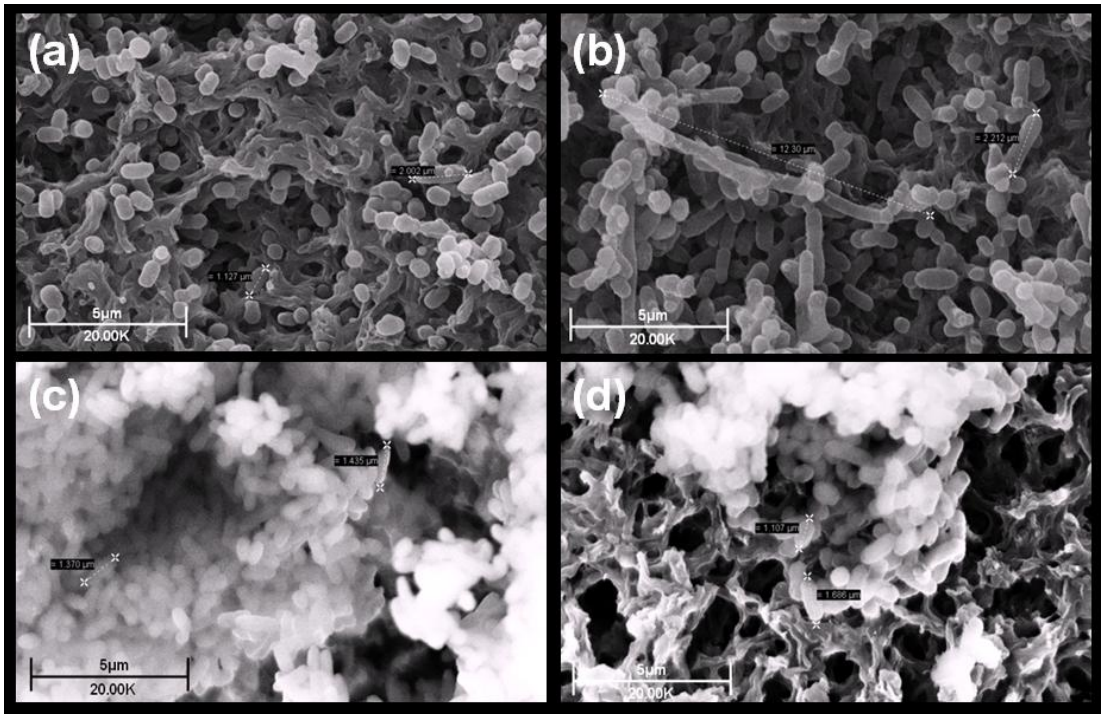

Figure 6.59 a) Scanning electron micrograph of $1x10^6$ cfu/ml *E. coli* exposed to NP108 for 168 hours: (a) control (b) 0.0125 mg/ml ($1/20^{th}$ MIC) (c) 0.25 mg/ml (MIC) and (d) 0.5 mg/ml (2xMIC). Viability after 168 hours; *E. coli* control $1.0x10^9$ cfu/ml; *E. coli* incubated with $1/20^{th}$ MIC NP101 $6.0x10^8$ cfu/ml; *E. coli* incubated with MIC NP101 $1.0x10^3$ cfu/ml and *E. coli* incubated with 2xMIC NP101 was < 10 cfu/ml

Blebbing of the cell surfaces of these $1/20^{th}$ MIC bacteria was apparent (higher magnification images Figure 6.59 b)) in conjunction with indented cell exteriors and what appeared to be leakage of intracellular material from some bacterial cells. Initiation of cross wall formation in *E. coli* can be clearly seen in the higher magnification SEM image, which was never completed. Though cross wall formation was inhibited, peripheral wall growth occurred, suggesting two separate processes may control such synthesis and only the cross wall formation is affected by NP108. An aggregated mass of bacteria exhibiting a gelled appearance was displayed on both the MIC and 2xMIC sample surface. The MIC bacteria were still replicating at

six hours but from that experimental sample time, no MIC bacteria exhibited active division for the remaining experimental period.

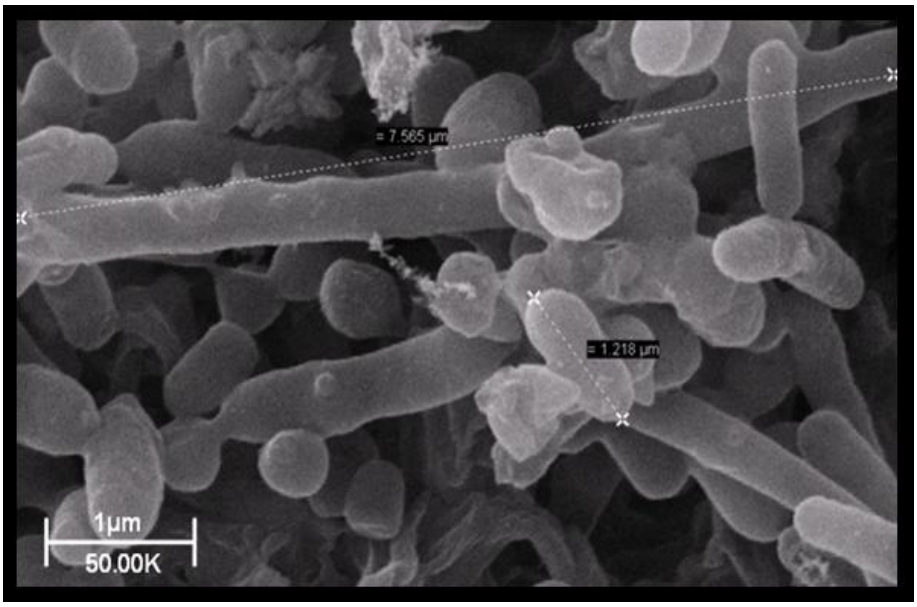

Figure 6.59 b) High magnification scanning electron micrograph of 1x10^{6} cfu/ml *E. coli* exposed to 1/20th MIC NP108 for 168 hours

b) *Staphylococcus aureus*

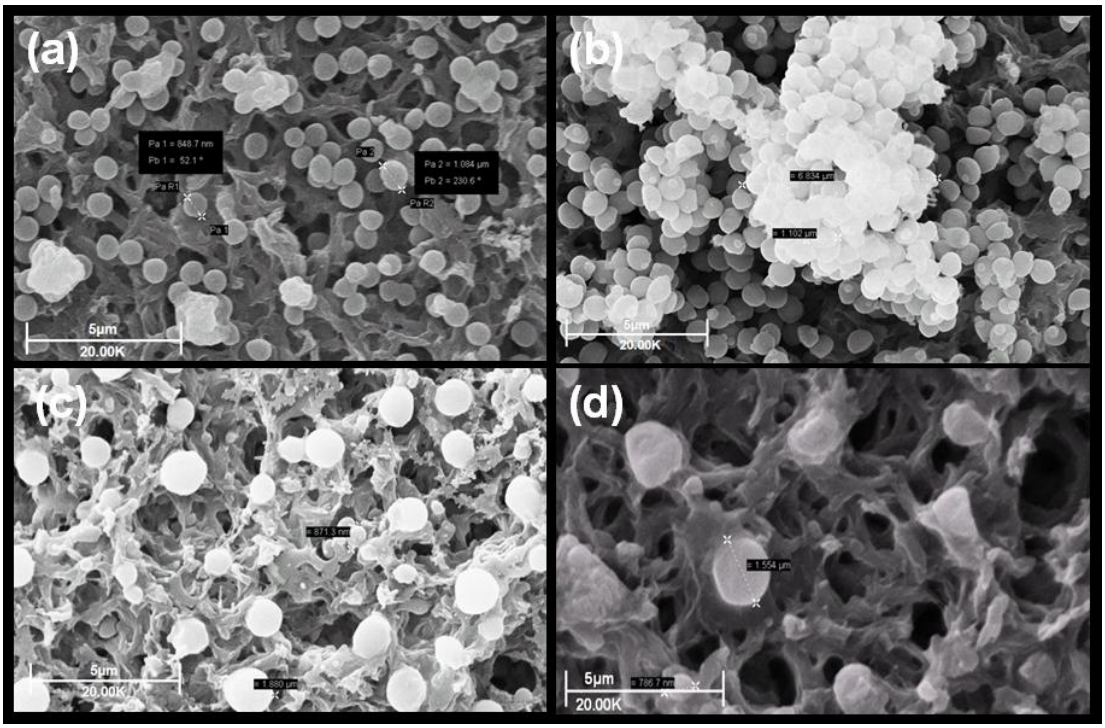

Figure 6.60 Scanning electron micrograph of 1x10^{7} cfu/ml *S. aureus* exposed to NP108 for 1 hour: (a) control (b) 0.0125 mg/ml (1/20th MIC) (c) 0.25 mg/ml (MIC) and (d) 0.5 mg/ml (2xMIC).

Exposure of *S. aureus* to NP108 for one hour (Figure 6.60) produced aggregated bacterial groups in the 1/20th MIC culture, while the MIC and 2xMIC incubated bacteria exhibited spherical cellular structures of different dimensions.

Aggregation of bacterial cells was visualised with *S. aureus* after three hours incubation with NP108 (Figure 6.61).

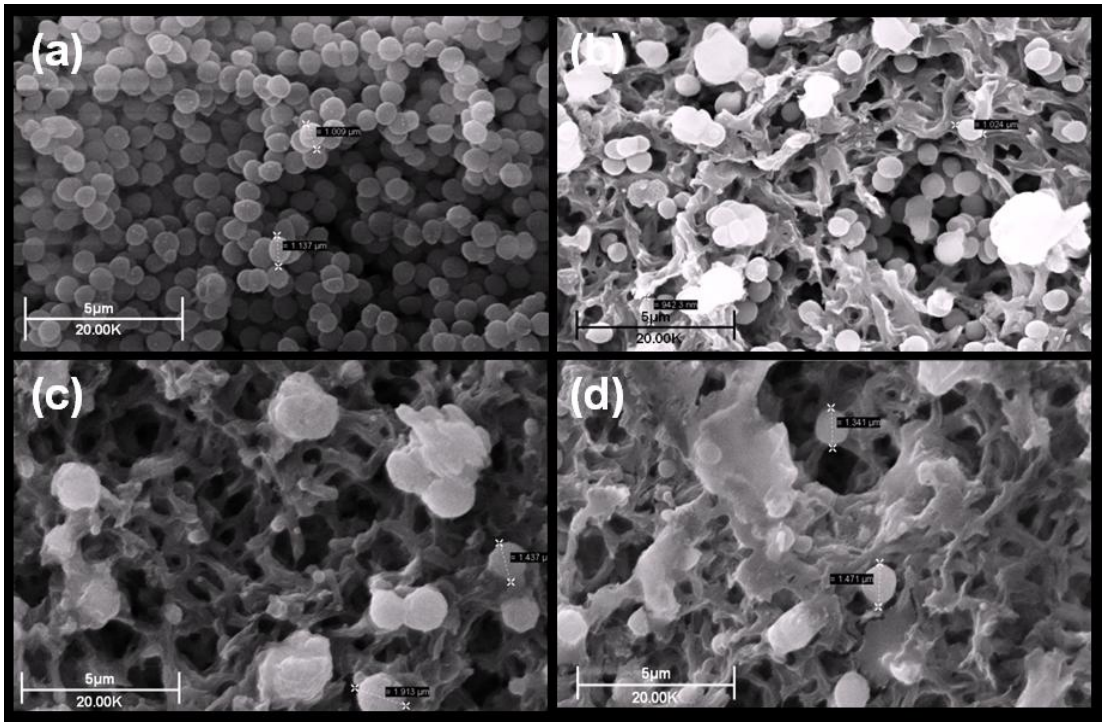

Figure 6.61 Scanning electron micrograph of 1x10^{7} cfu/ml *S. aureus* exposed to NP108 for 3 hours: (a) control (b) 0.0125 mg/ml (1/20th MIC) (c) 0.25 mg/ml (MIC) and (d) 0.5 mg/ml (2xMIC).

This aggregation was similar for all three test concentrations, with *S. aureus* exposed to the sub-inhibitory NP108 concentration retaining some degree of normal morphology.

The effects of the longer incubation time of six hours on *S. aureus* (Figure 6.62 a)) were more severe. Blebbed and distorted bacterial membranes together with aggregation were visible in the 1/20th MIC NP108 culture. Bacteria in the MIC culture formed one cohesive group, from which appeared to have extruded intracellular material (Figure 6.62 b)). In addition to this extruded material the

spherical cellular structures present had diameters ranging in size between 200 – 900 nm. Bacteria in the 2xMIC concentration displayed gelled spherical structures.

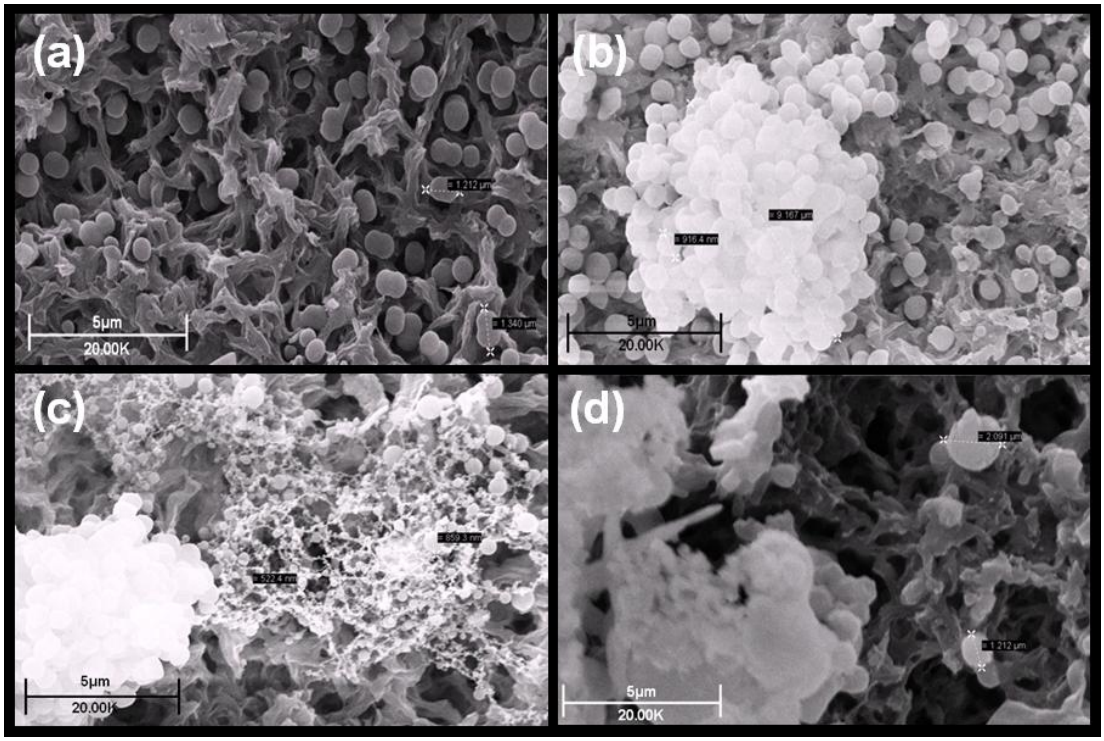

Figure 6.62 a) Scanning electron micrograph of $1x10^7$ cfu/ml *S. aureus* exposed to NP108 for 6 hours: (a) control (b) 0.0125 mg/ml ($1/20^{th}$ MIC) (c) 0.25 mg/ml (MIC) and (d) 0.5 mg/ml (2xMIC). Viability after 6 hours; *S. aureus* control $2.8x10^9$ cfu/ml; *S. aureus* incubated with $1/20^{th}$ MIC NP108 $1.8x10^8$ cfu/ml; *S. aureus* incubated with MIC NP108 $2.3x10^6$ cfu/ml; *S. aureus* incubated with 2xMIC was < 10 cfu/ml

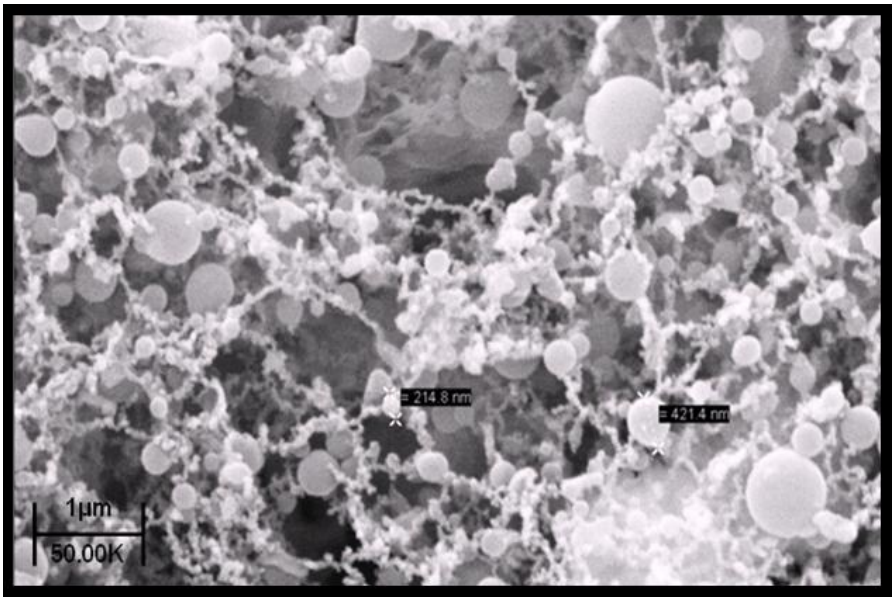

Figure 6.62 b) High magnification scanning electron micrograph of $1x10^7$ cfu/ml *S. aureus* exposed to MIC NP108 for 6 hours

S. aureus control and sub-inhibitory incubated bacteria were similar in size and shape at 24 hours (Figure 6.63). The bacteria revealed in the MIC SEM micrographs had formed into a large group of cells, each cell similar in size to control bacteria. *S aureus* in the 2xMIC culture adopted two forms, one as part of a gelled bacterial mass, while smaller spherical structures with a roughened exterior, different to the smooth exterior of control cells, were also present.

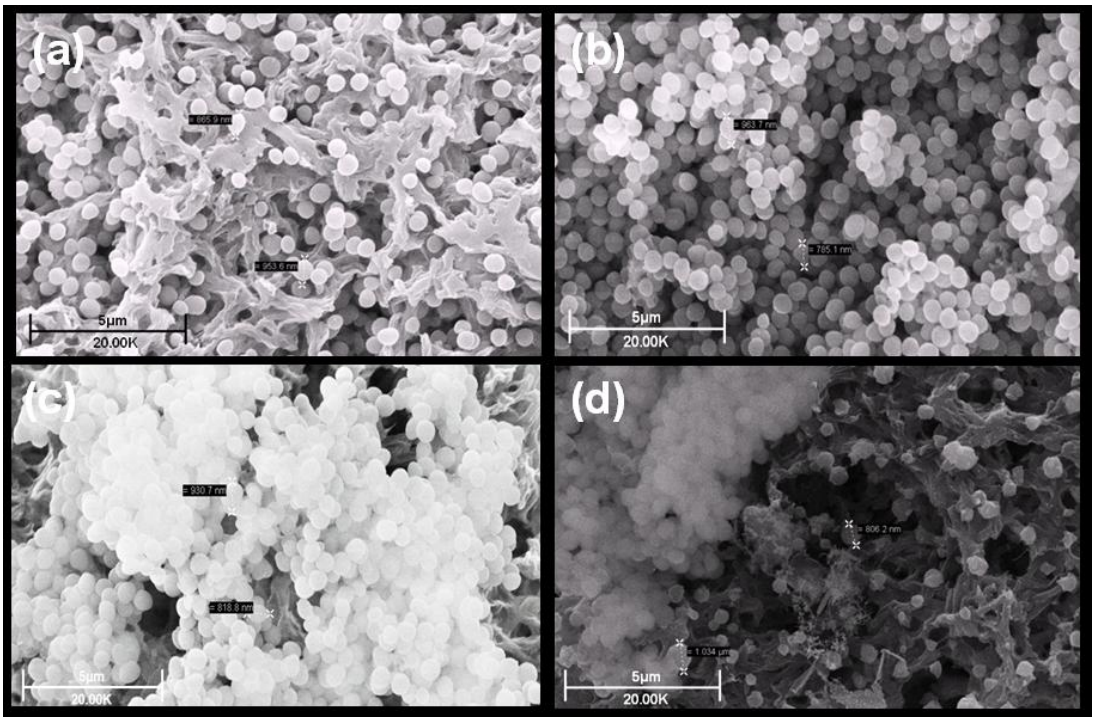

Figure 6.63 Scanning electron micrograph of 1x107 cfu/ml S. aureus exposed to NP108 for 24 hours: (a) control (b) 0.0125 mg/ml (1/20th MIC) (c) 0.25 mg/ml (MIC) and (d) 0.5 mg/ml (2xMIC). Viability after 24 hours; *S. aureus* control 5.5x10^{11} cfu/ml; *S. aureus* incubated with 1/20th MIC NP108 3.0x10^{11} cfu/ml; *S. aureus* incubated with MIC NP108 6.2x10^{3} cfu/ml; *S. aureus* incubated with 2xMIC was < 10 cfu/ml

Data gathered by flow cytometry regarding these cultures and presented in Chapter 5 (Figure 5.14) had identified the control and sub-inhibitory incubated bacteria as similar in size and shape. However, neither MIC nor 2xMIC cultures were detected due to low bacterial density in these cultures, which is certainly obvious from the 2xMIC SEM data. Bacterial density in the MIC culture had improved from the six-hour sample, which is in accordance with the viability data described in Figure 5.14 (d).

SEM images at 72 hours display similarity between control, 1/20th MIC and MIC incubated bacteria (Figure 6.64). The MIC incubated bacteria had reverted from one aggregated mass to the more normal sized and evenly distributed *S. aureus*. Very few bacteria were revealed in the supra-inhibitory concentration and those that were present expressed slightly gelled exteriors.

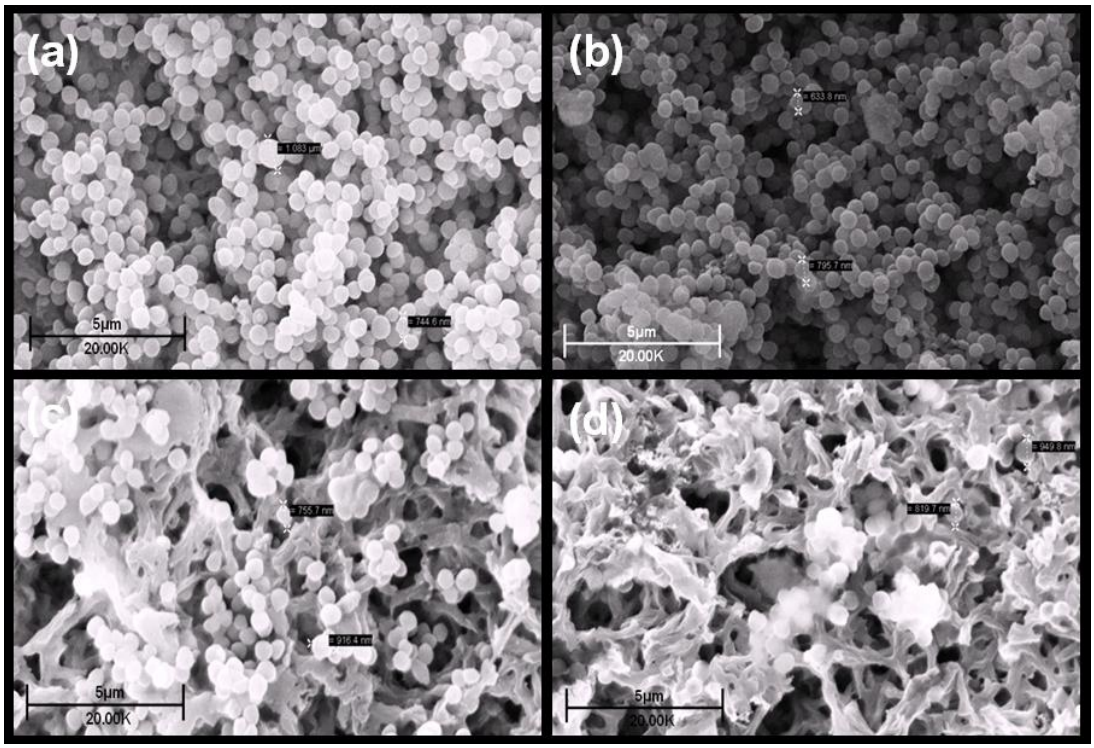

Figure 6.64 Scanning electron micrograph of 1x10^{7} cfu/ml *S. aureus* exposed to NP108 for 72 hours: (a) control (b) 0.0125 mg/ml (1/20th MIC) (c) 0.25 mg/ml (MIC) and (d) 0.5 mg/ml (2xMIC). Viability after 72 hours; *S. aureus* control 4.2x10^{10} cfu/ml; *S. aureus* incubated with 1/20th MIC NP108 8.0x10^{9} cfu/ml; *S. aureus* incubated with MIC NP108 1.14x10^{5} cfu/ml; *S. aureus* incubated with 2xMIC was < 10 cfu/ml

SEM micrographs at 168 hours exposed partial aggregation in the 1/20th MIC cultures (Figure 6.65) but size and bacterial shape were similar to control. Bacterial density in the MIC culture had fallen dramatically from the 24 and 72 hour levels and only spherical cellular aggregates were visible via SEM. A few spherical entities were also present in the 2xMIC sample surface. Viability and flow cytometry results (Figure 5.14) support this SEM data which identified similarity between control and

sub-inhibitory incubated bacterial cultures, with very low density in the inhibitory and supra-inhibitory concentrations.

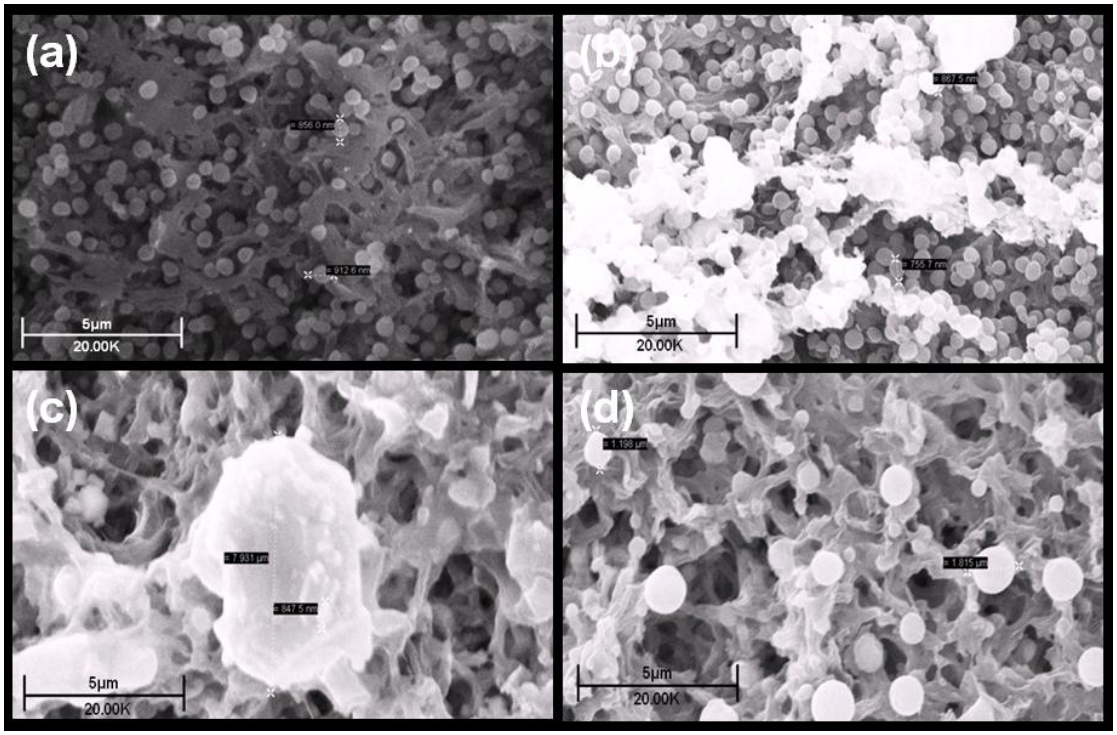

Figure 6.65 Scanning electron micrograph of $1x10^7$ cfu/ml *S. aureus* exposed to NP108 for 168 hours: (a) control (b) 0.0125 mg/ml ($1/20^{th}$ MIC) (c) 0.25 mg/ml (MIC) and (d) 0.5 mg/ml (2xMIC). Viability after 168 hours; *S. aureus* control $1.0x10^{11}$ cfu/ml; *S. aureus* incubated with $1/20^{th}$ MIC NP108 $7.8x10^{10}$ cfu/ml; *S. aureus* incubated with MIC NP108 $1.0x10^3$ cfu/ml; *S. aureus* incubated with 2xMIC was < 10 cfu/ml

c) *Pseudomonas aeruginosa*

NP108 caused partial aggregation of *P. aeruginosa* when incubated at the sub-inhibitory and inhibitory concentrations for one hour (Figure 6.66). Exposure to 2xMIC concentration for the same time period resulted in spherical structures, probably forming from cellular debris

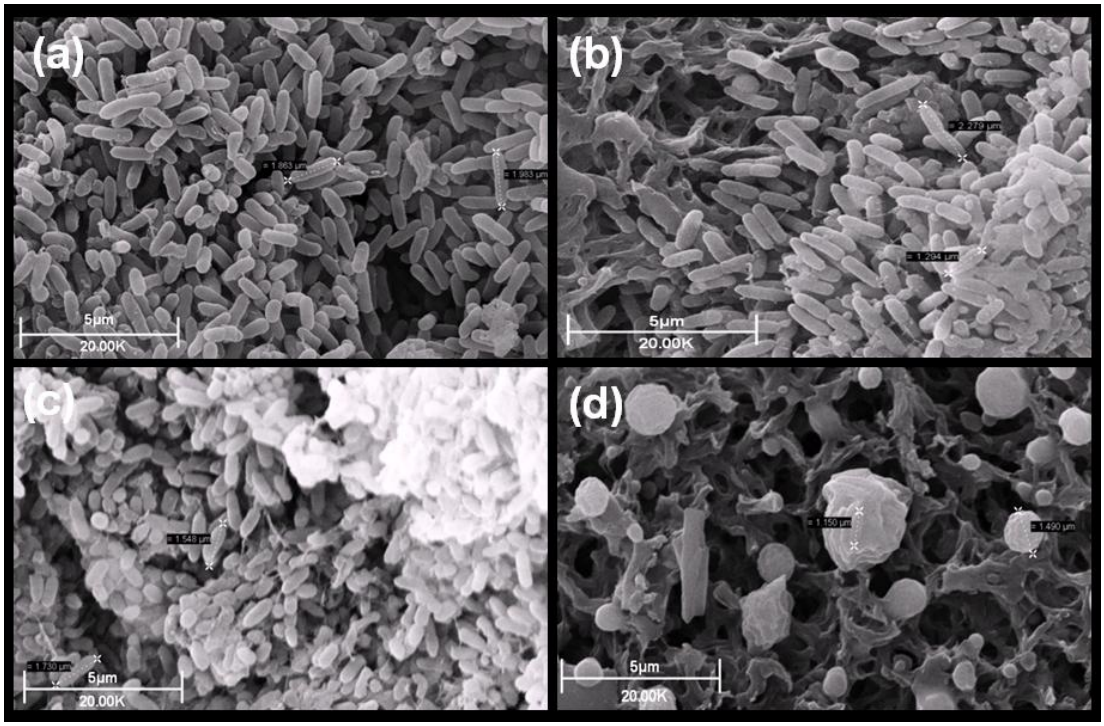

Figure 6.66 Scanning electron micrograph of 1x10^{7} cfu/ml *P. aerugionsa* exposed to NP108 for 1 hour: (a) control (b) 0.025 mg/ml (1/20th MIC) (c) 0.5 mg/ml (MIC) and (d) 1.0 mg/ml (2xMIC).

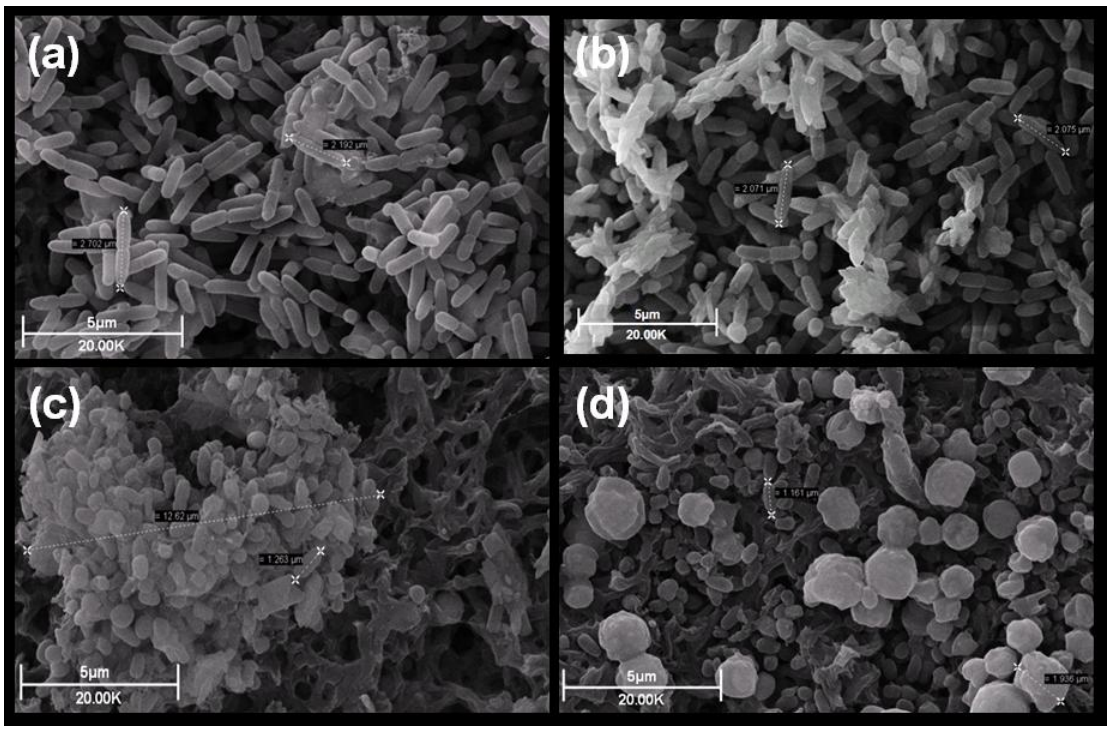

Figure 6.67 Scanning electron micrograph of 1x10^{7} cfu/ml *P. aerugionsa* exposed to NP108 for 3 hours: (a) control (b) 0.025 mg/ml (1/20th MIC) (c) 0.5 mg/ml (MIC) and (d) 1.0 mg/ml (2xMIC).

Bacterial aggregation had increased in the 1/20TH MIC and MIC cultures with the longer incubation of three hours (Figure 6.67). The shape and size of *P. aeruginosa* exposed to the sub-inhibitory concentration were similar to control, with bacteria in the inhibitory culture substantially shorter and rounder than control cells. Spherical structures of varying diameter continued to be present in the 2xMIC sample.

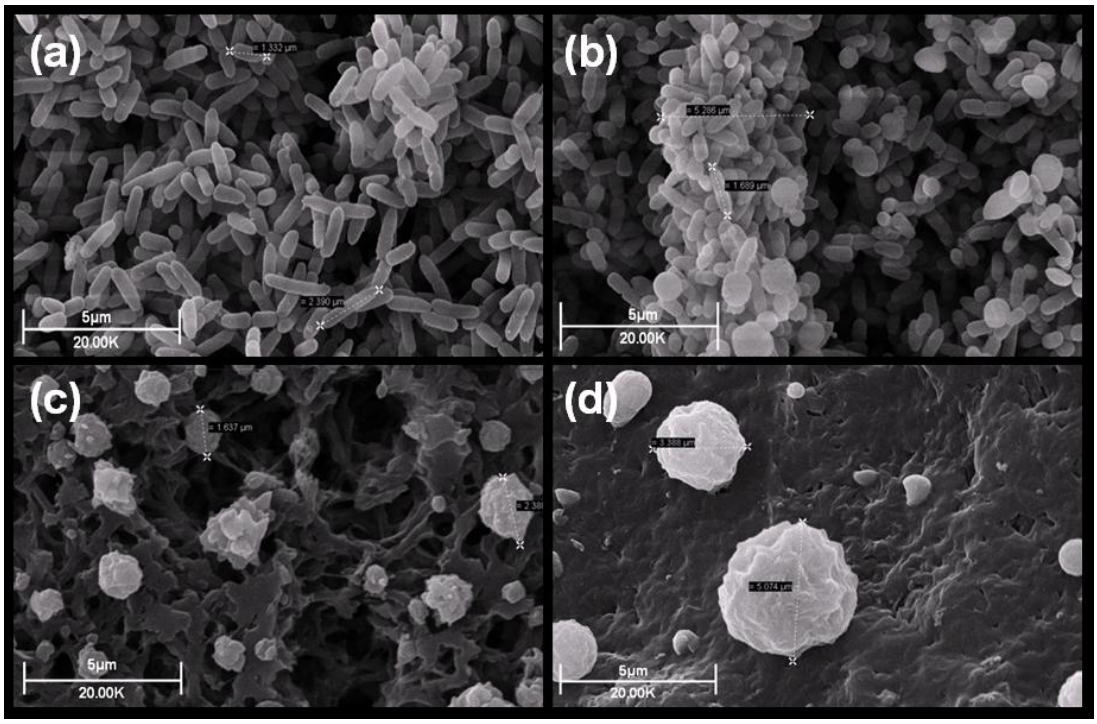

Figure 6.68 Scanning electron micrograph of 1x10^{7} cfu/ml *P. aerugionsa* exposed to NP108 for 6 hours: (a) control (b) 0.025 mg/ml (1/20th MIC) (c) 0.5 mg/ml (MIC) and (d) 1.0 mg/ml (2xMIC). Viability after 6 hours; *P. aeruginosa* control 5.6x10^{10} cfu/ml; *P. aeruginosa* incubated with 1/20th MIC NP108 5.0x10^{10} cfu/ml; *P. aeruginosa* incubated with MIC NP108 4.0x10^{2} cfu/ml; *P. aeruginosa* incubated with 2xMIC was < 10 cfu/ml

At six hours, bacteria treated with 1/20th MIC concentration, revealed a more rounded exterior, some spherical cellular entities and elongated groups of aggregated bacteria. The MIC and 2xMIC cultures displayed smaller spherical entities rather than one large structure, with the cell density of the 2xMIC culture radically reduced.

Surprisingly incubation of *P. aeruginosa* with NP108 for twenty-four hours (Figure 6.69), revealed a reversion to normal bacterial shape for the MIC and 2xMIC cultures. The 1/20th MIC incubated bacteria continued to exhibit a more rounded

bacterial shape. As with the 6-hour culture a long fibrous entity of possibly cellular material, with attached cells, was displayed by the sub-inhibitory culture.

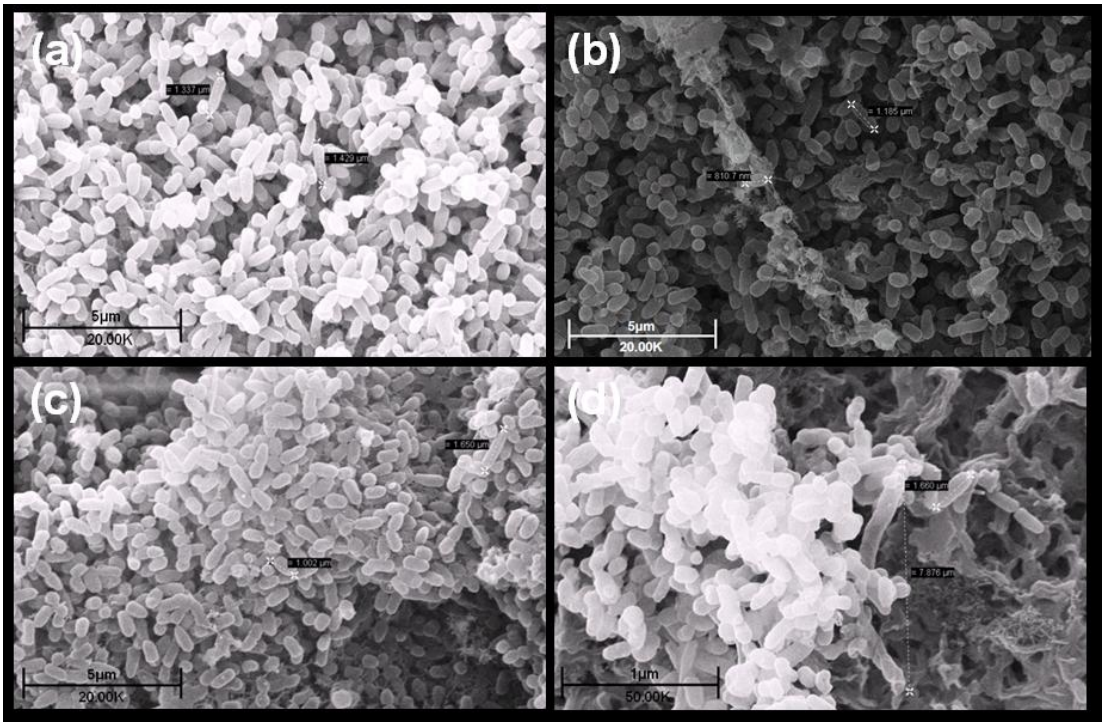

Figure 6.69 Scanning electron micrograph of $1x10^7$ cfu/ml *P. aerugionsa* exposed to NP108 for 24 hours: (a) control (b) 0.0125 mg/ml ($1/20^{th}$ MIC) (c) 0.25 mg/ml (MIC) and (d) 0.5 mg/ml (2xMIC). Viability after 24 hours; *P. aeruginosa* control $5.0x10^{11}$ cfu/ml; *P. aeruginosa* incubated with $1/20^{th}$ MIC NP108 $5.0x10^{11}$ cfu/ml; *P. aeruginosa* incubated with MIC NP108 $6.0x10^2$ cfu/ml; *P. aeruginosa* incubated with 2xMIC was < 10 cfu/ml

The SEM micrographs after 72 hours incubation with NP108 (Figure 6.70), showed the now familiar strand of material with attached bacteria in the sub-inhibitory concentration. Non-septation and spheronisation of cells were two other effects of the $1/20^{th}$ MIC NP108 on *P. aeruginosa.* Both inhibitory and supra-inhibitory incubated bacteria contained spherical cellular aggregated, with a much lower bacterial density in the higher NP108 concentration.

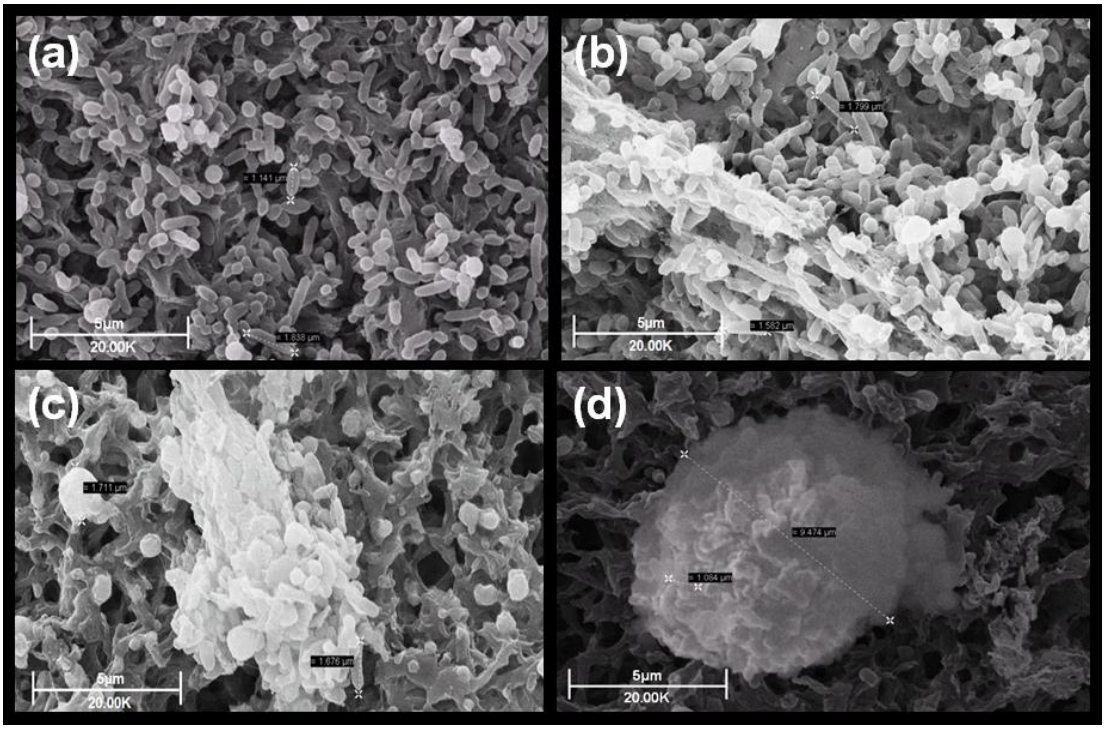

Figure 6.70 Scanning electron micrograph of $1x10^7$ cfu/ml *P. aerugionsa* exposed to NP108 for 72 hours: (a) control (b) 0.0125 mg/ml ($1/20^{th}$ MIC) (c) 0.25 mg/ml (MIC) and (d) 0.5 mg/ml (2xMIC). Viability after 72 hours; *P. aeruginosa* control $5.0x10^{11}$ cfu/ml; *P. aeruginosa* incubated with $1/20^{th}$ MIC NP108 $5.0x10^{11}$cfu/ml; *P. aeruginosa* incubated with MIC NP108 $1.0x10^5$cfu/ml; *P. aeruginosa* incubated with 2xMIC was < 10 cfu/ml

The effects of incubation for 168 hours with NP108 on *P. aeruginosa* were dependent on the concentration employed (Figure 6.71 a)). The $1/20^{th}$ MIC bacteria possessed significantly distorted, dented and blebbed exteriors (SEM Figure 6.71 b)). Only spherical cellular structures were visible in the MIC and 2xMIC cultures.

Flow cytometry data for *P. aeruginosa* incubated with NP108 (Figure 5.15) supports the SEM images showing control and $1/20^{th}$ MIC cultures to be similar in size and shape over the 168 hour period. The MIC and 2xMIC cultures due to low bacterial density, were not detected by flow cytometry; supported by the low bacterial density of these cultures revealed by the SEM micrographs.

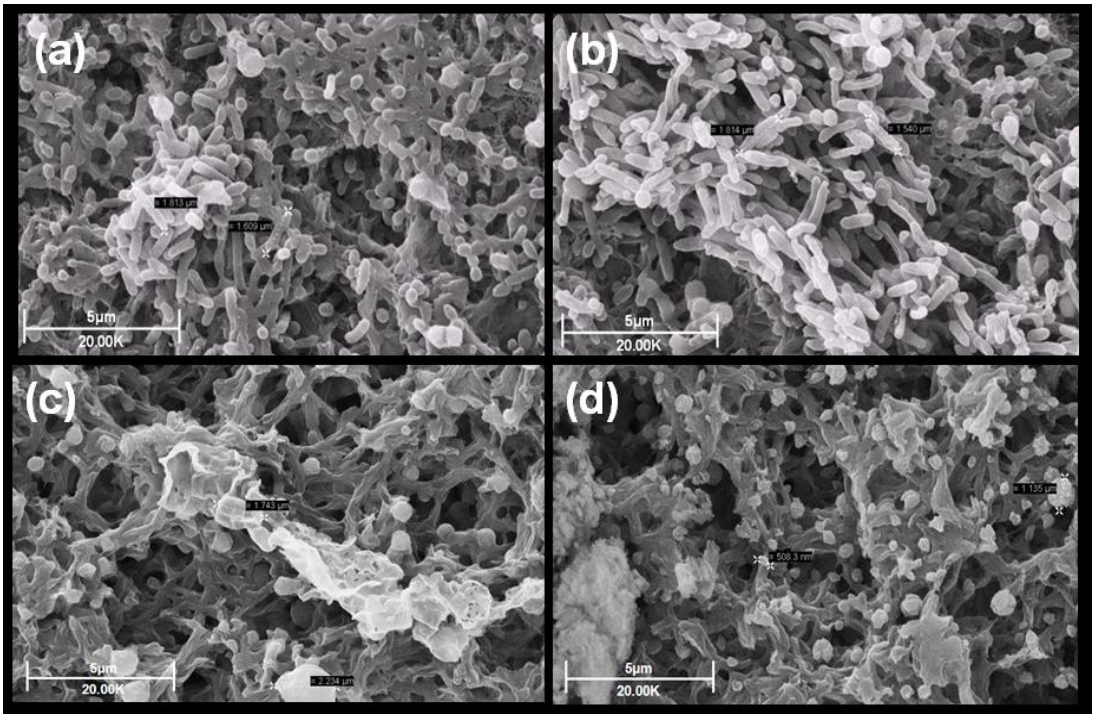

Figure 6.71 a) Scanning electron micrograph of $1x10^7$ cfu/ml *P. aerugionsa* exposed to NP108 for 168 hours: (a) control (b) 0.0125 mg/ml ($1/20^{th}$ MIC) (c) 0.25 mg/ml (MIC) and (d) 0.5 mg/ml (2xMIC). Viability after 168 hours; *P. aeruginosa* control $5.0x10^{11}$ cfu/ml; *P. aeruginosa* incubated with $1/20^{th}$ MIC NP108 $2.9x10^{10}$cfu/ml; *P. aeruginosa* incubated with MIC NP108 $1.14x10^5$cfu/ml; *P. aeruginosa* incubated with 2xMIC was < 10 cfu/ml

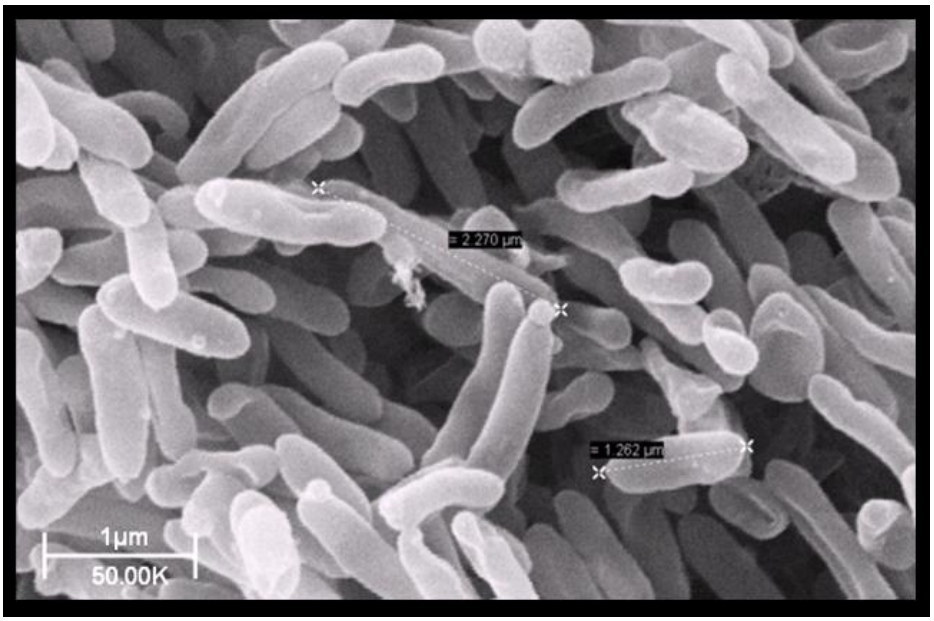

Figure 6.71 b) High magnification scanning electron micrograph of $1x10^6$ cfu/ml *P. aeruginosa* exposed to MIC NP108 for 168 hours

6.4 Discussion

6.4.1 Introduction

Bacteria respond to environmental stresses through alteration of their genetics, physiology, biochemistry that probably lead to changes in cellular morphology to permit continued cell growth and division (Dynes et al. 2009). This was apparent from the responses of the test bacteria upon their exposure to cationic antibacterial agents used in this investigation. Some of the most surprising results collected, were those bacterial reactions to incubation with sub-inhibitory antibacterial concentrations. The inhibition of normal septation in *S. aureus* and *S. bovis* exposed to sub-inhibitory concentrations of penicillin had been reported by Lorain *et al* (Lorian 1975). In this investigation results of incubation with sub-inhibitory concentrations of cationic antibacterials have included; non-septation, bacterial aggregation; the probable release of cellular filaments to form extracellular fibres, filaments or films linking cells; blebbing; deformation; and formation of large spherical structures, probably aggregates of viable or non-viable cells or debris derived from such cells. This is to some extent surprising in view of the growth inhibition data shown in Chapter 3, when the $1/20^{th}$ MIC revealed no adverse effect on the rate or extent of growth.

The reactions of *P. aeruginosa* to the presence of triclosan, to which the bacterium is continuously referred to being resistant, were un-expected as they matched the responses observed in *E. coli,* which is not triclosan resistant. The normal rod-shaped *P. aeruginosa* cells have been shown to adopt a smaller coccoid shape during under nutritionally challenging conditions (Dynes et al. 2009). In the SEM images presented here the response of *P. aeruginosa* from four hours incubation with the inhibitory triclosan concentration has also been to adopt a coccoid shape.

Responses of bacteria such as *E. coli* and other un-related bacterial species to transition into stationary-phase conditions by size reduction and the subsequent exhibition of spherical or ovoid exteriors, through induction of expression of the alternative sigma factor σ^S that controls the morphological phenotype, is well reported (Lange and Hengge-Aronis 1991). The SEM images of *E. coli* incubated with various colistin concentrations from one to 168 hours presented here, has also shown reduction in bacterial size and exhibition of spheroid exteriors as a result of exposure to this antibacterial.

The reaction of *S. aureus* within 30 minutes exposure to the presence of colistin, by the adoption of an aggregated spherical structure was also un-expected (Figure 6.24). Little information exists on the effect of colistin on Gram-positive bacteria such as *S. aureus*, as a consequence of this antibacterial agent not being used clinically to treat Gram-positive infections, so these results were intriguing.

As NP101 and NP108 are novel antibacterials, bacterial reaction to incubation with these agents through morphological alteration was un-known. However SEM micrographs revealed alterations in outer bacterial morphology, similar to those reported for other CAPs such as inhibition of normal bacterial septation and membrane blebbing (Hale and Hancock 2007)(Zhang and Falla 2006).

6.4.2 Changes in morphology of *E. coli*, *S. aureus* and *P. aeuginosa* induced by triclosan

6.4.2.1 Sub-inhibitory concentration

Incubation with 1/20th MIC triclosan produced different effects upon the Gram-positive and Gram-negative bacteria. Effects visualised in *E. coli* and *P. aeruginosa* was a rounding of the normal rod-shaped exterior and inhibition of normal bacterial septation. Aggregation combined with non-septation was present in *E.coli* incubated

with the sub-inhibitory triclosan concentration from 24 hours onwards. A longer exposure time of eight hours, to the presence of 1/20th MIC triclosan, was required before non-septated *P. aeruginosa* became apparent. Limiting factors such as the solubility of triclosan and high level triclosan resistance possessed by *P. aeruginosa* as a result of its MDR efflux pumps which actively extrudes triclosan from the bacterium, meant an MIC could only be determined for a maximum of 32 hours (Chuanchuen, Karkhoff-Schweizer and Schweizer 2003). However, by 24 hours incubation and again at 32 hours incubation with the sub-inhibitory triclosan concentration, *P. aeruginosa* had begun to form bacterial sheets interlinked with what appeared to be fine extracellular strands or fibres as well as distinct long co-joined bacterial cells.

The response of the Gram-positive *S. aureus* to incubation with sub-inhibitory triclosan concentration from one to 168-hours was shown to be bacterial aggregation. The most striking example of this phenomenon was displayed by *S. aureus* after 24 hours incubation (Figure 6.11), when co-joined *S. aureus* chains were visualised at this concentration

6.4.2.2 Inhibitory concentration

In *E. coli*, elongation or non-septation was apparent in MIC incubated bacteria from one hour onwards. By six hours, this phenomenon of non-septation had developed a further dimension as the non-septated bacteria now exhibited a budding or blebbing effect, that suggested growth in *E. coli* was now occurring not only longitudinally but also in other dimensions to the bacterial chain, indicative of an adverse impact upon peptidoglycan synthesis (Figure 6.4). Non-septated *P. aeruginosa* were visible in the MIC concentration after four hours incubation, with the 24/32 hour samples also populated with spherical aggregates bearing a corrugated appearance. *S. aureus* response to incubation with the inhibitory

triclosan concentration was shown to be bacterial aggregation. Elaborate, large apparently hollow spherical structures were produced by *S. aureus* after 24 hours incubation with triclosan (Figure 6.11).

6.4.2.3 Supra-inhibitory concentration

The supra-inhibitory triclosan concentration produced a gelling of *E. coli* cells after incubation times of 24 to 168 hours; a phenomenon observed in bacteria exposed to biocides that have been reported by other researchers (Barrett-Bee, Newboult and Edwards 1994). Exposure of *S. aureus* to 10xMIC triclosan concentration also resulted in production of spherical cellular or acellular structures of varying dimensions.

6.4.2.4 Summary of bacterial responses to triclosan

A similar response by all three test bacteria to treatment with triclosan was the inability to undergo normal bacterial septation. Non-septation in coccoid and rod-shaped bacteria resulting from exposure to an antibacterial agent has been reported by other researchers (Lorian 1975). Well established antibacterial effects of triclosan effects are the inhibition of both membrane biogenesis and fatty acid synthesis (Escalada et al. 2005)(Rock and Jackowski 2002)(Levy et al. 1999). The SEM images presented tend to support the results of both these reported inhibitory effects in all three test species.

A reduction in size of *E. coli* incubated with the inhibitory triclosan concentration and a change in shape of *P. aeruginosa* from rod to spheroid shape after incubation with the inhibitory triclosan concentration for 32 hours was also noted. It has already been mentioned that induction of alternative sigma factor σ^S responsible for controlling bacterial phenotypes is induced by depletion of available nutrients and results in smaller bacterial size and shape changes (Lange and Hengge-Aronis 1991). It is possible that this factor is also triggered by the stress of incubation with

an antibacterial agent such as triclosan as both smaller bacterial size and changes in bacterial structure were visualised in the SEM images presented here (Lange and Hengge-Aronis 1991). A common response by *S. aureus* observed with all triclosan concentrations at most time points was demonstrated to be bacterial aggregation. Whether this aggregatory effect on *S. aureus* was as a result of the inability of *S. aureus* bacteria to septate normally and therefore forced to remain co-joined and form larger and larger structures of aggregated cells remains to be elucidated. However it is probable that aggregation was the reason, as the appearance of large aggregates occurred within one hour of incubation with triclosan.

6.4.3 Changes in morphology of *E. coli*, *S. aureus* and *P. aeuginosa* induced by colistin

6.4.3.1 Sub-inhibitory concentration

Spherical cellular aggregates of *E. coli* were present in the sub-inhibitory culture after incubation from one to 72 hours with colistin. SEM images at 72 hours revealed the de-aggregation of these spherical structures into smaller groups. Rounding of *E. coli* cell shape as well as smaller bacterial size was noted at 72 and 168-hours incubation.

The response of *S. aureus* to the presence of sub-inhibitory colistin was the rapid formation of spherical structures, regressing at three hours into normal sized *S. aureus* groups displaying blebbed membranes. Subsequent SEM images at 24, 72 and 168 hours revealed bacterial exteriors similar to un-treated bacteria.

Reactions by *P. aeruginosa* to this colistin concentration produced interlinked bacterial sheets until eight hours with the bacteria reverting to normal control-like bacterial appearance at that time. Inhibition of bacterial septation was also observed in *P. aeruginosa* at 72 and 168 hours.

6.4.3.2 Inhibitory concentration

Incubation with the inhibitory (and supra-inhibitory) colistin concentrations resulted in a similar reaction to both concentrations by *E. coli* in the formation of spherical structures throughout the experimental period. A very low bacterial density was also noticed in all SEM samples for both these concentrations. Whilst incubated with MIC and 10xMIC colistin *E. coli* was not observed to undergo binary fission, though bacterial division was noted in un-treated and sub-inhibitory incubated *E. coli*.

Incubation of *S. aureus* with MIC colistin produced spherical structures until 24 hours whereupon reversion to control-type bacterial groupings occurred. Recognisable *S. aureus* groups persisted until 168 hours at which point *S. aureus* cells were visualized as one cohesive mass.

P. aeruginosa produced interlinked bacterial sheets in reaction to the stress of the inhibitory colistin concentration up to eight hours, then appearing to exist as single, smaller bacteria with blebbed and indented exteriors observed at eight hours. Spherical structures were observed in the 24 hour SEM image, with cellular aggregation at 72 hours. By 168 hours incubation *P. aeruginosa* had formed a mat of interconnected bacteria, interwoven with what appeared to be filaments or fibres almost certainly of bacterial origin.

6.4.3.3 Supra-inhibitory concentration

Supra-inhibitory colistin concentrations resulted in the formation of spherical structures by *S. aureus* over the experimental period. The density of bacteria in all the SEM images was very low but as binary fission was not observed in the supra-inhibitory incubated *S. aureus*, inhibition of cell replication would in part be responsible for this.

Individual *P. aeruginosa* cells had adopted a spherical shape in response to the presence of 10xMIC colistin at two, four and eight hours, producing an aggregated

spherical structure at 24-hours. Very few *P. aeruginosa* cells were identified in the 72 and 168 hour cultures, with these revealing deformed exteriors. Bacterial replication was not observed in the inhibitory or supra-inhibitory colistin concentrations during the experiment. However, as the density of the MIC culture had increased dramatically between 24 and 168 hours, binary fission must have occurred. Failure to replicate could account for the low bacterial density observed in the supra-inhibitory cultures throughout these experiments.

6.4.3.4 Summary of bacterial responses to colistin

The production of spherical aggregates, rounding of bacterial cells, blebbing of bacterial membranes and non-septation were the effects of sub-inhibitory colistin concentration on the test bacteria. Colistin is attributed as being a membrane active agent, yet the examination of two Gram-negative and one Gram-positive bacterium at concentrations ranging from $1/20^{th}$ MIC to 10xMIC has not disclosed burst or ruptures bacterial cells. Blebbing of bacterial membranes, distortion of cell shapes and indentation of bacterial surfaces are all effects visualised by SEM. It has been postulated (Clausell et al. 2003) that colistin acts in a different way on the bacterial membrane at the MIC concentration, probably through effects on the lipid bilayer surrounding the periplasmic space.

Incubation with the inhibitory and supra-inhibitory colistin concentrations resulted in spherical aggregation, blebbing of bacterial membranes, reduced bacterial size and low bacterial density. This is in agreement with a report by Mortensen *et al* that the bacterial surface of *P. aeruginosa* had changed to a wrinkled phenotype after 3 hours incubation and cell length had decreased after exposure to 10 μg/ml colistin (Mortensen et al. 2009). A concentration of 10 μg/ml colistin is equivalent to 7xMIC used in the current investigation of *P. aeruginosa*. Clauselle *et al* revealed colistin has more than one mechanism of action; at high concentrations several times the

MIC value the mechanism of action has been reported to be through membrane permeability, although no significant K^+ loss was observed when *P. aeruginosa* was treated with 10xMIC in this study (Clausell et al. 2003).

Binary fission was not observed in *E. coli* either at inhibitory or sub-inhibitory concentrations, or in *S. aureus* or *P. aeruginosa* at the supra-inhibitory concentrations. This agrees with Mortensen *et al* who reported colistin reduced the rate of bacterial cell division five–fold in *P. aeruginosa* incubated for one hour with 10 μg/ml colistin compared to *P. aeruginosa* untreated cultures. The bactericidal effect of colistin is likely due in part to prevention of normal bacterial replication above certain concentrations. Mortensen *et al* suggested colistin incubated *P. aeruginosa* were arrested in proliferation after septum formation, preventing elongation in mother and daughter cells (Mortensen et al. 2009).

6.4.4 Changes in morphology of *E. coli*, *S. aureus* and *P. aeuginosa* induced by CAPs

6.4.4.1 Sub-inhibitory concentration

Bacterial responses to incubation with NP101 and NP108 were very similar and these novel CAPs will therefore be considered together. Incubation with the sub-inhibitory CAP concentrations produced the following myriad effects in *E. coli* and *P. aeruginosa* cells: shortening and rounding of cells; extrusion of intracellular contents; and non-septation. Filaments or fibres of possible cellular origin were observed to interlink *P. aeruginosa* cells after 24 hours incubation with $1/20^{th}$ MIC NP101 and after 72 hours incubation with $1/20^{th}$ MIC NP108. Whether these materials were extruded intracellular matter or specifically produced by the bacterium in response to the antibacterial stress of incubation with NP101 or NP108 remains to be determined.

6.4.4.2 Inhibitory and supra-inhibitory concentrations

Similar responses to those exhibited by the test bacteria incubated with sub-inhibitory CAP concentration were also seen at the MIC and 2xMIC concentrations, but to a more severe degree. Specifically the effects were indentation, corrugated and misshapen bacterial exteriors, interruption in bacterial septation, blebbing of bacterial membranes, extrusion of intracellular material and formation of spherical structures. The production of aggregated bacterial layers was noted in *P. aeruginosa* in response to incubation with NP101. Gelling of *E. coli* cells by inhibitory and supra-inhibitory NP108 concentrations and *S. aureus* by supra-inhibitory NP108 concentration were also observed. As with the supra-inhibitory colistin concentration, binary fission was not observed in the test bacteria in either 2xMIC NP101 or NP108 concentrations, (except for *P. aeruginosa* incubated with 2xMIC NP101 up to six hours, but absent thereafter). Significantly different to colistin, *E. coli* incubated with MIC NP108 underwent binary fission at 6 hours but not subsequently, while dividing *P. aeruginosa* cells were seen after 24 hours incubation with MIC NP108 but no cell division in this culture was observed afterwards. The low bacterial density of these cultures was most likely due to prevention of cell replication by NP101 and NP108.

6.4.4.3 Summary of bacterial responses to CAPs

Responses of test bacteria to incubation with either NP101 or NP108 were similar to those observed for colistin; changes to bacterial shape and size, extrusion of intracellular material, blebbing of bacterial membranes, inhibition of septation and prevention of binary fission. CAPs are primarily reported in literature as membrane active agents; regardless of whether they act on intracellular targets, CAPs still have to interact with the bacterial membrane to reach their intracellular target (Reddy, Yedery and Aranha 2004)(Brogden 2005). Many of the visualised reactions

of the test bacteria to NP101 and NP108 are typical of bacterial responses to the presence of a cationic antimicrobial peptide (Hancock and Chapple 1999)(Hale and Hancock 2007)(Zhang and Falla 2006)(Hancock and Sahl 2006).

Chapter Seven

The production of lyophilised wafers as a formulation vehicle for the topical delivery of CAPs

7.1 Introduction

Human skin is a complex organ possessing many in-built protective mechanisms. (Supp and Neely 2008)(Martin and Dodds 2006) These protective mechanisms include desquamation of the outer skin layers with subsequent microbial shedding and secretion of antimicrobial peptides in response to organisms that have penetrated the epithelium (Zaiou 2007)(Martin and Dodds 2006). Skin components such as lipids also possess substantial antimicrobial activity (Martin and Dodds 2006). Skin therefore is not a passive barrier but is constantly vigilant against microbial attack with continuous monitoring systems and excellent rapid responses to ensure an infection free status (Schauber and Gallo 2008)(Martin and Dodds 2006).

Human skin is colonised by commensal organisms, including amongst others *S. aureus* and *S. epidermidis* that do not cause infection unless the physical barrier of the skin is breached, whereupon these organisms can cause opportunistic infections (Martin and Dodds 2006).

7.1.2 Wounded and burned skin

Normal human interaction with the environment occasionally results in damage to the skin and underlying dermis; in the US alone more than a million skin burns occur annually (Supp and Neely 2008). One main factor is responsible for deaths resulting from burns, being infection developing in the wound environment (Bhat and Milner 2007). A severe burn destroys the skin's protective barrier and the burn's protein rich environment is ideal for bacterial colonization (Bhat and Milner

2007)(Supp and Neely 2008). Immediately after the burn has occurred the wound surface is sterile but quickly becomes colonized by commensal bacteria from sweat glands and hair follicles from intact skin (Bhat and Milner 2007).

Apart from burns, chronic wounds are extended in duration for many reasons; the patient may be immuno-compromised, malnourished or suffer from other long-term medical conditions such as diabetes mellitus that reduce normal healing processes (Supp and Neely 2008). The microorganisms that colonise chronic wounds are also found in burn environments, with a recent US study identifying *S. aureus* as the most commonly isolated wound organism, closely followed by *P. aeruginosa* (Supp and Neely 2008). The current cost of treating chronic wounds in the US, where over 2 million people are treated for chronic wounds annually, is $1 billion per year (Supp and Neely 2008). The current gold standard in burn and chronic wound treatment is by skin graft, however if these wounds are large, locating donor sites can be difficult and further complicated by being painful or un-successful due to poor patient healing (Supp and Neely 2008).

7.1.3 Application of CAPs as topical therapeutic agents

The ever-increasing rise in bacterial resistance to current antimicrobial agents is cause for concern (Shukla et al. 2010). MRSA has now become widespread in community as well as hospital settings despite efforts to limit the spread of the superbug from hospital environments (Shukla et al. 2010). Also adding to the problems of bacterial resistance within individual countries; injured soldiers returning from conflict situations in other countries are regularly diagnosed with multidrug resistant infections (Shukla et al. 2010). New therapeutic agents as well as innovative methods in treating bacterial infections are urgently required and an

area being investigated for new therapeutic options is antimicrobial peptides (Hale and Hancock 2007).

CAPs have been shown to be effective against Gram-positive and negative bacteria, viruses, fungi as well as multi-drug resistant bacteria (Shukla et al. 2010). A recent investigation examined the role of multidrug resistance efflux pumps in mediating resistance to innate antimicrobial peptides in *E. coli*, *S. aureus* and *P. aeruginosa* (Rieg et al. 2009). Neither the RND efflux pumps of *E. coli*, the MexAB-OprM pumps of *P. aeruginosa,* nor the MF family member NorA in *S. aureus* conferred resistance to the endogenous peptides tested (Rieg et al. 2009). This demonstrated that differences in secondary peptide structure, net charge, amphipathicity or mechanism of action are not determinants of efflux-mediated CAP resistance in these bacterial multidrug resistance pumps.

Another positive factor possessed by CAPs relate to recent reports that have shown the ability of antimicrobials peptides such as lactoferrin to effectively block biofilm formation (Shukla et al. 2010). Dead tissue supports the development of sessile bacterial communities, leading to further tissue damage and resulting in the shedding of planktonic bacteria and the spread of infection (Shukla et al. 2010). The most effective method in treating these biofilms is to successfully prevent initial bacterial attachment to either the dead tissue or to medical device surfaces (Shukla et al. 2010). Current methods in the development of CAPs as therapeutic agents are their inclusion in polyelectrolyte multilayer films permitting time controlled drug release from various substrates with several potential applications (Shukla et al. 2010).

7.1.4 Lyophilised wafers as topical drug delivery systems

Traditionally, treatment of small burns and chronic wounds has been delivered through the use of systemic or topical agents or via occlusive dressings, which may or may not contain antimicrobial compounds (Supp and Neely 2008). Lyophilised wafers offer a new topical delivery system in wound treatment, allowing the sustained release of an incorporated antibacterial agent thus assuring a steady-state concentration of the selected agent in the wound environment (Matthews et al. 2005). The wafer can be applied directly to the wound necessitating minimum human contact, thus the use of lyophilised wafers in wound healing offers several advantages over conventional topical treatments (Matthews et al. 2008). Lyophilised wafers absorb water when applied to the wound surface, changing state from glassy, porous solids to viscous gels (Matthews et al. 2005). Release of the antimicrobial agent from lyophilised wafers occurs through diffusion when the glassy polymer absorbs water, thereby producing a gel and releasing the active agent (Boateng et al. 2009)(Boateng et al. 2010). The diffusion rate of the water-soluble antimicrobial agent into the wound environment has been shown to be time dependent (Boateng et al. 2009). The lyophilised wafers in this investigation were produced by freeze-drying the polymeric carrier, guar gum (Table 7.1) with NP101 and NP108.

7.1.5 Freeze-drying process

The three stages in the lyophilisation process are freezing, primary drying followed by secondary drying. During freezing, the gel mixture undergoing lyophilisation is cooled and the water forms ice, freeze concentrating the polymer vehicle and peptide in a separate phase. Some non-freezing water remains in this freeze-concentrated phase. The pressure is reduced and the primary drying cycle

commences. The shelf temperature is slowly increased in a series of thermal ramps over a period of 14 hours from -80 to +20°C. There is thermal lag attributable to the polystyrene tray used as a mould for wafers. At some point in this thermal cycle, all of the ice has been removed and only residual amounts of non-freezing water remain in the glassy polymer structure. Continued low pressure (vacuum) causes desorption of this water to the gas phase. This is the secondary drying cycle.

7.1.6 Chemical nature of NP101 and NP108

NP101 is a 25.2 KDalton peptide while NP108 is half the molecular weight of NP101 at 10.5 KDalton. The components of NP101 are unknown; however, NP108 is a poly-L-lysine cationic antimicrobial peptide.

7.1.7 Selection of polymeric carrier

As NP101 and NP108 are cationic antimicrobial peptides, potential interaction between gel and CAPs required the exclusion of a number of gels as appropriate bases, as illustrated in Table 7.1.

Polymer type	Overall chemical charge	Source	Molecular weight (Daltons)
Guar gum	Non-ionic	Guar gum bean *Cyamopsis tetragonolobus*	220,000 – 250,000
Xanthan gum	Anionic	Polysaccharide from *Xanthomonas campestris*	250,000+ depending on grade used
Karaya gum	Anionic	Acetylated polysaccharide (composed of galactose, rhamnose, glucuronic and galacturonic acids)	5,000,000 – 8,000,000
Chitosan	Cationic	Derived from the exoskeleton of shellfish	3,800 – 20,000

Table 7.1 Chemical nature and source of polymers

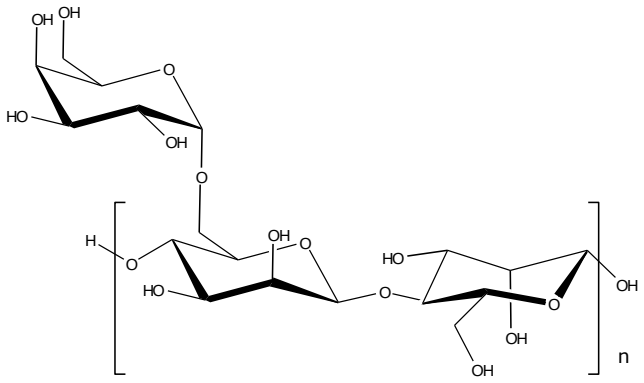

Figure 7.1 Chemical structure of guar gum

The non-ionic guar gum (Figure 7.1) was selected as the most suitable polymer type to use as the carrier for the freeze dried wafers, as the weakest and lowest level of bonding between CAP and carrier was expected from this combination. It was appreciated that as a natural gum, guar could be contaminated with native/natural bacterial flora, necessitating the sterilisation of the lyophilised wafers by gamma radiation prior to use as a wound therapy (Matthews et al. 2006). In this investigation the lyophilised wafers were not gamma-irradiated, however, only the presence of test bacteria was detected on examination.

7.1.7 Objective of current investigation

The antimicrobial potencies of NP101 and NP108 were established in Chapter 3. However the development of a safe, effective formulation vehicle for topical delivery to the wound environment, to avoid systemic problems such as stability and antigenicity of CAPs, would be very beneficial. The purpose of this area of investigation was to formulate cohesive, non-friable lyophilised antimicrobial wafers as CAP topical delivery vehicles to aid wound healing.

7.2 Methodologies

7.2.1 Preparation of guar gum gel

Control and antimicrobial batches of gel were prepared as described in Section 2.10.1.

7.2.2 Freeze drying process

After formulation of gels, the freeze-drying process to prepare lyophilised wafers was undertaken as described in Section 2.10.2.

7.2.3 Rheological analysis of gels

Analysis of control and antimicrobial gels were performed as described in Section 2.10.3

7.2.4 Preparation of agarose plates

Agarose plates were prepared according to Section 2.3.6.1 and 2.3.6.2, to determine activity through a disc diffusion assay and measurement of resulting zones of growth inhibition of NP101 and NP108 against the test bacterial species.

7.2.5 Determination of zones of inhibition

Analysis of zones of inhibition of NP101 and NP108 were determined as described in Section 2.3.6.3.

7.3 Results

7.3.1 Rheological analysis of pre-lyophilised gels

The rheological properties of the polymeric carrier with and without CAPs were examined prior to lyophilisation for comparison with the behaviour in physical state post hydration from lyophilised wafers into gel form.

Polymer	η' (Pa.s)	σ_o (Pa)	Rate Index	Standard error
2% Guar gum control	51.56 ±5.89	77.67 ±3.19	0.10	5.58
2% Guar gum + NP101	52.86 ±3.80	87.37 ± 6.73	0.11	6.02
2% Guar gum + NP108	72.61 ±9.14	89.69 ± 4.09	0.09	6.73

Table 7.2 Viscosity coefficient (consistency) η' (Pa.s), yield stress σ_o (Pa), rate index for control, NP101 and NP108 polymers in aqueous solution as analysed by the Herschel-Bulkley model

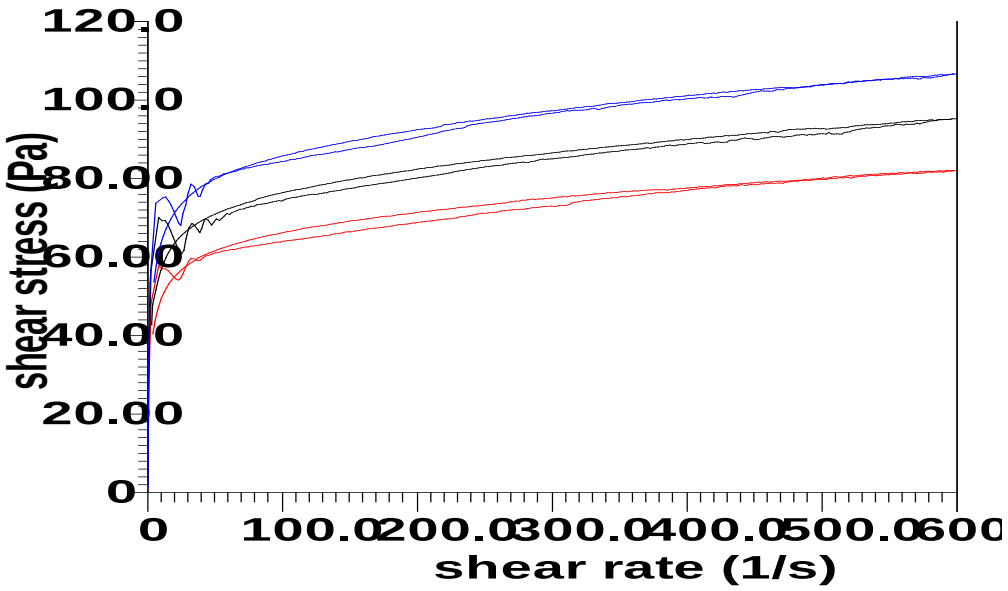

Figure 7.2 Rheological analysis of pre-lyophilised gels; ascending and descending flow curves of 2% guar gum control ■ 2% guar gum + NP101 ■ 2% guar gum + NP108 ■

Analysis of the rheological properties of guar gum with and without CAPs was undertaken, under controlled conditions and temperature (Table 7.2). The variation in the initial part of the ascending flow curve was due to the uneven dissolution of the guar gum in water, which was more apparent when either NP101 or NP108 was added to the gel solution. Each of the three gels displayed shear thinning with pseudoplastic (verging on classic plastic flow) type flow curves. None of the three curves intersected the origin, revealing significantly high yield stresses, as displayed in Figure 7.2. The yield stress increased as the CAPs were added to guar gum (Table 7.2), with the 2% control gel exhibiting the lowest yield stress, followed by NP101 and then NP108.

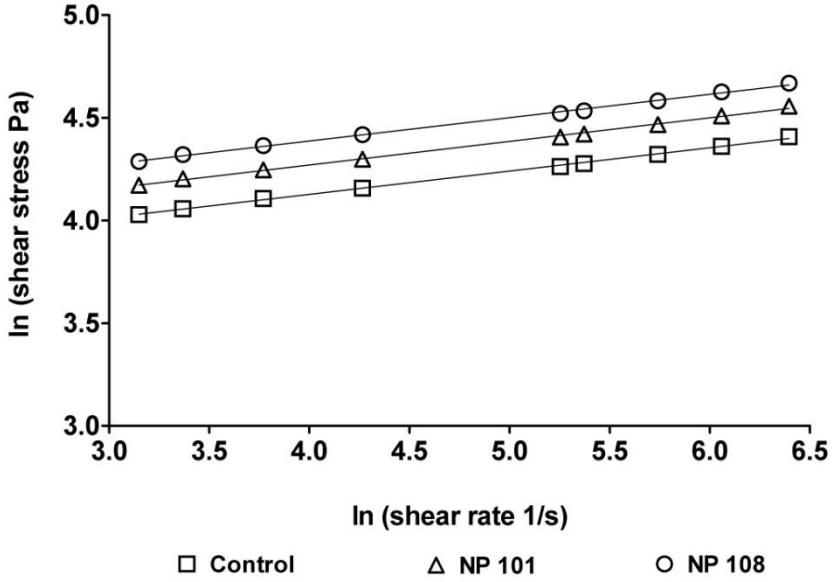

Figure 7.3 Determination of log shear stress against log shear rate

Plots of log shear stress against log shear rate were linear (Figure 7.3) indicating that under the shear rates experienced, the behaviour of all three gels can be represented by the Herschel-Bulkley equation as stated in Section 2.10.3. The viscosity coefficient (η') increased from control to NP101 with the highest value recorded for NP108 (Table 7.2). The rate index was highest for the control gel,

followed by NP101 with NP108 recording the lowest value, as is normal for gels with increasing consistency.

Small differences in the ascending and descending flow curves were attributed to very mild thixotropic properties. Thixotropy is a time dependent change in consistency displayed by certain gels; for example gels that are viscous under normal conditions can become more viscous over time. It can be seen from Figure 7.2 that NP108 is improving the gel properties of guar gum and giving more structure to guar gum than NP101.

7.3.2 Freeze dried lyophilised wafers

The temperature profile of the freeze-drying process of the guar gum and CAP mixture is highlighted in Figure 7.4. The total time taken for the freeze-drying process from start to finish was 24 hours.

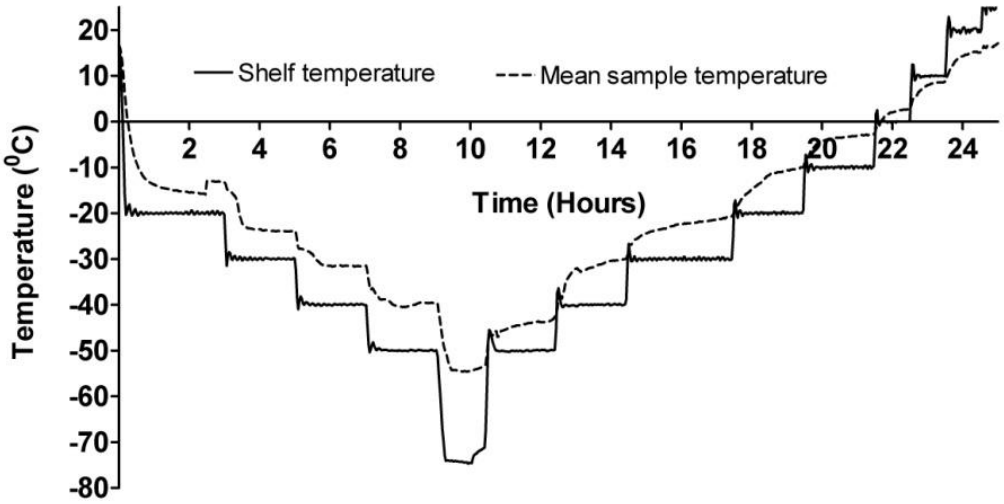

Figure 7.4 Temperature profile of freeze-drying process

7.3.3 Determination of expansion and inhibition ratios of lyophilised 2% guar gum wafers via spread plates

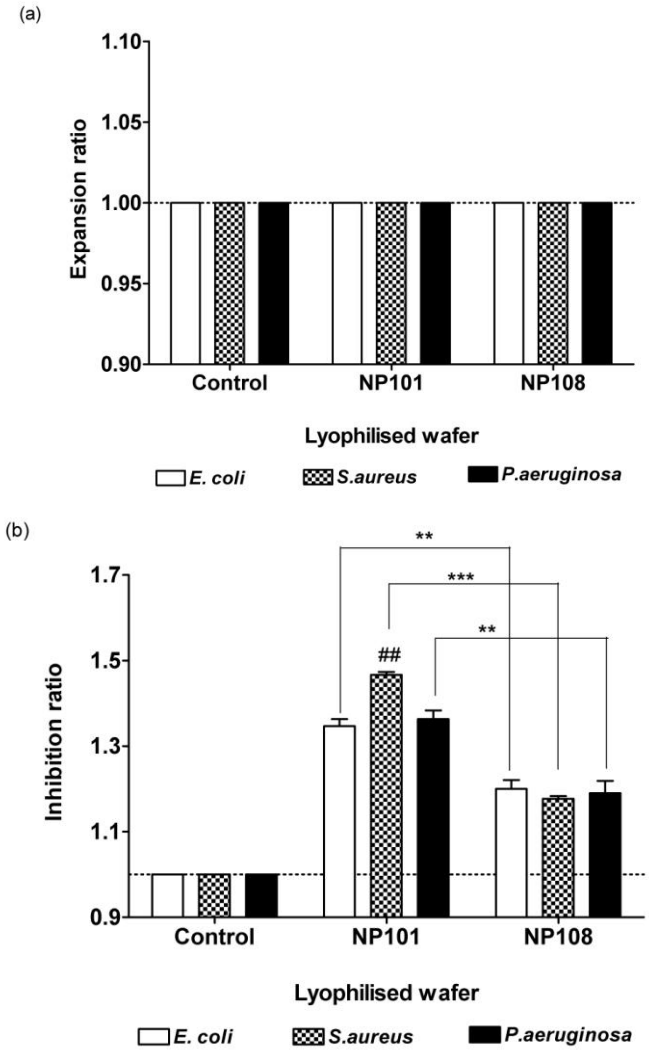

Figure 7.5 Expansion (a) and inhibition (b) ratios of lyophilised wafers. * indicates a statistically significant difference between the zone of inhibition recorded for NP101 and NP108 against a bacterial species: * indicates *p*-value < 0.05, ** indicates *p*-values < 0.01, *** indicates *p*-value < 0.001. # indicates a statistically significant difference between the zones of inhibition recorded for NP101 against the test bacteria: # indicates *p*-value < 0.05, ## indicates *p*-values < 0.01, ### indicates *p*-value < 0.001

(a) Expansion ratios of 2% guar gum lyophilised wafers; control, 2xMIC NP101, 2xMIC NP108, determined on spread plates
(b) Inhibition ratios of 2% guar gum lyophilised wafers; control, 2xMIC NP101, 2xMIC NP108, determined on spread plates

Neither Guar gum control, NP101 nor NP108 wafers experienced expansion (Figure 7.5 (a)) after 24 hours contact with the agarose plate. Therefore the swollen polymer, due to the significantly high polymer yield stress, did not exhibit flow. If

the polymer yield stress were lower, when the wafer absorbed water from the agarose plate, the polymer would flow causing expansion. Diffusion of both NP101 and NP108 from the lyophilised wafers occurred and clear zones of inhibition against all three test bacterial species were observed surrounding the lyophilised wafers after incubation.

The inhibition zone recorded for NP101 against *E. coli*, *S aureus* and *P. aeruginosa* was statistically significantly higher than the zone of inhibition achieved by NP108 against *E. coli*, *S. aureus* and *P. aeruginosa.* A statistically significant difference was also recorded in the zones of inhibition achieved by NP101 against *S. aureus* compared to those recorded against *E. coli* and *P. aeruginosa*. Given that the MIC of NP101 against *E. coli* (0.5 mg/ml) was twice that of NP101 against *S. aureus* (0.25 mg/ml)*,* it was not un-expected that a smaller zone of inhibition was recorded for *E. coli* than *S. aureus.*

The MIC of NP108 recorded against all three test bacteria was 0.25 mg/ml and this was reflected by the non-statistically significant difference recorded in the zones of inhibition against all three bacterial species. Due to possessing a lower molecular weight, NP108 was anticipated to migrate more easily from the gel matrix and exhibit a larger zone of inhibition against the test bacteria as a result of the higher concentration of NP108 in the agarose gel. This did not occur and a smaller inhibition zone was recorded for NP108 compared to NP101 against the three test bacteria. As only limited information was available for both NP101 and NP108, which did not include the chemical structures, it can only be surmised that NP108 bound more strongly to guar gum and therefore dissolution of NP108 from the lyophilised wafer was retarded resulting in the recording of a smaller zone of inhibition against the test bacteria.

7.3.3 Determination of expansion and inhibition ratios of guar gum 2% lyophilised wafers via pour plates

As previously described for spread plates, no expansion ratios were determined for control, NP101 or NP108 wafers after 24 hours incubation on pour plates (Figure 7.6 (a)).

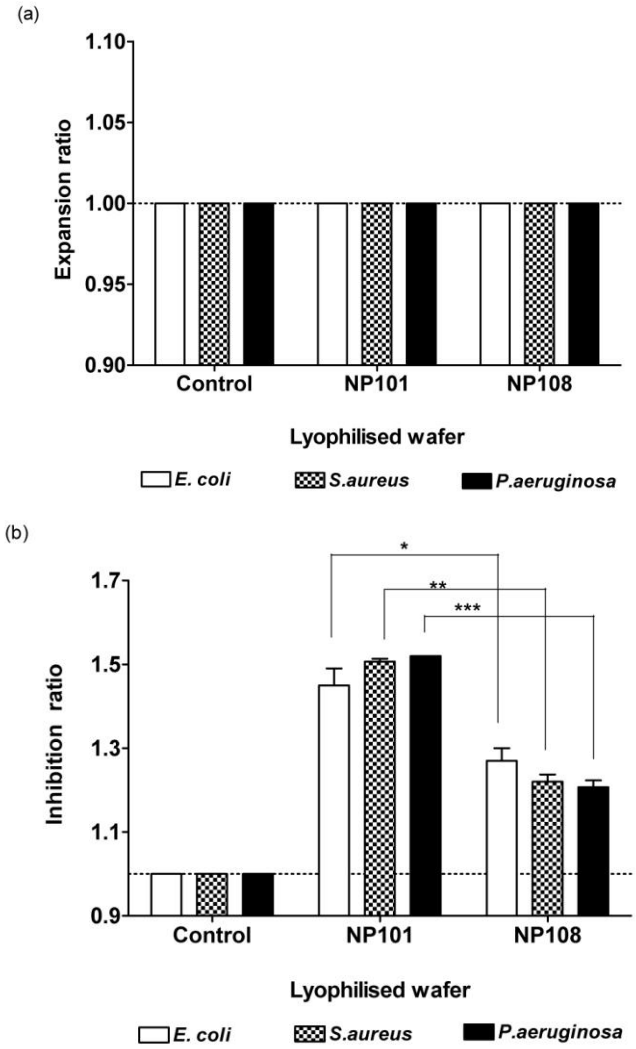

Figure 7.6 Expansion (a) and Inhibition (b) ratios of lyophilised wafers. * indicates a statistically significant difference between the zone of inhibition recorded for NP101 and NP108 against a bacterial species: * indicates *p*-value < 0.05, ** indicates *p*-values < 0.01, *** indicates *p*-value < 0.001.

(a) Expansion ratios of 2% guar gum lyophilised wafers; control, 2xMIC NP101, 2xMIC NP108, determined on pour plates
(b) Inhibition ratios of 2% guar gum lyophilised wafers; control, 2xMIC NP101, 2xMIC NP108, determined on pour plates

As with the spread plates, a smaller zone of inhibition was recorded for NP101 against *E. coli* than for *S. aureus* and *P. aeruginosa,* which was not un-expected as the MIC for NP101 against *E. coli,* is twice that of the other two bacteria. A statistically significant zone of inhibition (Figure 7.6 (b)) was recorded between the zones of inhibition recorded for NP101 and NP108 against each test bacterial species. As previously mentioned, NP108 appeared to bind far more strongly to guar gum than NP101, thus lower zones of inhibition against all bacteria tested were recorded for this CAP.

7.4 Discussion

7.4.1 Determination of inhibition ratios

The inhibition ratios determined by pour plate against all three test bacterial species were higher than those determined by spread plate. There are a number of factors that could have contributed to this result being obtained. Firstly, pour plates are prepared by introducing the required bacterial density into an empty Petri dish and adding the molten agarose at a temperature of approximately 50 ^{0}C. Due to thermal lysis, a proportion of these bacteria are killed, therefore a lower bacterial density may be present within pour plates compared to spread plates, thus a larger zone of inhibition will be recorded for the agent being tested against the bacteria. Secondly, as pour plates have the bacteria present throughout the agar plate, a lower bacterial density per unit volume is present in pour plates than in spread plates, where the required bacterial density is spread over the agarose surface.

Smaller zones of inhibition are regularly recorded in our laboratory for spread plates compared to pour plates for reasons outlined above. (A. Lamb, 2011, personal communication)

7.4.2 Lyophilised wafers as topical formulations

From the results reported in Sections 7.3.2 and 7.3.3. lyophilised wafers of 2% Guar gum are effective formulations for the topical delivery of CAPs *in vitro.* Dissolution of NP101 and NP108 from the wafers occurred and zones of inhibition were recorded for both CAPs against the three test bacteria. Having a molecular weight half that of NP101, a greater concentration of NP108 would be expected to diffuse from the wafer into the agarose gel. However, tighter binding of NP108 to

guar gum, resulted in less NP108 released over the incubation time, with resultant recording of lower zones of incubation compared to NP101.

7.4.3 CAP cell selectivity

The current view amongst researchers is that CAPs exhibit cell selectivity (Matsuzaki 2009). Based on numerous reports of the non-haemolytic activity of CAPs at concentrations several times higher than MIC values determined against numerous microorganisms, CAPs selectively kill bacterial cells without exerting significant toxicity against host cells (Matsuzaki 2009). This cell selectivity of CAPs is partly due to their cationicity; the surfaces of bacterial membranes are more highly negatively charged than mammalian membranes (Matsuzaki 2009). The *in-vitro* binding of the antimicrobial peptide magainin to *S. aureus* but not to surrounding epithelium has previously been demonstrated (Matsuzaki 2009). CAPs have been also been shown to act synergistically with other CAPs and conventional antibacterials to induce bacterial death (Marr, Gooderham and Hancock 2006). Randomised double-blind Phase III trials were conducted in 1991/2 examining the effect of 1% pexiganan acetate (synthetic analogue of the antimicrobial peptide magainin 2) and oral ofloxacin on infected diabetic foot ulcers, which reported a 90% cure rate (Zhang and Falla 2006)(Zheng, Sohn and Kim 2009). The development of a topical formulation containing pexiganan for the treatment of diabetic ulcers is on-going (Zhang and Falla 2006).

In the search for new therapeutic agents one of the essential requirements is that the antimicrobial under development displays cell selectivity as continued development of a therapeutic agent is curtailed if, in addressing microbial infection, damage is also inflicted by the agent on host cells.

7.4.4 Factors controlling drug residence in tissues

Before an antimicrobial agent can be effective, it must first be released from the formulation vehicle, bind to and remain in the target site at sufficient concentration to elicit an effect, also have a long half-life before being excreted by the host (Lu and Tonge 2010). The efficacy of any medicament is linked with the length of time the active agent is present in the area under treatment (Lu and Tonge 2010). In this investigation the incorporation of two novel antimicrobial peptides into lyophilised wafers has been shown to be effective against the most commonly found bacteria in human wounds, namely, *S. aureus* and *P. aeruginosa*. These lyophilised wafers deliver the antibacterial agent directly to the treatment area; allow the controlled release of the incorporated antimicrobial over time directly into the wound environment, therefore assuring sufficient drug/target residence time (Matthews et al. 2005). Resistance to these CAPs is not mediated by the efflux systems of the test bacteria and CAPs have been shown to exhibit cell selectivity. Further investigation is now required to examine the *in vivo* efficacy of the combination of CAPs and lyophilised wafers in the treatment of topical wounds.

7.5 Conclusion

Guar gum is a suitable polymer for the preparation of lyophilised wafers containing NP101 and NP108 for use as topical preparations in the treatment of wounds. Release of both NP101 and NP108 occurred from the lyophilised wafers, with substantial zones of inhibition recorded against *E. coli*, *S. aureus* and *P. aeruginosa,* each of which are commonly found in wounded and burned skin.

Chapter Eight

Discussion

8.1 Introduction

Excessive use of antibiotics in clinical practice since their discovery, without due consideration for inevitable ensuing bacterial resistance, coupled with the dearth in development of new antibacterials over the past few decades, has resulted in a world wide increase in bacterial resistance, closely correlating antibiotic usage (Carlet et al. 2011). Many factors have contributed and continue to add to the escalating bacterial resistance including; ageing immuno-suppressed populations in the developed world and poor sanitation, malnutrition and freely available generic antibacterials in the developing countries (Projan 2002). There is an urgent immediate global need for alternatives to classic antibiotics, (Fernebro 2011) which CAPs as a class provide a viable alternative to conventional antibacterial agents (Lohner and Blondelle 2005).

8.2 Measures to reduce antibacterial resistance

The focus of the WHO's World Health Day in 2011 was antimicrobial resistance (Carlet et al. 2011). This has helped to highlight the level of bacterial resistance globally and to promote wiser prescribing strategies for the effective antibacterials remaining to humans. Recognition that increased use of an antibacterial agent is swiftly followed by increased bacterial resistance to that agent is being actively promoted worldwide. One consequence of increased antibacterial resistance to existing therapeutic agents is that the empirical use of carbapenems has been adopted (Carlet et al. 2011). Carbapenems are currently the last effective class of antibacterials against most Gram-negative bacteria, a resource that must be

husbanded or resistance to this agent will surely occur if standard first–line therapy is adopted worldwide (Carlet et al. 2011).

However, the development of new agents while critical is not the only measure that must be adopted worldwide: informed use of existing agents must be promoted, strategies implemented to address the development of bacterial resistance by methods other than the use of antimicrobials must be investigated and more responsible prescribing policies must be encouraged in all health practitioners. Consideration of all these factors leads to the current investigation. Triclosan though in clinical use for many decades has recently come under FDA scrutiny due to reports of hormone effects in humans and fears of furthering antimicrobial resistance. Colistin was abandoned clinically from 1970-2000 due to adverse neurotoxic and nephrotoxic effects and is now used as a last resort treatment for multidrug resistant bacteria. However there is a great lack of information about the effects of colistin on bacteria as it was licensed in an era when existing regulatory requirements were not necessary for products and due to being discarded, as a therapeutic agent studies into the activity of colistin were not undertaken. NP101 and NP108 are novel cationic antimicrobial peptides, with the potential for development as therapeutic agents.

Therefore, this investigation examined triclosan, colistin, NP101 and NP108 in order to gain more information as to the bacteriostatic/bactericidal effects of these antimicrobials. Each agent has been shown to be effective against *E. coli*, *S, aureus* and *P. aeruginosa*. Though triclosan has been used clinically for many years it has retained its anbacterial efficacy. The abandonment of colistin from clinical practice from 1970s–2000 due to safety concerns has contained the development of resistance to this antibacterial, which currently remains the only active therapeutic agent against several multi-drug resistant bacteria.

8.2 Membrane active agents

Triclosan, colistin and CAPs are each attributed as being membrane active agents. Membrane active agents can exert their activity on bacterial membranes through alteration of the membrane potential, effects on membrane associated enzymes or activity on membrane structure and/or permeability (Denyer and Russell 2004) (Singleton 1999). Thus, the ranges of activities through which membrane active agents can exert bactericidal or bacteriostatic effects are extensive.

8.2.1 Membrane potential

The bacterial membrane is impermeable to protons, the extrusion of which from the cell interior forms the proton-motive force (PMF). This PMF drives the energy-requiring activities of the cell, including adenosine triphosphate synthesis (Denyer and Russell 2004)(Singleton 1999). The PMF also controls the up-take and metabolism of cellular components such as amino acids and sugars within the bacterium. Therefore, membrane active agents, by affecting the membrane potential, can un-couple bacterial metabolism from the energy processes which fuel catabolic activity essential for bacterial survival, resulting in bacterial death (Denyer and Russell 2004)(Singleton 1999).

8.2.2 Membrane enzymes

In aerobic bacteria, action on the electron transport chain by membrane active agents causes the inhibition of all metabolic processes, followed by bacterial death. These agents can also cause inhibition of ATPase and therefore inhibit metabolic processes in anaerobic bacteria. Membrane and cytoplasmic enzymes containing thiol groups such as the dehydrogenases (which are involved in redox reactions)

are also targeted by membrane active agents, with lethal results (Denyer and Russell 2004).

8.2.3 Membrane permeability

Effects on membrane permeability can produce bacteriostatic or bactericidal results depending on the concentration of antibacterial employed or the length of time to which the bacterium is exposed to the antimicrobial agent. Bacterial reactions therefore, can vary from slight leakage of intracellular components such as potassium ions to total cell lysis and bacterial death (Denyer and Russell 2004).

8.3 Quorum sensing

The phenomenon of quorum sensing is achieved through all the cells in a bacterial population secreting signal molecules; upon attainment of a certain cell density (quorum) these molecules accumulate until a level is reached where certain genes are activated within bacterial cells (Denyer and Russell 2004)(Singleton 1999). As previously detailed, homoserine lactones act as autoinducers in Gram–negative bacteria; once a certain concentration is reached they diffuse into bacterial cells, bind to a cytoplasmic protein and induce transcription of a specific gene. Thus, quorum sensing regulates gene expression in response to increased cell density (Otto 2004). Changes in gene expression and reduced growth rate occur in *E. coli* when the bacterium is exposed to the stress of an antimicrobial agent, to ensure survival (Rand et al. 2002). Biofilm formation by *S. aureus* has been shown to increase in response to inhibition of quorum sensing (Otto 2004). The acquisition of multidrug resistance genes by *P. aeruginosa* is also thought to affect the quorum sensing control of gene expression and release of virulence factors (Deptula and Gospodarek 2010). During *P. aeruginosa* colonization, quorum-sensing mutants benefit from molecules produced by wild-type isolates by rapid multiplication,

without any metabolic cost to these bacteria, which therefore have a fitness advantage (Kohler et al. 2010). A macrolide antibiotic, azithromycin exerts its antibacterial activity through interference with the quorum-sensing circuit, inhibiting expression of several extracellular virulence factors (Kohler et al. 2010).

8.4 Small colony variants and persister cells

S. aureus small colony variants result from exposure of planktonic cells to antimicrobials and amass as a drug-resistant sub-population, reducing sensitivity to antimicrobials through slow growth, reduced intake of cationic antibacterials and increased survival rates (Seaman, Ochs and Day 2006). The phenotype of small colony variants is due to defects in the electron transport chain, which can prove genetically inheritable or a transient colony type (Singh et al. 2009). *S. aureus* small colony variants have been shown to arise from antibacterial exposure, in particular exposure to aminoglycosides and Seaman *et al* have also reported the development of small colony variants in *S. aureus* as a result of exposure to 1 µg/ml triclosan (eighteen times higher than the MIC determined for *S. aureus* exposed to triclosan in this study) (Seaman, Ochs and Day 2006). These small colony variants displayed substantially increased resistance to triclosan, tolerating a concentration of 7.5 µg/ml triclosan for two hours while wild-type *S. aureus* were killed in less than 20 minutes. Subsequent analysis proved this triclosan resistance possessed by small colony variants was not due to mutation of *fabI,* clearly inferring *fabI* is not the only target affected by triclosan.

Persister cells are small populations of bacterial cells possessing a highly protected phenotype (Lai, Tremblay and Deziel 2009). Persisters do not possess specific resistance mechanisms and yet survive exposure to lethal concentrations of antimicrobials (Singh et al. 2009). Resistance in these persister cells is as a result

of a transient phenotypic switch, which reverts on re-culture to wild-type with new persister cells arising within this population (Singh et al. 2009). Persisters are not the result of antimicrobial exposure nor are they formed in response to quorum sensing but pre-exist in bacterial populations (Singh et al. 2009). Large numbers of persister cells are found in biofilms but small numbers of these cells have also been reported in planktonic cultures.

8.5 Antibacterial mechanism of action of triclosan

The responses of all three test species to incubation with triclosan were longer replication times and reduced metabolic activity. The growth inhibitory ability of triclosan against *E. coli* and *S. aureus* is due to blocking lipid synthesis by inhibiting FabI (Russell 2003). McMurray *et al* demonstrated blockage of lipid synthesis in *E. coli* within two hours incubation in 0.15 µg/ml triclosan (twice the MIC determined for *E. coli* in this study), directly inhibiting the bacterial growth rate by 50% (McMurray, Oethinger and Levy 1998). Triclosan has also been credited with having multiple target sites in the cytoplasmic membrane inhibiting not only lipid but also RNA and protein synthesis, resulting in membrane damage and bacterial death (Suller and Russell 2000).

The growth pattern of un-treated *S. aureus* was also revealed to be different to that displayed by *S. aureus* incubated with triclosan. Onset of a more rapid second phase of exponential bacterial growth was visible in *S. aureus* several hours after logarithmic bacterial growth had already commenced in the bacterium. This onset of a second phase of logarithmic bacterial growth was absent from *S. aureus* incubated with triclosan. This further onset of exponential growth in un-treated bacteria could perhaps be attributed to quorum sensing; once the bacterial population has assessed that adequate nutritional supplies and optimum growing

conditions are available to the community, a trigger is lifted and already occurring exponential bacterial growth proceeds at a faster rate. Exposure to sub-lethal triclosan prevents this trigger being lifted and a single phase of significantly reduced exponential growth occurs.

Assessment of membrane permeability in bacteria incubated with triclosan showed that a statistically significant K^+ loss linked to concentration and length of exposure to the bisphenol was detected from *E. coli* incubated with inhibitory or supra-inhibitory triclosan concentrations. McMurray *et al* demonstrated incubation with 8 µg/ml triclosan induced lysis in *E. coli* within two hours incubation (McMurray, Oethinger and Levy 1998). This is equivalent to 115xMIC determined for *E. coli* against triclosan in this study. Triclosan is adsorbed into bacterial cells by a Z adsorption pattern; the entry of triclosan into cells commences, a sudden cessation in triclosan adsorption follows after which adsorption resumes at a faster rate (Russell 2003). This type of adsorption indicates triclosan causes the structural breakdown of the bacterial cell wall/membrane and generates new sites through which it can then access within the bacterial cell (Russell 2003). In contrast to *E. coli*, K^+ loss from *S. aureus* exposed to triclosan was un-affected by concentration and exposure time and was not statistically significant. Villalaín *et al* demonstrated triclosan destabilizes structures in bacterial cells, compromising cell membrane integrity but not resulting in bacterial lysis (Villalaín et al. 2001). Examination of the effects of triclosan on bacterial populations by flow cytometry revealed different responses in control and triclosan incubated cultures. Exposure of both these bacterial species to sub-inhibitory triclosan concentrations was well tolerated; viability patterns and bacterial size of sub-inhibitory and un-treated bacteria were very similar, indicating exposure to this triclosan concentration exerted minimal stress and limited fitness cost on the bacteria. As 99.999% of *E. coli* and *S. aureus*

die when incubated with the inhibitory triclosan concentration; the remaining 0.001% slowly grow and after a long period their progeny cells are detected by flow cytometry at 72 hours. Contrary to the inhibitory triclosan concentration, *E. coli* or *S. aureus* cells do not survive exposure to the supra-inhibitory triclosan concentration. Changes in morphology of these test bacteria by SEM examination revealed a similar response to incubation with triclosan causing interference with the ability of cells to undergo normal septation. Interrupted cell division in *S. aureus* incubated with triclosan has been demonstrated by Seaman *et al* (Seaman, Ochs and Day 2006). Aggregation of *S. aureus* cells was seen in all triclosan concentrations over the experimental period, probably attributable to the inability of bacteria to separate properly.

8.5 Antibacterial mechanism of action of colistin

A concentration dependent retardation in onset of logarithmic bacterial growth with little or no reduction in final bacterial density was seen with all three test bacteria incubated with colistin. In contrast to triclosan, onset of the second phase of logarithmic bacterial growth was observed in both un-treated and colistin incubated *S. aureus* cells. This highlights the clear distinction between the effects that colistin and triclosan exerted on the growth kinetics of *S. aureus*.

A concentration dependent, significant K^+ loss was observed in *S. aureus* and *E. coli* when incubated with colistin. However, the concentration of colistin required inducing this K^+ loss in *S. aureus* was thirty-three times higher than that used to treat *E. coli*. Importantly incubation of *P. aeruginosa* with colistin did not result in leakage of K^+ as no difference in the quantity of K^+ lost was detected between un-treated and treated cells. Therefore the fact that colistin is active against *P.*

aeruginosa, but no loss of K^+ is observed, this suggests that K^+ loss in the other test species are a secondary consequence of the primary action of this agent.

Exposure to the supra-inhibitory colistin concentration proved bactericidal for all three test bacteria. *P. aeruginosa* and *S. aureus* but not *E. coli,* displayed tolerance to the presence of the inhibitory colistin concentration between 24 and 72 hours. Small colony variants observed to permit bacterial survival were detected during viability counts with *P. aeruginosa* exposed to colistin at inhibitory and supra-inhibitory concentrations. Neither *E. coli* nor *S. aureus* in response to incubation with colistin produced these small colony variants.

Changes in bacterial morphology over 168 hours revealed by SEM, disclosed incubation of *E. coli*, *S. aureus* and *P. aeruginosa* with sub-inhibitory colistin concentrations produced spherical cellular aggregates, rounding of rod-shaped bacteria, interference with normal bacterial septation and membrane blebbing. Adaptive resistance to the presence of colistin has been shown previously for *P. aeruginosa* and other Gram-negative bacteria (Skiada et al.). Adaptive resistance is a self-regulated bacterial phenomenon, where resistance to an antibacterial through phenotypic alterations is displayed by the bacterium in the presence of the antibacterial, lost when the antibacterial compound is removed (Skiada et al.). The effect underpinning such resistance are changes in bacterial cell surface, alteration in outer membrane architecture and lipid composition and reduction in Mg^{++} and Ca^{++} content of LPS, all of which decreases outer membrane permeability and result in reduced binding of colistin (Skiada et al.). Exposure of *P. aeruginosa* to sub-inhibitory colistin concentrations activates the two-component regulatory system, triggering adoption of adaptive resistance and LPS alterations. MexAB-OprM efflux systems, which are overexpressed in *P. aeruginosa* biofilms, have also been shown to confer an adaptive resistant phenotype to colistin (Skiada et al.).

Alterations upon bacterial morphology in response to sub-inhibitory colistin concentrations were also visualised at the inhibitory and supra-inhibitory concentrations; specifically the presence of spherical aggregated cells, membrane blebbing and non-septation in conjunction with very low bacterial density at these colistin concentrations.

8.6 Antibacterial mechanism of action of NP101 and NP108

The effects exerted by NP101 and NP108 were different and depended not on the bacterial species with which they were incubated but on the density of the bacterial culture. At a lower density an all or nothing effect was seen with all test species; this changed to delayed onset of logarithmic growth coupled with reduced final bacterial densities when a higher bacterial innoculum was employed. The ability of CAPs to inhibit planktonic growth in bacteria has been shown to be linked to the peptide length; with hexa and octameric peptides successfully inhibiting *E. coli* growth whereas tetrameric peptides did not (Hou et al. 2010). Until recently it was believed there were no specific receptors for cationic peptides on the surfaces of micro-organisms. However this viewpoint requires revision since it appears that histatins bind specifically to Ssa1/2 proteins on the surface of *Candida albicans* (Pereira 2006). Vylkova *et al* demonstrated in 2006 that salivary histatin 5 (Hst 5) kills *Candida albicans* by a multi step process involving binding to Ssa 1/2 proteins on the cell surface requiring the Trk1 potassium transporter as an essential tool (Vylkova et al. 2006).

As previously observed with *S. aureus* incubated with triclosan, the second onset of logarithmic bacterial growth displayed by un-treated bacteria was not present in the growth of *S. aureus* exposed to either of the CAPs.

Being membrane active agents, assessment on changes to membrane permeability through detection of K^+ loss resulting from exposure to NP108, resulted in swift and statistically significant K^+ loss in all three test species. The concentration dependent K^+ loss recorded was greatest for *E. coli,* with *P. aeruginosa* requiring a higher concentration of NP108 before K^+ loss was significant. Low outer membrane permeability forms the basis of the reduced susceptibility of *P. aeruginosa* to most antibacterials (Breidenstein, de la Fuente-Núñez and Hancock 2011). This low membrane permeability is 12-100 times less than that of *E. coli* (Breidenstein, de la Fuente-Núñez and Hancock 2011). Exposure of *P. aeruginosa* to sub-inhibitory concentrations of antibiotics has resulted in the subsequent development of resistance to that antibacterial, through overexpression of genes encoding efflux pumps. In chronic cystic fibrosis infections *P. aeruginosa* switches to a biofilm lifestyle with resistance to conventional antibacterials (Breidenstein, de la Fuente-Núñez and Hancock 2011). *E. coli* revealed what looked like development of tolerance to the inhibitory concentration of NP101 but not to NP108. Neither *P. aeruginosa* nor *S. aureus* tolerated the inhibitory or supra-inhibitory NP101 or NP108 concentrations. To illustrate the diversity of CAPs, there appears to be no general peptide cross-resistance mechanism whereby bacteria are resistant to every single peptide (Marr, Gooderham and Hancock 2006). *S. aureus* and *Ps. aeruginosa* have evolved a degree of generalised CAP resistance by increasing the amount of positively charged protein in their membranes. *S. aureus* transports D-alanine from the cytoplasm to the surface teichoic acid to reduce the net negative charge by introducing basic amino groups (Brogden 2005). Another method by which bacteria develop resistance to CAPs is by production of proteolytic enzymes; for example, LL-37 is cleaved and inactivated by a *S. aureus* metalloproteinase, aureolysin (Brogden 2005). A two-component system ParR-ParS is significant in the

adaptive resistance of *P. aeruginosa* to cationic peptides, through activation of the lipopolysaccharide modification operon. Small colony variants were produced by all test bacterial species in response to CAP incubation, to increase bacterial survival.

Changes in bacterial morphology as elucidated by SEM revealed bacterial size and shape alterations: extrusion of intracellular material: blebbed bacterial membranes: inhibition of bacterial septation and interruption of binary fission. Other proposed mechanisms of action include activity on intracellular targets after membrane permeabilization, such as activation of autolytic enzymes and inhibition of DNA and protein synthesis. For example; attacins block synthesis of integral membrane proteins, pyrrhocoricin (insect peptide) has been demonstrated to kill bacteria by binding to a protein target called DnaK, preventing DnaK from performing its protein repair function resulting in death (Zaiou 2007).

During this investigation, the statistically significant *in vitro* efficacy of two novel CAPs against the microorganisms most commonly found contaminating chronic wounds and burns has been demonstrated. One of the principal factors limiting the use of CAPs as clinical therapeutics is their short systemic half-life owing to proteolytic degradation (Marr, Gooderham and Hancock 2006). Research is on going in the development of protease resistant CAPs; Marsh *et al* have shown that fluorination of naturally existing peptides increases their resistance to proteolytic degradation to twenty times longer than their non-fluorinated counterparts (Ritter 2007). However, there are no known topical toxicities, which make topical delivery the most suitable current application for the antibacterial action of CAPs (Marr, Gooderham and Hancock 2006).

Utilisation of antimicrobial peptides to promote wound healing is well established since manuka honey was introduced into topical therapy (Ratcliffe et al. 2011). The antibacterial activity and re-granulation effect of manuka honey can be attributed in

part to the constituents of honey, including the insect antimicrobial peptide bee defensin-1. (Ratcliffe et al. 2011) Delivery of these antimicrobials directly into the wound bed was possible by incorporating the CAPs into lyophilised wafers. Lyophilised wafers are being developed as novel topical therapeutic delivery formulations, delivering sustained release, with resultant constant concentration of the therapeutic agent in the wound environment.

8.7 Future work

A transcriptional analysis of *E. coli, S. aureus* and *P. aeruginosa* is now required to determine the individual cellular genetic responses of these bacteria to triclosan, colistin, NP101 and NP108. This will greatly add to the information already gathered during this study.

While SEM has elucidated several effects of all the test agents against the bacteria used in this investigation, analysis by TEM is the logical progression in further analysis of individual bacterial responses to these cationic antimicrobial agents.

During this investigation of the effects of the inhibitory concentration of NP101 on *E. coli*, the appearance of what appeared to be a tolerance to the effects of the inhibitory concentration of the CAP was revealed. Further investigation of this effect is required and if tolerance to NP101 is revealed, whether de-sensitisation to the peptide would result in the return of sensitivity to the agent.

8.8 Conclusions

The conclusions that can be drawn from the current investigation are;

a) Triclosan

Triclosan exerts a concentration dependent retardation in onset of logarithmic growth coupled with reduction in bacterial growth in all three test bacteria.

The inhibition of onset of second-phase logarithmic growth in *S. aureus*, by triclosan.

Minimal K^+ loss is induced from *E. coli* and *S. aureus* upon incubation with triclosan concentrations up to 10xMIC.

The inability of *E. coli* and *S. aureus* to withstand incubation with the supra-inhibitory triclosan concentration was evident from flow cytometry data. Development of tolerance by *E. coli* and *S. aureus* to the inhibitory triclosan concentration by 72 hours was elucidated by flow cytometry.

Examination of bacterial morphology via SEM revealed inhibition of normal bacterial septation and the formation of cellular aggregates in all test species.

b) Colistin

Concentration dependent retardation in onset of bacterial growth, without reduction in final bacterial density of all test species by colistin.

Incubation with colistin resulted in the induction of significant K^+ loss from *S. aureus* and *E. coli* but not *P. aeruginosa.*

P. aeruginosa and *S. aureus* but not *E. coli* developed resistance to the inhibitory colistin concentration over the experimental period.

The stress of incubation with colistin resulted in the production of small colony variants by *P. aeruginosa*.

SEM examination of bacterial morphology revealed colistin incubation produced the formation of spherical aggregates; membrane blebbing and inhibition of normal bacterial septation in all test bacteria.

c) NP101 and NP108

An all or nothing effect on bacterial growth of *E. coli*, *S. aureus* and *P. aeruginosa* by NP101 and NP108.

Suppression of second-phase logarithmic growth in *S. aureus* by both NP101 and NP108.

Incubation with NP108 resulted in significant K^+ loss in all test bacteria.

Examination of outer morphology of *E. coli*, *S. aureus* and *P. aeruginosa* after incubation with NP101 and NP108 produced bacterial size and shape alterations; induced extrusion of intracellular material; caused blebbing of membranes; inhibited bacterial septation and interrupted replication through binary fission.

Formulation of lyophilised wafers containing either NP101 or NP108 was undertaken, tested for *in vitro* topical antibacterial efficacy and found to possess antibacterial activity against all test species.

Bibliography

AHN, K.C. et al., 2008. In vitro biologic activities of the antimicrobials triclocarban, its analogs, and triclosan in bioassay screens: receptor-based bioassay screens. *Environmental Health Perspectives,* 116(9), pp. 1203-1210

AIELLO, A.E. et al., 2004. Relationship between triclosan and susceptibilities of bacteria isolated from hands in the community. *Antimicrobial Agents and Chemotherapy,* 48(8), pp. 2973-2979

ALANIS, A.J., 2005. Resistance to Antibiotics: are we in the post-antibiotic era? *Archives of Medical Research,* 36(6), pp. 697-705

ALEKSHUN, M.N. and LEVY, S.B., 2007. Molecular mechanisms of antibacterial multidrug resistance. *Cell,* 128(6), pp. 1037-1050

ALHANOUT, K. et al., 2010. New insights into the antibacterial mechanism of action of squalamine. *Journal of Antimicrobial Chemotherapy,* 65(8), pp. 1688-1693

ALLISON, D. and GILBERT, P., 2004. Bacteria. In: S. DENYER, N.A. HODGES and S.P. GORMAN, eds. *Hugo and Russell's Pharmaceutical microbiology.* 7th ed. Oxford: Blackwell Publishing. pp. 23-43

AL-RAJAB, A.J. et al., 2009. Impact of biosolids on the persistence and dissipation pathways of triclosan and triclocarban in an agricultural soil. *Science of the Total Environment,* 407(23), pp. 5978-85

ALTMAN, H. et al., 2006. In vitro assessment of antimicrobial peptides as potential agents against several oral bacteria. *Journal of Antimicrobial Chemotherapy,* 58(1), pp. 198-201

AMIRI, M. et al., 2007. Electrostatic accumulation and determination of triclosan in ultrathin carbon nanoparticle composite film electrodes. *Analytica Chimica Acta,* 593(1), pp. 117-122

ANDERSSON, D.I., 2006. The biological cost of mutational antibiotic resistance: any practical conclusions? *Current Opinion in Microbiology,* 9(5), pp. 461-465

AOKI, N. et al., 2009. Efficacy of colistin combination therapy in a mouse model of pneumonia caused by multidrug-resistant *Pseudomonas aeruginosa*. *Journal of Antimicrobial Chemotherapy,* 63(3), pp. 534-542

APPELT, C. et al., 2007. Design of antimicrobial compounds based on peptide structures. *Bioorganic & Medicinal Chemistry Letters,* 17(8), pp. 2334-2337

ARANCIBIA, R. et al., 2009. Triclosan inhibits tumor necrosis factor-alpha-stimulated urokinase production in human gingival fibroblasts. *Journal of Periodontal Research,* 44(6), pp. 726-35

ARCIDIACONO, S. et al., 2008. Cy5 labeled antimicrobial peptides for enhanced detection of *Escherichia coli* O157:H7. *Biosensors and Bioelectronics,* 23(11), pp. 1721-1727

ARCIOLA, C.R. et al., 2005. Antibiotic resistance in exopolysaccharide-forming *Staphylococcus epidermidis* clinical isolates from orthopaedic implant infections. *Biomaterials,* 26(33), pp. 6530-6535

ARCIOLA, C.R. et al., 2003. *Staphylococcus epidermidis*–fibronectin binding and its inhibition by heparin. *Biomaterials,* 24(18), pp. 3013-3019

ASSADIAN, O., BELOW, H. and KRAMER, A., 2009. The effect of triclosan-coated sutures in wound healing and triclosan degradation in the environment. *Journal of Plastic, Reconstructive & Aesthetic Surgery,* 62(2), pp. 264-265

AUCKEN, H. et al., 2002. A new UK strain of epidimic methicillin-resistant *Staphylococcus aureus* (EMRSA-17) resistant to multiple antibiotics. *Journal of Antimicrobial Chemotherapy,* 50(2), pp. 171-175

AYTON, G.S. and VOTH, G.A., 2009. Systematic multiscale simulation of membrane protein systems. *Current Opinion in Structural Biology,* 19(2), pp. 138-144

BADER, M.W. et al., 2005. Recognition of Antimicrobial Peptides by a Bacterial Sensor Kinase. *Cell,* 122(3), pp. 461-472

BALL, P., 2007. Conclusions: the future of antimicrobial therapy – Augmentin® and beyond. *International Journal of Antimicrobial Agents,* 30(Supplement 2), pp. 139-141

BARRETT-BEE, K., NEWBOULT, L. and EDWARDS, S., 1994. The membrane destabilising action of the antibacterial agent chlorhexidine. *FEMS Microbiology Letters,* 119(1-2), pp. 249-253

BECKER, D. et al., 2006. Robust Salmonella metabolism limits possibilities for new antimicrobials. *Nature,* 440(7082), pp. 303-307

BEHERA, B. et al., 2010. Evaluation of susceptibility testing methods for polymyxin. *International Journal of Infectious Diseases,* 14(7), pp. e596-e601

BEN JACOB, E. et al., 2004. Bacterial linguistic communication and social intelligence. *Trends in Microbiology,* 12(8), pp. 366-372

BESTER, K. and SCHAFER, D., 2009. Activated soil filters (bio filters) for the elimination of xenobiotics (micro-pollutants) from storm- and waste waters. *Water Research,* 43(10), pp. 2639-2646

BHARGAVA, H.N. and LEONARD, P.A., 1996. Triclosan: applications and safety. *American Journal of Infection Control,* 24(3), pp. 209-218

BHAT, S. and MILNER, S., 2007. Antimicrobial peptides in burns and wounds. *Current Protein & Peptide Science,* 8(5), pp. 506-520

BHAVSAR, A.P., GUTTMAN, J.A. and FINLAY, B.B., 2007. Manipulation of host-cell pathways by bacterial pathogens. *Nature,* 449(7164), pp. 827-834

BIROSOVA, L. and MIKULASOVA, M., 2009. Development of triclosan and antibiotic resistance in *Salmonella enterica* serovar Typhimurium. *Journal of Medical Microbiology,* 58(4), pp. 436-441

BISHOP, J.L. and FINLAY, B.B., 2006. Friend or foe? Antimicrobial peptides trigger pathogen virulence. *Trends in Molecular Medicine,* 12(1), pp. 3-6

BLAIR, J.M. and PIDDOCK, L.J., 2009. Structure, function and inhibition of RND efflux pumps in Gram-negative bacteria: an update. *Current Opinion in Microbiology,* 12(5), pp. 512-519

BOATENG, J.S. et al., 2010. Characterisation of freeze-dried wafers and solvent evaporated films as potential drug delivery systems to mucosal surfaces. *International Journal of Pharmaceutics,* 389(1-2), pp. 24-31

BOATENG, J.S. et al., 2009. In vitro drug release studies of polymeric freeze-dried wafers and solvent-cast films using paracetamol as a model soluble drug. *International Journal of Pharmaceutics,* 378(1-2), pp. 66-72

BÖHME, L. and RUDEL, T., 2009. Host cell death machinery as a target for bacterial pathogens. *Microbes and Infection,* 11(13), pp. 1063-1070

BOLON, M., 2011. Hand hygiene. *Infectious Disease Clinics of North America,* 25(1), pp. 21-43

BOYCE, J. et al., 2005. Meticillin-resistant *Staphylococcus aureus*. *The Lancet Infectious Diseases,* 5(10), pp. 653-663

BRADBURY, J., 2004. Antimicrobial peptides reveal their signature. *The Lancet Infectious Diseases,* 4(6), pp. 317

BRASSEUR, R. and DIVITA, G., 2010. Happy birthday cell penetrating peptides: Already 20 years. *Biochimica et Biophysica Acta (BBA) - Biomembranes,* 1798(12), pp. 2177-2181

BRAUSCH, J.M. and RAND, G.M., 2011. A review of personal care products in the aquatic environment: Environmental concentrations and toxicity. *Chemosphere,* 82(11), pp. 1518-1532

BREIDENSTEIN, E.B.M., DE LA FUENTE-NÚÑEZ, C. and HANCOCK, R.E.W., 2011. *Pseudomonas aeruginosa*: all roads lead to resistance. *Trends in Microbiology,* In Press, Corrected Proof

BRICKNER, S.J. and MOBASHERY, S., 2007. Prospects of therapies targeting resistant bacteria—New challenges 20 years post emergence of vancomycin-resistant enterococcus. *Current Opinion in Microbiology,* 10(5), pp. 425-427

BROGDEN, K.A., 2005. Antimicrobial peptides: pore formers or metabolic inhibitors in bacteria? *Nature Reviews Microbiology,* 3(3), pp. 238-250

BROGER, T. et al., 2011. Real-time on-line flow cytometry for bioprocess monitoring. *Journal of Biotechnology,* In Press, Corrected Proof

BRÖTZ-OESTERHELT, H. and BRUNNER, N.A., 2008. How many modes of action should an antibiotic have? *Current Opinion in Pharmacology,* 8(5), pp. 564-573

BRUINSMA, G.M. et al., 2006. Resistance to a polyquaternium-1 lens care solution and isoelectric points of *Pseudomonas aeruginosa* strains. *Journal of Antimicrobial Chemotherapy,* 57(4), pp. 764-766

BUCKI, R. et al., 2010. Cathelicidin LL-37: a multitask antimicrobial peptide. *Archivum Immunologiae et Therapiae Experimentalis,* 58(1), pp. 15-25

BUCKLING , A. and BROCKHURST, M., 2005.Microbiology: RAMP resistance. *Nature,* 438, pp. 170-171

BULITTA, J.B. et al., 2010. Attenuation of colistin bactericidal activity by high inoculum of *Pseudomonas aeruginosa* characterized by a new mechanism-based population pharmacodynamic model. *Antimicrobial Agents and Chemotherapy,* 54(5), pp. 2051-2062

CABANA, H. et al., 2009. Immobilization of laccase from the white rot fungus *Coriolopsis polyzona* and use of the immobilized biocatalyst for the continuous elimination of endocrine disrupting chemicals. *Bioresource Technology,* 100(14), pp. 3447-3458

CABANA, H., JONES, J.P. and AGATHOS, S.N., 2009. Utilization of cross-linked Laccase aggregates in a perfusion basket reactor for the continuous elimination of endocrine-disrupting chemicals. *Biotechnology and Bioengineering,* 102(6), pp. 1582-1592

CADIEUX, P.A. et al., 2009. Use of triclosan-eluting ureteral stents in patients with long-term stents. *Journal of Endourology,* 23(7), pp. 1187-1194

CAJTHAML, T. et al., 2009. Biodegradation of endocrine-disrupting compounds and suppression of estrogenic activity by ligninolytic fungi. *Chemosphere,* 75(6), pp. 745-750

CARLET, J. et al., 2011. Society's failure to protect a precious resource: antibiotics. *The Lancet,* In Press, Corrected Proof

CARSON, R.T. et al., 2008. Use of antibacterial consumer products containing quaternary ammonium compounds and drug resistance in the community. *Journal of Antimicrobial Chemotherapy,* 62(5), pp. 1160-1162

CHAMPLIN, F.R. et al., 2005. Effect of outer membrane permeabilisation on intrinsic resistance to low triclosan levels in *Pseudomonas aeruginosa*. *International Journal of Antimicrobial Agents,* 26(2), pp. 159-164

CHANG, S., CHANG, H. and LAI, M., 1999. Antibiotic usage in primary care units in Taiwan. *International Journal of Antimicrobial Agents,* 11(1), pp. 23-30

CHAPMAN, J.S., 2003. Disinfectant resistance mechanisms, cross-resistance, and co-resistance. *International Biodeterioration & Biodegradation,* 51(4), pp. 271-276

CHENG, C. et al., 2010. Safety and efficacy of intravenous colistin (colistin methanesulphonate) for severe multidrug-resistant Gram-negative bacterial infections. *International Journal of Antimicrobial Agents,* 35(3), pp. 297-300

CHIAPPETTA, D.A. et al., 2008. Triclosan-loaded poloxamine micelles for enhanced topical antibacterial activity against biofilm. *European Journal of Pharmaceutics and Biopharmaceutics,* 69(2), pp. 535-545

CHONGSIRIWATANA, N.P. and BARRON, A.E., 2010. Comparing bacterial membrane interactions of antimicrobial peptides and their mimics. In: A. GIULIANI and A. RINALDI, eds. *Antimicrobial peptides: methods and protocols.* New York: Humana Press. pp. 171-182

CHUANCHUEN, R., KARKHOFF-SCHWEIZER, R.R. and SCHWEIZER, H.P., 2003. High-level triclosan resistance in *Pseudomonas aeruginosa* is solely a result of efflux. *American Journal of Infection Control,* 31(2), pp. 124-127

CLAUSELL, A. et al., 2003. Influence of polymyxins on the structural dynamics of *Escherichia coli* lipid membranes. *Talanta,* 60(2-3), pp. 225-234

CLINICAL AND LABORATORY STANDARDS INSTITUTE (CLSI), 2006. *Methods for dilution antimicrobial susceptibility tests for bacteria that grow aerobically; Approved Standards-Seventh Edition (MA-A7) Vol. 26, No 2.* Wayne, PA.: CLSI

COMAS, J. and VIVES-REGO, J., 1998. Enumeration, viability and heterogeneity in *Staphylococcus aureus* cultures by flow cytometry. *Journal of Microbiological Methods,* 32(1), pp. 45-53

CONLON, J.M. et al., 2007. Strategies for transformation of naturally-occurring amphibian antimicrobial peptides into therapeutically valuable anti-infective agents. *Methods,* 42(4), pp. 349-357

COSTA, F. et al., 2011. Covalent immobilization of antimicrobial peptides (AMPs) onto biomaterial surfaces. *Acta Biomaterialia,* 7(4), pp. 1431-1440

COSTELLOE, C. et al., 2010. Effect of antibiotic prescribing in primary care on antimicrobial resistance in individual patients: systematic review and meta-analysis. *BMJ (Clinical research ed.),* 340, pp. c2096

COTTELL, A. et al., 2009. Triclosan-tolerant bacteria: changes in susceptibility to antibiotics. *Journal of Hospital Infection,* 72, pp. 71-76

CROFTON, K.M. et al., 2007. Short-term in vivo exposure to the water contaminant triclosan: Evidence for disruption of thyroxine. *Environmental Toxicology and Pharmacology,* 24(2), pp. 194-197

CUI, L. et al., 2003. Cell wall thickening is a common feature of vancomycin resistance in *Staphylococcus aureus*. *Journal of Clinical Microbiology,* 41(1), pp. 5-14

CUMMINS, J. et al., 2009. Subinhibitory concentrations of the cationic antimicrobial peptide colistin induce the pseudomonas quinolone signal in *Pseudomonas aeruginosa*. *Microbiology,* 155, pp. 2826-2837

DANIELS, C. and RAMOS, J.L., 2009. Adaptive drug resistance mediated by root-nodulation-cell division efflux pumps. *Clinical Microbiology and Infection,* 15, pp. 32-36

DAROUICHE, R.O. et al., 2009. Antimicrobial and antibiofilm efficacy of triclosan and DispersinB combination. *Journal of Antimicrobial Chemotherapy,* 64(1), pp. 88-93

DAVIES, A.J. and MAILLARD, J.-., 2001. Bacterial adaptation to biocides: the possible role of 'alarmones'. *Journal of Hospital Infection,* 49(4), pp. 300-302

DAVIES, A.J. and MAILLARD, J.-., 2002. Erratum: Bacterial adaptation to biocides: the possible role of 'alarmones'. *Journal of Hospital Infection,* 50(4), pp. 328-328

DAVIES, B. and COHEN, J., 2011. Endotoxin removal devices for the treatment of sepsis and septic shock. *The Lancet Infectious Diseases,* 11(1), pp. 65-71

DELCOUR, A.H., 2009. Outer membrane permeability and antibiotic resistance. *Biochimica et Biophysica Acta (BBA) - Proteins & Proteomics,* 1794(5), pp. 808-816

DEMING, T.J., 2007. Synthetic polypeptides for biomedical applications. *Progress in Polymer Science,* 32(8-9), pp. 858-875

DENYER, S. and RUSSELL, A.D., 2004. Non-antibiotic antibacterial agents: mode of action and resistance. In: S.P. DENYER, N.A. HODGES and S.P. GORMAN, eds. *Hugo and Russell's pharmaceutical microbiology.* 7th ed. Oxford: Blackwell Publishing. pp. 306-322

DENYER, S.P., 1995. Mechanisms of action of antibacterial biocides. *International Biodeterioration & Biodegradation,* , pp. 227-245

DEPTULA, A. and GOSPODAREK, E., 2010. Reduced expression of virulence factors in multidrug-resistant *Pseudomonas aeruginosa* strains. *Archives of Microbiology,* 192(1), pp. 79-84

DESBOIS, A.P. and SMITH, V.J., 2010. Antibacterial free fatty acids: activities, mechanisms of action and biotechnological potential. *Applied Microbiology and Biotechnology,* 85(6), pp. 1629-1642

DEUTSCHER, M. and FRIEDMAN, C., eds. 2010. Antibiotic resistance and implications for the appropriate use of antimicrobial agents. In: A.G.MAINOUS and C.POMEROY, eds. *Management of antimicrobials in infectious diseases.* New York: Springer. pp. 1-30

DIEN, B.S. and SRIENC, F., 1991. Bromodeoxyuridine labeling and flow cytometric identification of replicating *Saccharomyces cerevisiae* cells: lengths of cell cycle phases and population variability at specific cell cycle positions. *Biotechnology Progress,* 7(4), pp. 291-298

DONG, C. et al., 2006. Wza the translocon for *E. coli* capsular polysaccharides defines a new class of membrane protein. *Nature,* 444(7116), pp. 226-229

DOTSCH, A. et al., 2010. Evolutionary conservation of essential and highly expressed genes in *Pseudomonas aeruginosa*. *BMC Genomics,* 11, pp. 234

DURAI, R., NG, P.C.H. and HOQUE, H., 2010. Methicillin-Resistant *Staphylococcus aureus*: an update. *AORN,* 91(5), pp. 599-609

DYNES, J.J. et al., 2009. Morphological and biochemical changes in *Pseudomonas fluorescens* biofilms induced by sub-inhibitory exposure to antimicrobial agents. *Canadian Journal of Microbiology,* 55(2), pp. 163-178

DZIARSKI, R. and GUPTA, D., 2006. Mammalian PGRPs: novel antibacterial proteins. *Cellular Microbiology,* 8(7), pp. 1059-1069

EL SOLH, A.A. and ALHAJHUSAIN, A., 2009. Update on the treatment of *Pseudomonas aeruginosa* pneumonia. *Journal of Antimicrobial Chemotherapy,* 64(2), pp. 229-238

ENNE, V.I. et al., 2004. Enhancement of host fitness by the sul2-coding plasmid p9123 in the absense of selective pressure. *Journal of Antimicrobial Chemotherapy,* 53(6), pp. 958-963

EPSTEIN, W., 2003. The roles and regulation of potassium in bacteria. In: K. MOLDAVE, ed. *Progress in nucleic acid research and molecular biology.* San Diego, CA.: Academic Press. pp. 293-320

ESCALADA, M.G. et al., 2005. Triclosan inhibition of fatty acid synthesis and its effect on growth of *Escherichia coli* and *Pseudomonas aeruginosa*. *Journal of Antimicrobial Chemotherapy,* 55(6), pp. 879-882

EWIG, S., 2011. Nosocomial pneumonia: de-escalation is what matters. *The Lancet Infectious Diseases,* 11(3), pp. 155-157

FALAGAS, M.E. et al., 2006. The use of intravenous and aerosolized polymyxins for the treatment of infections in critically ill patients: a review of the recent literature. *Clinical Medicine & Research,* 4(2), pp. 138-146

FALAGAS, M.E. and RAFAILIDIS, P.I., 2009. Nephrotoxicity of colistin: new insight into an old antibiotic. *Clinical Infectious Diseases,* 48(12), pp. 1729-1731

FALAGAS, M.E. and BLIZIOTIS, I.A., 2007. Pandrug-resistant Gram-negative bacteria: the dawn of the post-antibiotic era? *International Journal of Antimicrobial Agents,* 29(6), pp. 630-636

FALAGAS, M.E. and MICHALOPOULOS, A., 2006. Polymyxins: old antibiotics are back. *The Lancet,* 367(9511), pp. 633-634

FALAGAS, M.E. et al., 2010. Colistin therapy for microbiologically documented multidrug-resistant Gram-negative bacterial infections: a retrospective cohort study of 258 patients. *International Journal of Antimicrobial Agents,* 35(2), pp. 194-199

FALAGAS, M.E., RAFAILIDIS, P.I. and MATTHAIOU, D.K., 2010. Resistance to polymyxins: mechanisms, frequency and treatment options. *Drug Resistance Updates,* 13(4-5), pp. 132-138

FALAGAS, M.E. et al., 2009. Inhaled colistin as monotherapy for multidrug-resistant gram (−) nosocomial pneumonia: a case series. *Respiratory Medicine,* 103(5), pp. 707-713

FALAGAS, M.E., VOULOUMANOU, E.K. and RAFAILIDIS, P.I., 2009. Systemic colistin use in children without cystic fibrosis: a systematic review of the literature. *International Journal of Antimicrobial Agents,* 33(6), pp. 503.e1-503.e13

FALKOW, S., 2006. Is persistent bacterial infection good for your health? *Cell,* 124(4), pp. 699-702

FERNÁNDEZ, L., BREIDENSTEIN, E.B.M. and HANCOCK, R.E.W., 2011. Creeping baselines and adaptive resistance to antibiotics. *Drug Resistance Updates,* 14(1), pp. 1-21

FERNEBRO, J., 2011. Fighting bacterial infections—future treatment options. *Drug Resistance Updates,* 14(2), pp. 125-139

FINCH, R. and HUNTER, P.A., 2006. Antibiotic resistance-action to promote new technologies:report of an EU intergovernmental conference held in Birmingham UK, 12-13 December 2005. *Journal of Antimicrobial Chemotherapy,* 58(S1), pp. i3-i22

FINKEL, S.E., 2006. Long-term survival during stationary phase: evolution and the GASP phenotype. *Nature Reviews Microbiology,* 4(2), pp. 113-120

FISCHBACH, M.A., 2009. Antibiotics from microbes: converging to kill. *Current Opinion in Microbiology,* 12(5), pp. 520-527

FOCUS ON SURFACTANTS, 2010a. FDA reviewing surfactants. *Focus on Surfactants*, 2010(6), p.5

FOCUS ON SURFACTANTS, 2010b. Triclosan under the spotlight again. *Focus on surfactants*, 2010(7), p.4

FU, W. et al., 2007. First structure of the polymyxin resistance proteins. *Biochemical and Biophysical Research Communications,* 361(4), pp. 1033-1037

FURCHTGOTT, L., WINGREEN, N.S. and HUANG, K.C., 2011. Mechanisms for maintaining cell shape in rod-shaped Gram-negative bacteria. *Molecular Microbiology,* In Press. Corrected Proof

GANAPATHY, H. et al., 2010. Use of colistin in treating multi-resistant Gram-negative organisms in a specialised burns unit. *Burns,* 36(4), pp. 522-527

GANT, V.A., WARNES, G. and PHILLIPS, I. AND SAVIDGE, G.F., 1993. The application of flow cytometry to the study of bacterial responses to antibiotics. *Journal of Medical Microbiology,* 39, pp. 147-154

GARCÍA-LARA, J., MASALHA, M. and FOSTER, S.J., 2005. *Staphylococcus aureus*: the search for novel targets. *Drug Discovery Today,* 10(9), pp. 643-651

GARIDEL, P. et al., 2007. Novel antiinflammatory and antiinfective agents. *Anti-Infective Agents in Medicinal Chemistry,* 6, pp. 185-200

GASINK, L.B. et al., 2007. The categorization of prior antibiotic use: Impact on the identification of risk factors for drug resistance in case control studies. *American Journal of Infection Control,* 35(10), pp. 638-642

GIACOMETTI, A. et al., 2005. In vitro activity of amphibian peptides alone and in combination with antimicrobial agents against multidrug-resistant pathogens isolated from surgical wound infection. *Peptides,* 26(11), pp. 2111-2116

GIAMARELLOU, H., 2010. Multidrug-resistant Gram-negative bacteria: how to treat and for how long. *International Journal of Antimicrobial Agents,* 36(Supplement 2), pp. S50-S54

GILBERG, K. et al., 2003. Analysis of medication use patterns: apparent overuse of antibiotics and under use of prescription drugs for asthma, depression and CHF. *Journal of Managed Care Pharmacy,* 9(1), pp. 232-237

GIULIANI, A., PIRRI, G. and RINALDI, A., 2010. Antimicrobial peptides: the LPS connection. In: A. GIULIANI and A.C.RINALDI, eds. *Antimicrobial peptides: methods and protocols.* New York: Humana Press. pp. 137-154

GOMEZ- ESCALADA, M. et al., 2005. Triclosan-bacteria interactions: single or multiple target sites? *Letters in Applied Microbiology,* 41, pp. 476-481

GUTSMANN, T. et al., 2005. Lipid-mediated resistance of Gram-negative bacteria against various pore-forming antimicrobial peptides. *Journal of Endotoxin Research,* II(3), pp. 167-173

HÄCKER, G., 2009. Introduction: the various deaths a cell can die, and their use in microbial infections. *Microbes and Infection,* 11(13), pp. 1047-1049

HALE, J.D.H. and HANCOCK, R.E.W., 2007. Alternative mechanisms of action of cationic antimicrobial peptides on bacteria. *Future Drugs,* 10, pp. 951-959

HALL, B.G., 1995. Adaptive mutations in *Escherichia coli* as a model for the multiple mutational origins of tumors. *Proceedings of the National Academy of Sciences of the United States of America,* 92(12), pp. 5669-5673

HANCOCK, R.E. and CHAPPLE, D.S., 1999. Peptide antibiotics. *Antimicrobial Agents and Chemotherapy,* 43(6), pp. 1317-1323

HANCOCK, R.E. and SAHL, H.G., 2006. Antimicrobial and host-defence peptides as new anti-infective therapeutic strategies. *Nature Biotechnology,* 24(12), pp. 1551-1557

HANSEN, M., KILK, K. and LANGEL, Ü., 2008. Predicting cell-penetrating peptides. *Advanced Drug Delivery Reviews,* 60(4-5), pp. 572-579

HARDER, J., 2008. Antimicrobial peptides: ancient molecules as modern therapeutics? *Expert Review Dermatology,* 3(1),

HARTMANN, M. et al., 2010. Damage of the bacterial cell envelope by antimicrobial peptides gramicidin S and PGLa as revealed by transmission and scanning electron microscopy. *Antimicrobial Agents and Chemotherapy,* 54(8), pp. 3132-3142

HARTZELL, J.D. et al., 2009. Nephrotoxicity associated with intravenous colistin (colistimethate sodium) treatment at a tertiary care medical center. *Clinical Infectious Diseases,* 48(12), pp. 1724-1728

HAY, A.G., DEES, P.M. and SAYLER, G.S., 2001. Growth of a bacterial consortium on triclosan. *FEMS Microbiology Ecology,* 36(2-3), pp. 105-112

HEATH, R.J. et al., 2000. The enoyl-[acyl-carrier-protein] reductases FabI and FabL from *Bacillus subtilis*. *Journal of Biological Chemistry,* 275(51), pp. 40128-40133

HENRY-STANLEY, M.J. et al., 2010. Selected factors affecting *Staphylococcus aureus* within silastic catheters. *Journal of Surgical Research,* 161(2), pp. 202-208

HIRAMATSU, K. et al., 1997. Methicillin-resistant *Staphylococcus aureus* clinical strain with reduced vancomycin susceptibility. *Journal of Antimicrobial Chemotherapy,* 40(1), pp. 135-146

HØIBY, N. et al., 2010. Antibiotic resistance of bacterial biofilms. *International Journal of Antimicrobial Agents,* 35(4), pp. 322-332

HOQ, M.I., AOKI, T. and IBRAHIM, H.R., 2009. Triclosan-lysozyme complex: a promising antimicrobial macromolecule stable against photooxidative damage. *Food Research International,* 42(2), pp. 298-306

HOQ, M.I. and IBRAHIM, H.R., 2011. Potent antimicrobial action of triclosan–lysozyme complex against skin pathogens mediated through drug-targeted delivery mechanism. *European Journal of Pharmaceutical Sciences,* 42(1-2), pp. 130-137

HOU, S. et al., 2010. Effects of Trp- and Arg-containing antimicrobial-peptide structure on inhibition of *Escherichia coli* planktonic growth and biofilm formation. *Applied and Environmental Microbiology,* 76(6), pp. 1967-1974

HUANG, Y., HUANG, J. and CHEN, Y., 2010. Alpha-helical cationic antimicrobial peptides: relationships of structure and function. *Protein & Cell,* 1(2), pp. 143-152

HUERTA-FONTELA, M., GALCERAN, M.T. and VENTURA, F., 2011. Occurrence and removal of pharmaceuticals and hormones through drinking water treatment. *Water Research,* 45(3), pp. 1432-1442

HUSSAIN, R., JOANNOU, C. and SILIGARDI, G., 2006. Identification and characterization of novel lipophilic antimicrobial peptides derived from naturally occurring proteins. *International Journal of Peptide Research and Therapeutics,* 12(3), pp. 269-273

IMRANUL HOQ, M., AOKI, T. and IBRAHIM, H.R., 2009. Triclosan–lysozyme complex: a promising antimicrobial macromolecule stable against photooxidative damage. *Food Research International,* 42(2), pp. 298-306

ISHII, K.J. et al., 2008. Host innate immune receptors and beyond: making sense of microbial infections. *Cell Host & Microbe,* 3(6), pp. 352-363

JAMES, E.S. and CRONAN, J.E., 2003. Never fat or gaunt. *Developmental Cell,* 4(5), pp. 610-611

JANG, H.J. et al., 2008. Microarray analysis of toxicogenomic effects of triclosan on *Staphylococcus aureus*. *Applied Microbiology and Biotechnology,* 78(4), pp. 695-707

JAYARMAN, R., 2009. Antibiotic resistance: an overview of mechanisms and a paradigm shift. *Current Science,* 96(11), pp. 1475-1484

JOHNSON, D.R. et al., 2009. Toxicity of triclosan, penconazole and metalaxyl on *Caulobacter crescentus* and a freshwater microbial community as assessed by flow cytometry. *Environmental Microbiology,* 11(7), pp. 1682-1691

JOHNSTON, M.D. et al., 2003. Membrane damage to bacteria caused by single and combined biocides. *Journal of Applied Microbiology,* 94(6), pp. 1015-1023

JONES, R.D. et al., 2000. Triclosan: a review of effectiveness and safety in health care settings. *American Journal of Infection Control,* 28(2), pp. 184-196

KATSURAGI, T. et al., 2000. Gel microdroplet technique leaving microorganisms alive for sorting by flow cytometry. *Journal of Microbiological Methods,* 42(1), pp. 81-86

KHANDELIA, H., IPSEN, J.H. and MOURITSEN, O.G., 2008. The impact of peptides on lipid membranes. *Biochimica et Biophysica Acta,* 1778(7-8), pp. 1528-1536

KIM, C. and KAUFMANN, S.H.E., 2006. Defensin: a multifunctional molecule lives up to its versatile name. *Trends in Microbiology,* 14(10), pp. 428-431

KIM, J. et al., 2009. Clinical characteristics and risk factors of colistin-induced nephrotoxicity. *International Journal of Antimicrobial Agents,* 34(5), pp. 434-438

KIM, Y. et al., 2011. Triclosan susceptibility and co-metabolism – a comparison for three aerobic pollutant-degrading bacteria. *Bioresource Technology,* 102(3), pp. 2206-2212

KINDRACHUK, J. et al., 2007. The PhQ-activating potential of antimicrobial peptides contributes to antimicrobial efficacy and is predictive of the induction of bacterial resistance. *Antimicrobial Agents and Chemotherapy,* 51(12), pp. 4374-4381

KING, M.A., 2000. Detection of dead cells and measurement of cell killing by flow cytometry. *Journal of Immunological Methods,* 243(1-2), pp. 155-166

KOCH, A.L., ROBERTSON, B.R. and BUTTON, D.K., 1996. Deduction of the cell volume and mass from forward scatter intensity of bacteria analyzed by flow cytometry. *Journal of Microbiological Methods,* 27(1), pp. 49-61

KOHLER, T. et al., 2010. Quorum sensing inhibition selects for virulence and cooperation in *Pseudomonas aeruginosa*. *PLoS Pathogens,* 6(5), pp. e1000883

KRISHNAN, K. et al., 2010. Biomonitoring equivalents for triclosan. *Regulatory Toxicology and Pharmacology,* 58(1), pp. 10-17

KUFER, T.A. and SANSONETTI, P.J., 2007. Sensing of bacteria: NOD a lonely job. *Current Opinion in Microbiology,* 10(1), pp. 62-69

KUMAR, A. and SCHWEIZER, H.P., 2005. Bacterial resistance to antibiotics: active efflux and reduced uptake. *Advanced Drug Delivery Reviews,* 57(10), pp. 1486-1513

KUMMERER, K., 2009. Antibiotics in the aquatic environment--a review--part I. *Chemosphere,* 75(4), pp. 417-434

KWA, A. et al., 2007. Polymyxin B: similarities to and differences from colistin (polymyxin E). *Expert Review of Anti-Infective Therapy,* 5(5), pp. 811-821

LAI, S., TREMBLAY, J. and DEZIEL, E., 2009. Swarming motility: a multicellular behaviour conferring antimicrobial resistance. *Environmental Microbiology,* 11(1), pp. 126-136

LAI, X.Z. et al., 2008. Ceragenins: cholic acid-based mimics of antimicrobial peptides. *Accounts of Chemical Research,* 41(10), pp. 1233-1240

LAMBERT, P., 2004. Mechanisms of action of antibiotics and synthetic anti-infective agents. In: S.P. DENYER, N.A. HODGES and S.P. GORMAN, eds. *Hugo and Russell's pharmaceutical microbiology.* 7th ed. Oxford: Blackwell Publishing. pp. 202-219

LANDINI, P. et al., 2010. Molecular mechanisms of compounds affecting bacterial biofilm formation and dispersal. *Applied Microbiology and Biotechnology,* 86(3), pp. 813-823

LANGE, R. and HENGGE-ARONIS, R., 1991. Growth phase-regulated expression of bolA and morphology of stationary-phase *Escherichia coli* cells are controlled by the novel sigma factor sigma S. *Journal of Bacteriology,* 173(14), pp. 4474-4481

LANGHAM, A.A., AHMAD, A.S. and KAZNESSIS, Y.N., 2008. On the nature of antimicrobial activity: a model for protegrin-1 pores. *Journal of the American Chemical Society,* 130(13), pp. 4338-4346

LARKIN, M., 2004. Lack of new anti-infectives spurs call for action. *The Lancet Infectious Diseases,* 4(6), pp. 317

LATOSIŃSKA, J.N., TOMCZAK, M.A. and KASPRZAK, J., 2008. Thermal stability and molecular dynamics of triclosan in solid state studied by 35Cl–NQR spectroscopy and DFT calculations. *Chemical Physics Letters,* 462(4-6), pp. 284-288

LAUTENBACH, E. et al., 2004. Longitudinal trends in fluoroquinolone resistance among enterobacteriaceae isolates from inpatient and outpatients, 1989-2000: differences in the emergence and epidemiology of resistance across organisms. *Clinical Infectious Diseases,* 38, pp. 655-662

LERNER, P., 2004. Producing penicillin. *New England Journal of Medicine,* 351(6), pp. 524-532

LEVY, S. and MARSHALL, B., 2004. Antibacterial resistance worldwide; causes, challenges and responses. *Nature Medicine,* 10((Suppl)), pp. S122-S129

LEVY, C.W. et al., 1999. Molecular basis of triclosan activity. *Nature,* 398(6726), pp. 383-384

LI, J. et al., 2005. Evaluation of colistin as an agent against multi-resistant Gram-negative bacteria. *International Journal of Antimicrobial Agents,* 25(1), pp. 11-25

LI, J. et al., 2006. Colistin: the re-emerging antibiotic for multidrug-resistant Gram-negative bacterial infections. *The Lancet Infectious Diseases,* 6(9), pp. 589-601

LI, M. et al., 2007. The antimicrobial peptide-sensing system aps of *Staphylococcus aureus*. *Molecular Microbiology,* 66(5), pp. 1136-1147

LIN, Y.M. et al., 2010. Outer membrane protein I of *Pseudomonas aeruginosa* is a target of cationic antimicrobial peptide/protein. *Journal of Biological Chemistry,* 285(12), pp. 8985-8994

LIU, F. et al., 2009. Terrestrial ecotoxicological effects of the antimicrobial agent triclosan. *Ecotoxicology and Environmental Safety,* 72(1), pp. 86-92

LOEWE, L., TEXTOR, V. and SCHERER, S., 2003. High deleterious genomic mutation rate in stationary phase of *Escherichia coli*. *Science,* 302(5650), pp. 1558-1560

LOHNER, K. and BLONDELLE, S.E., 2005. Molecular mechanisms of membrane perturbation by antimicrobial peptides and the use of biophysical studies in the

design of novel peptide antibiotics. *Combinatorial Chemistry & High Throughput Screening,* 8(3), pp. 241-256

LOOSE, C. et al., 2006. A linguistic model for the rational design of antimicrobial peptides. *Nature,* 443(7113), pp. 867-869

LORIAN, V., 1975. Some Effects of subinhibitory concentrations of penicillin on the structure and division of Staphylococci. *Antimicrobial Agents and Chemotherapy,* 7(6), pp. 864-870

LU, H. and TONGE, P.J., 2010. Drug–target residence time: critical information for lead optimization. *Current Opinion in Chemical Biology,* 14(4), pp. 467-474

LUCKNER, S.R. et al., 2010. A slow, tight binding inhibitor of InhA, the enoyl-acyl carrier protein reductase from *Mycobacterium tuberculosis*. *Journal of Biological Chemistry,* 285(19), pp. 14330-14337

LUPETTI, A. et al., 2003. Radiolabelled antimicrobial peptides for infection detection. *The Lancet Infectious Diseases,* 3(4), pp. 223-229

LYNCH, A.S., 2006. Efflux systems in bacterial pathogens: an opportunity for therapeutic intervention? An industry view. *Biochemical Pharmacology,* 71(7), pp. 949-956

LYON, G.J. and NOVICK, R.P., 2004. Peptide signaling in *Staphylococcus aureus* and other Gram-positive bacteria. *Peptides,* 25(9), pp. 1389-1403

MACADAM, H. et al., 2006. Investigating the association between antibiotic use and antibiotic resistance: impact of different methods of categorising prior antibiotic use. *International Journal of Antimicrobial Agents,* 28(4), pp. 325-332

MAILLARD, J.Y., 2005. Antimicrobial biocides in the healthcare environment: efficacy, usage, policies, and perceived problems. *Therapeutics and Clinical Risk Management,* 1(4), pp. 307-320

MAILLARD, J.-., 2007. Bacterial resistance to biocides in the healthcare environment: should it be of genuine concern? *Journal of Hospital Infection,* 65(Supplement 2), pp. 60-72

MAILLARD, J.Y. and DENYER, S.P., 2009. Emerging bacterial resistance following biocide exposure: should we be concerned? *Chimica Oggi-Chemistry Today,* 27(3), pp. 26-28

MARINELLI, F. and TOMASZ, A., 2010. Antimicrobials. *Current Opinion in Microbiology,* 13(5), pp. 547-550

MARR, A.K., GOODERHAM, W.J. and HANCOCK, R.E., 2006. Antibacterial peptides for therapeutic use: obstacles and realistic outlook. *Current Opinion in Pharmacology,* 6(5), pp. 468-472

MARTIN, N. and DODDS, C., 2006. Protective mechanisms of the body. *Anaesthesia & Intensive Care Medicine,* 7(12), pp. 459-461

MARTINEZ, J.L. et al., 2009. A global view of antibiotic resistance. *FEMS Microbiology Reviews,* 33(1), pp. 44-65

MATSUMOTO, K. et al., 2010. Flow cytometric analysis of the contributing factors for antimicrobial activity enhancement of cell-penetrating type peptides: case study on engineered apidaecins. *Biochemical and Biophysical Research Communications,* 395(1), pp. 7-10

MATSUZAKI, K., 2009. Control of cell selectivity of antimicrobial peptides. *Biochimica et Biophysica Acta (BBA) - Biomembranes,* 1788(8), pp. 1687-1692

MATTHEWS, K.H. et al., 2005. Lyophilised wafers as a drug delivery system for wound healing containing methylcellulose as a viscosity modifier. *International Journal of Pharmaceutics,* 289(1-2), pp. 51-62

MATTHEWS, K.H. et al., 2006. Gamma-irradiation of lyophilised wound healing wafers. *International Journal of Pharmaceutics,* 313(1-2), pp. 78-86

MATTHEWS, K.H. et al., 2008. Formulation, stability and thermal analysis of lyophilised wound healing wafers containing an insoluble MMP-3 inhibitor and a non-ionic surfactant. *International Journal of Pharmaceutics,* 356(1-2), pp. 110-120

MATTIUZZO, M. et al., 2007. Role of the *Escherichia coli* SbmA in the antimicrobial activity of proline-rich peptides. *Molecular Microbiology,* 66(1), pp. 151-163

MAVIGLIA, R., NESTORINI, R. and PENNISI, M., 2009. Role of old antibiotics in multidrug resistant bacterial infections. *Current Drug Targets,* 10(9), pp. 895-905

MAYER, M.L. and HANCOCK, R.E.W., 2010. Cathelicidins link the endocrine and immune systems. *Cell Host & Microbe,* 7(4), pp. 257-259

MCBAIN, A.J. and GILBERT, P., 2001. Biocide tolerance and the harbingers of doom. *International Biodeterioration & Biodegradation,* 47(2), pp. 55-61

MCBAIN, A.J. et al., 2004. Selection for high-level resistance by chronic triclosan exposure is not universal. *Journal of Antimicrobial Chemotherapy,* 53(5), pp. 772-777

MCBRIDE, M.C. et al., 2009. Persistence of antimicrobial activity through sustained release of triclosan from pegylated silicone elastomers. *Biomaterials,* 30(35), pp. 6739-47

MCMURRAY, L.A., OETHINGER, M. and LEVY, S.B., 1998. Triclosan targets lipid synthesis. *Nature,* 394, pp. 531-532

MCNAMARA, P.J. et al., 2009. Surfactants, aromatic and isoprenoid compounds, and fatty acid biosynthesis inhibitors suppress staphylococcus aureus production of

toxic shock syndrome toxin 1. *Antimicrobial Agents and Chemotherapy,* 53(5), pp. 1898-1906

MEADE, M.J., WADDELL, R.L. and CALLAHAN, T.M., 2001. Soil bacteria *Pseudomonas putida* and *Alcaligenes xylosoxidans* subsp. *denitrificans* inactivate triclosan in liquid and solid substrates. *FEMS Microbiology Letters,* 204(1), pp. 45-48

MELICHERCÍKOVÁ, V., URBAN, J. and GORONCY-BERMES, P., 2010. Residual effect of antiseptic substances on human skin. *Journal of Hospital Infection,* 75(3), pp. 238-239

MÉNDEZ-SAMPERIO, P., 2008. Role of antimicrobial peptides in host defense against mycobacterial infections. *Peptides,* 29(10), pp. 1836-1841

MEYER, B. and COOKSON, B., 2010. Does microbial resistance or adaptation to biocides create a hazard in infection prevention and control? *Journal of Hospital Infection,* 76(3), pp. 200-205

MEYLAN, E., TSCHOPP, J. and KARIN, M., 2006. Intracellular pattern recognition receptors in the host response. *Nature,* 442(7098), pp. 39-44

MICHALEK, M. et al., 2009. The human antimicrobial protein psoriasin acts by permeabilization of bacterial membranes. *Developmental and Comparative Immunology,* 33(6), pp. 740-746

MILNE, K.E. and GOULD, I.M., 2010. Combination testing of multidrug-resistant cystic fibrosis isolates of *Pseudomonas aeruginosa*: use of a new parameter, the susceptible breakpoint index. *Journal of Antimicrobial Chemotherapy,* 65(1), pp. 82-90

MIMA, T. et al., 2007. Identification and characterization of TriABC-OpmH, a triclosan efflux pump of *Pseudomonas aeruginosa* requiring two membrane fusion proteins. *Journal of Bacteriology,* 189(21), pp. 7600-7609

MISHRA, S. et al., 2008. Design, synthesis, and application of novel triclosan prodrugs as potential antimalarial and antibacterial agents. *Bioorganic & Medicinal Chemistry,* 16(10), pp. 5536-5546

MOELLERING JR., R.C., 2011. Discovering new antimicrobial agents. *International Journal of Antimicrobial agents,* 37(1), pp. 2-9

MONTANARO, L., CAMPOCCIA, D. and ARCIOLA, C.R., 2007. Advancements in molecular epidemiology of implant infections and future perspectives. *Biomaterials,* 28(34), pp. 5155-5168

MONTERO, M. et al., 2009. Effectiveness and safety of colistin for the treatment of multidrug-resistant *Pseudomonas aeruginosa* infections. *Infection,* 37(5), pp. 461-465

MORTENSEN, N.P. et al., 2009. Effects of colistin on surface ultrastructure and nanomechanics of *Pseudomonas aeruginosa* cells. *Langmuir : the ACS Journal of Surfaces and Colloids,* 25(6), pp. 3728-3733

MURRAY, C.J. and LOPEZ, A.D., 1997. Mortality by cause for eight regions of the world: Global Burden of Disease Study. *The Lancet,* 349(9061), pp. 1269-1276

MUSK, D.J.,JR and HERGENROTHER, P.J., 2008. Chelated iron sources are inhibitors of *Pseudomonas aeruginosa* biofilms and distribute efficiently in an in vitro model of drug delivery to the human lung. *Journal of Applied Microbiology,* 105(2), pp. 380-388

MYGIND, P.H. et al., 2005. Plectasin is a peptide antibiotic with therapeutic potential from a saprophytic fungus. *Nature,* 437(7061), pp. 975-980

NASNAS, R., SALIBA, G. and HALLAK, P., 2009. The revival of colistin: an old antibiotic for the 21st century. *Pathologie Biologie,* 57(3), pp. 229-235

NATION, R.L. and LI, J., 2009. Colistin in the 21st century. *Current Opinion in Infectious Diseases,* 22(6), pp. 535-543

NEBE-VON-CARON, G. et al., 2000. Analysis of bacterial function by multi-colour fluorescence flow cytometry and single cell sorting. *Journal of Microbiological Methods,* 42(1), pp. 97-114

NEONAKIS, I.K., SPANDIDOS, D.A. and PETINAKI, E., 2011. Confronting multidrug-resistant *Acinetobacter baumannii*: a review. *International Journal of Antimicrobial Agents,* 37(2), pp. 102-109

NIZET, V., 2007. Understanding how leading bacterial pathogens subvert innate immunity to reveal novel therapeutic targets. *Journal of Allergy and Clinical Immunology,* 120(1), pp. 13-22

NORDMANN, P. et al., 2007. Superbugs in the coming new decade; multidrug resistance and prospects for treatment of *Staphylococcus aureus, Enterococcus* spp. and *Pseudomonas aeruginosa* in 2010. *Current Opinion in Microbiology,* 10(5), pp. 436-440

NUDING, S. et al., 2006. A flow cytometric assay to monitor antimicrobial activity of defensins and cationic tissue extracts. *Journal of Microbiological Methods,* 65(2), pp. 335-345

NURYASTUTI, T. et al., 2009. Effect of cinnamon oil on icaA expression and biofilm formation by *Staphylococcus epidermidis. Applied and Environmental Microbiology,* 75(21), pp. 6850-6855

OTTO, M., 2004. Quorum-sensing control in Staphylococci -- a target for antimicrobial drug therapy? *FEMS Microbiology Letters,* 241(2), pp. 135-141

OUBERAI, M. et al., 2011. The *Pseudomonas aeruginosa* membranes: a target for a new amphiphilic aminoglycoside derivative? *Biochimica et Biophysica Acta (BBA) - Biomembranes, 1808*(6), pp. 1716-1727

PAPAGIANNI, M., 2003. Ribosomally synthesized peptides with antimicrobial properties: biosynthesis, structure, function, and applications. *Biotechnology Advances,* 21(6), pp. 465-499

PAPPAS, G., SAPLAOURA, K. and FALAGAS, M.E., 2009. Current treatment of pseudomonal infections in the elderly. *Drugs & Aging,* 26(5), pp. 363-379

PARISIEN, A. et al., 2008. Novel alternatives to antibiotics: bacteriophages, bacterial cell wall hydrolases, and antimicrobial peptides. *Journal of Applied Microbiology,* 104(1), pp. 1-13

PAUL, K.B. et al., 2010. Short-term exposure to triclosan decreases thyroxine in vivo via upregulation of hepatic catabolism in Young Long-Evans rats. *Toxicological Sciences,* 113(2), pp. 367-379

PEARCE, H., MESSAGER, S. and MAILLARD, J.Y., 1999. Effect of biocides commonly used in the hospital environment on the transfer of antibiotic-resistance genes in *Staphylococcus aureus*. *Journal of Hospital Infection,* 43(2), pp. 101-107

PEARSON, H., 2005. A nod in the right direction. *Nature,* 433, pp. 594

PEREIRA, H.A., 2006. Novel therapies based on cationic antimicrobial peptides. *Current Pharmaceutical Biotechnology,* 7(4), pp. 229-234

PERRON, G.G., ZASLOFF, M. and BELL, G., 2005. Experimental evolution of resistance to an antimicrobial peptide. *Proceedings of the Royal Society B,* 273, pp. 251-256

PIZARRO-CERDÁ, J. and COSSART, P., 2006. Bacterial adhesion and entry into host cells. *Cell,* 124(4), pp. 715-727

PORTER, J. and PICKUP, R.W., 2000. Nucleic acid-based fluorescent probes in microbial ecology: application of flow cytometry. *Journal of Microbiological Methods,* 42(1), pp. 75-79

PROJAN, S.J., 2002. New (and not so new) antibacterial targets – from where and when will the novel drugs come? *Current Opinion in Pharmacology,* 2(5), pp. 513-522

PROJAN, S.J. and BRADFORD, P.A., 2007. Late stage antibacterial drugs in the clinical pipeline. *Current Opinion in Microbiology,* 10(5), pp. 441-446

QIAN, L., GUAN, Y. and XIAO, H., 2008. Preparation and characterization of inclusion complexes of a cationic β-cyclodextrin polymer with butylparaben or triclosan. *International Journal of Pharmaceutics,* 357(1-2), pp. 244-251

QUADRI LUIS, E.N., 2007. Strategic paradigm shifts in the antimicrobial drug discovery process of the 21st century. *Infectious Disorders - Drug Targets,* 7(3), pp. 230-237

QUECKENBERG, C. et al., 2010. Absorption, pharmacokinetics, and safety of triclosan after dermal administration. *Antimicrobial Agents and Chemotherapy,* 54(1), pp. 570-572

RADTKE, A.L. and O'RIORDAN, M.X.D., 2006. Intracellular innate resistance to bacterial pathogens. *Cellular Microbiology,* 8(11), pp. 1720-1729

RAND, J.D., DANBY, S.G., GREENWAY, D.L.A. and ENGLAND, R.R., 2002. Increased expression of the multidrug efflux genes acrAB occurs during slow growth of *Escherichia coli*. *FEMS microbiology letters,* 207(1), pp. 91-95

RANDALL, L.P. et al., 2007. Commonly used farm disinfectants can select for mutant *Salmonella enterica serovar Typhimurium* with decreased susceptibility to biocides and antibiotics without compromising virulence. *Journal of Antimicrobial Chemotherapy,* 60(6), pp. 1273-1280

RATCLIFFE, N.A., MELLO, C.B., GARCIA, E.S., BUTT, T.M. and AZAMBUJA, P., 2011. Insect natural products and processes: New treatments for human disease. *Insect biochemistry and molecular biology,* In Press, Corrected Proof

RATTANAUMPAWAN, P., UNGPRASERT, P. and THAMLIKITKUL, V., 2011. Risk factors for colistin-associated nephrotoxicity. *Journal of Infection,* 62(2), pp. 187-190

REDDY, K.V.R., YEDERY, R.D. and ARANHA, C., 2004. Antimicrobial peptides: premises and promises. *International Journal of Antimicrobial Agents,* 24(6), pp. 536-547

REDFERN, R.L., REINS, R.Y. and MCDERMOTT, A.M., 2011. Toll-like receptor activation modulates antimicrobial peptide expression by ocular surface cells. *Experimental Eye Research,* 92(3), pp. 209-220

RENZONI, A. et al., 2010. Exploring innate glycopeptide resistance mechanisms in Staphylococcus aureus. *Trends in Microbiology,* 18(2), pp. 55-56

RICE, L.B., 2006. Antimicrobial resistance in gram-positive bacteria. *American Journal of Infection Control,* 34(5, Supplement 1), pp. S11-S19

RIEG, S. et al., 2009. Resistance against antimicrobial peptides is independent of *Escherichia coli AcrAB, Pseudomonas aeruginosa MexAB* and *Staphylococcus aureus NorA* efflux pumps. *International Journal of Antimicrobial Agents,* 33(2), pp. 174-176

RIESEBERG, M. et al., 2001. Flow cytometry in biotechnology. *Applied Microbiology Biotechnology,* 56, pp. 350-360

RITTER, S.K., 2007. Fluorous peptides get ready to heal. *Chemical & Engineering News: Science & Technology,* 85(37), pp. 36-37

ROCK, C.O. and JACKOWSKI, S., 2002. Forty years of bacterial fatty acid synthesis. *Biochemical and Biophysical Research Communications,* 292(5), pp. 1155-1166

ROKITSKAYA, T.I. et al., 2011. Indolicidin action on membrane permeability: Carrier mechanism versus pore formation. *Biochimica et Biophysica Acta (BBA) - Biomembranes,* 1808(1), pp. 91-97

ROOSILD, T.P. et al., 2009. KTN (RCK) domains regulate K+ channels and transporters by controlling the Dimer-Hinge conformation. *Structure,* 17(6), pp. 893-903

RUSSELL, A.D., 2001. Mechanisms of bacterial insusceptibility to biocides. *American Journal of Infection Control,* 29(4), pp. 259-261

RUSSELL, A.D., 2004. Whither triclosan? *Journal of Antimicrobial Chemotherapy,* 53(5), pp. 693-695

RUSSELL, A.D., 2002. Mechanisms of antimicrobial action of antiseptics and disinfectants: an increasingly important area of investigation. *Journal of Antimicrobial Chemotherapy,* 49(4), pp. 597-599

RUSSELL, A.D., 2003. Similarities and differences in the responses of microorganisms to biocides. *Journal of Antimicrobial Chemotherapy,* 52(5), pp. 750-763

RUSSELL, A.D., 2004. Bacterial adaptation and resistance to antiseptics, disinfectants and preservatives is not a new phenomenon. *Journal of Hospital Infection,* 57(2), pp. 97-104

RUSSELL, A.D. and MCDONNELL, G., 2000. Concentration: a major factor in studying biocidal action. *Journal of Hospital Infection,* 44(1), pp. 1-3

RUSSELL, A., 2003. Biocide use and antibiotic resistance: the relevance of laboratory findings to clinical and environmental situations. *The Lancet Infectious Diseases,* 3(12), pp. 794-803

SADER, H.S. and JONES, R.N., 1992. Historical overview of the cephalosporin spectrum: Four generations of structural evolution. *Antimicrobic Newsletter,* 8(12), pp. 75-82

SALTON, M.R.J. and KIM, K.S., 1996. Structure. In: S. BARON, ed. *Medical Microbiology.* 4th ed. Galveston (TX): The University of Texas Medical Branch at Galveston. 326-359

SANDBORGH-ENGLUND, G. et al., 2006. Pharmacokinetics of triclosan following oral ingestion in humans. *Journal of Toxicology and Environmental Health.Part A,* 69(20), pp. 1861-1873

SASAKAWA, C. and HACKER, J., 2006. Host-microbe interaction: bacteria. *Current Opinion in Microbiology,* 9(1), pp. 1-4

SAXENA, S. and GOMBER, C., 2010. Surmounting antimicrobial resistance in the millenium superbug: *Staphylococcus aureus*. *Central European Journal of Medicine,* 5(1), pp. 12-29

SCHAUBER, J. et al., 2006. Control of the innate epithelial antimicrobial response is cell-type specific and dependent on relevant microenvironmental stimuli. *Immunology,* 118, pp. 509-519

SCHAUBER, J. and GALLO, R.L., 2008. Antimicrobial peptides and the skin immune defense system. *Journal of Allergy and Clinical Immunology,* 122(2), pp. 261-266

SCHNEIDER, T. and SAHL, H., 2010. An oldie but a goodie – cell wall biosynthesis as antibiotic target pathway. *International Journal of Medical Microbiology,* 300(2-3), pp. 161-169

SCHWEIZER, H.P., 2001. Triclosan: a widely used biocide and its link to antibiotics. *FEMS Microbiology Letters,* 202(1), pp. 1-7

SEAMAN, P.F., OCHS, D. and DAY, M., 2006. Small-colony variants: a novel mechanism for triclosan resistance in methicillin-resistant *Staphylococcus aureus*. *Journal of Antimicrobial Chemotherapy,* 59, pp. 43-50

SENGUPTA, D. et al., 2008. Toroidal pores formed by antimicrobial peptides show significant disorder. *Biochimica et Biophysica Acta (BBA) - Biomembranes,* 1778(10), pp. 2308-2317

SHAI, Y., 1999. Mechanism of the binding, insertion and destabilization of phospholipid bilayer membranes by alpha-helical antimicrobial and cell non-selective membrane-lytic peptides. *Biochimica et Biophysica Acta,* 1462(1-2), pp. 55-70

SHAPIRO, H.M., 2000. Microbial analysis at the single-cell level: tasks and techniques. *Journal of Microbiological Methods,* 42(1), pp. 3-16

SHLAES, D. and MOELLERING, R., 2002. The United States Food and Drug Administration and the end of antibiotics. *Clinical Infectious Diseases,* 34(4), pp. 420-422

SHUKLA, A. et al., 2010. Controlling the release of peptide antimicrobial agents from surfaces. *Biomaterials,* 31(8), pp. 2348-2357

SINGH, R. et al., 2009. Role of persisters and small-colony variants in antibiotic resistance of planktonic and biofilm-associated *Staphylococcus aureus*: an in vitro study. *Journal of Medical Microbiology,* 58(Pt 8), pp. 1067-1073

SINGLETON, P., 1999. *Bacteria, in biology, biotechnology and medicine.* 5th ed. Chichester: John Wiley and Sons Ltd. pp. 39-40, 88-89, 252-253

SKIADA, A. et al., 2011. Adaptive resistance to cationic compounds in *Pseudomonas aeruginosa*. *International Journal of Antimicrobial Agents,* 37(3), pp. 187-193

SMALL, P.L. and VAN DER GOOT, G., 2007. Editorial overview. *Current Opinion in Microbiology,* 10(1), pp. 1-3

STALLMANN, H.P. et al., 2006. Antimicrobial peptides: review of their application in musculoskeletal infections. *Injury,* 37(2, Supplement 1), pp. S34-S40

STEEN, H.B., 2000. Flow cytometry of bacteria: glimpses from the past with a view to the future. *Journal of Microbiological Methods,* 42(1), pp. 65-74

STEINBERG, D.A. et al., 1997. Protegrin-1: a broad-spectrum, rapidly microbicidal peptide with in vivo activity. *Antimicrobial Agents and Chemotherapy,* 41(8), pp. 1738-1742

SULLER, M.T. and RUSSELL, A.D., 1999. Antibiotic and biocide resistance in methicillin-resistant *Staphylococcus aureus* and vancomycin-resistant enterococcus. *Journal of Hospital Infection,* 43(4), pp. 281-291

SULLER, M.T. and RUSSELL, A.D., 2000. Triclosan and antibiotic resistance in *Staphylococcus aureus*. *Journal of Antimicrobial Chemotherapy,* 46(1), pp. 11-18

SUPP, D.M. and NEELY, A.N., 2008. Cutaneous antimicrobial gene therapy: engineering human skin replacements to combat wound infection. *Expert Review Dermatology,* 3(1), pp. 73-84

SUTTERWALA, F.S. and FLAVELL, R.A., 2008. Immunology: cascade into clarity. *Nature,* 451(7176), pp. 254-255

TAKAHASHI, D. et al., 2010. Structural determinants of host defense peptides for antimicrobial activity and target cell selectivity. *Biochimie,* 92(9), pp. 1236-1241

TAM, V.H. et al., 2010. Prevalence, resistance mechanisms, and susceptibility of multidrug-resistant bloodstream isolates of *Pseudomonas aeruginosa*. *Antimicrobial Agents and Chemotherapy,* 54(3), pp. 1160-1164

TATTAWASART, U. et al., 1999. Development of resistance to chlorhexidine diacetate and cetylpyridinium chloride in *Pseudomonas stutzeri* and changes in antibiotic susceptibility. *Journal of Hospital Infection,* 42(3), pp. 219-229

TATTAWASART, U. et al., 2000. Outer membrane changes in *Pseudomonas stutzeri* resistant to chlorhexidine diacetate and cetylpyridinium chloride. *International Journal of Antimicrobial Agents,* 16(3), pp. 233-238

TATTOLI, I. et al., 2007. The Nodosome: Nod1 and Nod2 control bacterial infections and inflammation. *Seminars in Immunopathology,* 29(3), pp. 289-301

TELES, R.P. and TELES, F.R.F., 2009. Antimicrobial agents used in the control of periodontal biofilms: effective adjuncts to mechanical plaque control? *Brazilian Oral Research,* 23(Supplement 1), pp. 39-48

TENOVER, F. et al., 2004. Vancomycin-resistant *Staphylococcus aureus* isolate from a patient in Pennsylvania. *Antimicrobial Agents and Chemotherapy,* 48(1), pp. 275-280

TENOVER, F.C. and MCGOWAN JR., J.E., 2008. Antimicrobial Resistance. In: K. HEGGENHOUGEN, ed. *International Encyclopedia of Public Health.* Oxford: Academic Press. pp. 211-219

THOMPSON, A. et al., 2005. The fate and removal of triclosan during wastewater treatment. *Water Environment Research,* 77(1), pp. 63-67

TKACHENKO, O. et al., 2007. A triclosan-ciprofloxacin cross-resistant mutant strain of *Staphylococcus aureus* displays an alteration in the expression of several cell membrane structural and functional genes. *Research in Microbiology,* 158(8-9), pp. 651-658

TREVORS, J.T., 2011. Viable but non-culturable (VBNC) bacteria: Gene expression in planktonic and biofilm cells. *Journal of microbiological methods,* 86(2), pp. 266-273

UDOMTHAVORNSUK, B., TATSANAVIVAT, P. and PATJANASOONTORN, B., 1991. Intervention of inappropriate antibiotic use at a teaching hospital. *Journal of the Medical Association of Thailand,* 74(10), pp. 429-436

UENO, S. et al., 2010. An enhancer peptide for membrane-disrupting antimicrobial peptides. *BMC Microbiology,* 10, pp. 46

VAARA, M., 2010. Polymyxins and their novel derivatives. *Current Opinion in Microbiology,* 13(5), pp. 574-581

VALDIVIA, R.H. and FALKOW, S., 1998. Flow cytometry and bacterial pathogenesis. *Current Opinion in Microbiology,* 1(3), pp. 359-363

VAN BAMBEKE, F. et al., 2008. The bacterial envelope as a target for novel anti-MRSA antibiotics. *Trends in Pharmacological Sciences,* 29(3), pp. 124-134

VAN BLOOIS, E. et al., 2011. Decorating microbes: surface display of proteins on *Escherichia coli*. *Trends in Biotechnology,* 29(2), pp. 79-86

VAUGHAN, A.M. et al., 2009. Type II fatty acid synthesis is essential only for malaria parasite late liver stage development. *Cellular Microbiology,* 11(3), pp. 506-520

VEAL, D.A. et al., 2000. Fluorescence staining and flow cytometry for monitoring microbial cells. *Journal of Immunological Methods,* 243(1-2), pp. 191-210

VELICER, G.J., 2003. Social strife in the microbial world. *Trends in Microbiology,* 11(7), pp. 330-337

VELKOV, T. et al., 2010. Structure--activity relationships of polymyxin antibiotics. *Journal of Medicinal Chemistry,* 53(5), pp. 1898-1916

VERDURMEN, W.P.R. and BROCK, R., 2011. Biological responses towards cationic peptides and drug carriers. *Trends in Pharmacological Sciences,* 32(2), pp. 116-124

VILLALAÍN, J. et al., 2001. Membranotropic effects of the antibacterial agent triclosan. *Archives of Biochemistry and Biophysics,* 390(1), pp. 128-136

VULIC, M. and KOLTER, R., 2001. Evolutionary cheating in *Escherichia coli* stationary phase cultures. *Genetics,* 158(2), pp. 519-526

VYLKOVA, S. et al., 2006. Distinct antifungal mechanisms: beta-defensins require *Candida albicans Ssa1* protein, while Trk1p mediates activity of cysteine-free cationic peptides. *Antimicrobial Agents and Chemotherapy,* 50(1), pp. 324-331

WALSH, S.E. et al., 2003. Development of bacterial resistance to several biocides and effects on antibiotic susceptibility. *Journal of Hospital Infection,* 55(2), pp. 98-107

WANG, G., 2010. Structure, dynamics and mapping of membrane-binding residues of micelle-bound antimicrobial peptides by natural abundance 13C NMR spectroscopy. *Biochimica et Biophysica Acta (BBA) - Biomembranes,* 1798(2), pp. 114-121

WANG, G., 2007. Tool developments for structure-function studies of host defense peptides. *Protein & Peptide Letters,* 14, pp. 57-69

WANG, H. et al., 2011. Comparison of methods for measuring viable *E. coli* cells during cultivation: Great differences in the early and late exponential growth phases. *Journal of Microbiological Methods,* 84(1), pp. 140-143

WATANABE, M. et al., 1990. In vitro emergence of quinolone-resistant mutanta of *Escherischia coli*, *Enterobacter cloacae*, and *Serratia marcescens*. *Antimicrobial Agents and Chemotherapy,* 34(1), pp. 173-175

WEBBER, M.A. and PIDDOCK, L.J.V., 2003. The importance of efflux pumps in bacterial antibiotic resistance. *Journal of Antimicrobial Chemotherapy,* 51(1), pp. 9-11

WHITE, D.G. and MCDERMOTT, P.F., 2001. Biocides, drug resistance and microbial evolution. *Current opinion in microbiology,* 4(3), pp. 313-317

WOOD, P.J., 2006. The immune system: recognition of infectious agents. *Anaesthesia & Intensive Care Medicine,* 7(6), pp. 179-180

WOODS, C.R., 2006. Antimicrobial resistance: mechanisms and strategies. *Paediatric Respiratory Reviews,* 7(Supplement 1), pp. S128-S129

WRIGHT, G.D., 2005. Bacterial resistance to antibiotics: enzymatic degradation and modification. *Advanced Drug Delivery Reviews,* 57(10), pp. 1451-1470

WRIGHT, H.T. and REYNOLDS, K.A., 2007. Antibacterial targets in fatty acid biosynthesis. *Current Opinion in Microbiology,* 10(5), pp. 447-453

XIA, G., KOHLER, T. and PESCHEL, A., 2010. The wall teichoic acid and lipoteichoic acid polymers of *Staphylococcus aureus*. *International Journal of Medical Microbiology,* 300(2-3), pp. 148-154

XU, Y., TILLMAN, T.S. and TANG, P., 2009. Membranes and drug action. In: M. HACKER, W. MESSER and K. BACHMANN, eds. *Pharmacology.* San Diego: Academic Press. pp. 31-61

YACOBY, I. and BENHAR, I., 2007. Targeted anti bacterial therapy. *Infectious Disorders - Drug Targets,* 7(3), pp. 221-229

YANG, D. et al., 2000. Human neutrophil defensins selectively chemoattract naive T and immature dendritic cells. *Journal of Leukocyte Biology,* 68(1), pp. 9-14

YANG, L. et al., 2010. Evaluation of *enoyl-acyl carrier protein reductase* inhibitors as *Pseudomonas aeruginosa* quorum-quenching reagents. *Molecules,* 15(2), pp. 780-792

YOO, B. and KIRSHENBAUM, K., 2008. Peptoid architectures: elaboration, actuation, and application. *Current Opinion in Chemical Biology,* 12(6), pp. 714-721

YU, B.J., KIM, J.A. and PAN, J.G., 2010. Signature gene expression profile of triclosan-resistant *Escherichia coli*. *Journal of Antimicrobial Chemotherapy,* 65(6), pp. 1171-1177

ZAIOU, M., 2007. Multifunctional antimicrobial peptides: therapeutic targets in several human diseases. *Journal of Molecular Medicine,* 85(4), pp. 317-329

ZAVASCKI, A.P., GOLDANI, L.Z., LI, J. and NATION, R.L., 2007. Polymyxin B for the treatment of multidrug-resistant pathogens: a critical review. *The Journal of antimicrobial chemotherapy,* 60(6), pp. 1206-1215

ZHANG, L. and FALLA, T.J., 2006. Antimicrobial peptides: therapeutic potential. *Expert opinion on pharmacotherapy,* 7(6), pp. 653-663

ZGURSKAYA, H.I. et al., 2009. Structural and functional diversity of bacterial membrane fusion proteins. *Biochimica et Biophysica Acta,* 1794(5), pp. 794-807

ZHANG, H., MACHUTTA, C.A. and TONGE, P.J., 2010. Fatty acid biosynthesis and oxidation. In: L. MANDER and H. LIU, eds. *Comprehensive natural products II.* Oxford: Elsevier. pp. 231-275

ZHANG, L. et al., 2005. Antimicrobial peptide therapeutics for cystic fibrosis. *Antimicrobial Agents and Chemotherapy,* 49(7), pp. 2921-2927

ZHANG, L. and FALLA, T.J., eds. 2010. Potential therapeutic application of host defense peptides. In: A. GIULIANI and A.C.RINALDI, eds. *Antimicrobial peptides: methods and protocols.* New York: Humana Press. pp. 303-327

ZHENG, C.J., SOHN, M.J. and KIM, W.G., 2009. Vinaxanthone, a new *FabI* inhibitor from Penicillium sp. *Journal of Antimicrobial Chemotherapy,* 63(5), pp. 949-953

ZHU, L. et al., 2010. Triclosan resistance of *Pseudomonas aeruginosa PAO1* is due to *FabV*, a triclosan-resistant enoyl-acyl carrier protein reductase. *Antimicrobial Agents and Chemotherapy,* 54(2), pp. 689-698

ZIEGLER, A., 2008. Thermodynamic studies and binding mechanisms of cell-penetrating peptides with lipids and glycosaminoglycans. *Advanced Drug Delivery Reviews,* 60(4-5), pp. 580-597

ZORKO, M. and JERALA, R., eds. 2010. Production of recombinant antimicrobial peptides in bacteria. In: A. GIULIANI and A.C.RINALDI, eds. *Antimicrobial peptides: methods and protocols.* New York: Humana Press. pp. 61-76

Conference Publications

Society for General Microbiology Harrogate UK March 30th – April 2nd 2009: Poster presentation entitled; Effect of Triclosan upon morphology and cell integrity of *Escherichia coli.*

British Pharmaceutical Conference Manchester Sept 3rd -5th 2009: Poster presentation entitled; Investigation of the activity of Triclosan on growth, morphology and cell integrity of bacteria.

Robert Gordon University Aberdeen Novel Antimicrobial Agents Meeting June 15th 2010: Podium presentation entitled; Cationic antimicrobial peptides: novel alternatives to existing antibiotics.

Society for General Microbiology Nottingham UK September 6th – 9th 2010: Poster presentation entitled; Investigation of the Antibacterial Effect of Cationic Antimicrobial Peptides upon *Pseudomonas aeruginosa.*

International Conference on Antimicrobial Research (ICAR 2010) Valladolid Spain 3rd – 5th November 2010: Podium presentation entitled; Investigation of the effect of cationic antimicrobial peptides on bacteria.